University of Glasgow

Lignin Conversion to Fine Chemicals

Danielle Munick de Albuquerque Fragoso

A thesis submitted to the University of Glasgow for the degree of Doctor of Philosophy

Supervisor: Professor S.D. Jackson
School of Chemistry
College of Science and Engineering
University of Glasgow

September 2018

"It always seems impossible until it's done."

Nelson Mandela

Abstract

The large availability of Kraft lignin as an industrial by-product and its polyaromatic characteristic, is ideal to consider the potential for recycling it into fine chemicals. To depolymerise lignin, solvolysis and hydrogenolysis experiments were performed. This research considered whether the low yields of products (fine chemicals) were related to the low content of β-O-4 bonds or if it was also associated to the dissolution of lignin in the solvent solution employed in the reactions. The type of solvents chosen to check the dissolution effect were those with low cost and were more sustainable than traditional solvents. Water, ethanol, isopropanol (IPA) and acetone were used. The water mixtures were applied in the tests in various proportions (25:75, 50:50, 75:25 solvent/water v:v). Due to their ability to break C-C and C-O bonds in lignin model compounds [1][2], the efficiency of platinum and rhodium in these reactions supported on alumina was also studied. It was found that the non-catalysed (solvolysis) and catalysed reactions showed different selectivities but similar overall yields ~ 10 % wt of monomeric phenols. The difficulty in increasing yields was mainly associated with the highly condensed character of Kraft lignin and re-polymerisation issues.

To achieve an understanding of Kraft lignin depolymerisation, isotopic labelling reactions were completed in the presence of deuterated solvents as well as deuterium gas. This gave information on how Kraft lignin depolymerises, the influence of solvent to products formation and the involvement of hydrogen in the rate determining steps in the reactions. These results have led to an initial mechanistic understanding on how this complex molecule may yield alky-phenolic compounds. It was revealed that the solvent was directly involved in the products' formation and that they were not generated by simple thermolysis. In addition, the presence of catalysts and hydrogen influenced product formation. The compounds showed different kinetic isotopic values, suggesting that each of these molecules came from individual mechanisms, highlighting the complexity of their formation. This was a relevant study as most of lignin depolymerisation mechanistic insights are based on model compounds and not on lignin itself.

It was of interest to this project to explore not only different catalysts and their relationship to lignin depolymerisation, but also different lignin types. A simple pre-treatment for lignin extraction using sawdust (from oak and birch wood) in a Parr autoclave reactor in the presence of hydrogen, solvent and high temperature was developed. The lignins obtained after the pre-treatment were named parr-lignin and successfully resulted in polyaromatic molecules with less condensed character compared to lignins from Soda or Kraft pulping. Reactions were carried out with these lignins and a sugar-cane lignin.

Different catalytic systems with these lignins were investigated and how depolymerisation was affected by the metal and support used. The catalysts involved in the reactions included platinum, rhodium, nickel and iron. Various supports such as alumina, zirconia and carbon were tested along with the metals described. It was found that the supports were not inert in these experiments presenting catalytic activity. Materials with low surface area (zirconium catalysts) gave a poor performance compared to the others. In addition, nickel, a non-noble metal, showed as good a catalytic effect in the depolymerisation of these lignins as Pt and Rh. The components in the system influenced the reactions to different extents, especially product distribution. The catalysts had different selectivities and the solvents were not only dissolving lignin but also influencing the results.

GPC analysis was performed to give an overview of the condensed level of these lignins and degrees of depolymerisation compared to the original material. GC-MS enabled the identification and quantification of 18 monomeric compounds. The post reaction characterisation of selected alumina catalysts (Pt/Al_2O_3, Ni/Al_2O_3 and Al_2O_3) was performed using XRD, BET, CHN, TPO and Raman Analysis to study the nature of the carbonaceous layer deposited on these materials. The work showed that after reaction the catalysts turned black in colour and the carbon laydown consisted of not only one simple type of carbon, and included graphitic species. The amount of carbon deposited depended on the type of lignin. Oak and birch parr-lignins had the highest and lowest amount of carbon over the catalysts respectively. No obvious trend relating to the type of catalyst, lignin and solvent used to the carbon nature was identified.

This work showed that lignins with less condensed nature were less susceptible to solvolysis and more to hydrogenolysis. For example, sugar-cane lignin gave 3.9% of phenolic compounds in the solvolysis while reaction with Rh/Al_2O_3 gave 12.9% of products. This indicated that more selective cleavage of bonds were promoted by heterogenous catalysts. The results suggested that some compounds were mainly generated via dealkylation and hydrodeoxygenation, allowing a future possibility to generate target molecules. These results were mainly due to the presence of more labile bonds, vulnerable to hydrogenolysis. Highlighting that prior to depolymerisation, the pre-treatment used to extract lignin must be appropriate to avoid depletion of the alkyl-aryl ether bonds (β-O-4 bonds, especially) relevant for fine chemicals generation.

Dedication

To my beloved mother, my source of love and inspiration.

Acknowledgement

First, I would like to acknowledge my parents, Bartolomeu and Lucia. My father has always incentivised my career and he has been open to help both professionally and personally. Thank you for your love and kindness. To my mother, I am very grateful about the opportunity of having such admirable woman as a mother. Thank you for the amazing support that you have been given to me in my life. All of this would be much harder without the support of my family. Thank you for such love and friendship from my sisters Cris and Pati; my nieces Pri and Sarah; my nephew Lauro and all my relatives.

To my friend Anny, thank you for your friendship and supporting me over the last three years. To Valesca, thank you for listening to me, especially in the hard moments. You are a great friend and an amazing support. Emma, I have no words to describe how special you are to me. You have been amazing, thank you so much for everything over the last few years.

To the Heterogenous Catalysis group and my dear friends Cory, Kate, Yalinu, Angela, Kathleen, Adam, Mustapha, Ihfaf, Raul, John and Lygia. Thanks also to Ashley, especially for the help at the beginning of my PhD and many other times throughout. Thanks to Nicola for a great friendship and for being there whenever I needed. To the University of Glasgow technical support. To Michael Beglan, many thanks for always being ready to help and for such gentleness. To my second supervisor, Professor Justin for his mentoring throughout my PhD.

Especially, I would like to acknowledge my supervisor Professor David, who has been so present and always open to teach and help me in such a difficult project. Your support has been invaluable. Thank you for this great opportunity.

I would like to acknowledge the Conselho Nacional de Desenvolvimento Científico e Tecnológico (CNPq) for the scholarship and the opportunity. This work was financed by CNPq, Ministério da Ciência, Tecnologia, Inovações e Comunicações, Brazil.

Declaration

I declare that this thesis is the result of my own work, except where indicated by referencing to other authors. This is an original work and has not been submitted for any other degree at the University of Glasgow or any other institution.

Table of Contents

List of Tables

List of Figures

List of Equations

1 Introduction

1.1 Biomass and repurposing waste

The waste produced from vegetal and animal species can be defined as biomass [3]. Currently, biomass is contributing about 10 % of the global energy supply. It can be used directly as a fuel or transformed to numerous materials in solid, liquid or gaseous phases. The type of application varies geographically with the Americas mostly using biomass for biofuel production, Asia and Africa for fuel wood and charcoal, while Europe uses it for combined heat and power generation [4]. Demand for fossil fuels remained high in 2017, accounting for 81 % of the world's total energy consumption with main uses from oil, natural gas and coal. However, renewables had a considerable growth rate especially with increases in wind, solar and hydropower [5]. In accordance with the Sustainable Development goals [6] and various initiatives such as the Paris Climate Change Agreement [7], global awareness of the need to pursue non-renewable resources and mitigation measures to reduce the impact of climate change has increased. Thus, interest in biomass from both academy and industry has risen to draw significant focus over the recent years.

The production of fuels and valuable chemicals from biomass has the potential to help reduce reliance on fossil fuels. This could decrease the use of harmful products and cause less damage to the environment than traditional industrial processes. Several methods of transforming biomass into useful products have been studied over the years. Lignocellulosic materials which includes wood and plant based species are one of the most promising and abundant biomass feedstocks with annual production of about 170 billion metric tons [8]. A wide range of high value chemicals from the transformation of lignocellulose components (hemicellulose, cellulose and lignin) has been reported and includes the production of compounds such as organic acids, alcohols, furfural and alkyl-phenolic monomers. Some of these materials are highly relevant and can be used as platform chemicals that could undergo transformations to numerous value-added compounds [9]–[12]. Converting waste to valuable materials could allow for an additional use for lignocellulose and expand this field of knowledge.

1.2 Composition of lignocellulose

The plant cell is one of the basic components of lignocellulose. The plant cell wall is mainly composed of cellulose, hemicellulose and lignin, as illustrated in Figure 1. The content of

these three constituents differ depending on the type of feedstock used, however, an average ratio of 4:3:3 can be considered [13]-[14].

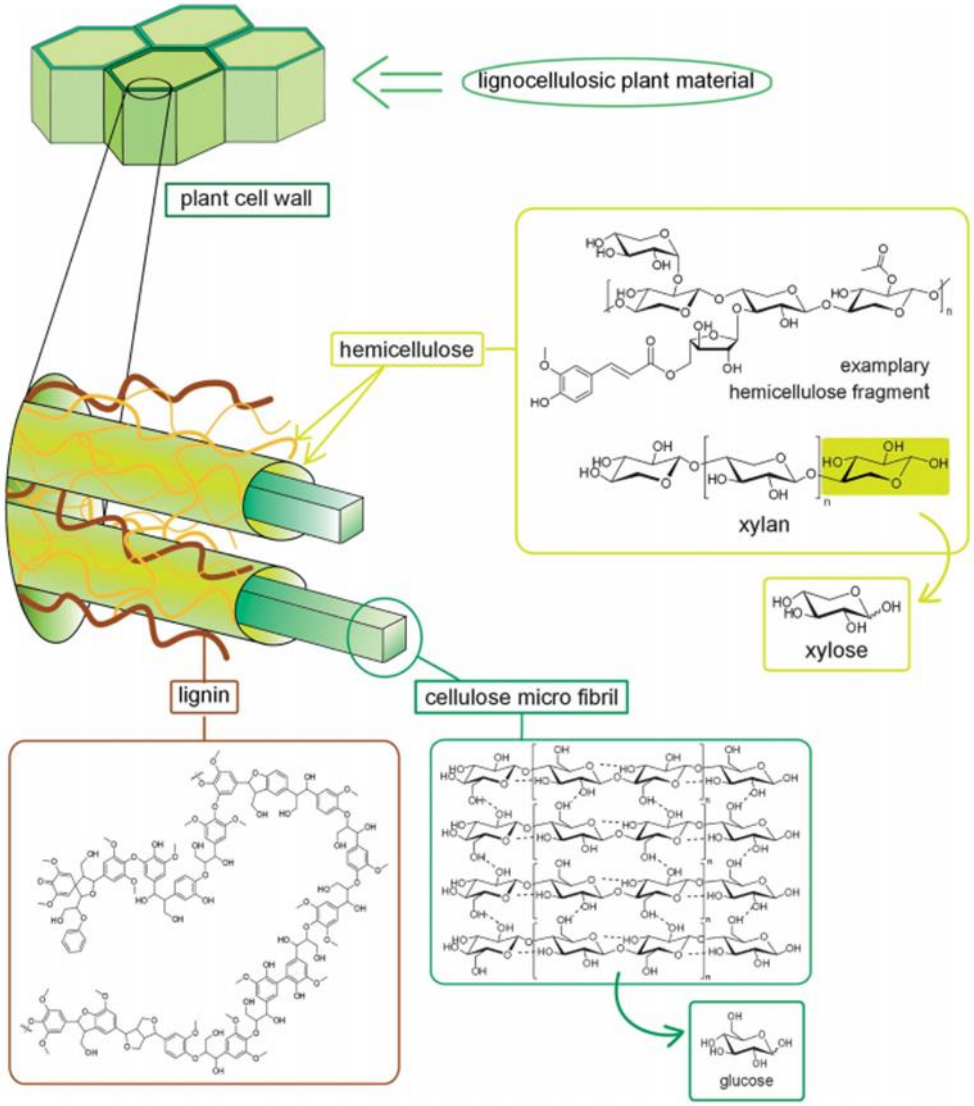

Figure 1 Schematic of plant cell wall components: cellulose, hemicellulose and lignin [14]

Cellulose $(C_6H_{10}O_5)n$ is the most abundant component in lignocellulose, comprising 30-50 % of its weight [8]. It is an insoluble polysaccharide with a linear chain of many (1-4)-linked D-glucose units, having a macromolecular structure that includes crystalline and amorphous regions [13].

Like cellulose, hemicellulose is also carbohydrate based. However, their differences rely on the composition of hemicellulose, which is a type of amorphous heteropolysaccharide constituted mainly of pentoses, hexoses and some uronic acids. These different constituents allow the generation of a non-uniform polymerised structure with side chains. Their

distribution varies depending on the type of plant, but xylose (pentose) is generally the most abundant [8], [13], [14]. One of the main characteristics of hemicellulose is that it contributes to the cross-linked interaction between cellulose and lignin that reinforces the cell wall [15]. The mechanical strength of wood is associated to this complex matrix composed of hemicellulose, cellulose and lignin [16], this stiffness leads to hard degradation of lignocellulose materials, making access to these components difficult.

Lignin is an amorphous, polyphenolic molecule which does not have a defined chemical structure, generated by a complex polymerisation process of three phenylpropanoid monomers, coniferyl, sinapyl and p-coumaryl alcohols (Figure 2) [17]. These monolignols are linked by radical coupling reactions forming a highly complex chemical structure with many types of bonds. These linkages can be ether C-O-C types, such as β-O-4, α-O-4, and 4-O-5 or C-C like β-β, β-5, and β-1 [18], [19] as shown in Figure 3. These bonds have been mostly studied by NMR, which together with the use of model compounds allowed the identification of specific bonds in native lignin [20]. The nature of formation includes many types of radical coupling reactions, leading to a molecule that does not follow ordered repeating units, resulting in a still not fully determined structure. The main voids in lignin contribute to water maintenance, protection and physical strength in plants [21], [22]. Diaryl ether linkages 4-O-5 and alkyl-aryl ethers β-O4, α-O-4, represent about 4-9 %, 45-62 % and 3-12 % in lignin, respectively [23].

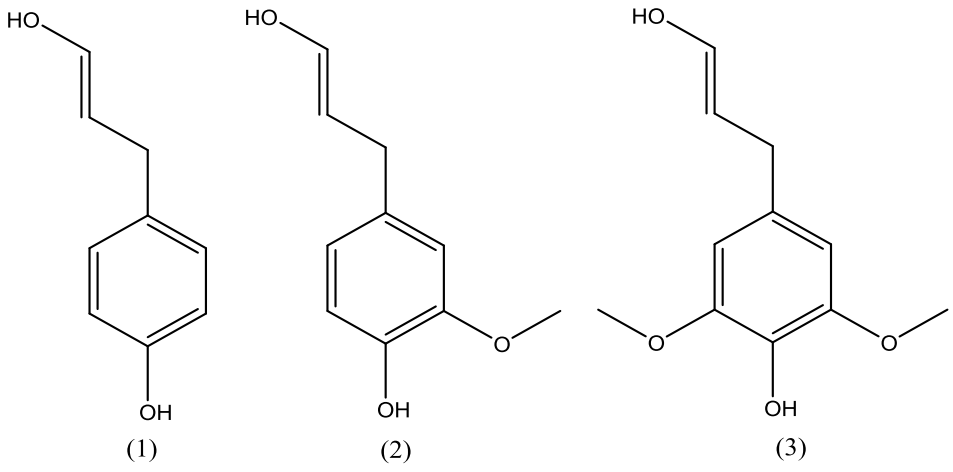

Figure 2 The three phenylpropanoid monomers of lignin. Key: (1) *p*-coumaryl alcohol, H unit; (2) Coniferyl alcohol, G unit; and (3) Sinapyl alcohol, S unit. [24].

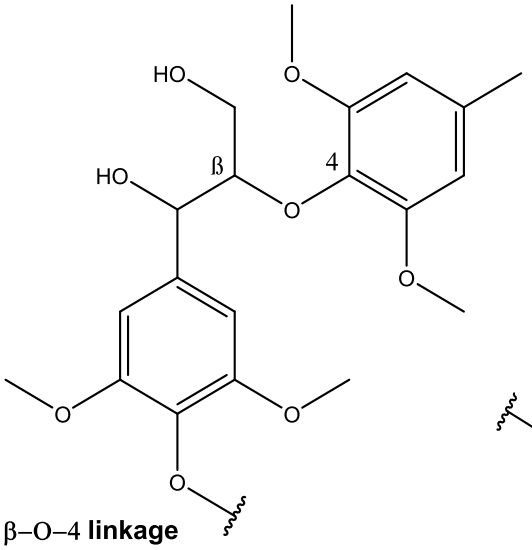

β–O–4 **linkage**

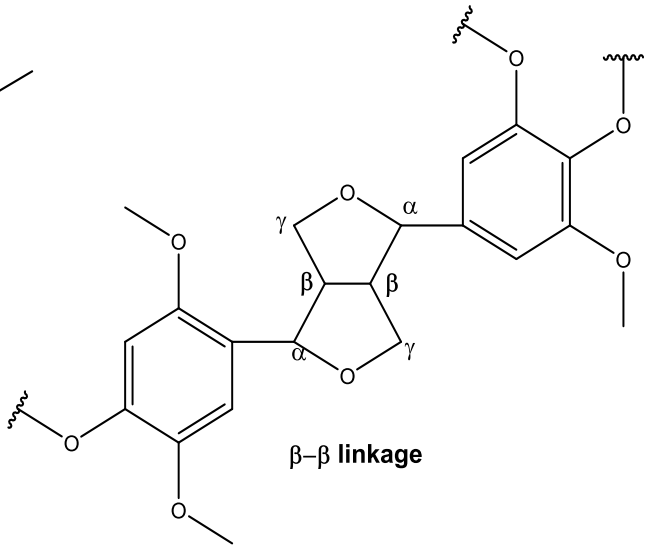

β–β **linkage**

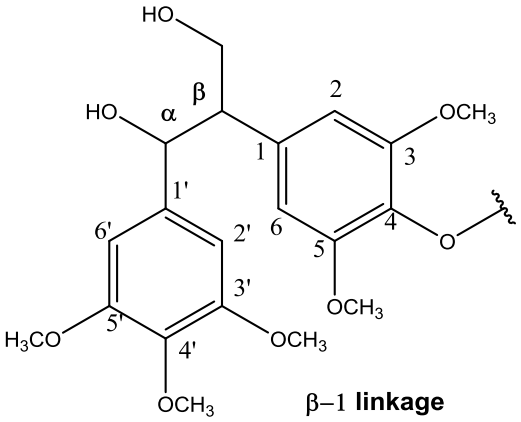

β–1 **linkage**

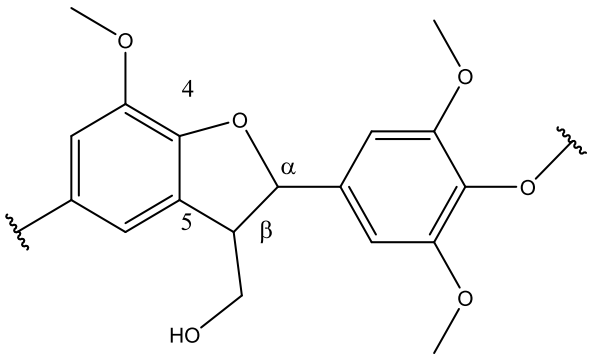

α–O–4 **linkage**

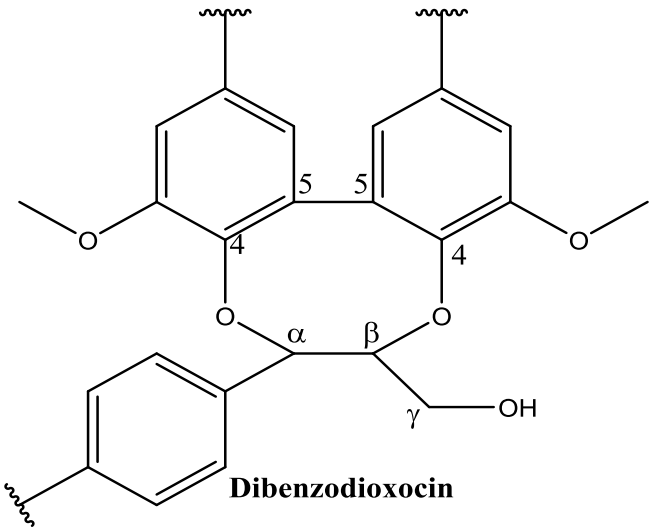

Dibenzodioxocin

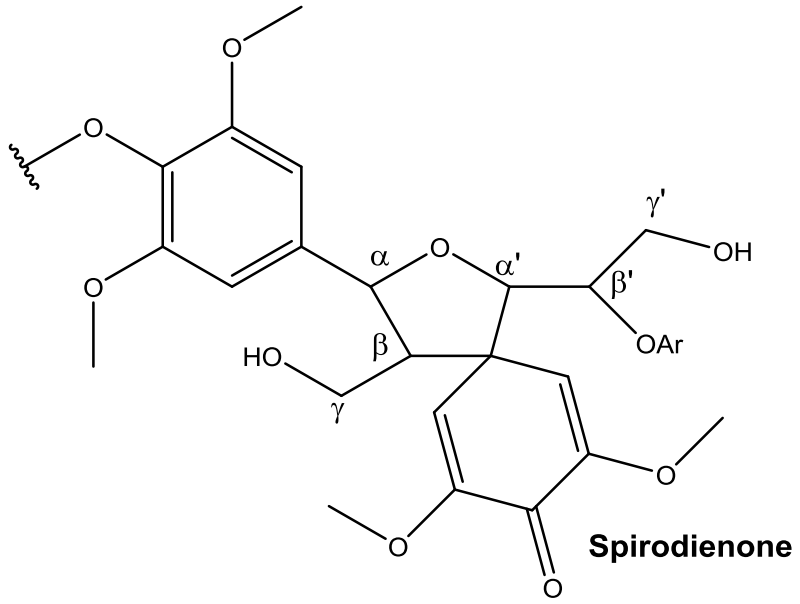

Figure 3 Representation of lignin linkages [25].

Among the most popular sources of wood, there are hardwoods and softwoods. Hardwoods are angiosperm trees mainly consisted of coniferyl and sinapyl units while softwoods are gymnosperms mostly (~ 95 %) comprised by coniferyl structures. The term "soft" does not necessarily mean that one type of wood would be "softer" than other, as there are variations and different characteristics in the trees from each group [17]. One of the most abundant linkages in lignin is the β-O-4. However, its content varies depending on the lignocellulosic feedstock. Table 1 summarises the linkages content in various wood types.

Table 1 Linkages content in various wood sources [26].

Wood type	β-O-4 (%)	β-1 (%)	β- β (%)	β-5 (%)	4-O-5 (%)	5-5 (%)
Poplar	57.8	2.1	2.1	1.8	0.7	0.7
Spruce	31.5	2.1	0.4	2.5	0.5	2.7
Pine	11.3	1.9	0.3	1.2	0.2	0.6
Birch	15.4	47.0	24.5	6.8	3.4	2.5

1.3 Biorefinery and lignocellulose

Petroleum refineries use oil, a non-renewable source, for the obtainment of various products while a Biorefinery uses biomass as a feedstock for the generation of energy, fuels and value-added chemicals. The main processes used by biorefineries consist of cellulose transformation, into fermentable glucose or paper [27]. However, due to its complexity, lignocellulosic materials are still challenging to manipulate and utilization of their full potential is still under development. One of the main problems is to efficiently control the separation of the lignocellulose components and keep their native characteristics after chemical processes, especially lignin. This directly affects the cost and transformation to value added materials [28].

The paper and pulp industries use wood to make several cellulose-based products. From this process, a huge amount (~ 100 million tons) of technical lignins are produced per year worldwide as a side product of these industries. The majority of this material is just burned as a low value fuel to provide power generation [29]. However, research has been showing that lignin holds an enormous potential and could be directed for several applications such as syngas, biodispersants, emulsifiers, carbon fibres, adhesives and aromatics. These are viable alternatives for petrol-based materials and could contribute to the further development of biorefineries [27].

Bulk chemicals or commodity chemicals are manufactured in large quantities, and include substances like acetone, acrylic acid and glycerine. Fine chemicals are highly pure substances, used as building blocks mainly for the obtainment of fragrances, food additives and for the pharmaceutical industry. The expensive cost involved in their industrial processes, including several steps like synthesis, biotechnology and extraction, results in high prices and small production [30]. Lignin's chemical framework holds a great potential for the generation of aromatic building blocks and BTX (benzene, toluene, xylene) due to its natural abundance and its aromatic structure [31]. This possibility of lignin being used as source of value-added chemicals has developed a vast research area that explores improvements in the fractionation of lignocellulosic materials and degradation of lignin. This is still a field in development and it has good prospects for great contributions in a Biorefinery context.

1.4 Sources of lignins

Common lignins available commercially are Kraft, lignosulphonates and soda. Most of the production is related to Kraft lignin, mainly because the sulfate treatment is able to remove the majority of the molecule present in the feedstock [19], [20]. The process consists of cooking wood fibres at high temperatures (435-448 K) with sodium hydroxide and sodium sulfite to generate wood pulp through the cleavage of bonds between cellulose, hemicellulose and lignin. From this method, a black liquor which contains lignin, is generated [21]. One of the main advantages is that the process is energetically favourable for industry, as this by-product can be used to create heat.

Lignosulphonates or sulfonated lignins originate from sulphate pulping to obtain cellulose, as distinct from Kraft lignin that uses sulfite. This lignin has sulfate groups (Figure 4) and it is soluble in water. Generally, it is used as a dispersant for concrete [32]. Soda pulping is an alkaline process (NaOH is used) at high temperatures (423-443 K), which uses straws and some hardwoods, or materials that do not present the same recalcitrant characteristics of most wood feedstocks [33]. The main difference between soda, Kraft and lignosulphonate lignins is that soda is a sulfur free process [27].

Another common procedure used in the lignin extraction is the Organosolv process. Among the most well-known lignins extracted by this process there is the commercial Alcell lignin [34]. Organolv lignin generation occurs through treatments with different types of organic solvents (e.g. alcohols, ketones and glycols). The most popular solvent used for lignin extraction is ethanol [17]. Commonly, the reaction includes a hydrolysis step, which can be catalysed in acidic medium by reagents such as H_2SO_4, HCl, acetic acid, formic acid or peroxiorganic acids. It also can happen in the absence of acid. This process can provide advantages, as it is sulfur free with a less aggressive treatment. In addition, the production of a liquor that contains lignin and hemicellulose favours the separation of these components by addition of water and decrease of the pH, resulting in lignin precipitation and the hemicellulose solubilised. However, Organosolv processes are still under development, as it involves high costs due to the use of solvents and extraction of the lignin is not 100 % [20], [27], [35], [36]. Acetone was also reported as a good solvent for lignin obtainment. Lignocellulosic fractionation at 478 K for 1 hour with 50 % acetone in water mixture resulted in 79 % delignification [37]. Organolv processes involving alkaline medium were also studied. Most of these lignins presented similarities to the soda lignin [38].

A study of catalytic reductive fractionation of lignocellulose to obtain platform chemicals from lignin and a carbohydrate-enriched pulp used various solvent water mixtures (ethanol and methanol) at milder conditions, in the presence of hydrogen and a Parr autoclave reactor. This showed that by increasing the amount of water the solubilisation of lignin and hemicellulose increased, producing cleaner cellulose. However, the decrease in the water content resulted in more lignin removal while the carbohydrates were not highly affected [39]. This strategy was used in the development of the methodology (Section 3.1) for the parr-lignins studied in this work.

As described, there are many methods already used and under development for lignin obtainment. These processes directly affect lignin and their impact on lignin structure were reviewed in the following section.

1.5 The effect of pre-treatment on lignin structure

One of the main challenges in lignin valorisation lies in developing better techniques to its obtainment. The β-ether units are in the majority in native lignins. However, despite a less than full understanding of lignin structure, it is found that there is a considerable decrease in β-O-4 content after chemical treatment. Presuming that these bonds are cleaved during the process, transformation of the molecular structure takes place and as a result, highly condensed bonds (C-C) are formed. The extent of transformation in the molecule is attributed mainly to the conditions used for the process, such as aggressive reagents, high temperature and duration of cooking [20], [40].

A variety of chemical processes to obtain lignin has emerged in the last years. The problem is that this results in lignins with different characteristics. In the case of Kraft lignin, the alteration in the molecule is very problematic. This treatment involves severe conditions, causing the introduction of thiol groups into the chemical framework, stilbene and the cleavage of the most labile bonds of the original molecule (Figure 4), leaving a lignin predominantly constituted with C-C bonds.

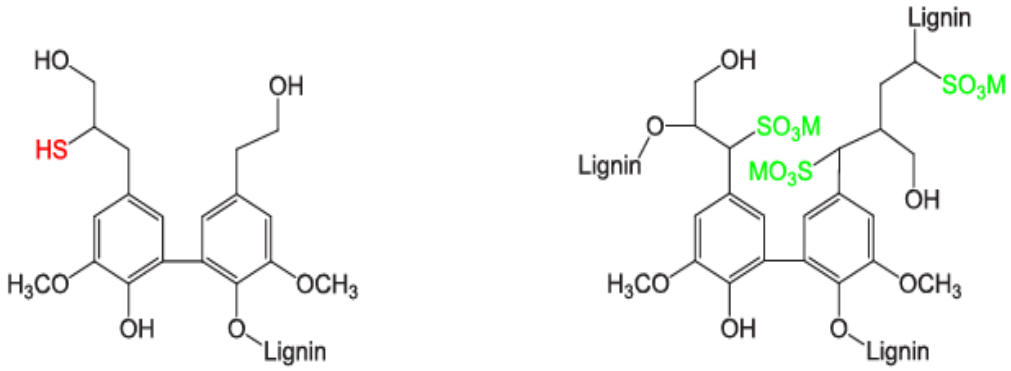

Figure 4 Introduction of thiol and sulfonate group in Kraft (left) and lignosulfonate (right) lignins [41]

Organosolv treatment can remove lignin from the lignocellulosic matrix [17]. In addition, the ether labile bonds of the native lignin can be preserved compared to processes such as Kraft and Soda [38]. It was found that at temperatures of 393 K, using high alcohol content and low acid concentration, a lignin with large amounts of β-aryl ether units, especially α-ethoxylated and α-butoxylated β-O-4 unit was produced [40]. Extraction of lignin from *Miscanthus gigantheus* using ethanol-water mixtures under reflux conditions resulted in a lignin with most of the linkages preserved. NMR analysis of this lignin showed that ethanol was incorporated at the benzylic position of the β-O-4 linkages [42], [40]. One of the advantages of the Organosolv processes is that by using alcohols, the alcohol can target the benzylic cations originated from the cleavage of lignin, forming benzylic ethers and this decreases the re-polymerisation of lignin to give highly condensed structures [17]. An extraction method using ammonia percolation highlighted the importance of pre-treatment methods, as a lignin rich in β-O-4 bonds was obtained [38].

These are examples of the variety of lignins that can be obtained by changing the extraction method. These modifications in the lignin structure are very difficult to avoid becoming one of the main challenges in the field.

1.5.1 Lignin depolymerisation

Several approaches have been studied for depolymerisation reactions involving lignin valorisation [43]–[45]. Most of this research focuses on the obtainment of high value aromatic monomers. Three main methods are currently explored: pyrolysis, oxidation and hydrotreating (hydrogenolysis, deoxygenation) [31].

1.5.1.1 Cleavage of bonds in lignin

The production of chemicals from lignin is directly related to the cleavage of the bonds present in this molecule. The yields and nature of products could be affected by their chemical structure. In hydrogenolysis, for example, lignins with more preserved β-O-4 bonds from its original framework had a better performance for fine chemicals obtainment. However, cleavage of linkages can be followed by repolymerisation, decreasing the yield of alkyl phenolic monomers even by using a less condensed starting material [2] and a very difficult task is preventing the condensation process from occurring. Figure 5 shows a scheme of these competition steps in depolymerisation of lignin.

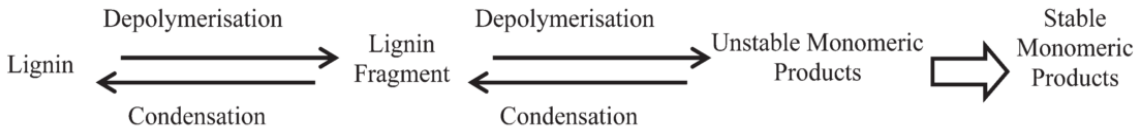

Figure 5 Depolymerisation and condensation processes affecting lignin depolymerisation [1].

Different linkages have different bond dissociation energy (BDE) values. Therefore, in lignin, certain linkages are harder to break than others. Figure 6 shows values of BDE evidencing that lignins having more C-C bonds will require more energy in their depolymerisation.

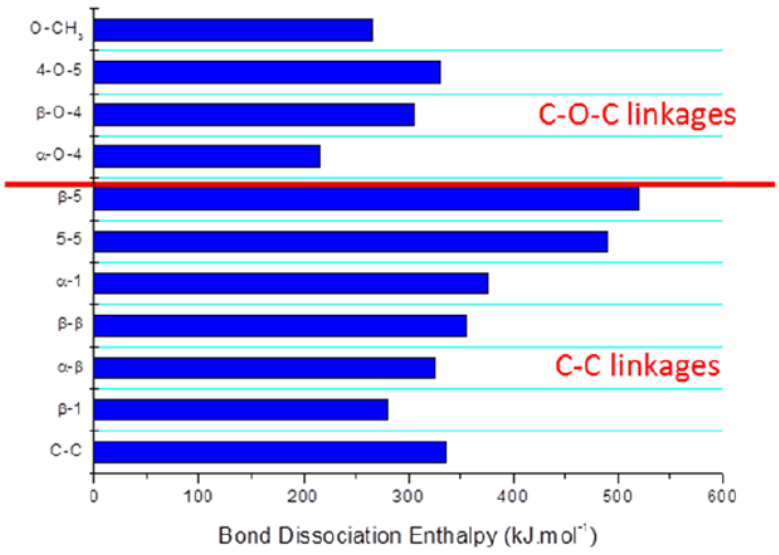

Figure 6 Bond dissociation energies in kJ/mol for various lignin linkages [26]

1.5.1.2 Acid/base and oxidative lignin depolymerisation

Generally, reactions using bases are carried out at high temperatures (~ 573K), pressure varying between 30 bar to 250 bar and base concentrations around 2 % to 10 % w/v [46]. Depolymerisation studies of Kraft and organosolv lignins using a range of bases showed that strong bases such as KOH and NaOH can generate lower molecular weight products than weaker bases. In addition, model compound reactions showed that solvolysis of the linkages was part of the reaction mechanism [47]. Phenoxy rings which have electron-withdrawing characteristics were described as promoters of the alkaline cleavage [48]. Although bases show good results for lignin depolymerisation, this method presents various disadvantages that include risk of equipment corrosion and loss of selectivity for the desired monomeric products.

Acid catalysts are common reagents in the fractionation process of lignocellulose [31], [17]. Acid catalysed depolymerisation of lignin uses reagents such as formic acid, chloric acid and sulfuric acid [49], [50]. Studies involving 10 wt % of formic acid and 77 % wt of ethanol at high temperatures showed that the depolymerisation of lignin had deoxygenation of methoxyphenols and catechols resulting in stable phenols [51]. Comparison of homogeneous (HCl and H_2SO_4) and heterogeneous catalyst performance in lignin depolymerisation under similar reaction conditions (initial pH of 2; 523 K; 30 min; water/methanol 1/5 v/v) revealed that for acids such as HCl and H_2SO_4 not all products were aromatic compounds and high molecular weight molecules were observed, with dealkaline lignin, dimers and oligomers predominating [49]. Using acids such as HCl or H_2SO_4 can result in disadvantages such as equipment corrosion, however, other alternatives (e.g. heterogeneous catalysts) may show benefits, such as the reaction occurring at mild conditions [52].

Oxidative reactions in lignin depolymerisation result mainly in aromatic aldehydes and carboxylic acids. Hydrogen peroxide, metal oxides, alkali or mineral acids have been explored in this area. It is reported that aromatics without high change in the structure and acyclic organic acids can be produced by oxidation methods [31]. This methodology is also known to cleave the resistant β-1 and β-5 linkages through metal-catalysed oxidation systems [53]. However, in lignin reactions, the product yield is not significantly high and the repolymerisation of lignin can lead to highly complex molecules [31].

1.5.1.3 Pyrolysis

Pyrolysis is a thermal degradation reaction which involves high temperatures in an inert environment [54]. Pyrolysis can be influenced by factors such as raw material constitution, pressure and heating rate [55]. As the process happens in the absence of oxygen, there is no combustion and depending on reaction conditions, three main products can be formed, bio-oil (e.g. mixture of phenols, guaiacol and catechol), bio-char and syngas [56]. The mechanisms involved in biomass or lignin pyrolysis are highly complex and are not clearly understood [57]. Usually for biomass, these reactions are divided in two main steps, one primary and one secondary. The first stage comprises decomposition of biomass into volatile compounds and char, followed by the secondary pyrolysis that consists in the degradation of the volatile compounds generated [58].

Lignin thermal degradation is a topic of relevance as most procedures involve high temperatures. In the pyrolysis of lignin, char, liquid oil, gases (e.g. hydrocarbons, carbon dioxide and carbon monoxide), generally compose the products found. If the lignin is from softwood, phenolic compounds derived from guaiacyl are produced. If it is hardwood, aromatics from guaiacyl and siryngyl are found [57]. According to Caballero *et al*., in the pyrolysis of Kraft lignin at 923 K, a range of primary products were generated, such as methane, ethane, acetaldehyde and carbon monoxide. With increasing temperature, methane and carbon oxides had higher yields while methanol, formaldehyde, acetaldehyde, and acetic acid decreased yields [55]. Mohd *et al*. reported thermogravimetric studies under nitrogen of lignin from softwoods and hardwoods. It was found that at high temperatures (~ 723 K), products such as catechols/pyrogallols and cresols/xylenols were found. With increasing temperature (> 823 K) these products were converted into gaseous molecules, mainly carbon monoxide [59]. In addition, Kraft lignins that originated from softwood and hardwood showed mass loss variations in step-wise pyrolysis from 473-1173 K. Between 473-573 K guaiacyl and syringyl units were released. Increasing temperature (> 673 K) resulted in the loss of phenols from hardwoods with no more release from 973 K. For the softwood lignins the temperature of decomposition was higher. Between 673-723 K was the major mass loss consisting mainly of phenol and cresol isomers and at 923 K some compounds could still be detected [60]. Hence, the type of biomass feedstock and treatment used to obtain lignin impacts on linkages distribution, as a result, different lignins show particular behaviour with changes in pyrolysis temperature [58]. Despite pyrolysis showing degradation of lignin into smaller molecules, the technique presents low product selectivity, limiting the practical use of the method.

Various lignins (e.g. Soda, Kraft, ammonia, AFEX, FR-AFEX, alkali and organosolv lignins) prepared through different methodologies were studied in a reduction environment by thermogravimetric analysis within the temperature range 298- 1273 K [26]. This allowed the investigation of decomposition in the presence of hydrogen. They presented different reduction temperatures, with variation in thermal stability. Especially due to the pre-treatment used in the extraction. Less condensed molecules reduced at lower temperatures, as they have a higher content of weaker bonds (especially C-O types). The results showed a broad decomposition between ~ 473-773 K and included four main areas. This signified the complexity of lignin and that the decomposition did not occur in only one step. Water was found to be lost at low temperature, 373 K and also in the main temperature zone, which could be due to dehydration of the OH groups on the β or γ carbons on the aliphatic region. A range of products were formed, such as aromatic hydrocarbons, phenolics, carbon oxides and methane [26].

Kraft lignin (Figure 7) in a reduction medium showed several derivative TPR peaks. The first peak was attributed to water by dehydration reactions. In a difference from less condensed molecules, the main peak appeared at higher temperature ~ 623 K and was accredited to the cleavage of C-C bonds, that required more energy than the ether linkages [26].

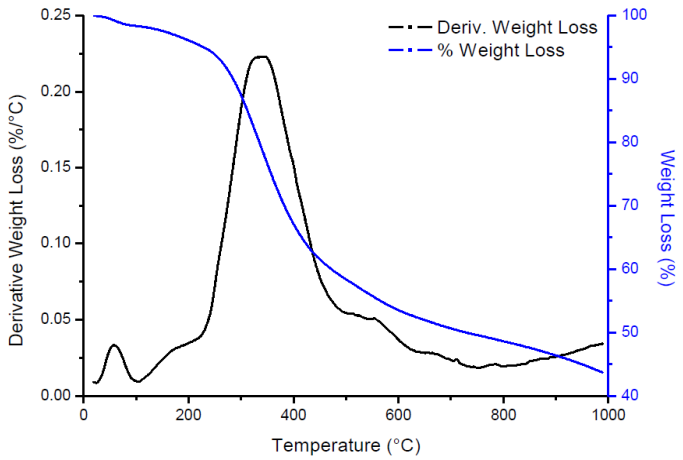

Figure 7 TPR profile of Kraft lignin [26]

1.6 Mechanistic studies of lignin and model compounds

Lignin has a highly complex chemical structure. The mechanism by which this molecule depolymerises to generate aromatic compounds is still unclear. To address this challenge,

several investigations with model compounds simulating lignin linkages have been explored. This helps to predict how a lignin fragment may cleave. Metals such as platinum, rhodium, nickel and iron over supports like alumina, silica and carbon showed a variety of results in terms of product distribution and selectivity for C-O-C and C-C bond cleavage [61]–[63]. Other studies showed that it is not only the metal that plays an important role in the mechanism but also the solvent used in the reaction [1], [26]. Wang *et al*. investigated the hydrogenolysis of diphenyl ether over a Raney nickel catalyst. It was found that the solvent used affected product distribution. Lewis basicity of solvent was not a positive aspect for the Raney nickel performance, however acidity improved catalyst activity [62].

Ethanol, acetone and isopropanol (IPA) can be interesting solvents for lignin depolymerisation. Ethanol is an alcohol that can be obtained from sugar-cane which is a renewable source [64]. Acetone already is produced commercially from fermentation of sugars derived from corn and other agricultural products [65]. IPA, despite not being derived from renewable sources, is a solvent that has a low commercial value and can be a hydrogen donor contributing to lignin reactions [66]. When water is used along with other solvents it contributes to the formation of compounds such as phenol, catechol, guaiacol and methoxy phenols due to hydrolysis of ether linkages [67].

During experiments carried out using ammonia lignin, different proportions of water and methanol revealed that by increasing solvent content, the lignin dissolution improved. The effect, in ammonia lignin depolymerisation, of changing the solvent composition at high temperature in the presence of hydrogen and Pt/Al_2O_3 catalyst showed that the use of 100 % methanol or a methanol-water mixture significantly decreased the condensation for the ammonia lignin. On the other hand, the absence of methanol in the reaction resulted in the formation of recalcitrant residues. The same experiment using IPA-water mixture yielded 24.3 % of monomeric products in comparison to 16.4 % obtained using the methanol-water mixture. Possibly, isopropanol underwent catalytic dehydrogenation to acetone giving isopropanol–acetone water mixture during the reaction. This contributed to the dissolution of lignin and stability of its intermediates [26]. Similar reactions in the presence of Rh/Al_2O_3 showed similar product distribution to Pt/Al_2O_3 with an overall of ~ 61 % syringyl, ~ 26 % guaiacyl and ~ 13 % p-hydroxyphenyl derived products [1].

Kraft lignin had a different behaviour compared to ammonia lignin. Depolymerisation of Kraft lignin in the presence of 100 % methanol showed that the overall yield to monomeric products dropped to 5.6 % compared to 9.2 % when a methanol-water 50:50 v/v solution

was used. The use of IPA-water 50:50 v/v in the reaction slightly increased the overall yield from 9.2 % to 9.8 % compared to methanol-water reaction. The char production considerably decreased in the reactions in the presence of IPA, which suggests that its hydrogen-donating characteristic contributed with Kraft lignin depolymerisation supressing condensation reactions [26].

Hydrogenolysis consists of a reaction that carbon-carbon or carbon-heteroatom bonds can be cleaved by hydrogen. When in this step oxygen is the heteroatom, it is named hydrodeoxygenation (HDO). Generally, these reactions are reported with the participation of catalysts and hydrogen [68]. One of the areas of main interest is the HDO of oxygenated compounds from lignocellulosic materials for bio-oil upgrading. This is already explored commercially. Neste pursues a vegetal oil refining methodology that includes HDO in the process. This allows the removal of oxygen from the plant oils contributing to the final quality of their biofuel [69]. CoMo and NiMo over alumina support are generally used in HDO processes. They were initially developed for the removal of sulfur and nitrogen in the bio oil molecules to avoid poisoning. Then, it was also found that these catalysts could promote HDO without increasing hydrogenation reactions [26]. Despite of these HDO reactions being studied for many years, the catalytic mechanism and deactivation are still not fully understood especially due to the complexity of products generated by the pyrolysis of lignocellulosic materials. Gutierrez *et al*. studied catalyst deactivation in HDO reactions with guaiacol and revealed the importance of noble metal catalysts in these reactions, being superior than traditional sulfided $CoMo/Al_2O_3$ [70]. In addition, the relevance of noble metals was investigated by Bouxin and co-authors in HDO experiments of *para*-methylguaiacol, over Rh/silica and Pt/silica catalysts. They found that the Rh/SiO_2 supplied by Johnson Matthey presented good performance and stability, being active for three days of reaction [71].

Bui and co-authors considered the HDO of 2-methoxyphenol over CoMo catalysts. They found that thermal conversion to catechol and very small quantities of phenol occurred in the absence of catalyst. In addition, detection of only traces of anisole indicated that the C-OH bond is the most difficult to cleave. In attempting to clarify the mechanism of lignin reactions, a great contribution is made by the study of reaction intermediates with these model molecules. Especially because in lignin depolymerisation, with much higher complexity, intermediates such as phenol can be present. Figure 8 shows mechanistic insights about HDO of guaiacol (2-methoxyphenol). Demethylation (DME) and demethoxylation (DMO) could lead to the formation of phenol. From this step, the removal

of oxygen could be caused by deoxygenation (DDO) but also hydrogenation generating cyclohexanol and cyclohexanone as intermediates, followed by water elimination giving non-oxygenated products. Methyl substitutions leading to methyl-catechols, methyl-phenols, and heavier products could be formed over acidic sites on the alumina support. Furthermore, CoMo catalyst favoured the DMO route while cobalt improved the HDO performance of the catalyst and C-O-Me cleavage [72].

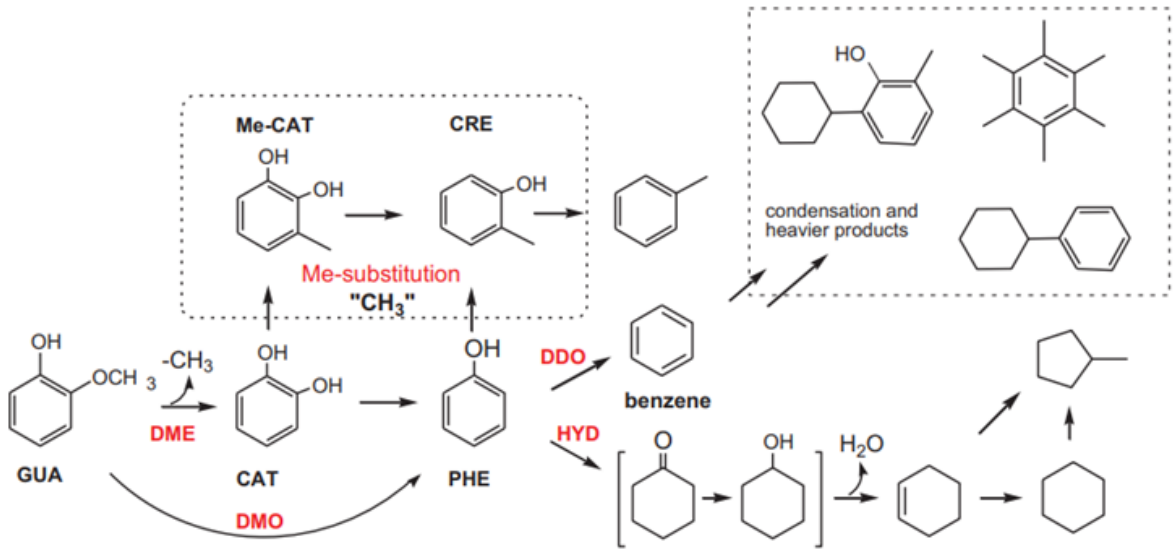

Figure 8 Reactions routes for the conversion of guaiacol [72].

Jiayue and co-authors studied the hydrogenolysis of C-O bonds in di-aryl ethers (4-O-5 linkage) over Ni/SiO_2 catalyst in aqueous phase at mild conditions. This bond cleavage over nickel was found to be the rate determining step. Even being a relatively small molecule, two major routes were considered. Primarily, hydrolysis was followed by hydrogenation resulting in cyclohexanol. Afterwards, hydrogenolysis and hydrogenation produced benzene and cyclohexanol. A minor step could involve hydrolysis, hydrogenolysis and hydrogenation resulting in cyclohexanol and benzene, or cyclohexanol and phenol [73].

Catalytic studies of C-O cleavage (α-O-4) in a model compound (benzyl phenyl ether) in liquid phase over Ni and zeolite-based catalysts was explored (Figure 9). The cleavage of the bond happened in the absence of catalyst thorough hydrolysis resulting in phenyl and benzyl alcohol (intermediates) ending in alkylation. Though, when nickel catalysts were present the predominant route was hydrogenolysis [74].

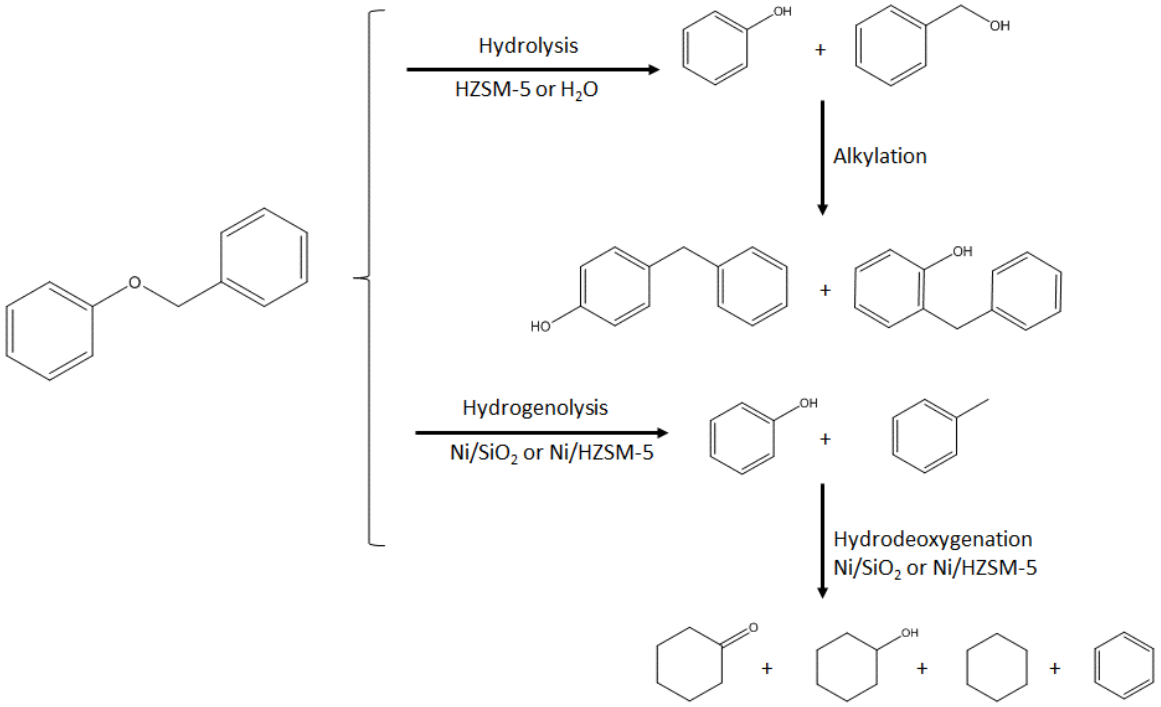

Figure 9 Proposed reaction mechanism for Benzyl phenyl ether in aqueous medium with and without nickel catalysts [74].

Yamaguchi *et al*. explored the cleavage of C-O (β-O-4) and C-C (β-1) bonds using 2-phenethyl phenyl ether and bibenzyl model compounds. The reaction was in supercritical water and carried out over Pd/C, Pt/C, Rh/C and Ru/C catalysts without hydrogen addition. The results confirmed the tendency of Ru to catalyse lignin gasification producing mostly carbon dioxide, methane and hydrogen. Hydrogenated products were not detected in this investigation. For reactions involving Pt and Rh, 2-phenethyl phenyl ether products showed that phenol was probably converted into benzene through hydrodeoxygenation, resulting in a low yield of phenol. Rh showed a relevant performance in the cleavage of C-C bonds in the bibenzyl molecule, as benzene and toluene were generated. Pt was a good catalyst for bibenzene dehydrogenation as phenanthrene was produced [63].

Iron catalysts in hydrogenolysis reactions with α-O-4 and β-O-4 model compounds revealed that Fe on activated carbon successfully cleaved α-O-4 bond resulting in high yields of toluene and phenol. In the case of the β-O-4 model molecule, an important aspect was the presence of an -OH vicinal group. The oxidation reaction of an α-carbon can decrease the bond dissociation energy of ether linkages improving products yield [61]. Hence, types of groups close to the linkages can influence the electronic environment and consequently how the reaction proceeds.

The Kraft lignin studied in this project contains ~ 3 % sulfur. Poisons are known to adsorb reversibly or irreversibly onto active sites in the catalyst. In the first case, the catalyst comes back to its normal performance and methods such as air oxidation and steaming can be used for poison removal. The problem with sulfur is that it can form strong S-metal bonds, competing for catalyst sites in the reaction medium. This can result in change of the catalyst selectivity with undesirable side reactions [75]. This is a challenge in this research, as the presence of sulfur in the Kraft lignin can lead to reduction in catalyst activity.

Despite contributions in clarifying how linkages cleave using heterogeneous catalysts with many model compounds, lignin depolymerisation is still a challenge. This variety of steps that can happen just by a change in a metal, model molecule or in the support, convey the difficulty in studying lignin due to the sometimes unpredictable changes, in reaction mechanisms, even in simple systems.

Different groups present various effects in the electronic configuration of the model molecules, influencing the way in which the linkages are cleaved. In lignin this becomes even more difficult. Especially because its chemical structure can change from source to source and the pre-treatment used to its extraction affects its final molecular composition. Therefore, research not only in small model molecules are important, but also in lignin itself. One of the focuses of this project is in study lignins with known linkages, with the intention to improve understanding of the complex chemistry of its depolymerisation.

1.7 Challenges in lignin depolymerisation and heterogeneous catalysis as a strategy

Reactions involving lignin are a relevant step in any conversion process such as the obtainment of fine chemicals or bio-oil. Nevertheless, many aspects of the depolymerisation are still debateable as the details and application of the models to predict the products obtained, enthalpy of the reaction and rate determining steps are not yet available. In addition, there are several parameters that can cause confusion or add complexity. Including the heterogeneity of the feedstocks, variations in the experimental methodologies, and the difficulty to characterise some products, especially transitory processes with simple techniques such as Gas Chromatography (GC).

Reactions with model compounds can provide valuable information. However, the complexity of lignin is much higher. Simple aspects such as choice of metal, support and

lignin purity (compared to a model compound) could affect the reaction pathways. One of the main desired achievements in lignin depolymerisation is a selective cleavage of C-C or C-O bonds in the molecule. This would allow the controlled production of desired bulk chemicals or functionalised molecules bringing the full potential of lignin in a Biorefinery context. In industry, about 90 % of processes include catalysis. For petrochemistry, cracking is a process in which complex molecules are converted into smaller ones by C-C bond cleavage involving catalysts and high temperature. Hence, the technology of large compound fragmentation has been already used commercially. In terms of lignocellulosic materials, cellulose receives more attention in industry than lignin, mostly because of the technical difficulties involved in lignin conversion. Part of lignin's role in the plant cell wall is protection against attacks, which makes this molecule not only highly complex, but also recalcitrant in its nature and resistant to chemical attack making its transformation very difficult.

As mentioned in Section 1.6, metals such as platinum, rhodium, nickel and iron have been studied in model compound bond cleavage. The experiments presented in the literature apply diverse conditions and results. This brings the possibility for a variety of new experiments, focused upon metals such as rhodium and iron that were not extensively researched. The type of support also has an important role along with the metal in the catalyst. In complex reactions such as lignin depolymerisation, supports with a high surface area can contribute to improve the results, as lignin fragments are not small molecules.

Thus, the development of efficient catalytic methods for lignin depolymerisation, such as the use of solvents improving lignin dissolution in the reaction medium and heterogeneous catalysts in hydrogenolysis reactions, is a viable alternative for lignin valorisation and can provide a great contribution to this field of science.

2 Project aims

The aim of this project is to study lignin depolymerisation to high value aromatic compounds (fine chemicals) using heterogeneous catalysis. This includes the characterisation of studied catalysts and evaluation of their activity and selectivity in reactions of lignin transformation.

3 Experimental Methods

3.1 Lignin sources and preparation methods

It was of interest in this project to explore not only different catalysts and their relationship to lignin depolymerisation, but also different lignin types. Hence, four different types of lignin were studied (Kraft, oak parr-lignin, birch parr-lignin and sugar-cane lignin). Their source and preparation methods are described in the following sections.

3.1.1 Kraft lignin

The Kraft process is used to produce cellulose fibres and consists in the most dominant chemical pulping technique. Kraft lignin is a by-product of this process. The method includes pulping with sodium hydroxide and sodium sulphide at high temperature resulting in a sulfur containing lignin [76]. The Kraft lignin used in this study was obtained from Norway Spruce, purchased from Sigma Aldrich and contains 3 % sulfur.

3.1.2 Parr-lignin

A simple pre-treatment for lignin extraction using sawdust (from oak and birch wood) in a Parr autoclave reactor, in the presence of hydrogen, solvent and high temperature was developed. The lignins obtained after the pre-treatment were named oak parr-lignin and birch parr-lignin.

The oak and birch sawdusts were purchased from Garden Secrets, England, and Gatehouse Firewood, Scotland, respectively. The first step in the parr-lignin preparation was to remove any extractives (e.g. fats, resins, waxes, terpenoids or steroids) present in the wood as they could interfere in further analyses. This procedure was carried out by using a soxhelet extraction system. The oak and birch sawdusts were sieved to a particle size range of 250-1000 µm. Approximately, 10 g of sawdust was weighed into a thimble which was submersed in 200 mL of ethanol/toluene mixture (2:1 v/v). The solvent was heated and allowed to boil for 15 minutes. The thimble was transferred to a soxhlet system containing the same solvent mixture and left for 3 hours. After the procedure, the sawdust was collected, washed with ethanol and left to dry overnight at 313 K. The sawdust samples were weighed before and after the soxhlet extraction. A mass loss of ~ 1.3 g was observed after the procedure. The parr-lignins were prepared by adding 10 g of previously treated sawdust, 130 mL of acetone/water mixture 70:30 v/v in a Parr autoclave reactor. Subsequently, the equipment

was pressurised to 20 bar with hydrogen and heated to 473 K. The reactor was left for 2 hours under 700 rpm mechanical stirrer. After the procedure, the equipment was allowed to cool and by filtration, the liquor containing the parr-lignin was collected. The lignin was precipitated in rapid stirring water at pH 2, recovered by filtration, washed and left to dry overnight at 313 K. The parr-lignin obtained was used in the experiments without further processing.

3.1.3 Sugar-cane lignin

The sugar-cane lignin used in this study was prepared by Professor Euzebio Santana Goulart at Federal University of Alagoas, Brazil.

3.2 Catalysts sources and preparation

Six different catalysts were selected to study their influence in the depolymerisation of lignin. The supports used were alumina, zirconia, carbon and the transition metals were iron, nickel, platinum and rhodium.

The catalysts Ni/alumina, Fe/alumina, Ni/zirconia, Fe/zirconia and Fe/carbon were prepared in house. The carbon and zirconia supports used were in the form of fine powders. Zirconium (IV) oxide was obtained from Sigma –Aldrich (purity 99 %), aluminium oxide from Johnson Matthey (pellets size ~ 5 mm, reference: 961), and carbon from Johnson Matthey (neutral, code: C952/89)

3.2.1 Support Impregnation

The metal precursors were nickel (II) nitrate hexahydrate (Alfa Aesar, purity 98 %, 4.95 g) and iron nitrate nonahydrate (ACROS Organic, purity 99 %, 7.2 g). The Fe/alumina, Ni/zirconia, Fe/zirconia and Fe/carbon catalysts were prepared by impregnation. The procedure consisted of simple wetness impregnation of the support using a solution that contained the stoichiometric amount of metal precursor. Subsequently, the material was left to dry overnight (12 hours) at 313 K. The volume of solution prepared for impregnation of 19 g of alumina, carbon and zirconia was enough for the free-flowing character of the support be lost due to wetness (For Al_2O_3 catalysts 0.7 mL/g, ZrO_2 0.3 mL/g and carbon 1.2 mL/g).

The preparation of Ni/alumina was carried out by using the HDC (Highly dispersed catalyst) technique. The preparation method included an increase in the solution pH in order to

improve the interactions between the alumina support and the metal in solution [77]. The HDC method can contribute to the production of a catalyst with better metal dispersion [78].

The metal precursor nickel (II) carbonate hydroxide tetrahydrate was purchased from Alfa Aesar (98 % purity), the ammonium carbonate from Alfa Aesar (NH_3 ca 30 %) and Ammonia water from Sigma Aldrich (25 % NH_3 bases). The nickel/alumina catalyst was prepared according to Gelder (2015) [78]. Ammonia solution (0.06 L) and distilled water (0.1 L) were gently added to a 0.5 L round-bottomed flask and mixed continuously. Ammonium carbonate chip (9.175 g) was added to the flask and the solution was kept under stirring until the dissolution of all chips was complete. Nickel carbonate (5.34 g) was added to the mixture, resulting in the formation of the nickel amine complex. Subsequently, 47.5 g of theta alumina were transferred to a round bottom flask and the precursor solution was added slowly to the stirred solution. The ammonia and water were distilled off by using a rotary evaporator concluding the metal dispersion into the support. The catalyst was washed in a Buchner flask and left to dry overnight (12 hours) at 323 K.

The conclusion of the catalyst preparation comprised a calcination step. In this procedure, the catalyst was submitted to high temperature for 1 hour in a furnace, in order to decompose the remaining precursor components. With respect to the Fe/C catalyst, it was submitted to the calcination step under argon atmosphere.

In order to determine the calcination temperature, Temperature Programmed Oxidation analyses (TPO) were carried out in the catalysts. The TPO profiles are described in Section 4.1.5.

3.2.2 1 wt % Platinum/alumina

A 1 wt % Platinum/alumina was supplied by Johnson Matthey (reference number 1074). XRD analyses showed that it was mainly composed of θ-alumina. The platinum dispersion was 56 % and it was measured by hydrogen chemisorption [26]. The BET analyses showed a catalyst surface area of 124 m^2g^{-1} with an average pore volume of 0.6 cm^3g^{-1}.

3.2.3 1 wt % Rhodium/alumina

The 1 wt % Rhodium/alumina catalyst was prepared by Dr. Gillan [79] using an impregnation method at University of Glasgow. XRD analyses identified that the support used was a mixture of theta and delta phase alumina. BET analyses presented a surface area

of 102 $m^2 g^{-1}$ and pore volume of 0.51 $cm^3 g^{-1}$, whilst the rhodium dispersion was quoted as being 121 % from CO chemisorption [26].

3.2.4 4.7 wt % Nickel/carbon

A 4.7 wt % Nickel/carbon was supplied by Johnson Matthey (code: C952/70).

3.3 Parr autoclave reactor

3.3.1 Set up description

A 300 mL 316 stainless steel Parr batch autoclave reactor was used to conduct all lignin extractions and the depolymerisation reactions. The Parr unit provides digital temperature control (± 1 K) and manual adjustment for the mechanical stirrer. The gases used in the reactions were provided by external gas cylinders connected to the equipment. Figure 10 shows detailed reactor set up and the internals of the reactor vessel.

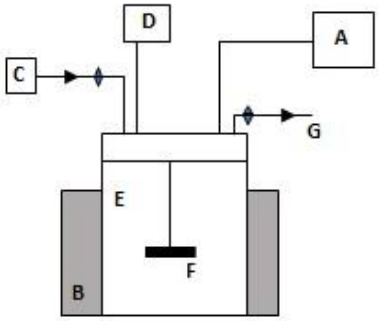

Figure 10: Parr autoclave reactor diagram

The reactor is comprised by the temperature and stirring controller (A), heater (B), gas inlet (C), pressure gauge (D), 300 mL reactor vessel (E), magnetic stirrer (F) and gas outlet (G).

3.3.2 Experimental procedure

The catalysts used were reduced prior to reaction in a flow microreactor. Initially, the alumina supported catalysts were crushed and sieved to obtain a particle size range of 250-425 µm. The catalyst (0.5 g) was added to a glass reactor tube and purged with argon at 30

mL.min^{-1} for 10 minutes. Afterwards, it was reduced as described in Table 2, in 2 % H_2/N_2 and following completion of the procedure it was cooled to room temperature under argon.

Table 2 Description of catalyst reduction conditions

Catalyst	Ramp rate ($^oC.min^{-1}$)	Final Temperature (K)	Dwell Time (h)
1 % Pt/Al_2O_3 [26]	10	523	2
1 % Rh/Al_2O_3 [26]	10	573	1
5 % Ni/Al_2O_3	10	850	1
5 % Fe/Al_2O_3	10	800	1
5 % Ni/ZrO_2	10	800	1
5 % Fe/ZrO_2	10	850	1

The lignin depolymerisation experiments were carried out in a Parr autoclave reactor as described: lignin (0.5 g) was added to the autoclave along with solvent mixture in the presence or absence of 0.1 g of pre-reduced catalyst. The solvents used in the experiments were ethanol (VWR chemicals, purity 99.96 %), isopropanol (Honeywell, purity 99.5 %) and acetone (Fisher scientific, purity 99.88 %) in different volume proportions with distilled water (25/75, 50/50, 75/25 100/0 v:v). The reactor was purged with hydrogen and pressurised to 20 bar. Subsequently, the reactor was heated to 574 K ($\pm$1K) under a mechanical stirring rate of 1000 rpm and stopped after 3 hours. The reactor was left to cool down and the products collected.

3.3.2.1 Kraft lignin product analyses

In order to analyse and quantify the products obtained in the Kraft lignin depolymerisation reactions, the method developed by Dr. McVeigh (2016) at The University of Glasgow (Method 1) was used. The reaction in the presence of acetone/H_2O 50:50 v/v and Pt/Al_2O_3 was carried out in triplicate and the standard deviation of individual compounds was calculated in order to show the consistency of the results. This information is presented in Figure 11 and Table 3. In this procedure, the reaction products were filtered using a glass filter (po.3) to recover the catalyst and separate insoluble products. The insolubilized residues were collected, solubilised in 200 mL of acetone and kept as Fraction 2. The filtered solvent-water sample was centrifuged and made up to 200 mL using the original solvent mixture and stored as Fraction 1 (fraction containing the fine chemicals).

For identification and quantification of products, a GC-MS described in Section 3.4.8 was used. The sample preparation for this analyses was carried out by taking 15 mL from the Fraction 1. This sample was mixed with 0.2 mL of 1 g/L hexadecane internal standard (ACROS Organics, purity 99 %) and acidified to pH 3 using hydrochloric acid, HCl (Sigma Aldrich, 36.5-38.0 %). It was followed by an extraction of the monomers products using dichloromethane (VWR chemicals, purity 99.9 %) and 1,4-dioxane (ACROS organics, purity 99.5 %) in a proportion of 8:2 v/v mixture. Finally, the solvent was removed using a rotary evaporator and the products solubilised in 2 mL dichloromethane (DCM). A 10 µL aliquot of this was mixed with 30 µL of pyridine (Sigma Aldrich, purity 99 %) and 70 µL of N,O-Bis(trimethylsilyl)trifluoroacetamide, BSTFA (ACROS organics, purity 98 %). The resulted mixture was left for 2 hours prior to analyses in the GC-MS equipment.

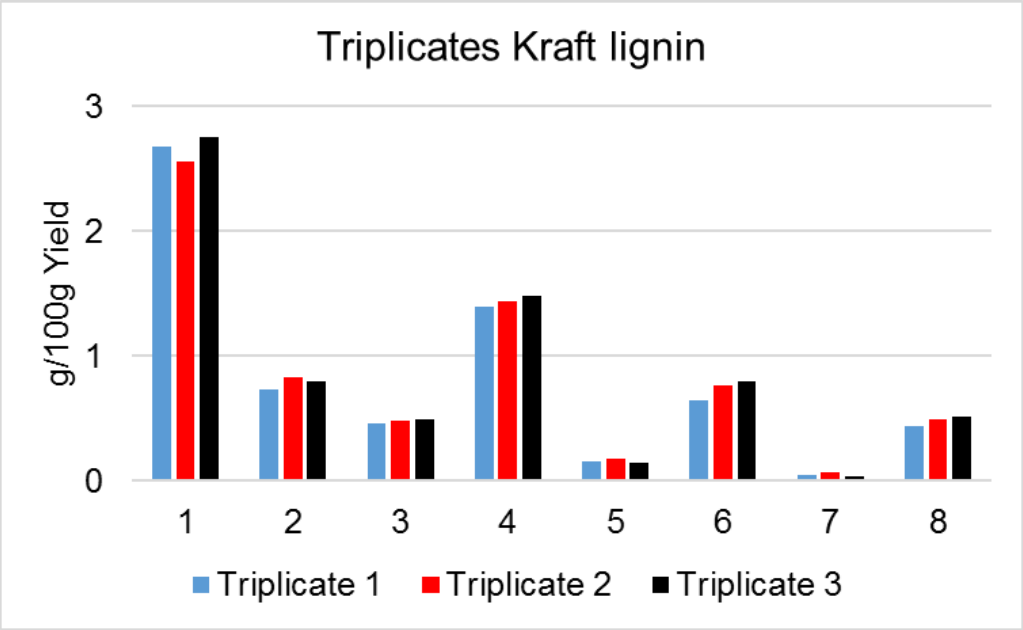

Figure 11 Kraft lignin reaction carried out in triplicate. Products identified and quantified by GC-MS. Key: (1) 2-methoxyphenol, (2) 4-methyl-2-methoxyphenol (3) 4-ethyl-2-methoxyphenol, (4) 4-propyl-2-methoxyphenol, (5) 1,2-dihydroxybenzene, (6) 4-ethylbenzene-1,2-diol, (7) 4-(3-hydroxypropyl)-2-methoxyphenol (8) 4-(3-methoxypropyl)-2-methoxy-phenol

Table 3 Standard deviation values for Kraft lignin triplicate product reactions

Compound							
1	2	3	4	5	6	7	8
Standard Deviation							
0.1	0.05	0.01	0.04	0.01	0.08	0.01	0.03

3.3.2.2 Parr-lignin and sugar-cane lignin product analyses

The methodology presented in Section 3.3.2.1 was simplified (Method 2) and the parr-lignins and sugar-cane lignin reaction products were analysed using this procedure. A comparison between reaction products from both methods showed minimal change in standard deviation, thus ensuring that the procedure was consistent as presented in Figure 12. The analyses was carried out as follows: the product was filtered using a glass filter (po. 3) and centrifuged. The solvent-water mixture portion was kept as Fraction 1 and the insoluble material was solubilised in 50 mL of acetone as Fraction 2. Fraction 1 contained the fine chemicals. The mixture was acidified to pH 2 using HCl and 0.2 mL of 1g/L hexadecane internal standard was added. The extraction process was conducted using DCM. A rotary evaporator was used in order to remove solvents and the product was solubilised in 25 mL of DCM. A volume of 10 µL of product was mixed with 30 µL of pyridine and 70 µL of BSTFA, the mixture was left for at least 2 hours prior to injection and analysed by GC-MS.

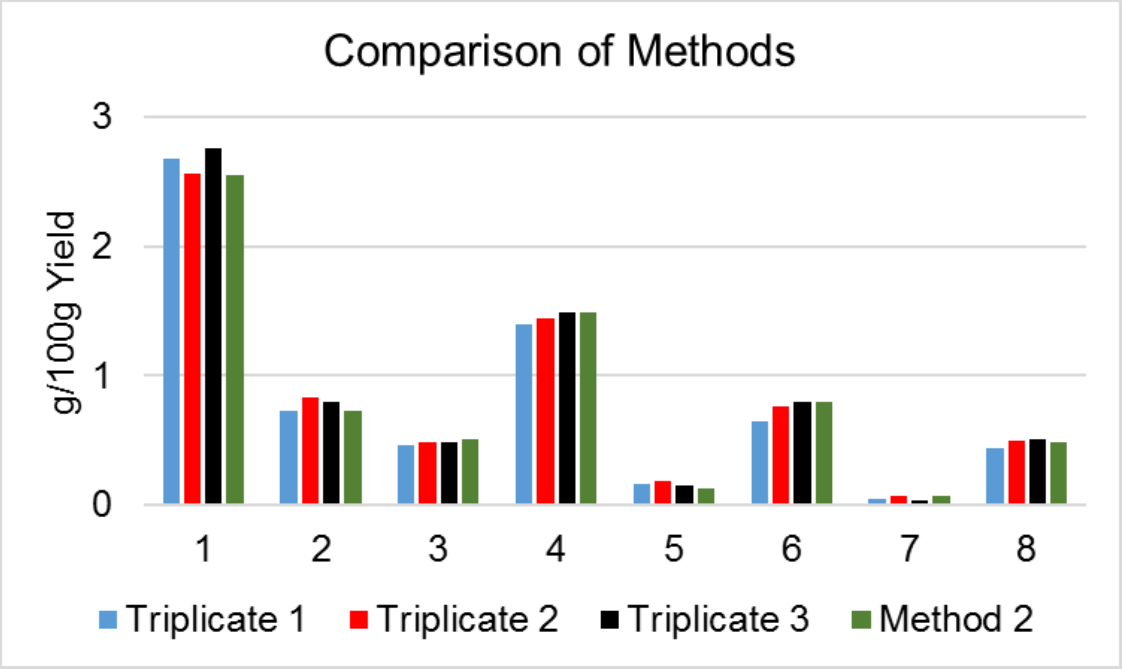

Figure 12 Comparison between Method 1 and Method 2 in the quantification of Kraft Lignin reaction products.

3.3.3 H/D exchange reactions of Kraft lignin

Conducive to improving the understanding of Kraft lignin depolymerisation and the breakdown mechanism of this molecule, isotopic labelling studies were carried out using deuterated acetone, $(CD_3)_2CO$ (ACROS organic, purity 99 %) deuterium oxide, D_2O

(ACROS organic, purity 99.8 %) and deuterium gas, D_2 (BOC, purity 100 %, code: UN 1957). The monomeric products were identified by GC-MS using the methodology described in Section 3.3.2.1.

3.3.3.1 Kinetic isotopic effect (KIE)

Kinetic isotopic effect is a phenomenon associated with isotopically substituted molecules exhibiting different reaction rates. Isotope effects such as KIEs are invaluable tools in both physical and biological sciences and are used to aid in the understanding of reaction kinetics, mechanisms, and solvent effects [80]. The KIE was calculated according to the following equation:

Equation 1 Kinetic isotopic effect calculation

$$\mathrm{KIE} = \frac{r_H}{r_D}$$

Where r_H and r_D are the rate of reaction for an individual compound in a protiated and deuterated experiment, respectively. They were obtained according to Equation 2.

Equation 2 Rate of reaction calculation for each individual product

$$\text{Rate of reaction (r)} = \frac{\text{Individual product yield}}{\text{Time (minutes)}}$$

3.4 Analyses Methods

3.4.1 Surface area and pore volume determination

For the determination of the surface area and pore volume of the catalysts used, Brunauer, Emmet and Teller (BET) analyses were done using a Micrometrics Gemini III 2375 Surface Area analyser at 77 K. Samples (0.04 g) were weighed in a glass tube and left overnight at 383 K under nitrogen. The sample was reweighed prior to analyses in order to obtain the proper catalyst weight.

The surface area, pore volume and pore diameter could be obtained according to Brunauer, Emmett and Teller (BET) [81] adsorption isotherm (Equation 3) and Equation 4.

Equation 3 The Brunauer, Emmett and Teller equation [81]

$$\frac{P}{V(P_0 - P)} = \frac{1}{V_m C} + \frac{(C-1)P}{V_m C P_0}$$

Equation 4 Equation for specific surface area obtainment [82]

$$SA = (\frac{Vm}{v})x\ (N)\ x\ (Am\ x\ 10^{-18})$$

Where, P = Pressure of the adsorbate, V = the volume of adsorbate adsorbed per unit mass of adsorbent at equilibrium pressure P, V_m = the volume of adsorbate required for complete monolayer coverage of the adsorbent, P_0 = saturated pressure of adsorbate gas, C = constant [81]. S_A = surface area of a substrate A, v = 0.0224 m^3 occupied by 1 mole of the adsorbate gas at STP, N= avogadro's number (6.022×10^{23} mol^{-1}) and Am= area of one molecule (which for N_2 is 0.162 x 10^{-18} m^2) [82].

In order to calculate the specific surface area of a substrate (m^2/g), $P/V(P_0-P)$ *versus* P/P_0 can be plotted and this should result in a straight line graph. Related to Equation 3, on the y-axis the intercept is $1/V_mC$ and the slope is $(C-1)V_mC$, therefore, C and V_m can be determined. By using Equation 4 and the values obtained, the specific surface area can be determined.

3.4.2 Thermogravimetric analyses

A combined TGA/DSC SDT Q600 thermal analyser coupled to an ESS mass spectrometer was used to perform the thermogravimetric analyses (TGA) in the catalysts. The procedure required 0.01-0.015 g of catalyst. The samples were heated from room temperature to 1273 K with a thermal ramp of 10 $Kmin^{-1}$ under 2 % H_2/N_2, O_2/Ar or Ar gas. Mr Andy Monaghan at The University of Glasgow carried out the TGA experiment.

3.4.2.1 Temperature programmed oxidation (TPO)

To determine the catalysts calcination temperature, the TPO analyses were accomplished after their preparation and the post reaction catalysts were submitted to this analyses to study carbon deposition onto catalyst surface. Typically, 0.01-0.015 g of catalyst sample was heated in a flow of 2 % O_2/Air (100 ml min^{-1}) from 303 K to 1273 K, at a ramp rate of 10

$Kmin^{-1}$. Desorbed fragments such as m/z 18(H_2O), 28 (CO), 44(CO_2), 30 (NO), 44 (N_2O), 48 (SO), 64 (SO_2), 50 (NO_2) were monitored.

3.4.2.2 Temperature programmed reduction (TPR)

The TPR analyses were carried out with a fresh catalyst to determine their reduction temperatures. The procedure consisted of 0.01-0.015 g of catalyst heated in a flow rate of 2 % H_2/ N_2 (100 ml min-1) to 1273 K from 303 K, at a ramp of 10 K min^{-1}. Desorbed fragments such as m/z 18 (H_2O) were monitored.

3.4.3 X-ray diffraction analyses (XRD)

The XRD analyses were performed using a Siemens D500 X-ray diffractometer (40 Kv, 40mA, monochromatised) with a CuK α source (1.5418 Å). Typically, the catalyst was crushed prior to experiment, placed in the sample holder and levelled for analysis. The scan range was between 5-85º 2θ and the scanning rate was 2 s/step with step size of 0.02º.

X-ray diffraction is commonly used to identify crystalline substances. In typical experiments, monochromatic X-rays are directed towards the sample and interference phenomena occur [83]. The interaction between the sample and the x-rays results in constructive (CI) or non-constructive interference (NCI). From CI, a diffracted ray is formed satisfying Bragg's law (Equation 5) [83]. This law relates the wavelength of the beam (λ), the incident angle (θ) and the spacing between diffracting planes (d). The patterns recorded in the detector from the diffracted x-rays are characteristic of the analysed substance, as they will depend upon the interplanar spacing (Equation 5) [83], [84]. Hence, the results can be interpreted as a fingerprint of the material.

Equation 5 Brag's law equation [83]

$$n\lambda = 2d\sin\theta$$

3.4.4 Raman spectroscopy

Raman Spectroscopy analyses were carried out on post reaction catalysts using a Horiba Jobin Yvon LabRAM High resolution spectrometer. As a source of excitation a Helium Cadmium IK3201R-F 325 nm UV laser was used. The sample was submitted to the laser light for 10 seconds using a 15x UV objective lens with 1200 cm^{-1} grating. The sample was

analysed in the range of 500 to 3000 cm^{-1}. A back scattering configuration was used to collect the scattered light and detected by a nitrogen cooled charge-coupled detector CCD.

3.4.5 CHN analyses

The CHN analyses were carried out using a CE-440 elemental analyser. Mr Gangi Ubbara at The University of Glasgow performed the experiments.

3.4.6 Atomic absorption spectroscopy analyses (AAS)

The AAS analyses was conducted using a Perkin Elmer analyst 400, atomic absorption spectrometer, with winlab 32. The analyses were carried out by Mr Michael Beglan at The University of Glasgow.

3.4.7 NMR analyses

Mr James Mongomery and Professor Nicholas Westwood performed the NMR analyses at The University of St Andrews.

Lignin NMR spectra was acquired on a Bruker Avance III 500 MHz spectrometer equipped with a nitrogen cooled BBO probe (prodigy). The central DMSO solvent peak was used as internal reference (δC 39.5, δH 2.49 ppm). The ^{1}H, ^{13}C-HSQC experiment was acquired using standard Bruker pulse sequence 'hsqcetgpsp.2' (phase sensitive gradient-edited-2D HSQC using adiabatic pulses for inversion and refocusing). Composite pulse sequence 'garp4' was used for broadband decoupling during acquisition. 2048 data points was acquired over 12 ppm spectral width (acquisition time 170 ms) in F2 dimension using 16 scans with 1 s interscan delay and the d4 delay was set to 1.8 ms (1/4J, J = 140 Hz). 128 increments were acquired in the F1 dimension (acquisition time 5.9 ms) with a spectral width of 86 ppm centred on 90 ppm. The spectrum was processed using squared cosinebell in both dimensions and LPfc linear prediction (32 coefficients) in F1. The total experimental time was 40 minutes.

The analysis calculated the number of linkages per 100 C9 units. If the lignin had only one type of aromatic unit present, the aromatic region was the reference. For lignins with various aromatic units (S, G and H) the linkages were used as a reference to in effect calculate the number of aromatic units per 100 linkage (β-O-4/β-5/β-β). By taking the reciprocal (1/x) of

this number, the number of linkages per 100 aromatic units were obtained. G2 S2/6 and H2/6 signals were used.

3.4.8 Gas chromatography – mass spectrometry (GC-MS)

The method developed by Dr. McVeigh (2016) was used to identify and quantify the reaction products. In order to perform the analyses, a Shimadzu GC-MS QP2010S coupled to a Shimazu GC-2010 equipped with a ZB-5MS capillary column (30 m x 0.25 nm x 0.25 µm) with He as carrier was used. The column was kept at 333 K for 2 minutes then heated to 533 K, where it was held for 10 min. A volume of 1 µL of sample was injected using split mode (50:1) and an injection temperature of 523 K.

3.4.8.1 Product identification and quantification

The reactions produced a wide-range of alkyl-phenolic compounds having many functional groups. Using the GC-MS technique, reference compounds and literature studies, it was possible to identify and semi-quantify 18 monomeric products, described in Table 5 and Figure 18.

Considering the high prices of fine chemicals, the semi-quantitative determination of these products was carried out after calibration with four authentic compounds (the molecules were derived from two Guaiacyl and two Syringyl lignin units) and relative to hexadecane, the internal standard. This enabled the obtainment of response factors (α), which were included in the products quantification as described in Equation 6. These compounds were: 2-methoxyphenol (Sigma Aldrich, purity 98 %), 4-ethyl-2-methoxyphenol (Sigma Aldrich, purity 98 %), 2,6-dimethoxyphenol (Sigma Aldrich, purity 99 %) and 4-methyl-2,6-dimethoxyphenol (Sigma Aldrich, purity 97 %). The concentrations used were 0.01, 0.05, 0.1, 0.5 and 1 g/L, where hexadecane, the internal standard, had a fixed concentration of 1g/L.

The identified compound peaks were integrated in order to establish their peak area. Hence, it was possible to plot a straight line, where the slope value corresponds to the response factor. Figure 14, Figure 15, Figure 16 and Figure 17 show the calibration curves used for each compound and the α values are outlined in Table 4.

As presented in Section 3.3.2, the product mixture was silylated using N,O-Bis(trimethylsilyl)trifluoroacetamide. This process allowed the hydroxyl groups present in

the product molecules be replaced with a [-Si$(CH_3)_3$] group. This technique, contributes to more volatile compounds [85]. Before the analyses of each molecule, the presence of this group was confirmed by mass fragment data analyses and the additional mass of 73 g/mol ([-Si$(CH_3)_3$] group) was taken in account onto the total mass of individual products. The reference compounds modification after the process is showed in Figure 13. The molecules showed are 2-methoxyphenol, 4-ethyl-2-methoxyphenol, 2,6-dimethoxyphenol and 2,6-dimethoxy-4-methylphenol, respectively.

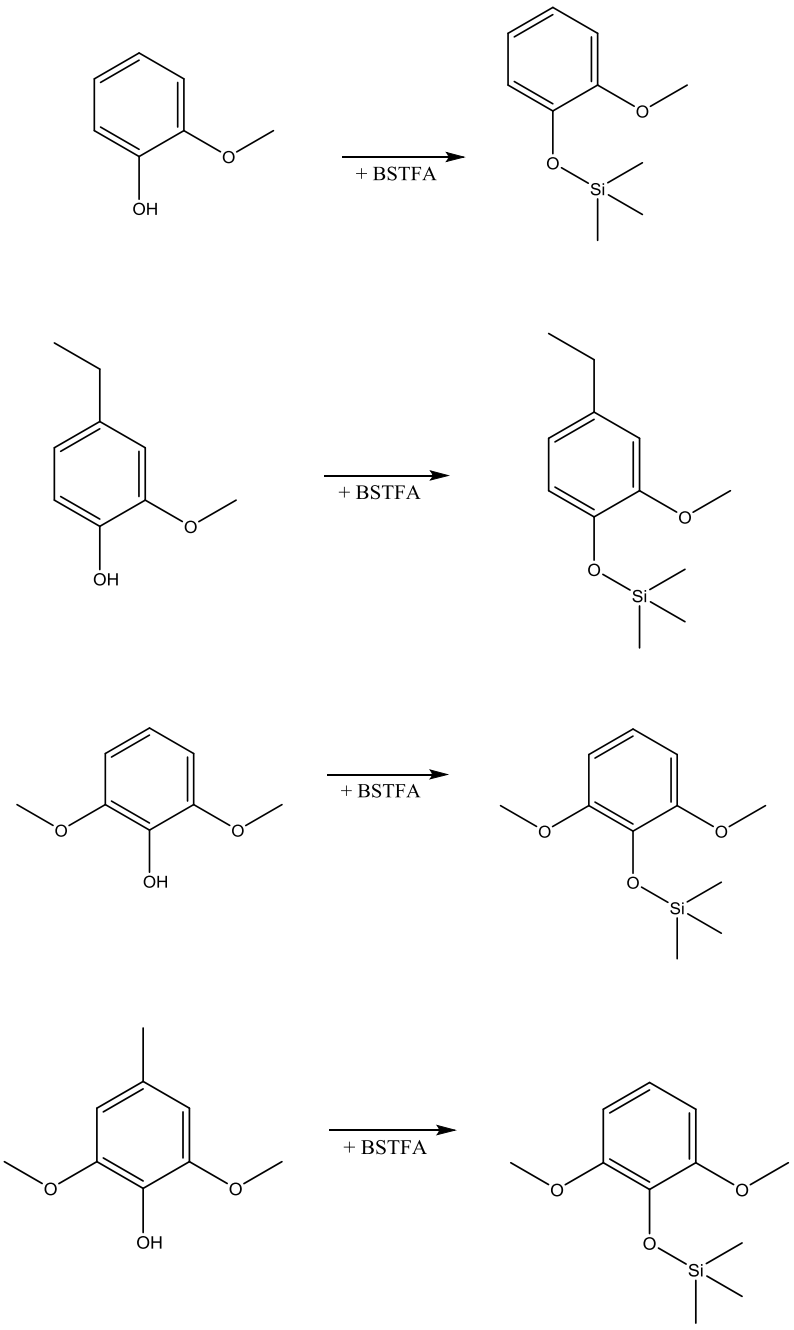

Figure 13 2-methoxyphenol, 4-ethyl-2-methoxyphenol, 2,6-dimethoxyphenol and 2,6-dimethoxy-4-methylphenol and their derivative forms.

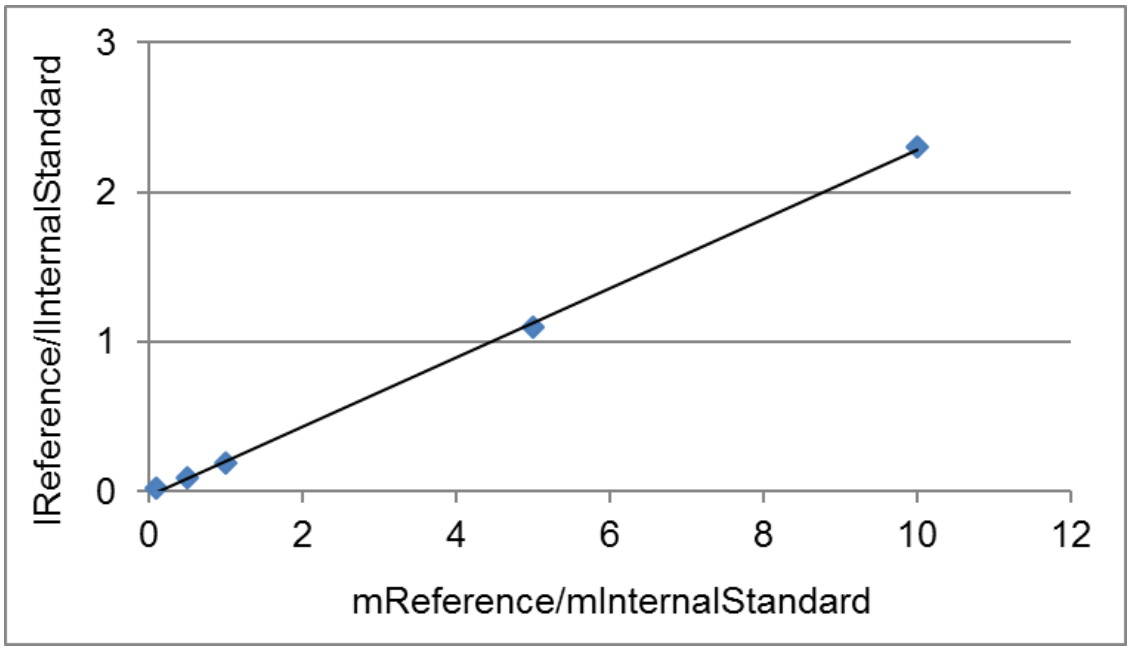

Figure 14 Calibration curve for 2-methoxyphenol. Key: intensity(I) and mass(m).

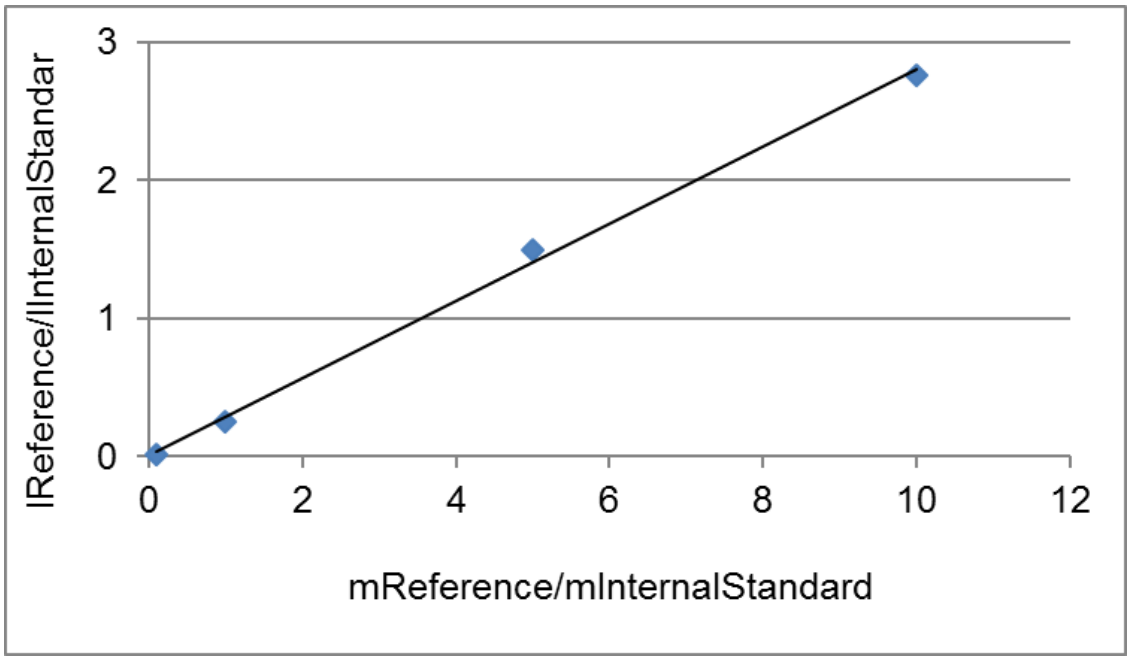

Figure 15 Calibration curve for 4-ethyl-2-methoxyphenol. Key: intensity(I) and mass(m).

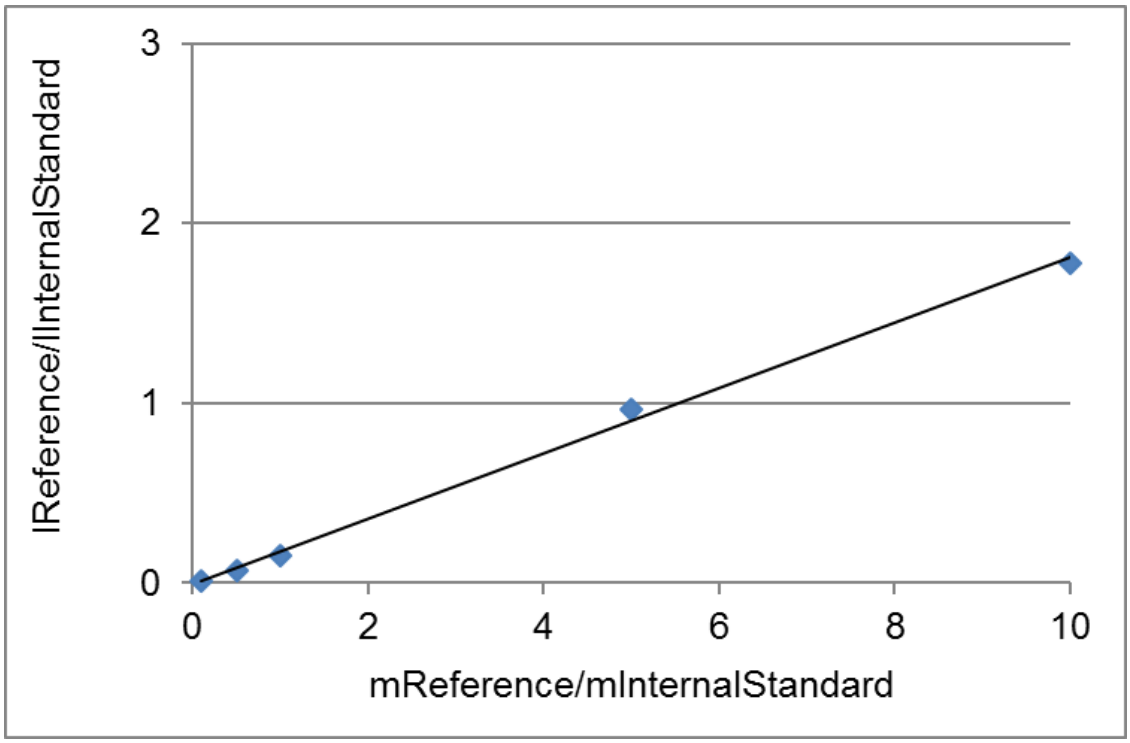

Figure 16 Calibration curve for 2,6-dimethoxyphenol. Key: intensity(I) and mass(m).

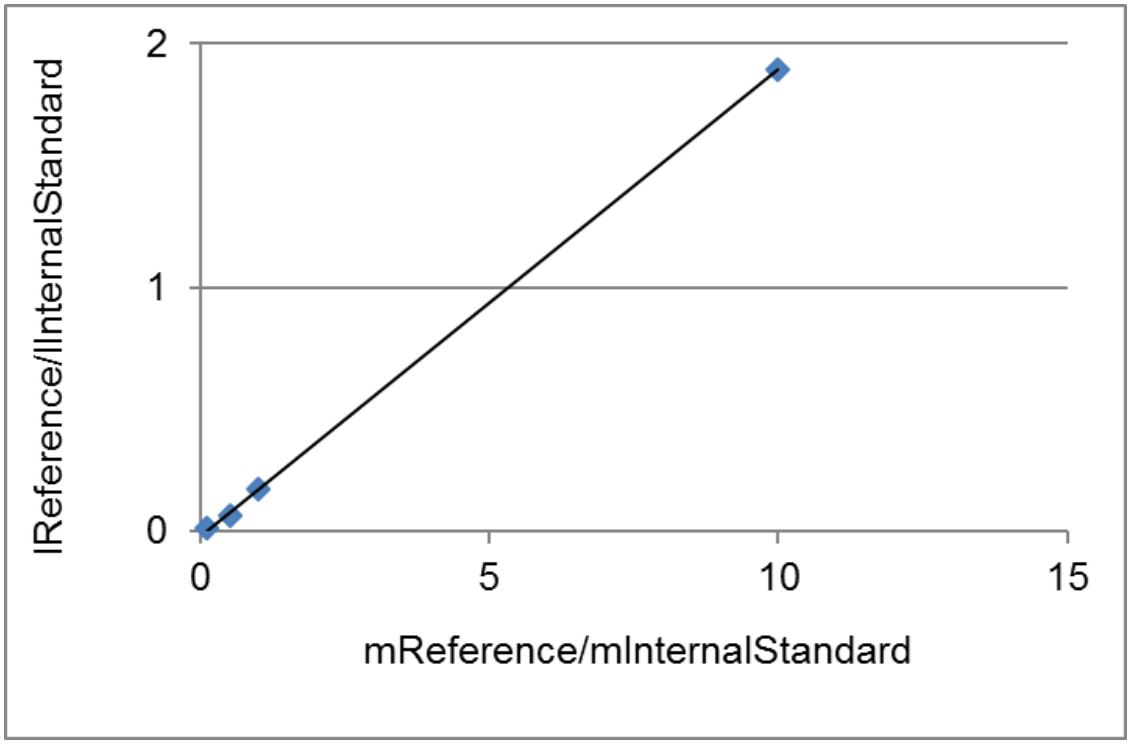

Figure 17 Calibration curve for 2,6-dimethoxy-4-methylphenol. Key: intensity(I) and mass(m).

Equation 6 Equation used to calculate the response factor for each individual compound

$$\alpha = \frac{\text{Intensity of reference}}{\text{Intensity of internal standard}} \text{x} \frac{\text{Mass of internal standard}}{\text{Mass of reference}}$$

The response factors obtained according to Equation 6 are presented in Table 4.

Table 4 Response factors obtained from Equation 6.

Compound	Lignin Unit	Response Factor (α)
2-methoxyphenol	Guaiacyl (G)	0.23
4-ethyl-2-methoxyphenol	Guaiacyl (G)	0.23
2,6-dimethoxyphenol	Syringyl (S)	0.19
2,6-dimethoxy-4-methylphenol	Syringyl (S)	0.18

According to Table 4 and the calibration curves showed in Figure 14, Figure 15, Figure 16 and Figure 17, a trend was found for the response factor (α) values related to the G units and S units. Therefore, in the quantification process, it was assumed for each molecule the α value of its correspondent unit structure. The values assumed for G and S units are 0.23 and 0.19, respectively.

3.4.8.2 Kraft lignin product quantification

As described in Section 3.3.2.1, after the reaction, 200 mL of Fraction 1 was prepared, which corresponds to the sample containing all the fine chemicals. The extraction process required a portion of 15 mL of this Fraction. After the complete procedure, 1 µL (0.001 mL) was injected in the GC-MS. By rearranging Equation 6, it was possible to calculate the mass of product present in 1 µL of sample injected (m1 µL). The identified compound peak was compared to the internal standard and the correspondent response factor was taken in account to give a relative quantity related to that peak, as presented in Equation 7.

Equation 7 Equation used to quantify the mass of individual products in 1 µL of injected sample.

$$\mathrm{m1\mu L} = \frac{\text{Intensity of Product}}{\text{Intensity of Internal Standard}} x \frac{\text{Mass of Internal Standard}}{\alpha}$$

In order to calculate the actual mass of each product, the mass present in 15 mL (m_{15mL}) of fraction was calculated according to Equation 8. Finally, the total of 200 mL Fraction 1 was factored in the calculation as well as the initial mass of lignin used in the reaction (0.5g). This was multiplied by 100 with the purpose of quote the product as gram of product per 100 g of lignin (g/100 g), as summarised in Equation 9.

Equation 8 Mass of product present in 15 mL of Fraction 1.

$$\mathrm{m15mL} = \frac{(\text{mass of product from Equation 7})\mathrm{x15}}{0.001}$$

Equation 9 Total mass of an individual product in g/100 g

$$\mathrm{m/100\ g} = \frac{\left(\frac{\text{mass of product from Equation 8 X 200}}{15}\right)}{0.5} \text{ x } 100$$

3.4.8.3 Parr-lignin and sugar-cane lignin products quantification

The products analyses of parr-lignin and sugar-cane lignin was described in Section 3.3.2.2. After the fine chemicals extraction and solvent removal procedure of Fraction 1, the sample containing all fine chemicals was solubilised in 25 mL DCM and 1 µL of the prepared sample injected for GC-MS analyses. By using Equation 7, it was possible to quantify the amount of an individual product present in 1µL (0.001 mL) of sample. Afterwards, the total mass of a product in 25 mL was considered and the initial mass of lignin used (0.5g). This was multiplied by 100 in order to present values in g/100 g of product, as described in Equation 10.

Equation 10 Total mass of an individual product in g/100 g

$$\mathrm{m\ g/100\ g} = \frac{\left(\frac{\text{mass of product from Equation 7 X 25}}{0.001}\right)}{0.5} \text{ x } 100$$

The Table 5 and Figure 18 below describe all 18 monomeric compounds identified in the reactions by mass fragment data analyses.

Table 5 List of identified compounds in product reactions

Compound Code	Compound Name
(1)	2-methoxyphenol
(2)	4-methyl-2-methoxyphenol
(2A)	4-ethylphenol
(3)	4-ethyl-2-methoxyphenol
(4)	4-propyl-2-methoxyphenol
(5)	1,2-dihydroxybenzene
(6)	4-ethylbenzene-1,2-diol
(6A)	2,6-dimethoxyphenol
(7)	4-(3-hydroxypropyl)-2-methoxyphenol
(8)	4-(3-methoxypropyl)-2-methoxyphenol
(9)	4-methyl-2,6-dimethoxyphenol
(10)	4-(2-hydroxyethyl)-2,6-dimethoxyphenol
(11)	4-ethyl-2,6-dimethoxyphenol
(12)	4-propenyl-2,6-dimethoxyphenol
(13)	4-(2-hydroxyethyl)-2-methoxyphenol
(14)	4-propyl-2,6-dimethoxyphenol
(15)	4-(1-hydroxy-2-methyl-pent-3-enyl)-2,6-dimethoxyphenol
(15A)	4-(3-hydroxypropyl)-2,6-dimethoxyphenol

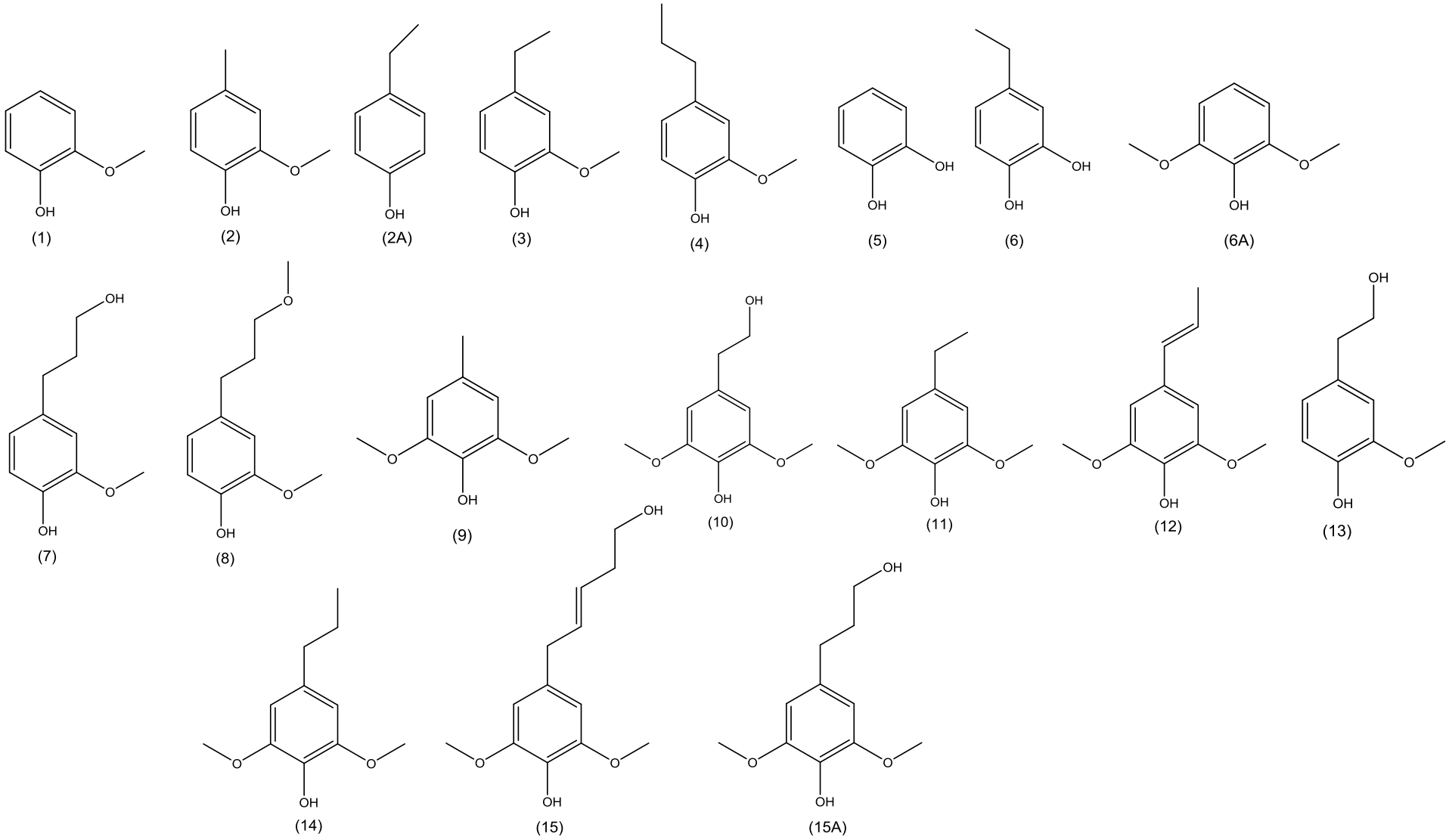

Figure 18 Identified molecules from GC-MS from Kraft, sugar-cane and parr-lignin depolymerisation

3.4.9 Gel permeation chromatography

The Gel Permeation Chromatography (GPC) is a technique commonly used to obtain the molecular weight distribution (Mw), molecular number (Mn) and polydispersity of lignin. The GPC analyses were performed according to the method developed by Dr Bouxin and Dr McVeigh (2016) at The University of Glasgow. Typically, 0.5 mL of pyridine and 0.5 mL of acetic anhydride (Sigma Aldrich, purity 99 %) were mixed with 0.5 g of lignin and left overnight, followed by removal of solvent under N_2. The final acetylated material was solubilised in 2 mL of tetrahydrofuran, THF (Fisher scientific, purity 99.9 %), to be ready for analyses. In order to compare the catalytic products with the initial lignin, the same volume of Fraction 1 (1 mL) and Fraction 2 (1 mL) were mixed and underwent the same procedure. The calibration was carried out by Dr Bouxin, and resulted in a line equation of $y = -0.031x^3 + 1.2581x^2 - 17.264x + 83.146$. Polystyrene standards were used and ranged from 474 to 28 000 $gmol^{-1}$ [26]. The GPC analyses was carried out on a Gilson pump system equipped with a UV detector (280nm). The columns PS/DVB (5 m, 300 x 7.5 nm, 50 and 500 Å, Polymer Lab) set at 303 K was used with an injection volume of 100 µL and THF as eluent (flow rate of 1 mL min^{-1}). The data produced was collected and analysed using the software ChromPerfect.

4 Catalyst characterisation

4.1 Pre-reaction catalyst characterisation

4.1.1 Atomic absorption spectroscopy (AAS) analysis

AAS analysis confirmed the deposition of the metals into the support. The content loaded of each metal is presented in Table 6.

Table 6 AAS analysis of pre-reaction catalysts

Catalyst	Metal loading (%)
Ni/Al_2O_3	4.7
Fe/Al_2O_3	4.5
Fe/C	5.4
Ni/ZrO_2	5.7
Fe/ZrO_2	4.3

4.1.2 BET analysis

BET surface areas, total pore volumes and average pore diameters of the pre-reaction catalysts are summarised in Table 7. According to this data, the surface areas of catalysts were related to the type of support used and increased as follows: carbon > alumina > zirconia catalysts.

Table 7 BET surface areas, total pore volumes and average pore diameters of the pre-reaction catalysts

Catalyst	S_{BET} (m^2/g)	V_p(cm^3/g)	D_p(Å)
Al_2O_3	104	0.5	116
Pt/Al_2O_3	124	0.6	146
Rh/Al_2O_3	102	0.5	145
Ni/Al_2O_3	106	0.5	126
Fe/Al_2O_3	90	0.4	145
Carbon	725	0.6	500
Ni/C	765	0.7	285
Fe/C	444	0.4	255
ZrO_2	2.6	0.07	19
Ni/ZrO_2	3.2	0.01	16
Fe/ZrO_2	5.0	0.02	15

Alumina catalysts presented in Table 7 showed the type IV isotherms with a characteristic hysteresis loop, as shown in the figures below.

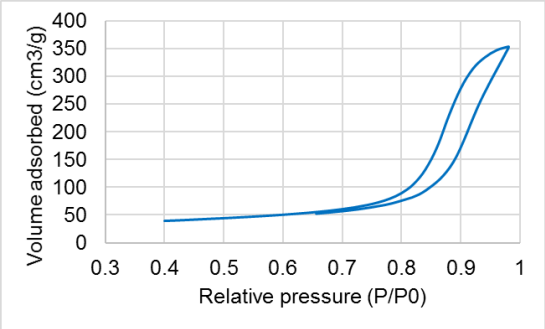

Figure 19 Nitrogen adsorption isotherm at 78 K for the Al_2O_3 support

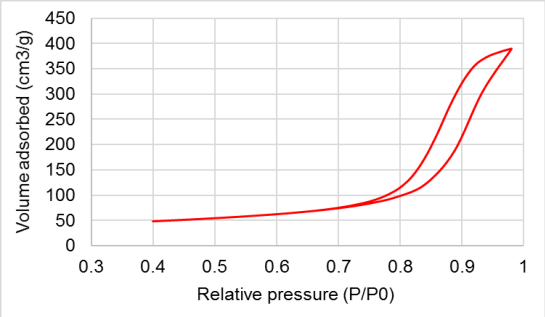

Figure 20 Nitrogen adsorption isotherm at 78 K for the Pt/Al_2O_3 catalyst

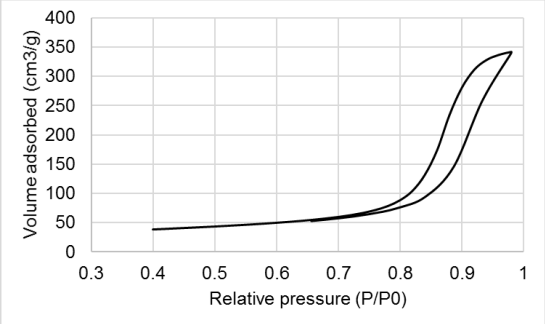

Figure 21 Nitrogen adsorption isotherm at 78 K for the Rh/Al_2O_3 catalyst

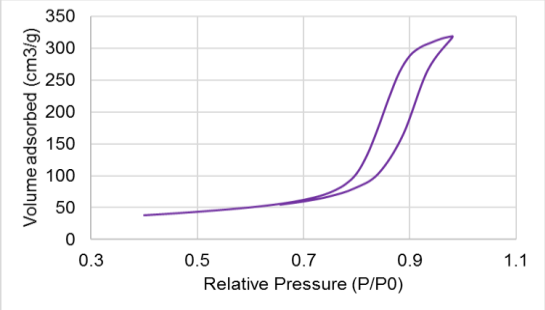

Figure 22 Nitrogen adsorption isotherm at 78 K for the Ni/Al_2O_3 catalyst

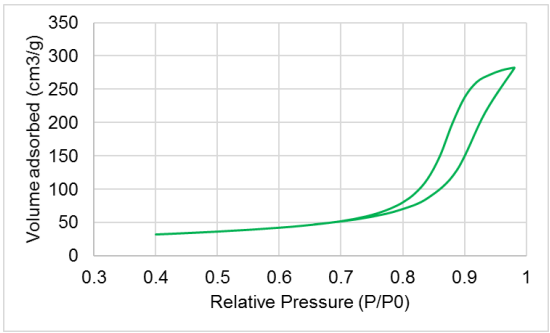

Figure 23 Nitrogen adsorption isotherm at 78 K for the Fe/Al_2O_3 catalyst

The zirconia and carbon supports and the catalysts presented isotherms which were similar to type IV, also with hysteresis loop, as shown in the Figure 24, Figure 25 and Figure 26.

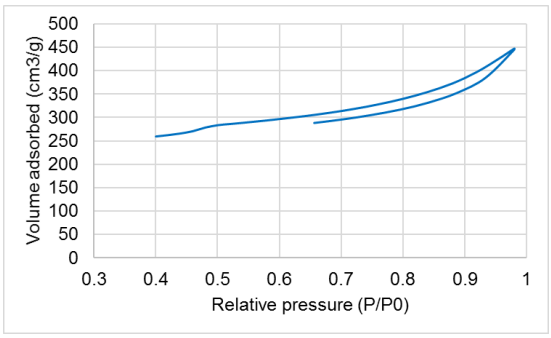

Figure 24 Nitrogen adsorption isotherm at 78 K for the Carbon support

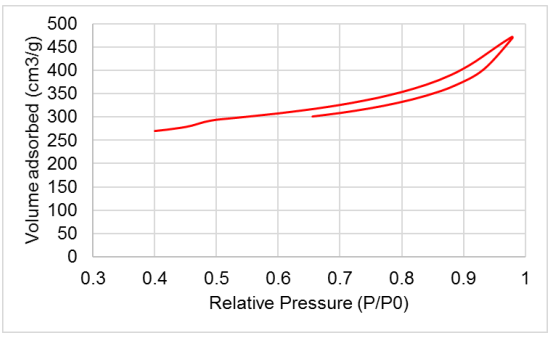

Figure 25 Nitrogen adsorption isotherm at 78 K for the Ni/C catalyst

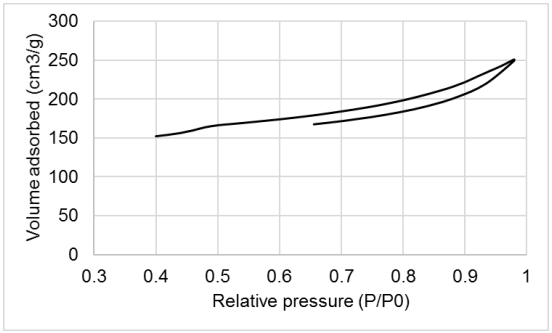

Figure 26 Nitrogen adsorption isotherm at 78 K for the Fe/C catalyst

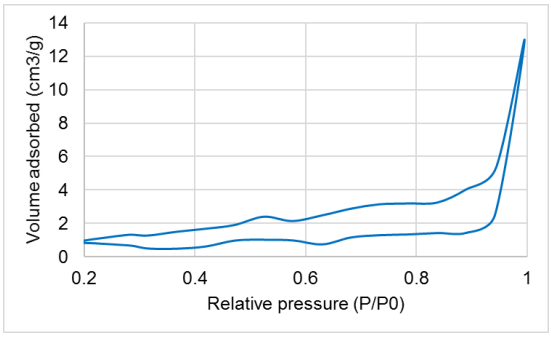

Figure 27 Nitrogen adsorption isotherm at 78 K for the ZrO_2 support

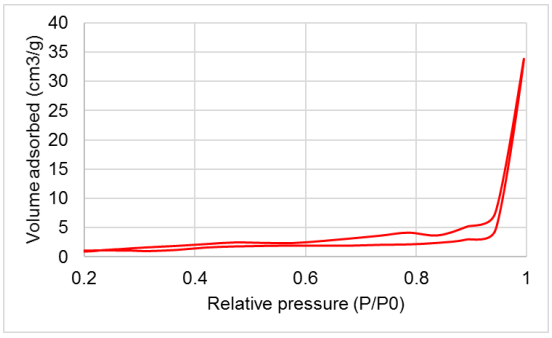

Figure 28 Nitrogen adsorption isotherm at 78 K for the Ni/ZrO_2 catalyst

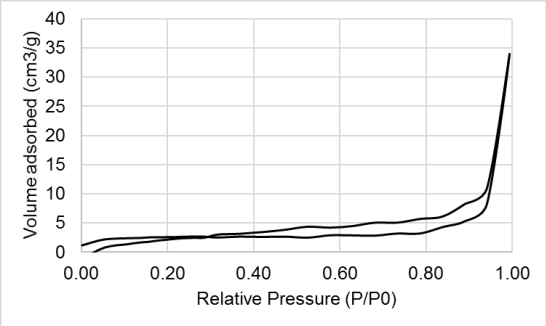

Figure 29 Nitrogen adsorption isotherm at 78 K for the Fe/ZrO_2 catalyst

4.1.3 XRD analysis

As previously reported [26][1][2] in the XRD of Rh/Al_2O_3 (Figure 30), the metal was not detected and the support was generally composed by theta and delta phases of alumina, while in Pt/Al_2O_3 (Figure 31), the alumina was mostly composed by theta alumina and due to low platinum load it was not detected.

For the alumina catalysts prepared in house, it was found through XRD analysis that the support was mostly composed by theta and delta alumina in agreement with JCPDS (reference 01-079-1559 and 00-046-1131). The XRD patterns are showed in Figure 32. The presence of metals could not be detected, only the support pattern.

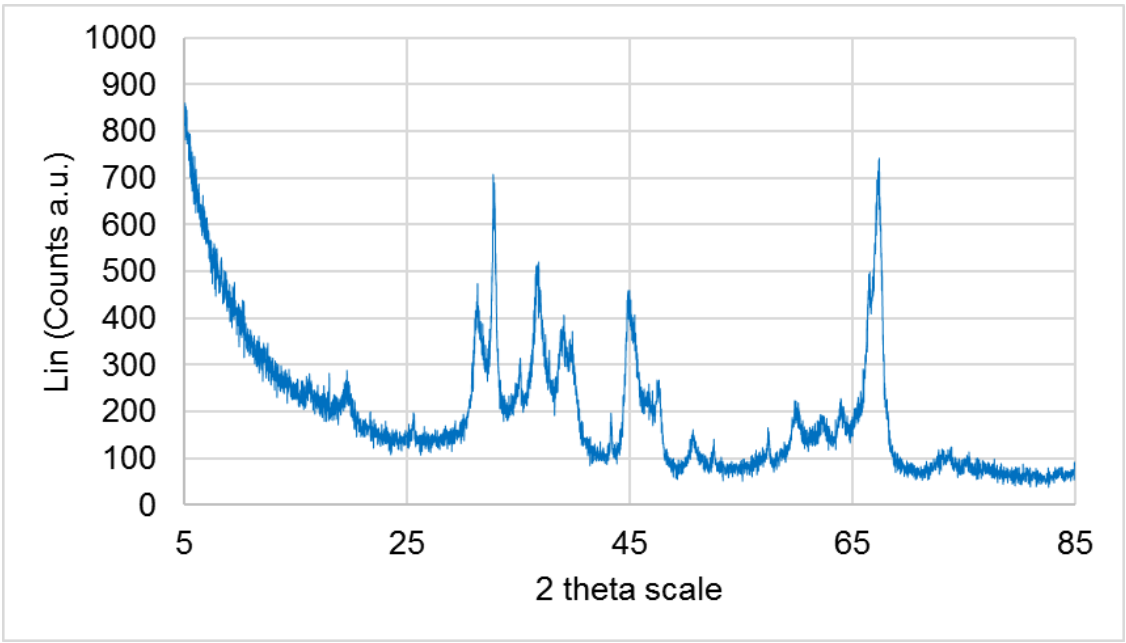

Figure 30 XRD pattern of pre-reaction Rh/Al_2O_3 catalyst

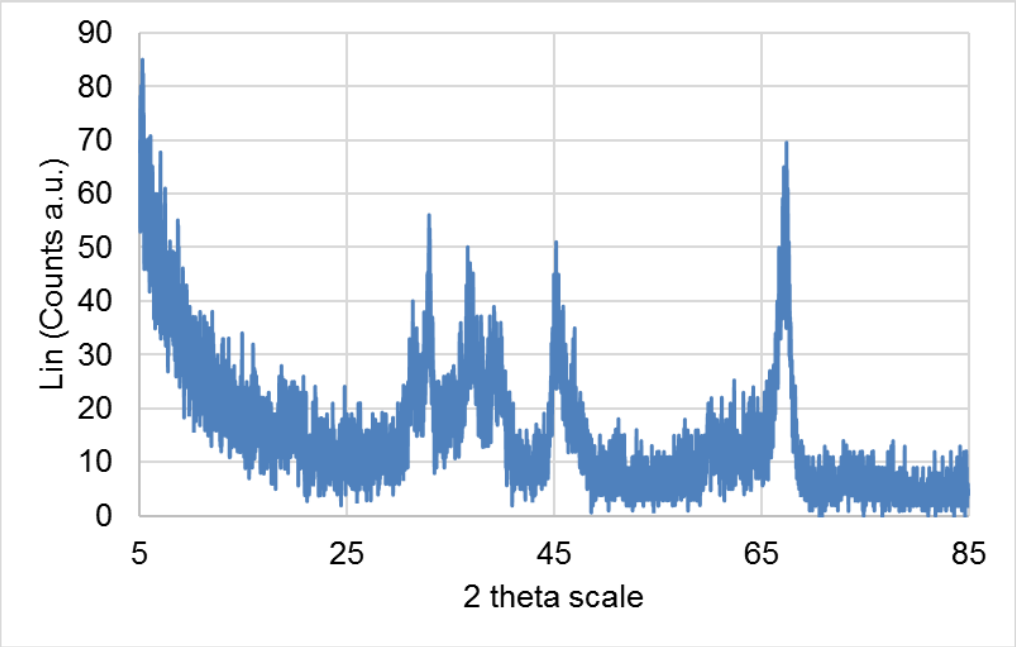

Figure 31 XRD pattern of pre-reaction Pt/Al_2O_3 catalyst

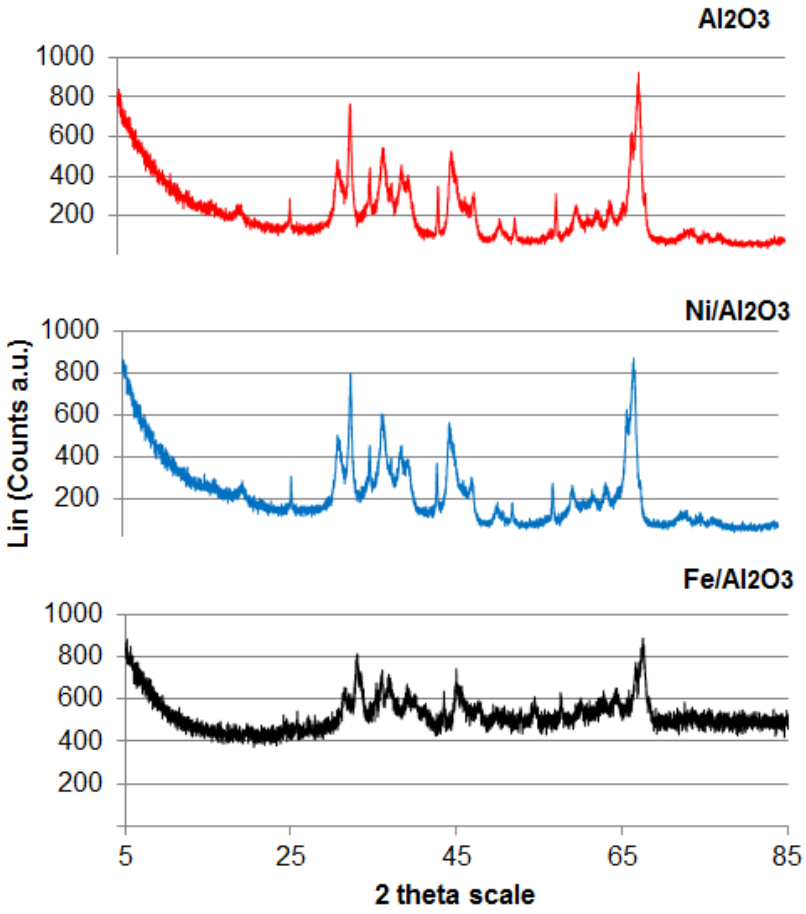

Figure 32 XRD patterns of pre-reaction Al_2O_3 support, Ni/Al_2O_3 and Fe/Al_2O_3 catalysts

The XRD pattern for ZrO_2 presented in Figure 33 showed the pattern of monoclinic ZrO_2, which is in agreement with the 01-074-0815 reference from the JCPDS. The metal oxides were not detected due to low metal loading and the possibility of peaks from the oxides overlapping with the alumina (two main peaks for NiO should appear at 37.2º and 43.5º, JCPDS reference number 01-071-6719; for Fe_3O_4 at 35º and 62.5º, JCPDS reference number 74-0748 and for Fe_2O_3 at 35º and 44.5º, JCPDS reference number 39-1346).

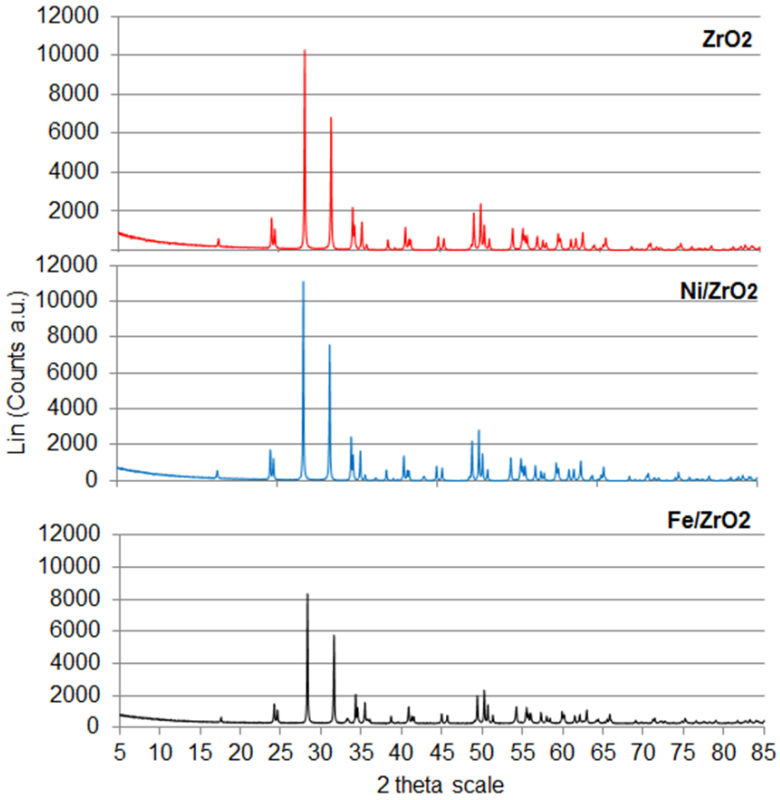

Figure 33 XRD patterns of pre-reaction ZrO_2 support, Ni/ZrO_2 and Fe/ZrO_2 catalysts

XRD patterns for carbon based catalysts presented in Figure 34 showed the reflection planes of a mixture of amorphous carbon and graphite (JCPDS reference number 01-071-3739). Ni/C showed a slightly different pattern than the support (Figure 35). According to the NiO pattern presented in the same Figure (JCPDS reference number 01-071-6719), these peaks could correspond to NiO species as there were peaks with low intensities in the same region. Additional peaks at 20.7º, 33.3º, 60.2º and 68.1º were found, however, it was not possible to specify to which species they were related to. In the case of Fe/C (Figure 36), the process of calcination affected carbon morphology, the XRD pattern became highly noisy and peaks difficult to distinguish. Hence, no evidence of iron oxide species could be detected, due to the noisy pattern and low metal loading.

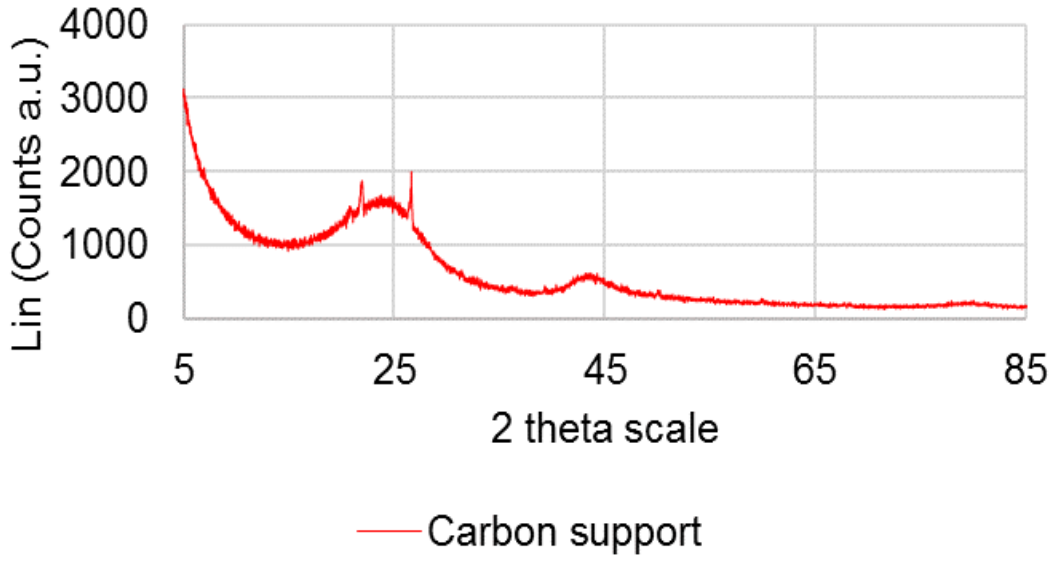

Figure 34 XRD pattern of pre-reaction carbon support

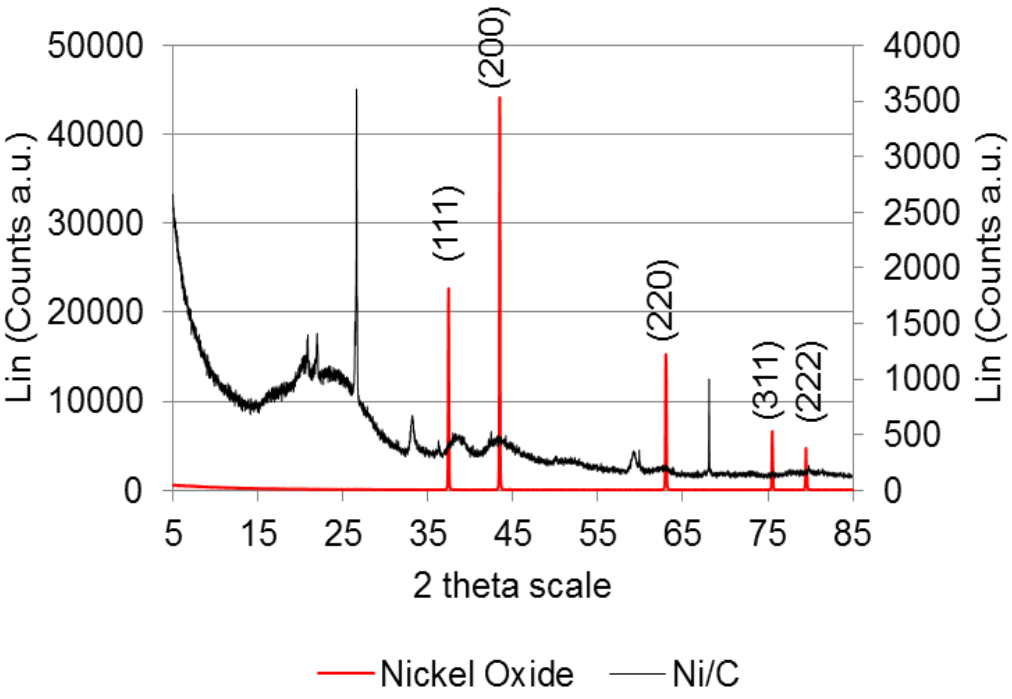

Figure 35 XRD pattern of pre-reaction Ni/C catalyst

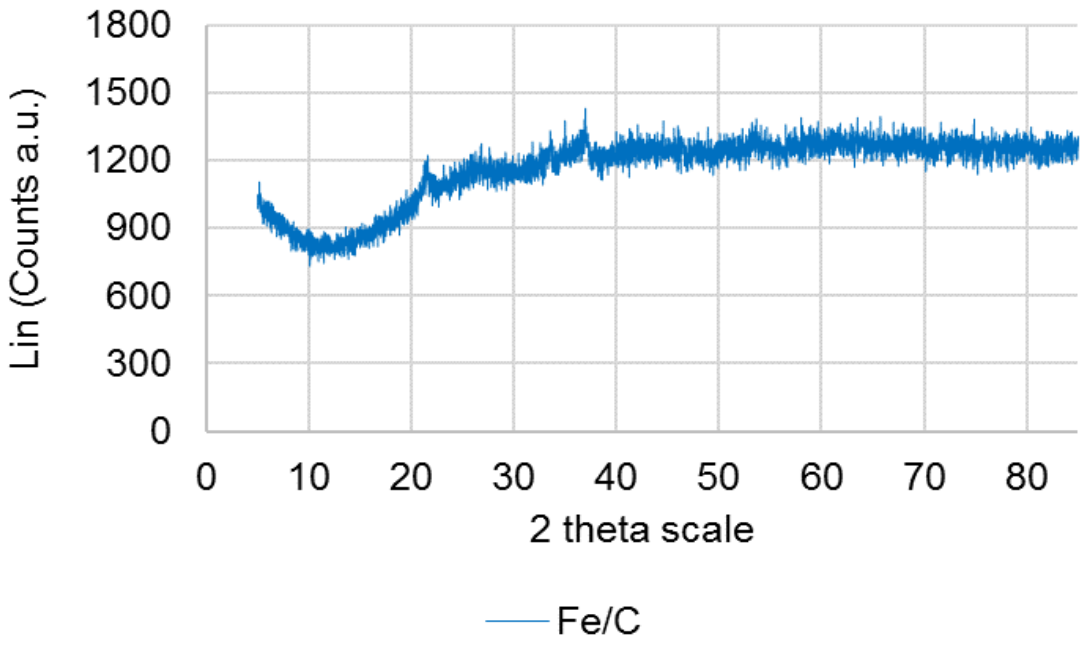

Figure 36 XRD pattern of pre-reaction Fe/C catalyst

4.1.4 Thermogravimetric analysis (TGA)

Ni/Al_2O_3, Fe/Al_2O_3, Ni/ZrO_2 and Fe/ZrO_2 catalysts were prepared in house, as described in Section 3.2, followed by the thermal activation processes of calcination (temperature programmed oxidation, TPO) and reduction (temperature programmed reduction, TPR). The main goal of these analyses was to find the temperatures necessary for the decomposition of metal precursors on the support leading to metal oxides, followed by reduction temperatures.

As previously reported [26] the reduction temperatures for Pt/Al_2O_3 and Rh/Al_2O_3 catalysts were 523 and 573 K, respectively. Ni/C catalyst was used without previous treatment.

4.1.5 Temperature programmed oxidation (TPO)

4.1.5.1 Ni/Al_2O_3 and Ni/ZrO_2 catalysts

Figure 37 presents the TPO plot for Ni/ZrO_2 catalyst. Nickel (II) nitrate hexahydrate reagent was used as precursor. There are two main regions of weight loss. In total, the weight loss corresponded to ~ 9 % of total sample's weight. There was an initial peak at ~370 K related to the evolution of water, followed by a main peak ~ 540 K and small peak at ~ 580 K. These last peaks matched NO and NO_2 ion current as displayed in Figure 38 and Figure 39. In terms of the decomposition of the nickel precursor, the amount of sample that should be lost to allow the formation of NiO was calculated as described in Table 8. This value should be

~ 9 % of total mass. The TPO presented a loss of ~ 9 % of total weight of the sample as shown in Figure 37. Signifying that the precursor was decomposed between 300 K and 680 K. According to the graph, from ~ 700 K there was no more weight loss, hence, calcination temperature defined for this catalyst was 700 K.

Table 8 Calculation of the decomposition of $Ni(NO_3)_2$ and NiO formation

After impregnation, water was evaporated from the catalyst (details in Experimental Section 3.2.1). Subsequently, for the TPO analysis, it was assumed the decomposition of $Ni(NO_3)_2$ not hydrated and the formation of NiO.

Loading of Ni metal into 100 g of support was 5.7 % (value obtained by AAS analysis, Section 4.1.1) or 5.7 g.

For $Ni(NO_3)_2$:

5.7 g of Ni corresponded to 0.09 mol of Ni, stoichiometrically equivalent to 0.18 mol of NO_3 or 11.16 g of NO_3. Hence, $Ni(NO_3)_2$ total mass: 16.86 g.

For NiO:

5.7 g of Ni corresponded to 0.09 mol of Ni, stoichiometrically equivalent to 0.09 mol of oxygen or 1.44 g of oxygen. Hence, NiO total mass: 7.14 g.

The difference in mass for this decomposition should be:

16.86 g - 7.14 g = 9.72 g.

Highlighting that 9. 72 g corresponded to 100 g of the sample, however, it was loaded into the TGA equipment 30.6 mg of catalyst sample. Adjusting the mass for mg and the amount loaded:

$$\frac{9.72 \times 10^3 \text{ mg} \times 30.6 \text{ mg}}{100 \times 10^3 \text{ mg}} = 2.9 \text{ mg or 9 \% of total sample.}$$

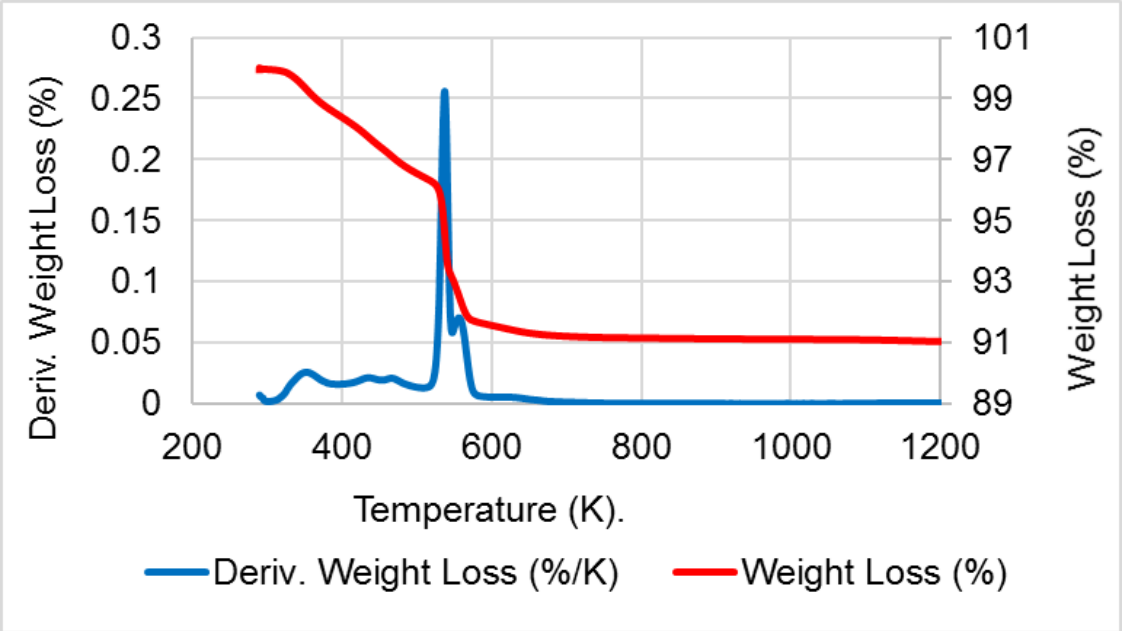

Figure 37 TPO analysis of pre-reaction Ni/ZrO_2 catalyst

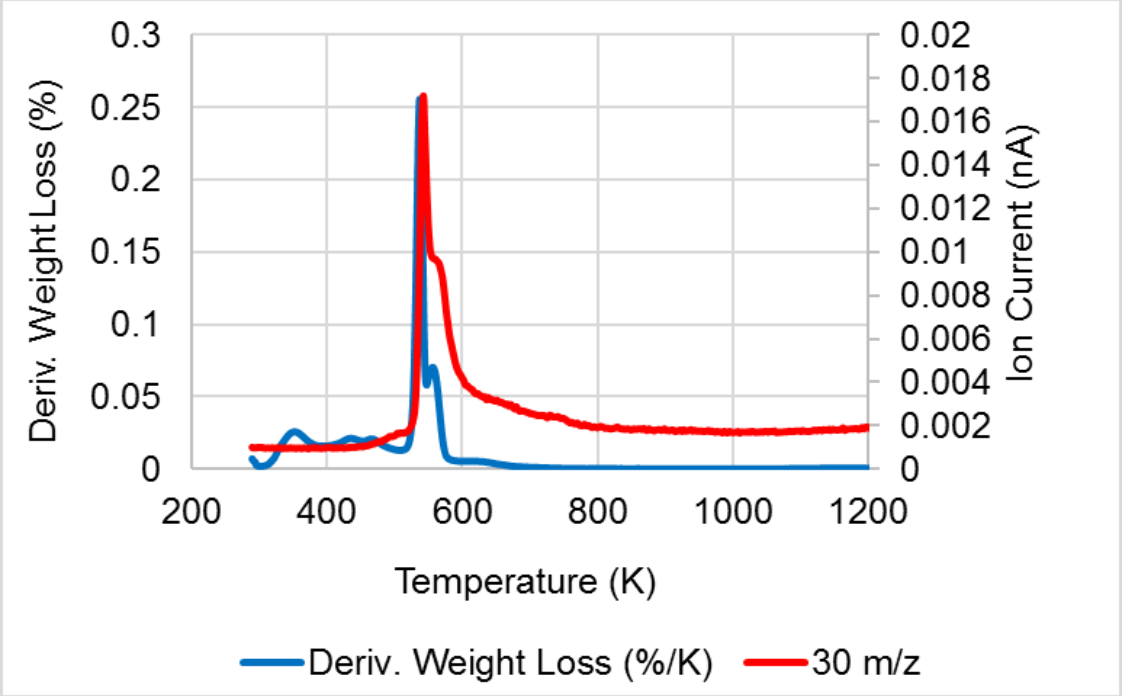

Figure 38 Derivative weight loss and NO m/z 30 evolution of pre-reaction Ni/ZrO_2 catalyst

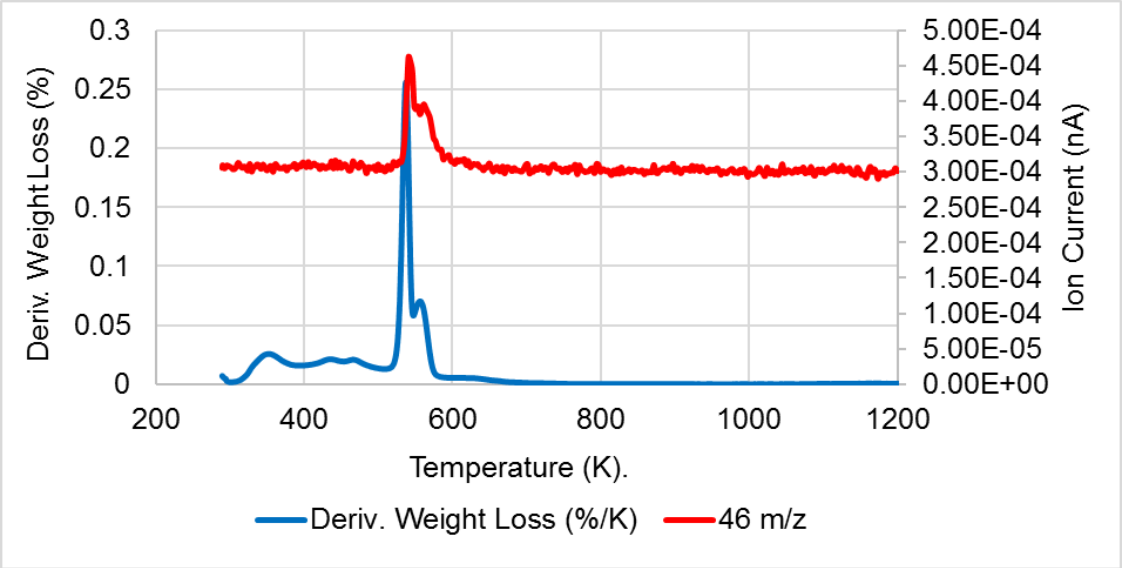

Figure 39 Derivative weight loss and NO_2 m/z 30 evolution of pre-reaction Ni/ZrO_2 catalyst

As described in Section 3.2.1, in the preparation of Ni/Al_2O_3 the basic solution allowed the dissociation of nickel (II) carbonate hydroxide tetrahydrate forming a nickel amine complex. The process also consisted of evaporation of ammonia and water, resulting in the formation of $NiCO_3$. The TPO plot in Figure 40 presents the derivative weight loss and weight loss percentage relative to temperature. In total, the weight loss corresponded to ~ 7.5 % of total sample's weight. The first weight loss of ~ 0.7 % was due to physisorbed water. From 320-500 K was the highest degree of change on the weight loss curve. This corresponded to ~ 3 % of total sample's weight. The following event (from ~ 500 K to ~ 650 K) was related to 2 % of loss. Both events were accompanied by the release of CO_2 as shown in Figure 41. Using the same concept shown in Table 8, in terms of the decomposition of $NiCO_3$, the amount of sample that should be lost to allow the formation of NiO should be 0.73 mg (as 4.7 % of nickel was loaded into the support, corresponding to 0.08 mol of Ni, stoichiometrically equivalent to 0.08 mol of CO_3). Hence, this transformation from $NiCO_3$ to NiO should mean a loss in 0.7 mg of sample or ~ 3 % of total mass (20.8 mg). The additional loss in mass may be associated to traces of ammonia (which could desorb as N_2O giving a m/z of 44) and water. According to the graph, from ~ 700 K there was no more weight loss, hence, calcination temperature defined for this catalyst was 700 K.

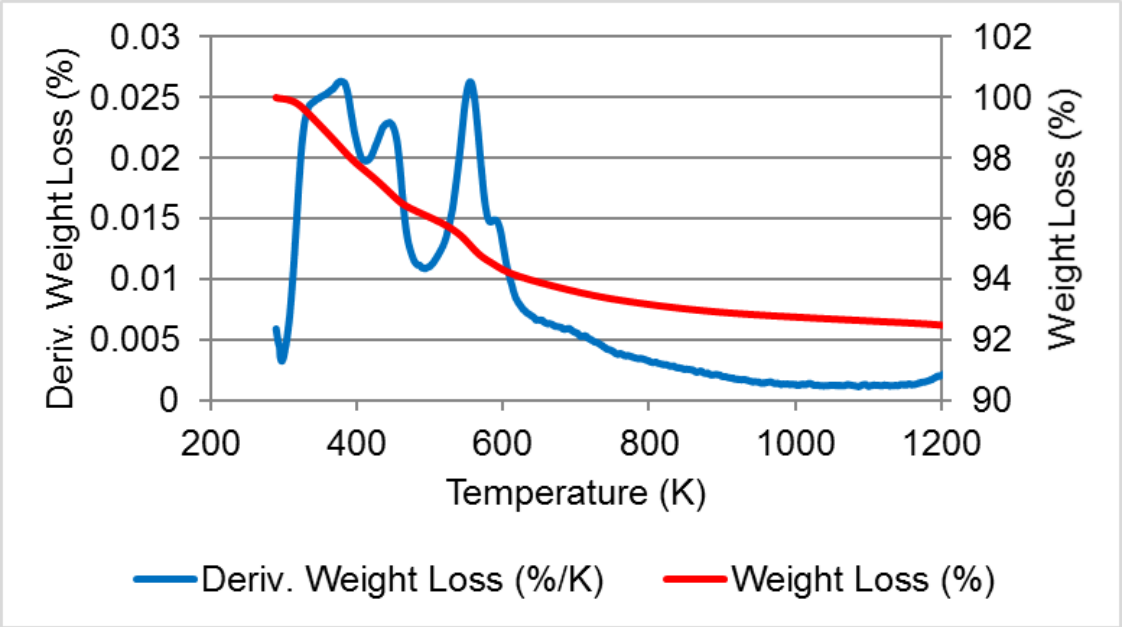

Figure 40 TPO analysis of pre-reaction Ni/Al_2O_3 catalyst

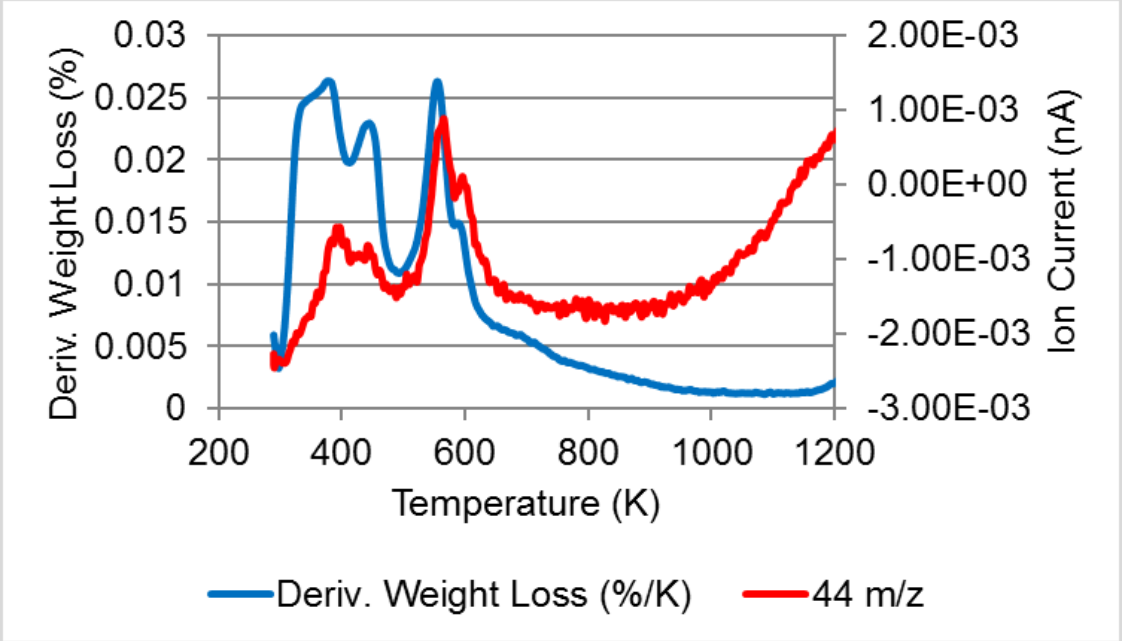

Figure 41 Derivative weight loss and CO_2 m/z 44 evolution of pre-reaction Ni/Al_2O_3 catalyst

4.1.5.2 Fe/Al_2O_3 and Fe/ZrO_2 catalysts

Synthesis of iron catalysts comprised the use of metal nitrate precursors, as described in Section 3.2.1. As expected, the TPO profiles in the next Figures showed the evolution of NO and NO_2 species for these catalysts.

Figure 42 presents the TPO plot for the Fe/Al_2O_3 catalyst. The graph showed one main oxidation area with peak maxima at ~ 400 K and a small peak at ~ 500 K. In total, the weight loss corresponded to 31 % of sample's weight. The peaks matched with NO and NO_2 ion current (Figure 44 and Figure 45). In terms of the decomposition of the iron precursor $Fe(NO_3)_3$, the amount of sample that should be lost to allow the formation of Fe_3O_4 (or $FeO_{4/3}$) and Fe_2O_3 (or $FeO_{1.5}$) should be 1.85 mg (as 4.5 % of iron was loaded into the support, corresponding to 0.08 mol of Fe stoichiometrically equivalent to 0.24 mol of NO_3). Hence, this transformation from $Fe(NO_3)_3$ to generate $FeO_{4/3}$ and $FeO_{1.5}$ should mean a loss in 1.85 mg of sample or ~ 6.8 % of total mass. The TPO presented a loss of ~ 30 % of total weight of the sample (27.1 mg) as shown in Figure 42. This signified that the precursor was decomposed in these temperature range. The additional loss in mass may be associated to water from dehydration of alumina at high temperature. From 700 K there was no more decomposition losses, hence 700 K was the temperature chosen for calcination.

TPO plot for Fe/ZrO_2 catalyst is presented in Figure 46. The graph showed more the one stage of weight loss due to oxidation. In total, the weight loss corresponded to ~ 5 % of total sample's weight. An initial loss at ~320-380 K was related to the evolution of water. In addition, two main peaks at ~500 K and 560 K corresponded to the evolution of NO as shown in Figure 47. In terms of the decomposition of the iron precursor $Fe(NO_3)_3$, the amount of sample that should be lost to allow the formation of Fe_3O_4 (or $FeO_{4/3}$) and Fe_2O_3 (or $FeO_{1.5}$) should be 1.3 mg (as 4.3 % of iron was loaded into the support, corresponding to 0.077 mol of Fe stoichiometrically equivalent to 0.23 mol of NO_3). Hence, this transformation from $Fe(NO_3)_3$ to generate $FeO_{4/3}$ and $FeO_{1.5}$ should mean a loss in 1.3 mg of sample or ~ 6 % of total mass. The TPO presented a loss of ~ 5 % of total weight of the sample (20 mg) between 348 K and 700 K as shown in Figure 46. This signified that the precursor was mostly decomposed in this temperature range. From ~ 700 K there was no more weight loss, hence, the calcination temperature defined for this catalyst was 700 K.

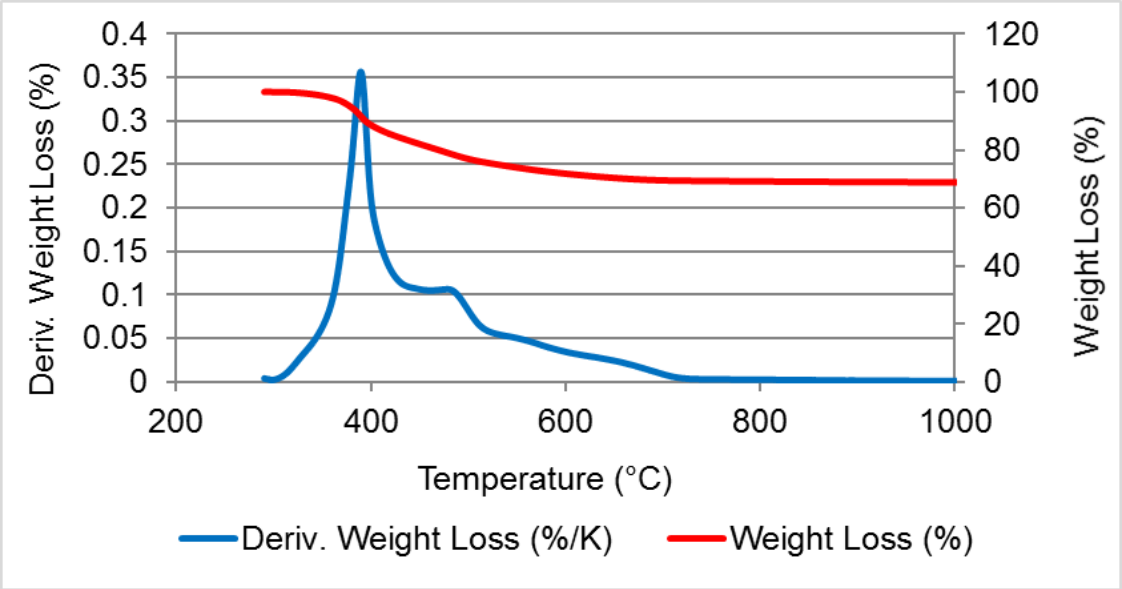

Figure 42 TPO of pre-reaction Fe/Al_2O_3 catalyst

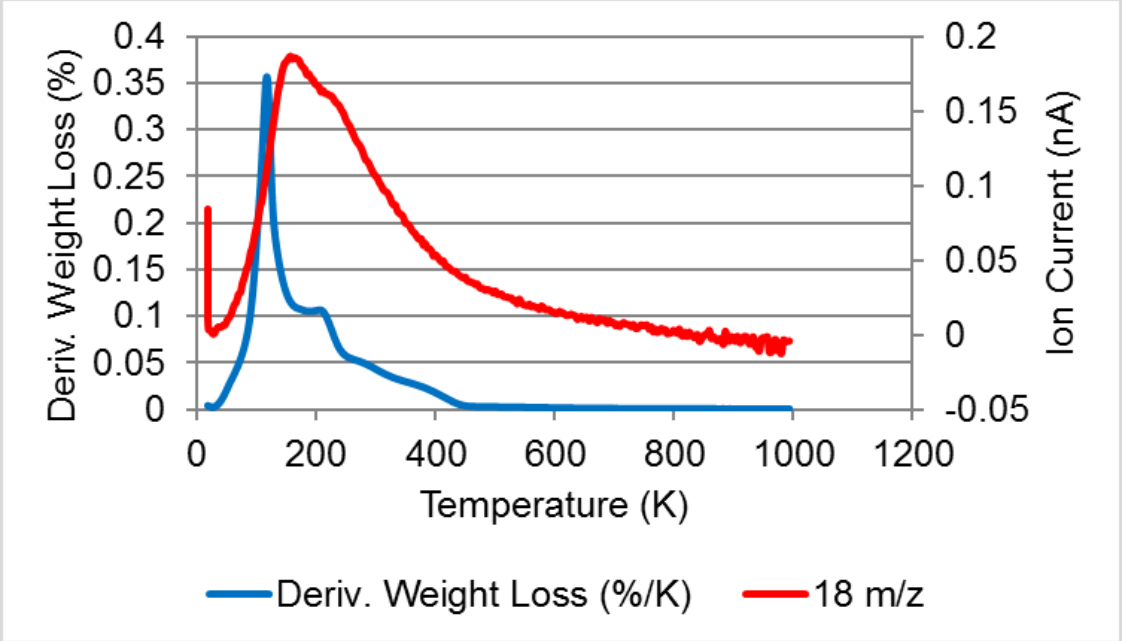

Figure 43 Derivative weight loss and H_2O m/z 18 evolution of pre-reaction Fe/Al_2O_3 catalyst

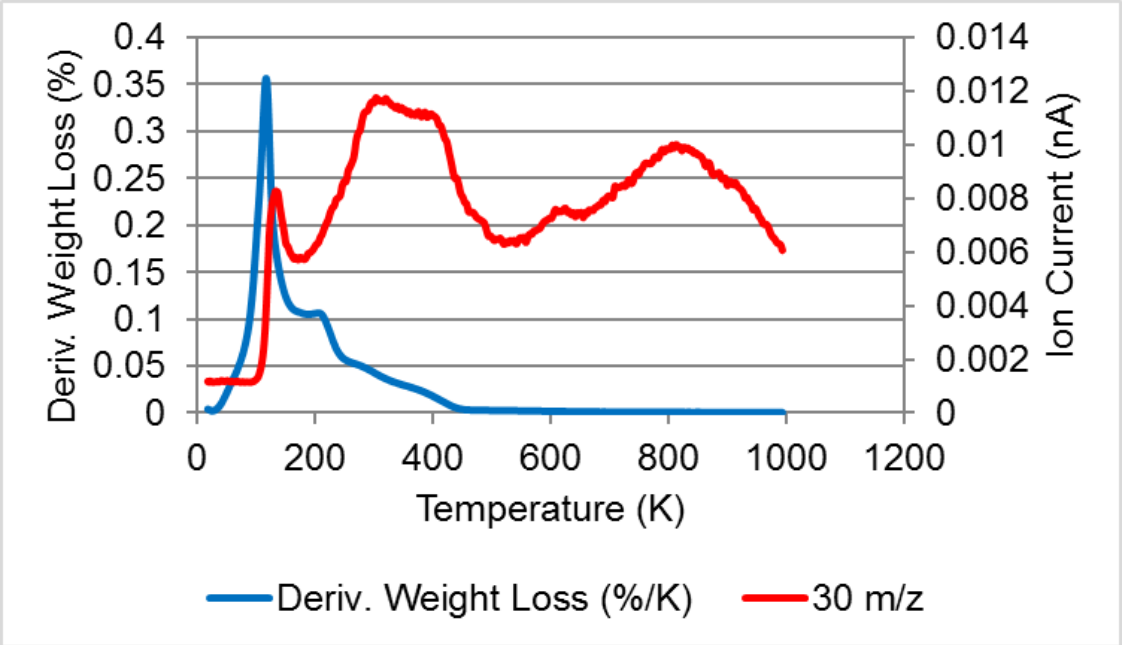

Figure 44 Derivative weight loss and NO m/z 30 evolution of pre-reaction Fe/Al_2O_3 catalyst

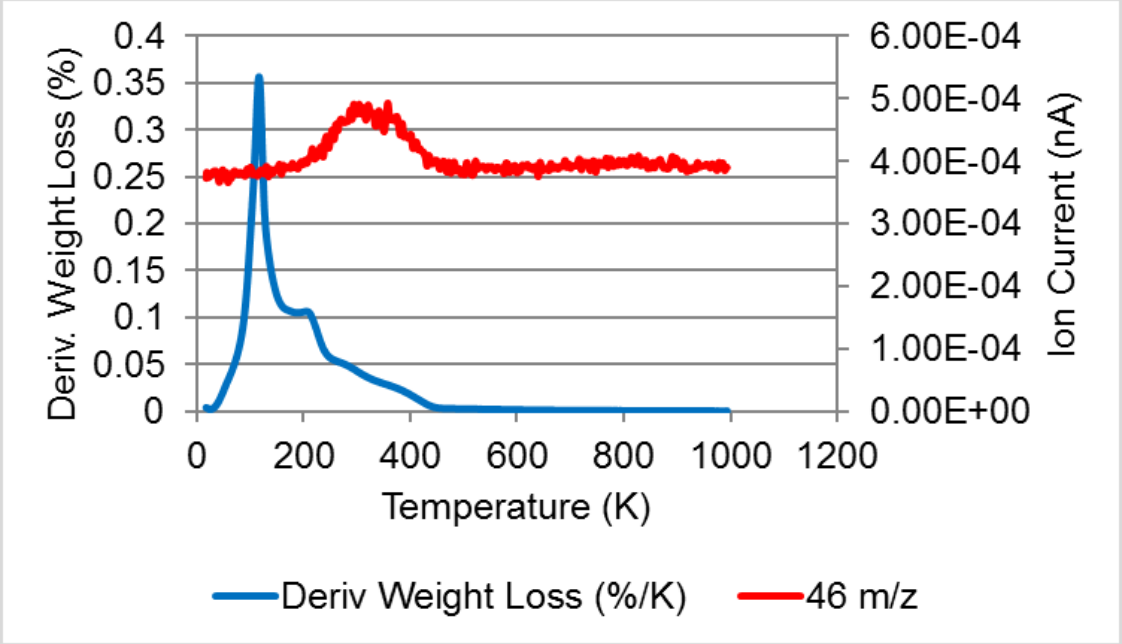

Figure 45 Derivative weight loss and NO_2 m/z 46 evolution of pre-reaction Fe/Al_2O_3 catalyst

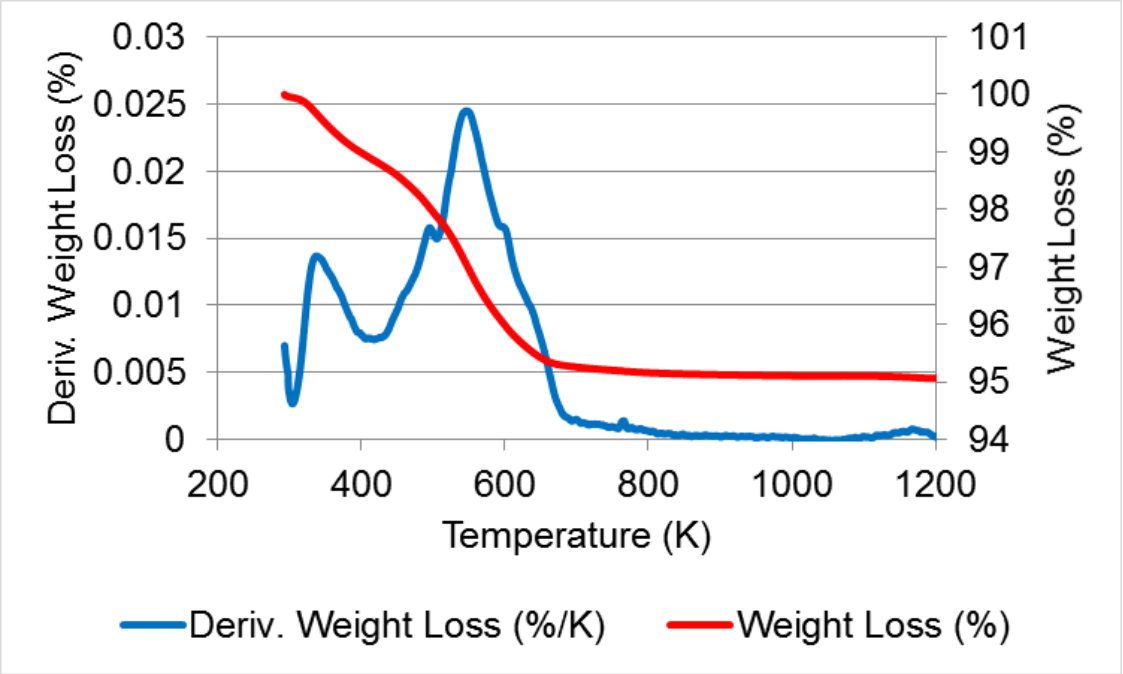

Figure 46 TPO of pre-reaction Fe/ZrO_2 catalyst

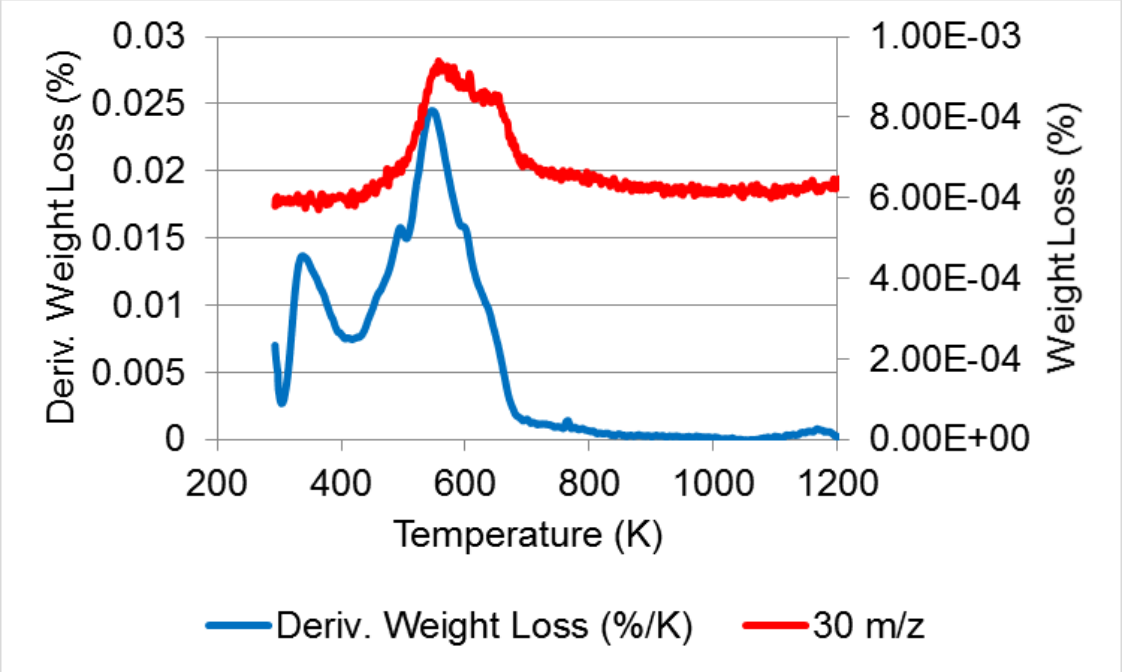

Figure 47 Derivative weight loss and NO m/z 30 evolution of pre-reaction Fe/ZrO_2 catalyst

4.1.5.3 TGA of Fe/C catalyst

This analysis was carried out under argon as described in Section 3.4.2. Figure 48 shows that the precursor decomposes in more than one step mainly within the temperature range ~ 376-541 K. In terms of the weight loss for the decomposition of iron precursor $Fe(NO_3)_3$ that should allow the formation of Fe_3O_4 ($FeO_{4/3}$) and Fe_2O_3 (or $FeO_{1.5}$), it should be ~ 1.2 mg (as 5.4 % of iron was loaded into the support, corresponding to 0.096 mol of Fe stoichiometrically equivalent to 0.29 mol of NO_3). Hence, this transformation from $Fe(NO_3)_3$ to $FeO_{4/3}$ and $FeO_{1.5}$ should mean a loss in 1.2 mg of sample or ~ 8 % of total mass). The TPO presented a total loss of ~ 8 % of total weight of the sample (14.7 mg) as shown in Figure 48. Signifying that the precursor decomposed between 300 K to 800 K. The calcination temperature was defined as 800 K under argon, no further reduction steps were adopted before reaction.

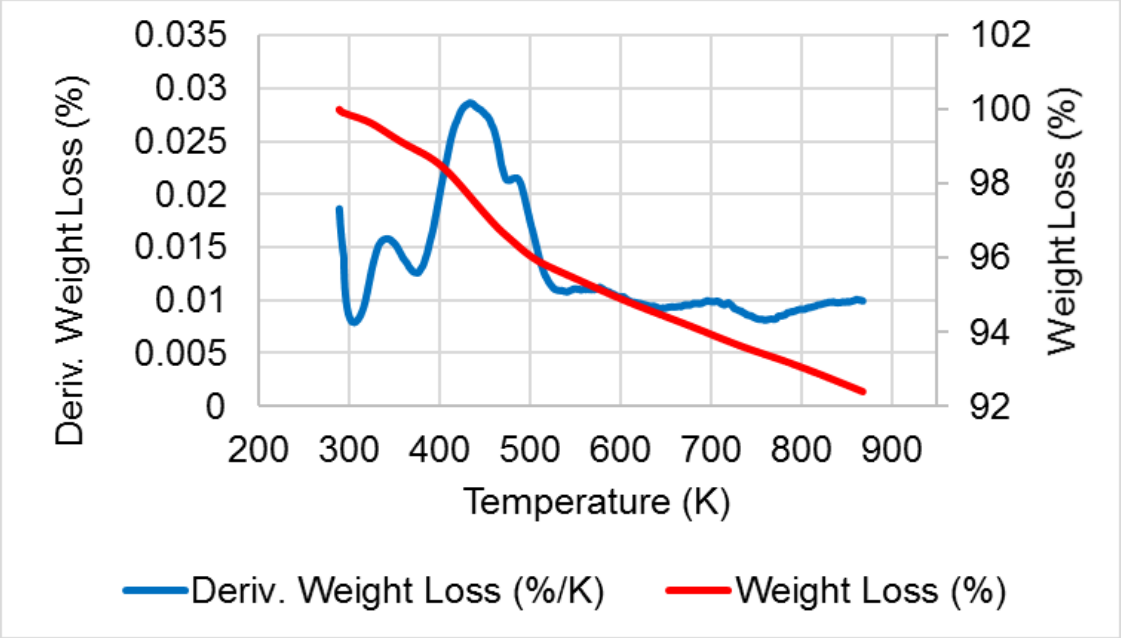

Figure 48 TGA analysis of Fe/C catalyst

4.1.6 Temperature programmed reduction (TPR)

4.1.6.1 Ni/Al_2O_3 and Ni/ZrO_2 catalysts

It was reported that on alumina support, three main nickel-based species can be found [86]–[88], bulk nickel with reduction temperature (RT) ~ 673 K, NiO bonded to the support (RT 673-973 K) and nickel incorporated in the support (RT above 900 K). In addition,

transformation of nickel oxide to spinel forms can be strongly associated to high reduction temperatures[86]–[88].

Figure 49 presents the TPR analysis for the Ni/Al_2O_3 catalyst. There were three weight loss ranges, corresponding in total to 5 % of the total weight. There was a peak at ~ 380 K, followed by another at ~ 800 K with a shoulder located about 1000K. The first peak was related to water while the second reduction peak ~ 800 K was assigned to reduction of nickel oxide. This high temperature can be attributed to strong interactions between NiO and the support, the identified shoulder was also found in the literature for Ni/Al_2O_3 catalysts submitted to the same calcination temperature range used in this work [86]. The temperature of 850 K was assumed for reduction.

For Ni/ZrO_2 catalyst (Figure 50) there was a different TPR profile, presenting only one main peak with maxima at ~ 680 K. This has been attributed to the reduction of metal +2 to zero valent state in accordance with similar systems published in the literature [89]. As no more reduction peaks were found, 800 K was assumed for reduction temperature.

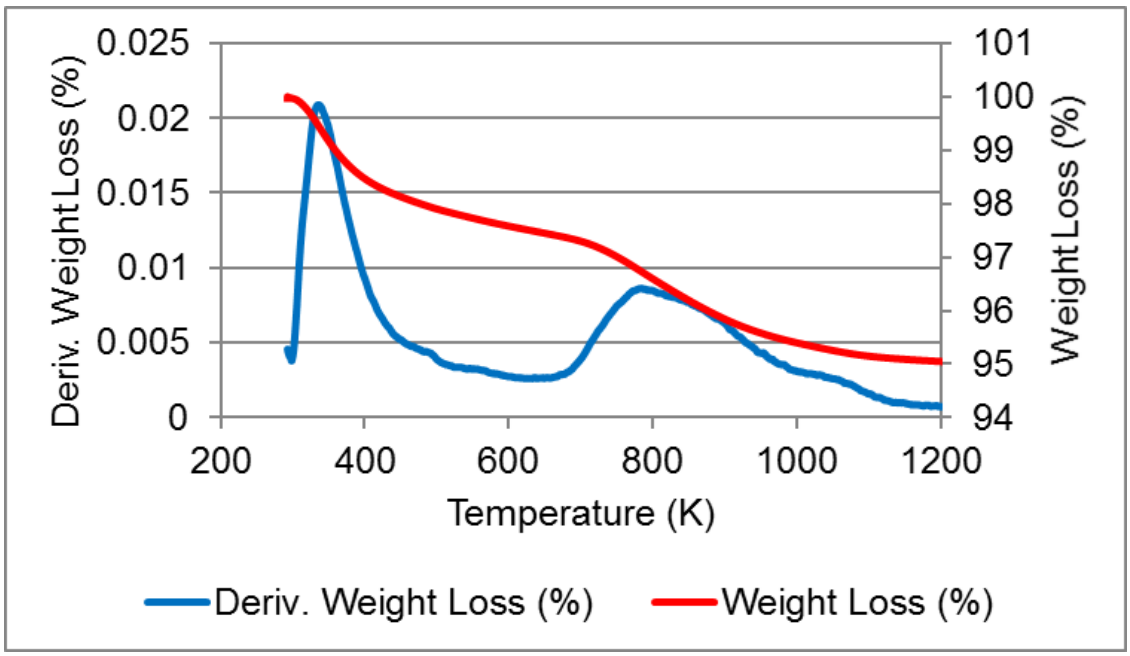

Figure 49 TPR analysis of pre-reaction Ni/Al_2O_3 catalyst

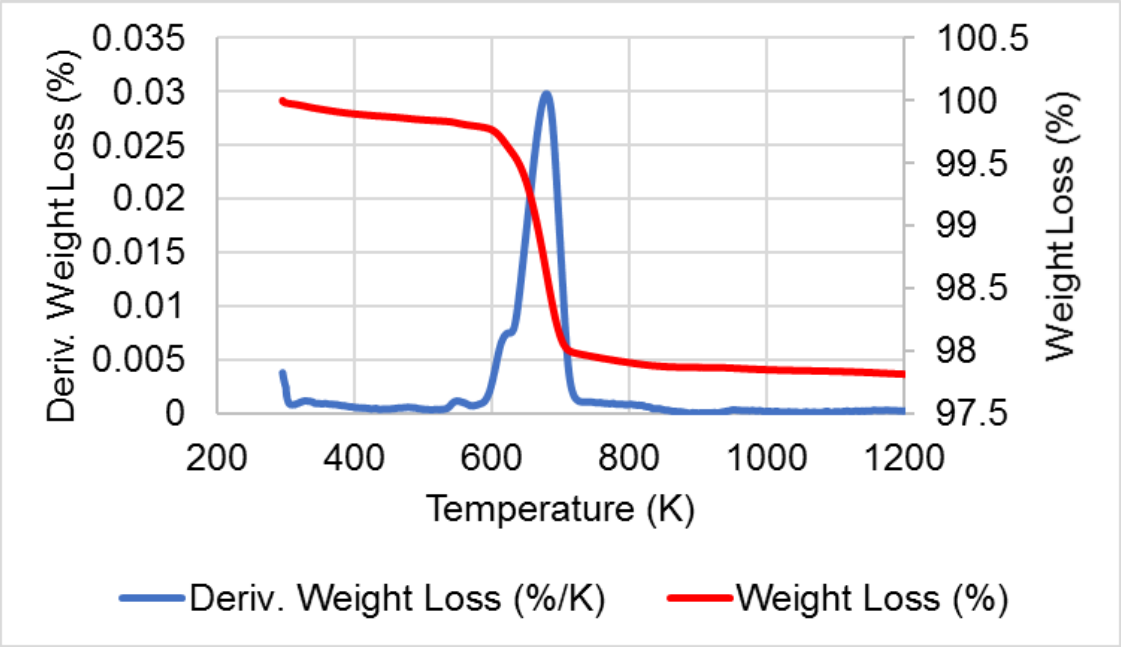

Figure 50 TPR analysis of pre-reaction Ni/ZrO_2 catalyst

4.1.6.2 Fe/Al_2O_3 and Fe/ZrO_2 catalysts

It was reported from combined TPR with *in situ* Mossbauer spectroscopy that iron zirconia catalysts with low metal loading can present mainly two reduction stages involving Fe_2O_3 to FeO and from FeO to metallic iron [90]. In Figure 51, the TPR presented a loss of ~ 4 % of total weight (52 mg). There was a main peak about 510-700 K with maxima at ~ 630 K. This corresponded to the loss of less than 1 % of total weight, which was the first reduction stage. The amount of oxygen that should be lost in this range to reduce Fe_2O_3 ($FeO_{1.5}$) to FeO is 0.2 mg (as 4.3 % of iron was loaded into the support, corresponding to 4 x 10^{-5} mols of Fe, stoichiometrically equivalent to 6 x 10^{-5} mol or 0.96 mg of oxygen atom in $FeO_{1.5}$. Hence, this transformation from $FeO_{1.5}$ to FeO should mean a loss in 0.2 mg of oxygen or 0.3 % of total mass. The reduction of FeO to Fe was found at about 850 K which should be a loss of 0.6 mg of oxygen or 1.2 % of total weight (as 4.3 % of iron was loaded into the support, corresponding to 4 x 10^{-5} mols of Fe, stoichiometrically equivalent to 4 x 10^{-5} mol or 0.6 mg of oxygen atom in FeO. Hence, this transformation from FeO to Fe should mean a loss of 0.6 mg of oxygen or 1.2 % of total mass. This reduction of iron oxides would be a loss of 1.5 % of total sample weight that corresponded to the amount lost on the temperature range assumed for reduction, 850 K.

In regards to Fe/Al_2O_3, Figure 52 shows an initial peak at ~ 380 K followed by two peaks at ~ 580 K and ~700 K, signifying that different oxidation species were also present and the

reduction process was occurring in more than one stage. The weight loss showed a total loss of ~ 6 % (for 21 mg of sample), which 1 % corresponded to the initial loss of water at ~ 380 K. The metal loading and amount of sample (21 mg) analysed is slightly different from the Fe/ZrO_2 catalyst, changing the loss of oxygen mass. Considering a full reduction for the TPR from Fe_2O_3 ($FeO_{1.5}$) to metallic iron should mean a total loss of 0.4 mg of oxygen or ~ 2 % of sample weight (as 4.5 % of iron was loaded into the support, corresponding to 1.68×10^{-5} mols of Fe, stoichiometrically equivalent to 2.5×10^{-5} mol or 0.4 mg of oxygen atom). Hence, from 400-800 K a loss of ~ 3 % was found in the experiment, confirming loss of oxygen and probably the additional mass can be attributed to the hydroxyls on the alumina support, indicating the full reduction of iron oxides. The reduction temperature adopted was 800 K.

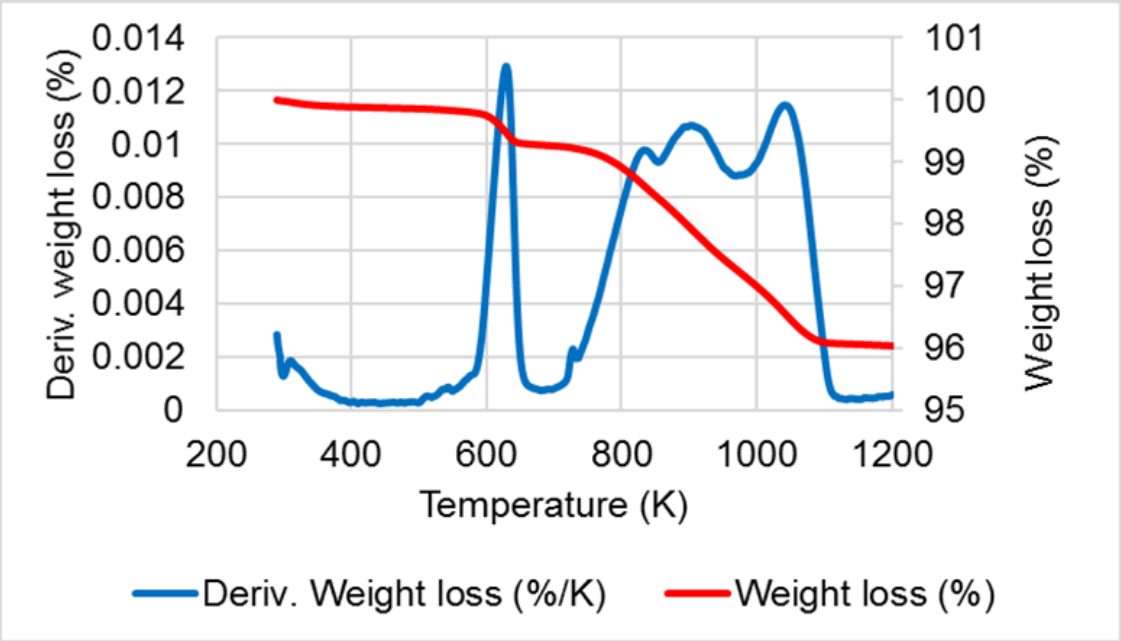

Figure 51 TPR analysis of pre-reaction Fe/ZrO_2 catalyst

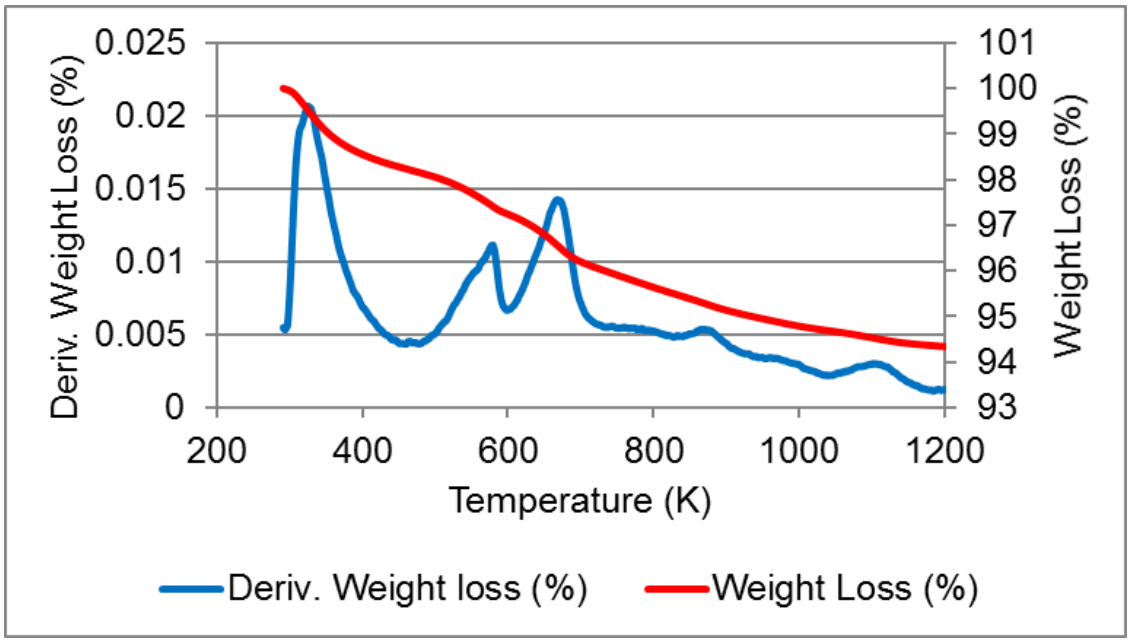

Figure 52 TPR analysis of pre-reaction Fe/Al_2O_3 catalyst

4.2 Post-reaction catalyst evaluation

To analyse the amount and nature of the carbonaceous material deposited on the catalysts, this section describes the TPO-MS, CHN, BET, XRD and Raman analysis of the spent Al_2O_3 support, Pt/Al_2O_3 and Ni/Al_2O_3 catalysts with water, acetone, IPA, deuterium oxide and deuterated acetone mixtures (solvent/water 50:50 v/v) in reactions with Kraft, Parr and sugar-cane lignins. This study could provide information about the changes in the type of coke material when different lignins, catalysts (support, noble metal and non-noble metal) and solvents were used.

4.2.1 TPO analysis

It was found that for all catalysts that the total weight loss of initial catalyst weight was similar, between 15-20 %, which the evolution of CO_2 corresponded to 8-10 % of this total.

The experiments presented that spent catalysts had an initial weight loss of physisorbed water around 250 K-380 K and a main derivative weight loss between ~ 400 K and 800 K. According to the online mass spectrometer, this main peak was related to the evolution of CO_2 as showed in the Figures below. It was not found throughout the TPO-MS data the loss of nitrogen or sulfur-based species, confirming the absence of highly prominent peaks for other masses. Hence, the weight loss found can be mainly associated to the elimination of

carbon, which the plot of carbon dioxide evolution matched the derivative weight profile for all samples.

Despite similarities in the temperature range for the evolution of H_2O and CO_2, all the derivative weight loss profiles were not identical in these experiments. For example, in Figure 55 there is a sharp peak at ~ 800 K while in Figure 61 this peak was very discreet. Figure 69 and Figure 71 showed a slight shoulder ~ 700 K in the plot, while Figure 79 had a prominent knee at about 620 K. Hence, differences were found in the shape of the graphs. This confirmed that depending on the type of metal, solvent and lignin, the carbonaceous material formed in each catalyst was complex and different in its nature. Therefore, different surface species were formed and deposited onto the catalyst.

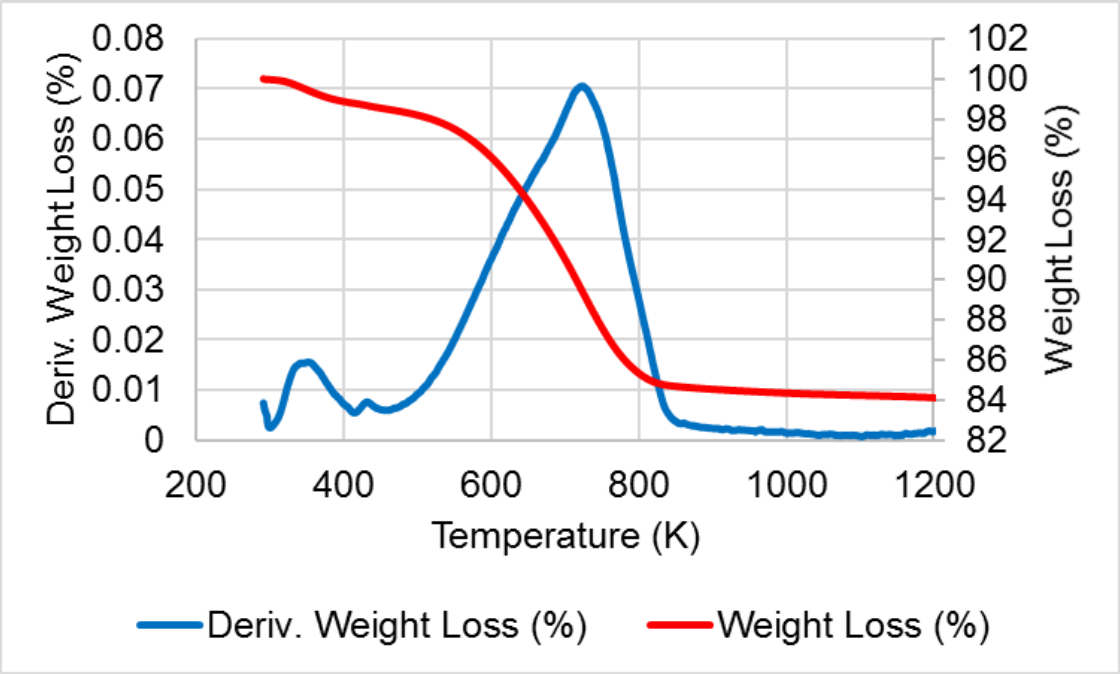

Figure 53 TPO of spent Pt/Al_2O_3 catalyst after $EtOH/H_2O$ reaction with the Kraft lignin

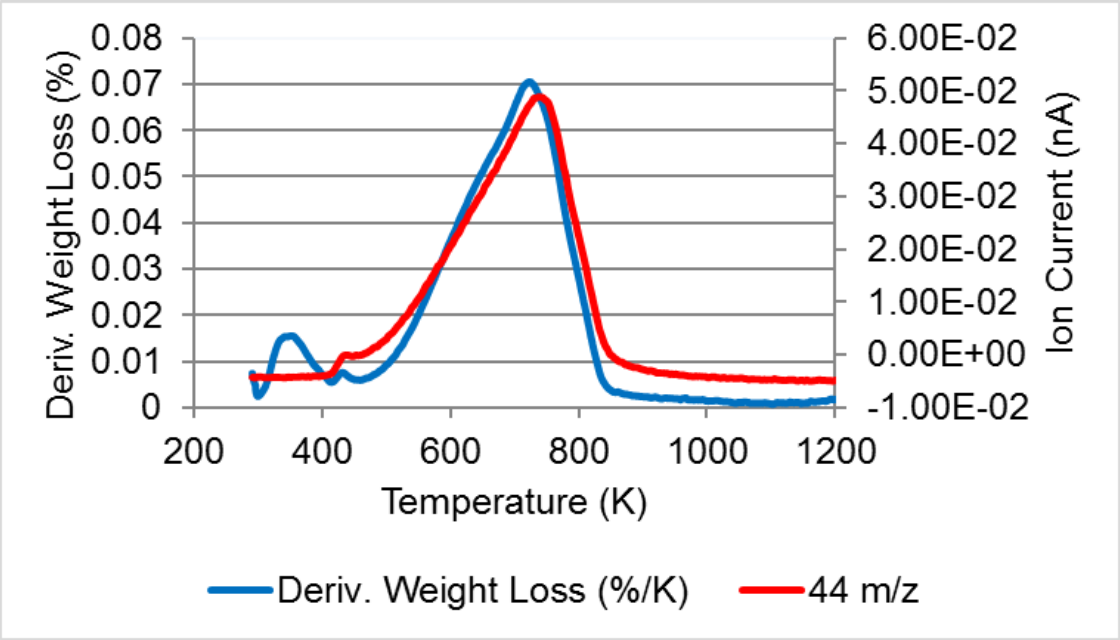

Figure 54 Derivative weight loss and CO_2 m/z 44 evolution of spent Pt/Al_2O_3 catalyst after $EtOH/H_2O$ reaction with the Kraft lignin

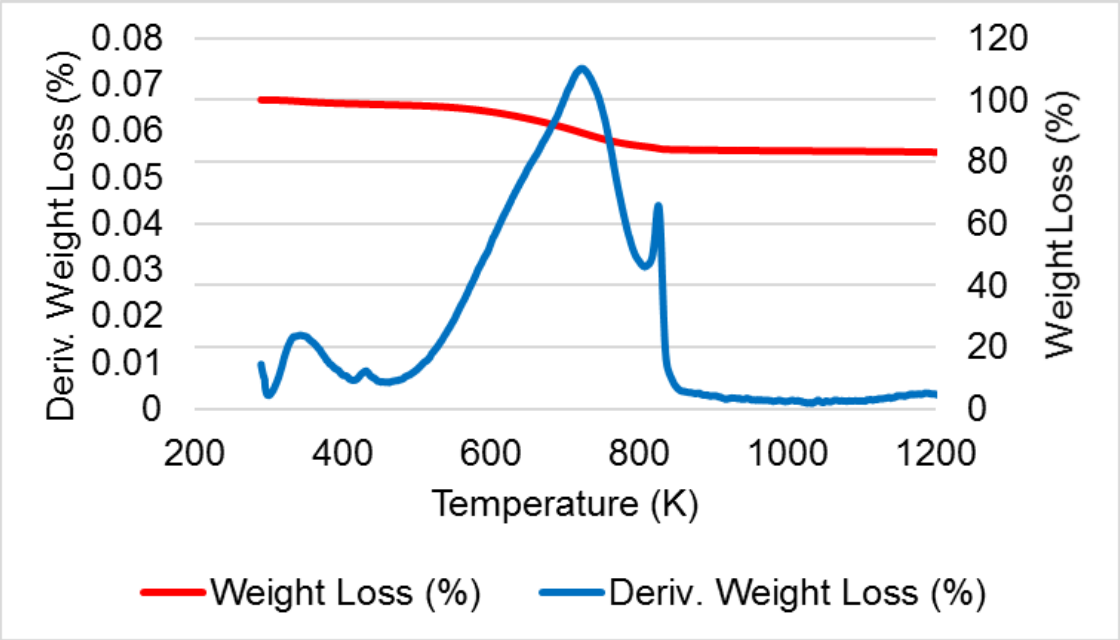

Figure 55 TPO of spent Pt/Al_2O_3 catalyst after acetone/H_2O reaction with the Kraft lignin

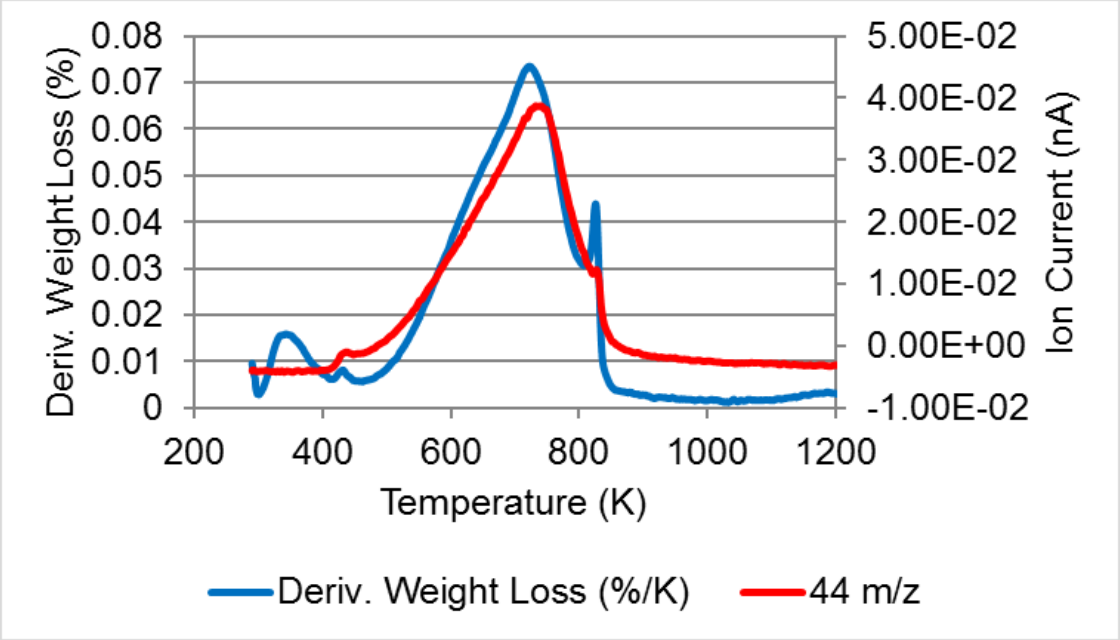

Figure 56 Derivative weight loss and CO_2 m/z 44 evolution of spent Pt/Al_2O_3 catalyst after acetone/H_2O reaction with the Kraft lignin

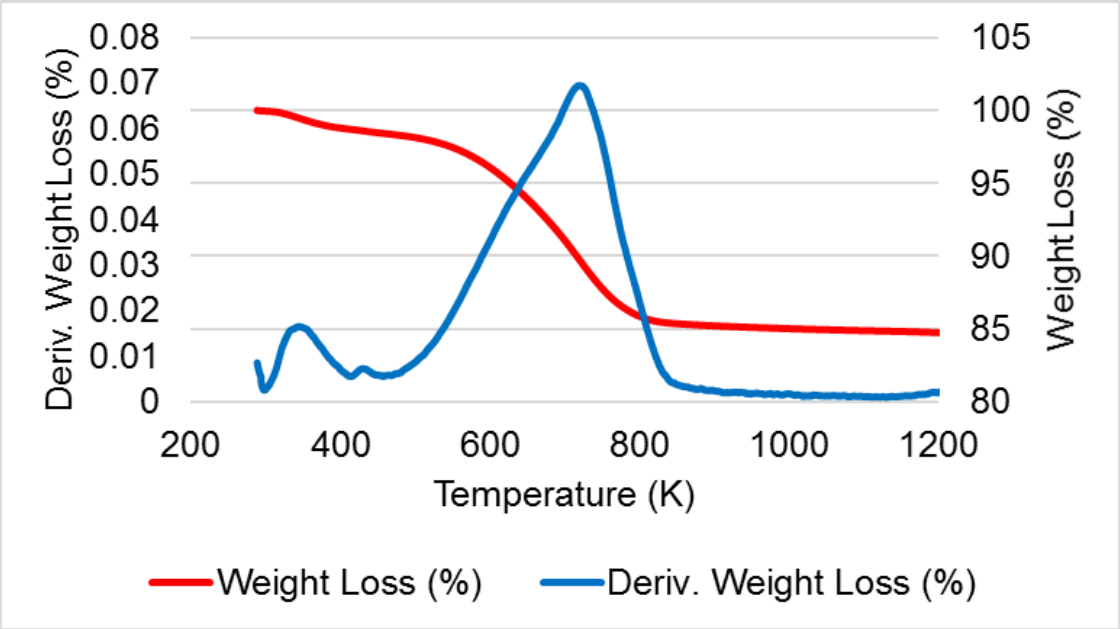

Figure 57 TPO of spent Pt/Al_2O_3 catalyst after IPA/H_2O reaction with the Kraft lignin

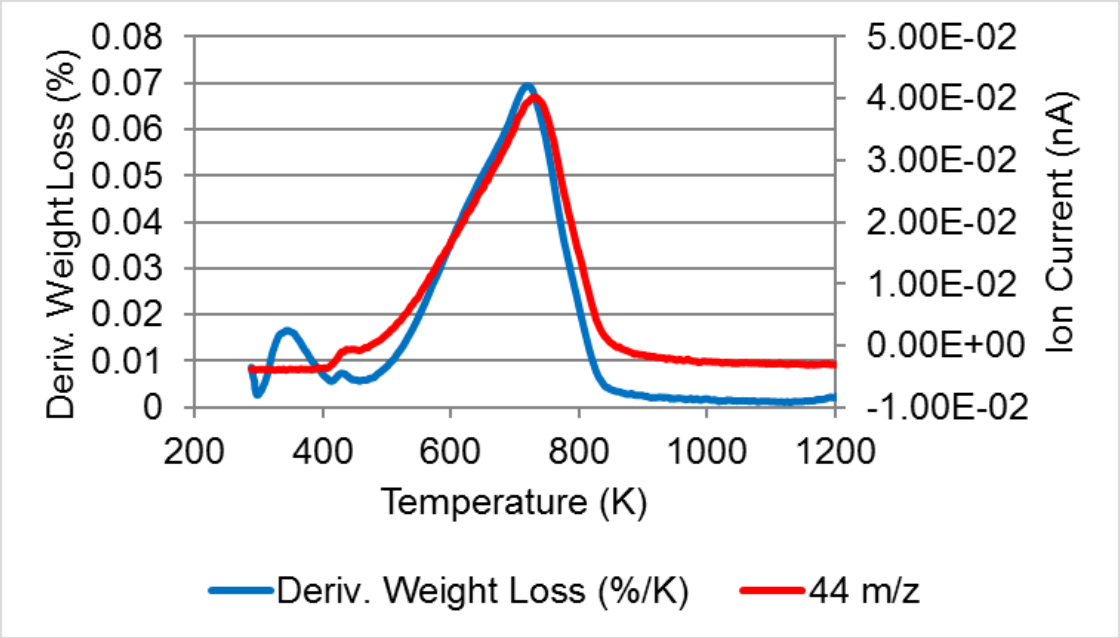

Figure 58 Derivative weight loss and CO_2 m/z 44 evolution of spent Pt/Al_2O_3 catalyst after IPA/H_2O reaction with the Kraft lignin

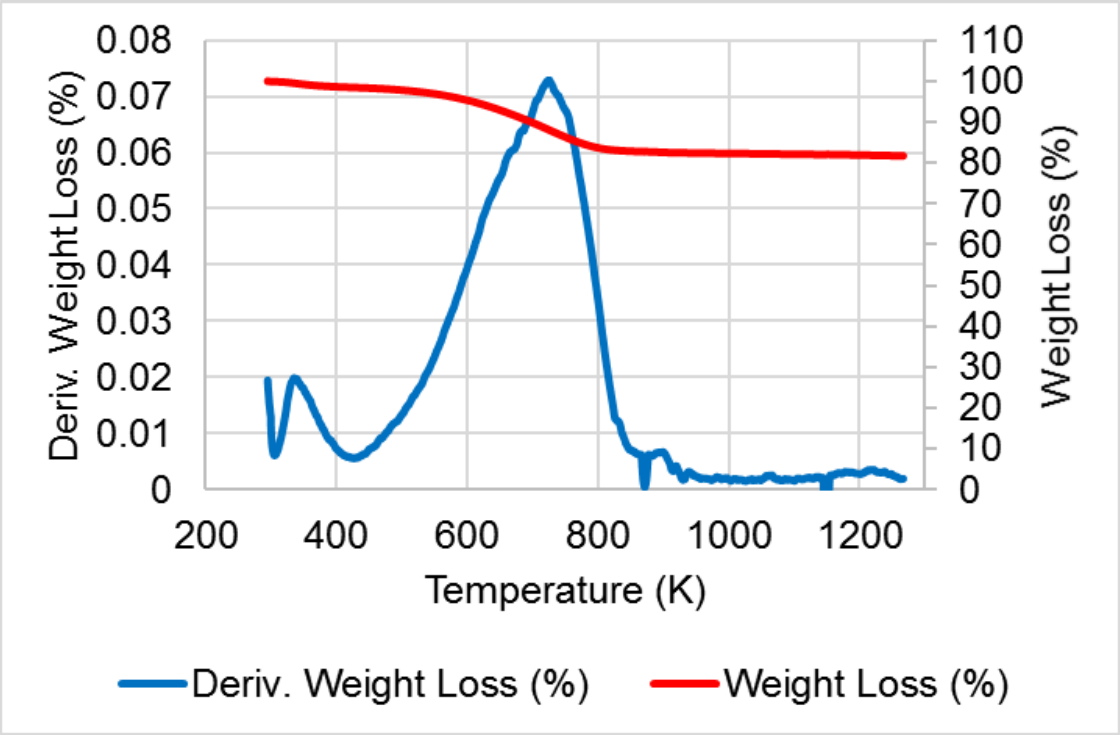

Figure 59 TPO of spent Pt/Al_2O_3 catalyst after partially deuterated reaction with the Kraft lignin

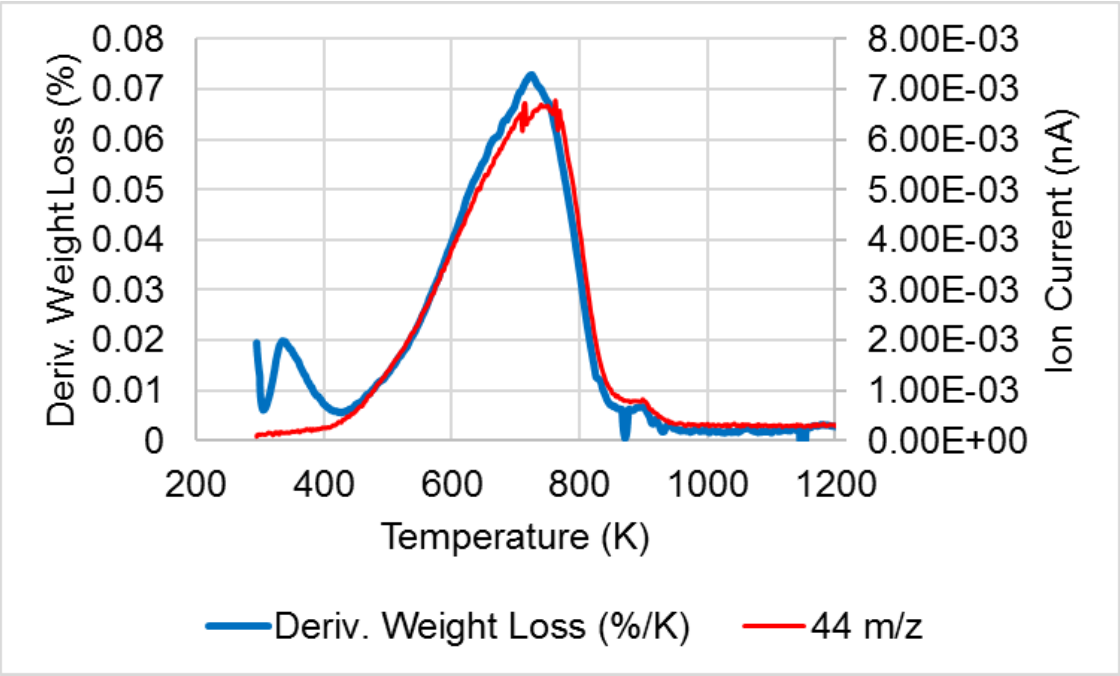

Figure 60 Derivative weight loss and CO_2 m/z 44 evolution of spent Pt/Al_2O_3 catalyst after partially deuterated reaction with the Kraft lignin

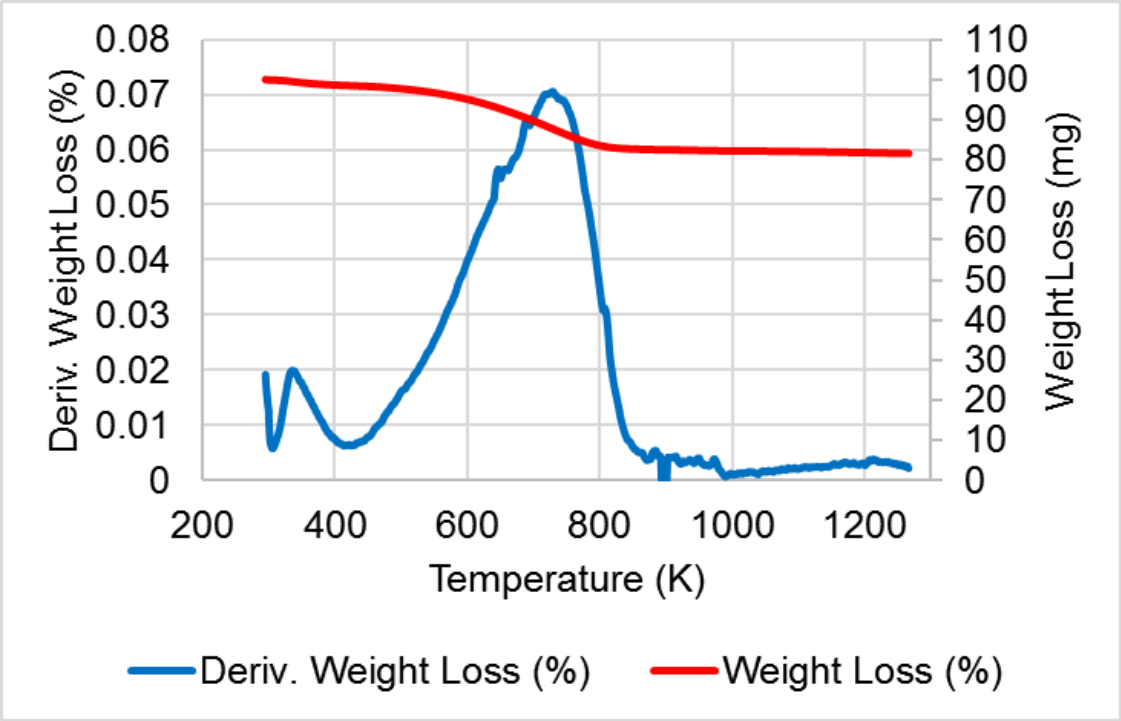

Figure 61 TPO of spent Pt/Al_2O_3 catalyst after fully deuterated reaction with the Kraft lignin

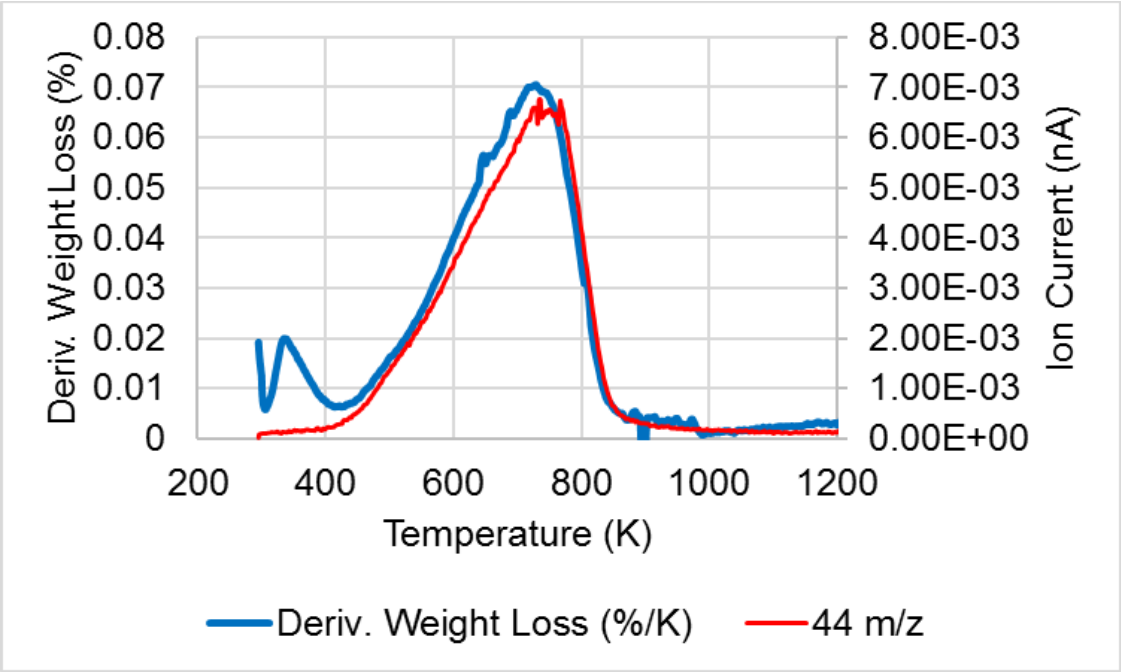

Figure 62 Derivative weight loss and CO_2 m/z 44 evolution of spent Pt/Al_2O_3 catalyst after fully deuterated reaction with the Kraft lignin

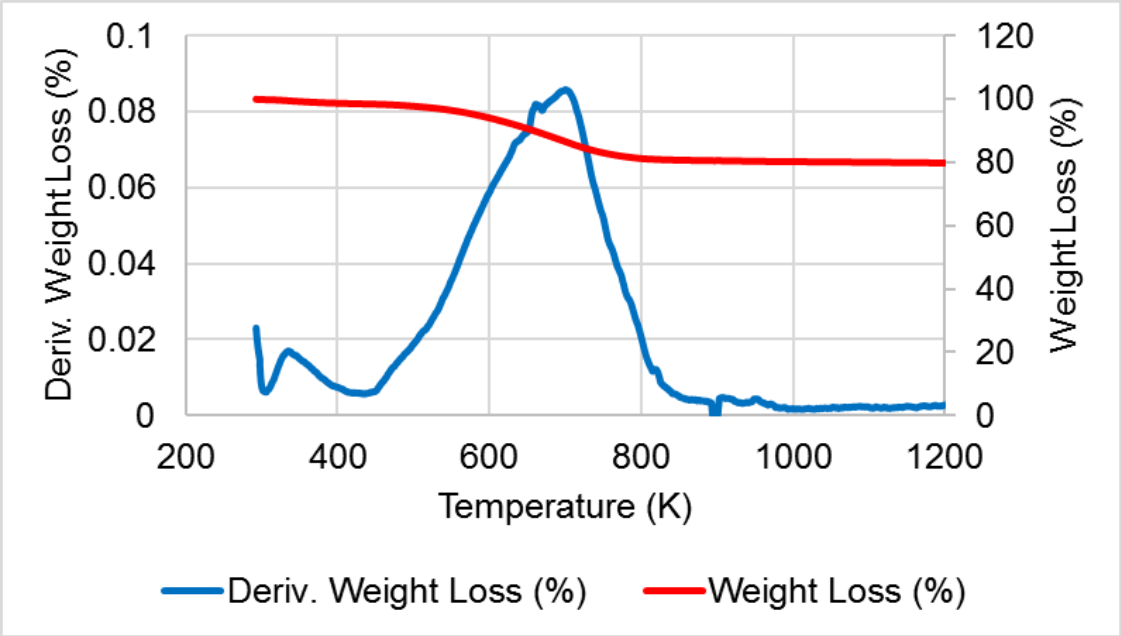

Figure 63 TPO of spent Pt/Al_2O_3 catalyst after IPA/H_2O reaction with the oak Parr-lignin

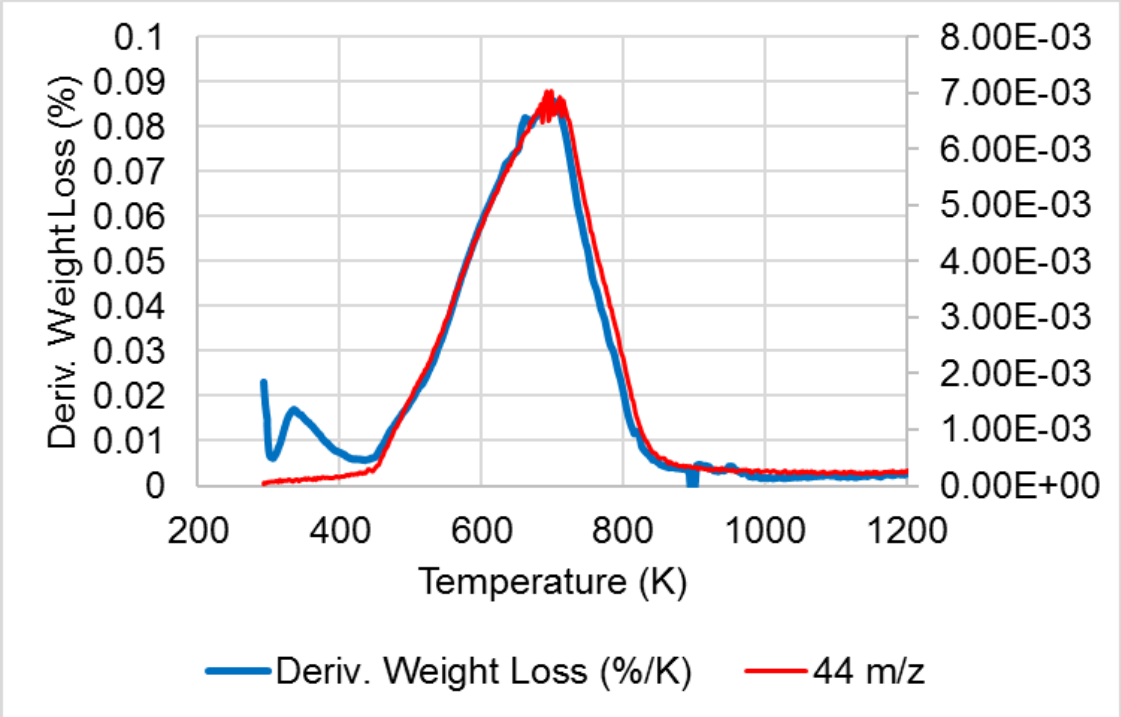

Figure 64 Derivative weight loss and CO_2 m/z 44 evolution of spent Pt/Al_2O_3 catalyst after IPA/H_2O reaction with the oak Parr-lignin

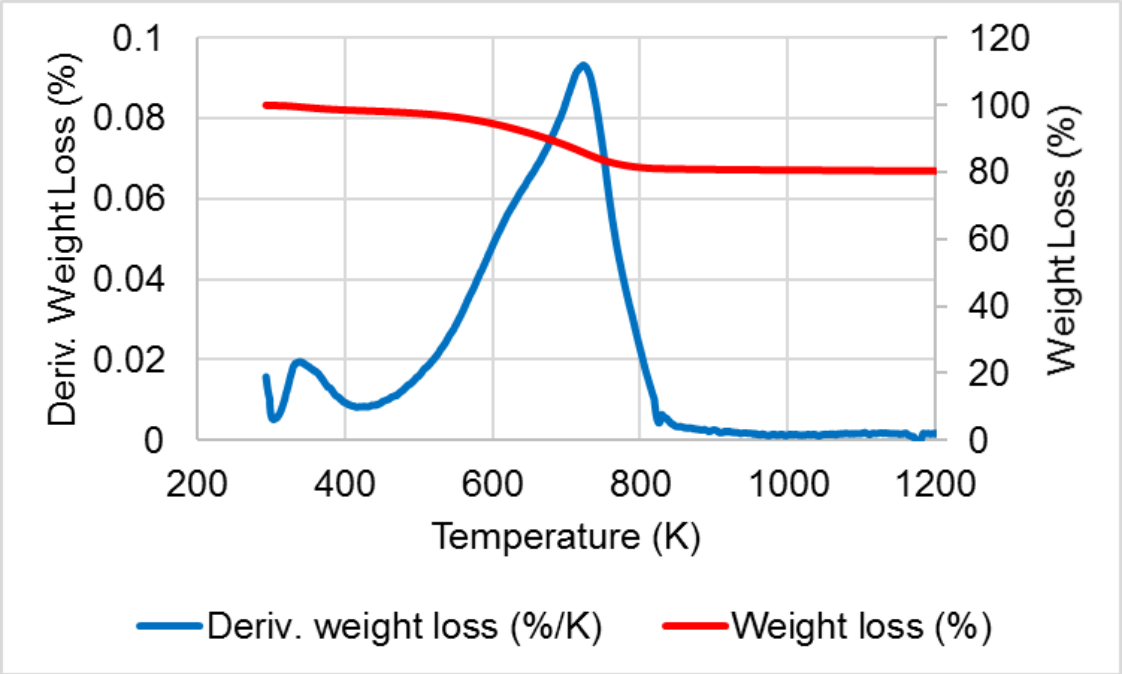

Figure 65 TPO of spent Pt/Al_2O_3 catalyst after acetone/H_2O reaction with the oak Parr-lignin

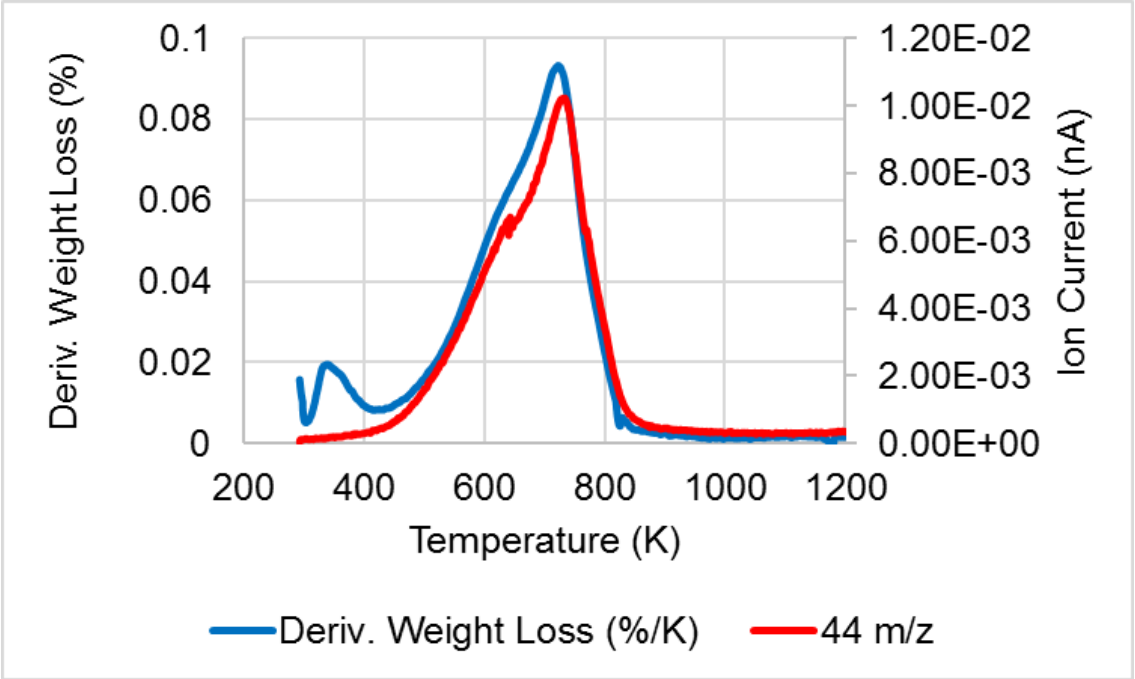

Figure 66 Derivative weight loss and CO_2 m/z 44 evolution of spent Pt/Al_2O_3 catalyst after acetone/H_2O reaction with the oak Parr-lignin

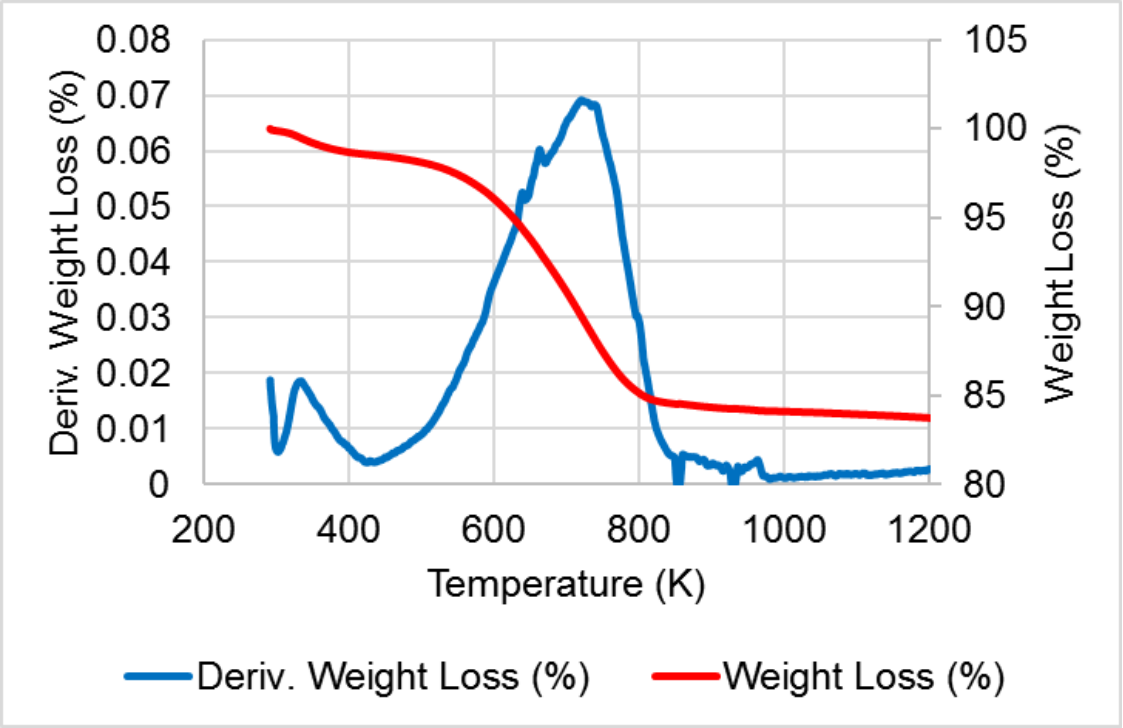

Figure 67 TPO of spent Pt/Al_2O_3 catalyst after acetone/H_2O reaction with the sugar-cane lignin

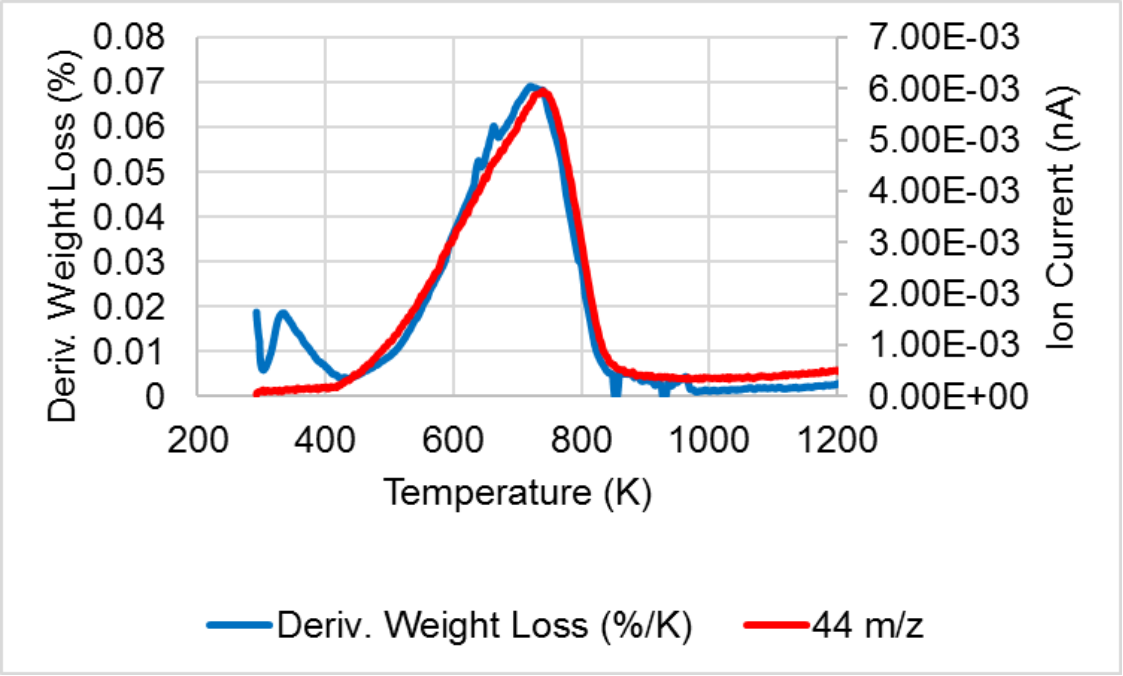

Figure 68 Derivative weight loss and CO_2 m/z 44 evolution of spent Pt/Al_2O_3 catalyst after acetone/H_2O reaction with the sugar-cane lignin

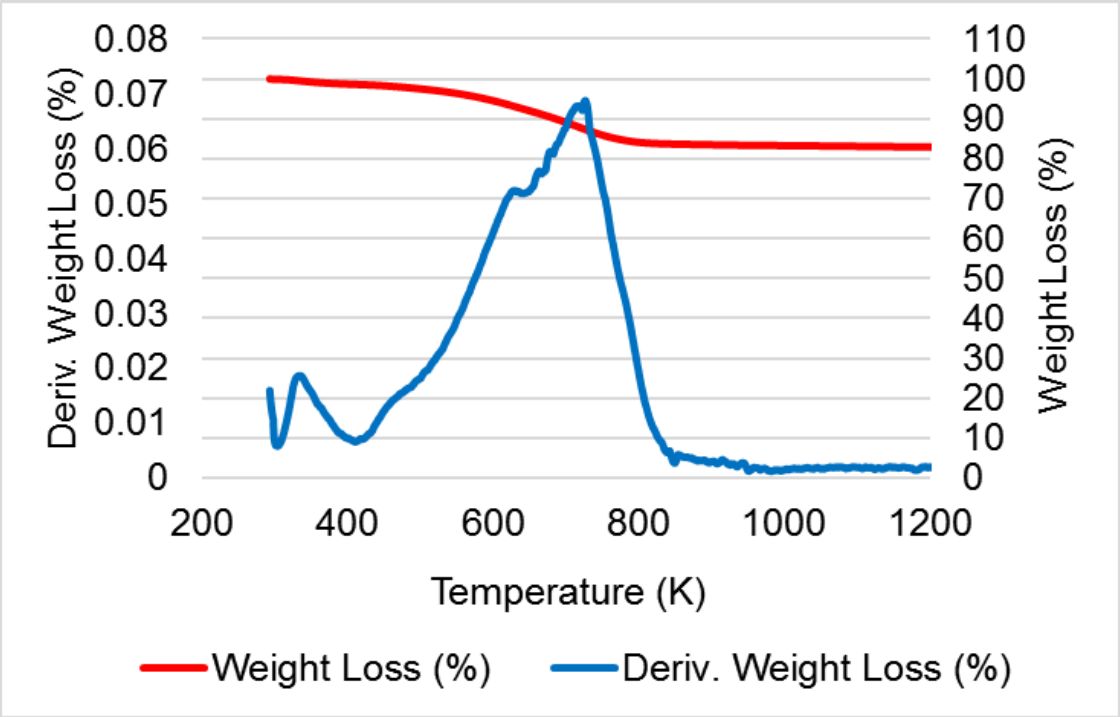

Figure 69 TPO of spent Pt/Al_2O_3 catalyst after acetone/H_2O reaction with the birch parr-lignin

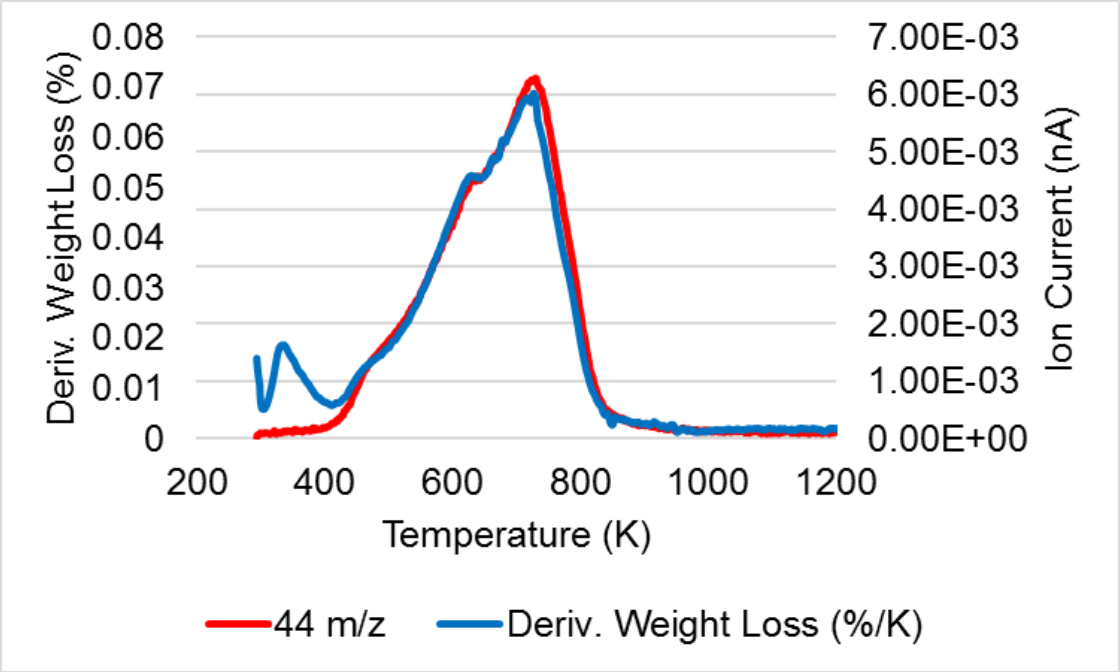

Figure 70 Derivative weight loss and CO_2 m/z 44 evolution of spent Pt/Al_2O_3 catalyst after acetone/H_2O reaction with the birch parr-lignin

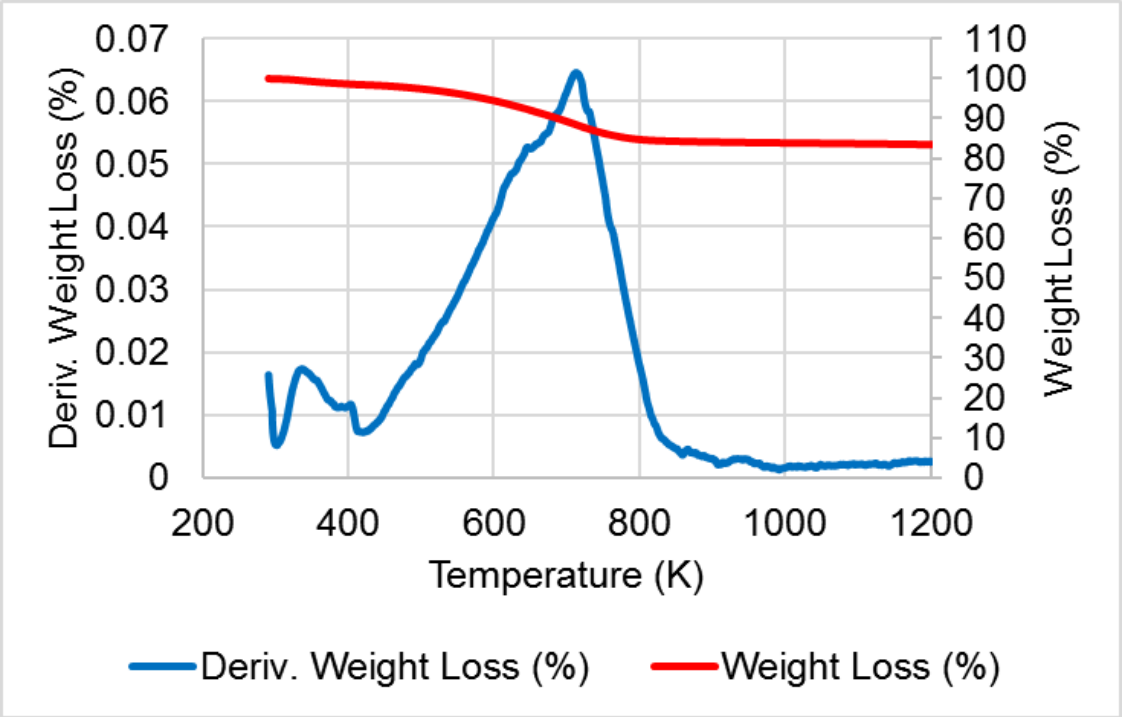

Figure 71 TPO of spent Pt/Al_2O_3 catalyst after IPA/H_2O reaction with the birch parr-lignin

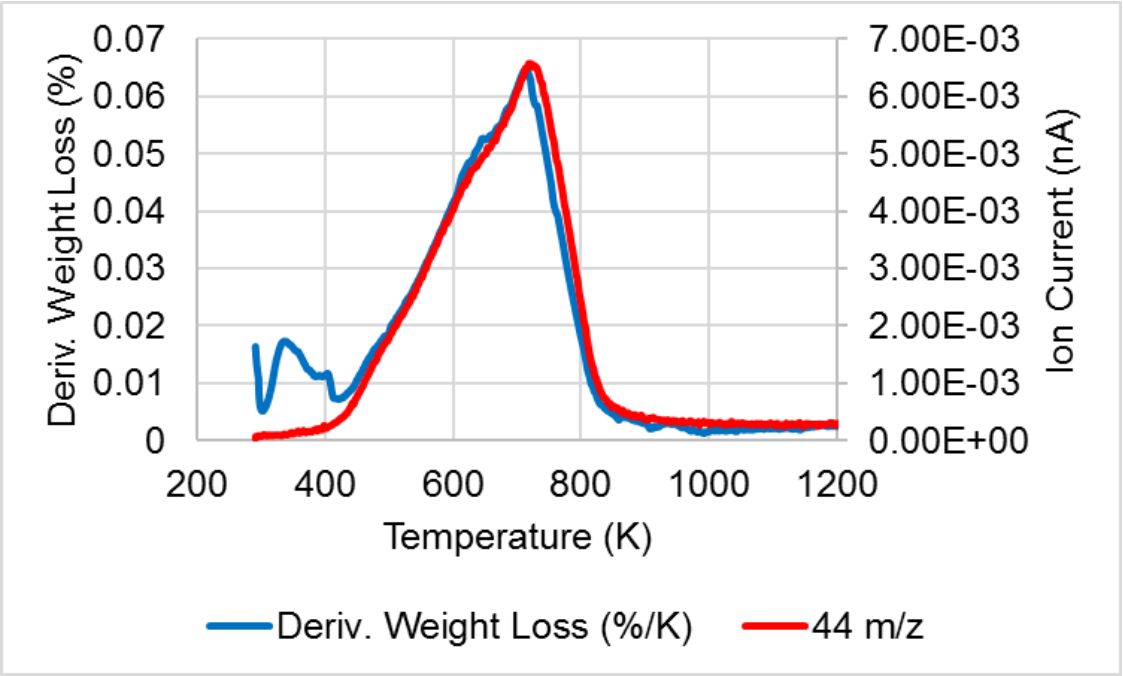

Figure 72 Derivative weight loss and CO_2 m/z 44 evolution of spent Pt/Al_2O_3 catalyst after IPA/H_2O reaction with the birch parr-lignin

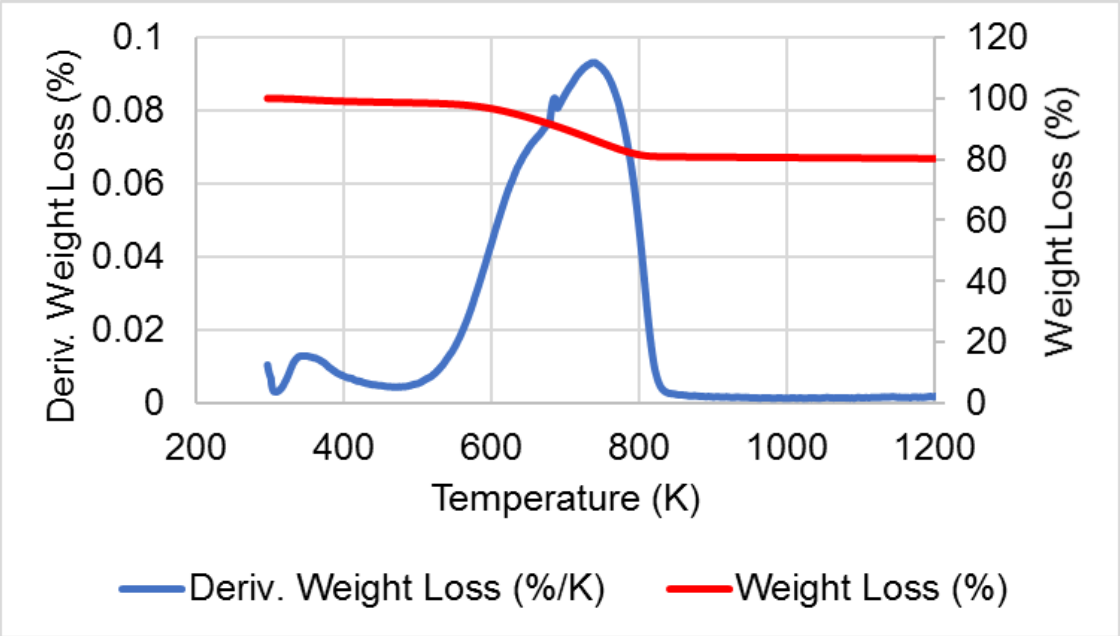

Figure 73 TPO of spent Al_2O_3 support after acetone/H_2O reaction with sugar-cane lignin

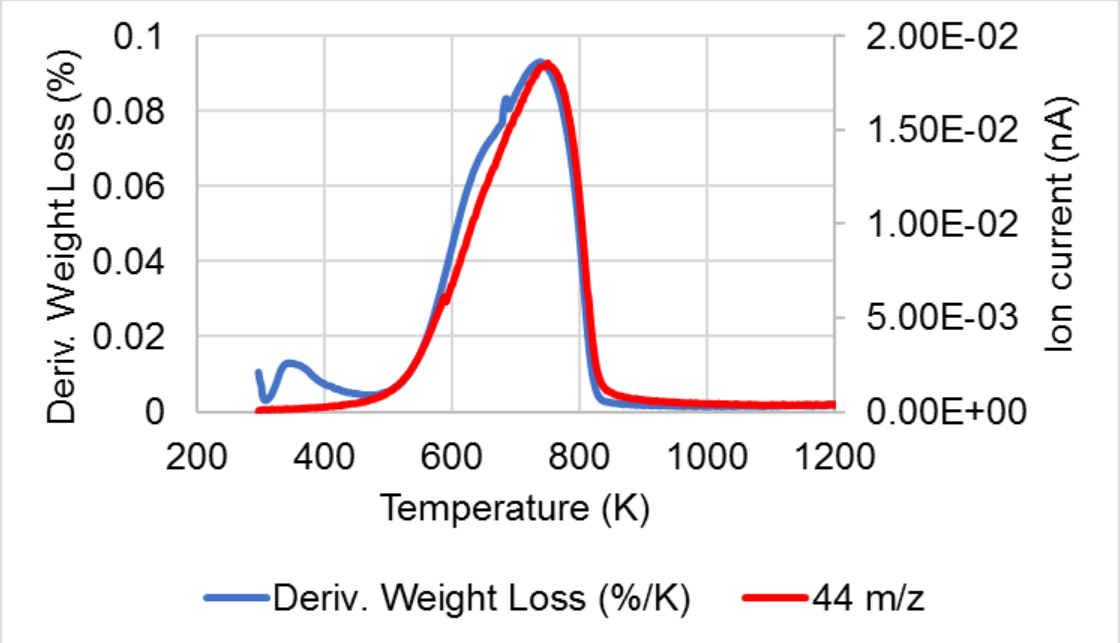

Figure 74 Derivative weight loss and CO_2 m/z 44 evolution of spent Al_2O_3 support after acetone/H_2O reaction with sugar-cane lignin

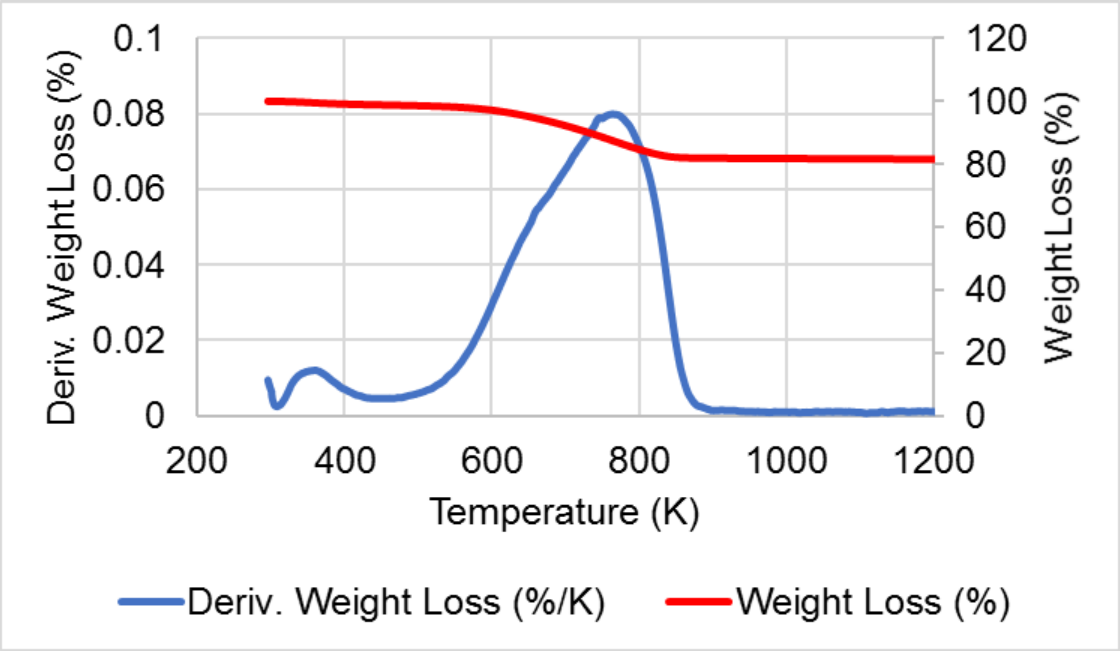

Figure 75 TPO of spent Al_2O_3 support after acetone/H_2O reaction with oak parr-lignin

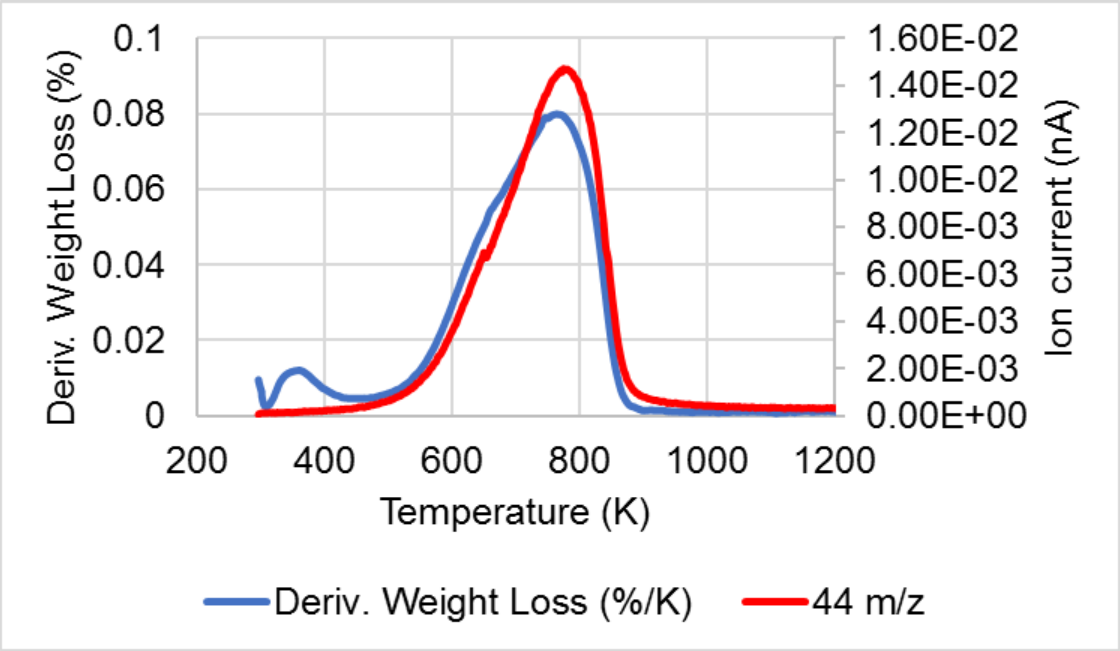

Figure 76 Derivative weight loss and CO2 m/z 44 evolution of spent Al_2O_3 support after acetone/H_2O reaction with oak parr-lignin

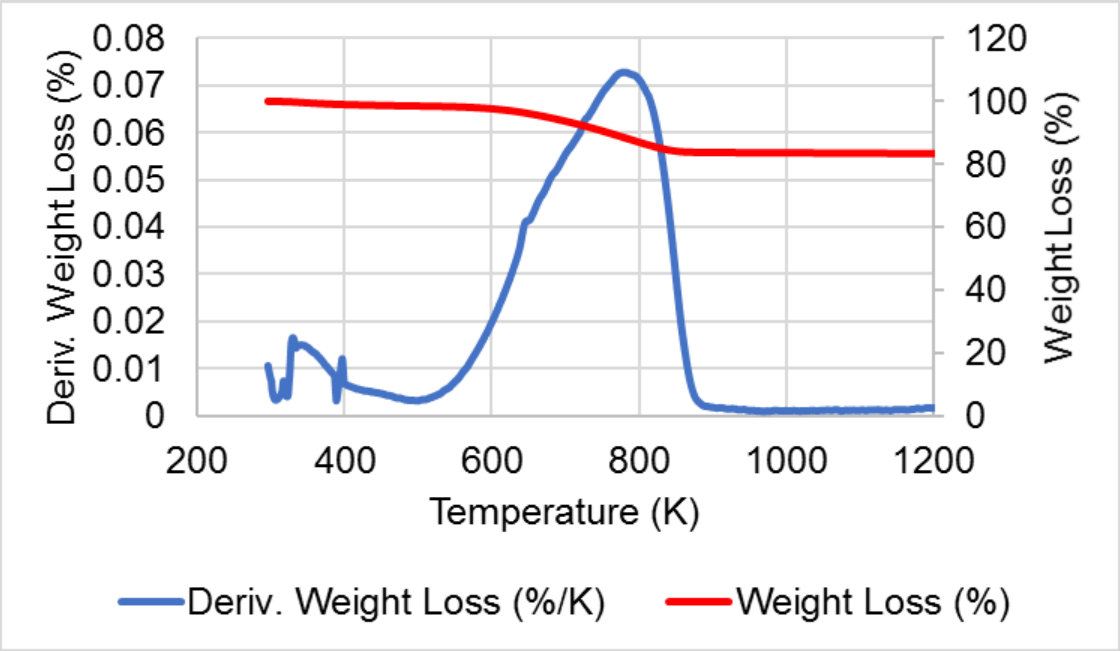

Figure 77 TPO of spent Al_2O_3 support after acetone/H_2O reaction with birch parr-lignin

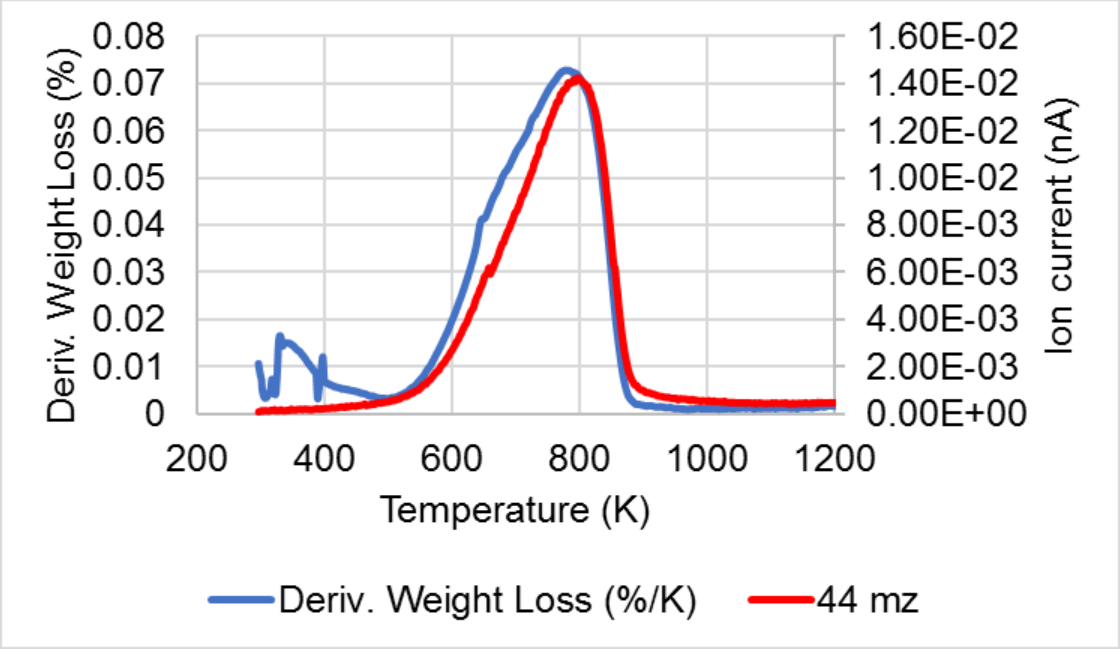

Figure 78 Derivative weight loss and CO_2 m/z 44 evolution of spent Al_2O_3 support after acetone/H_2O reaction with the birch parr-lignin

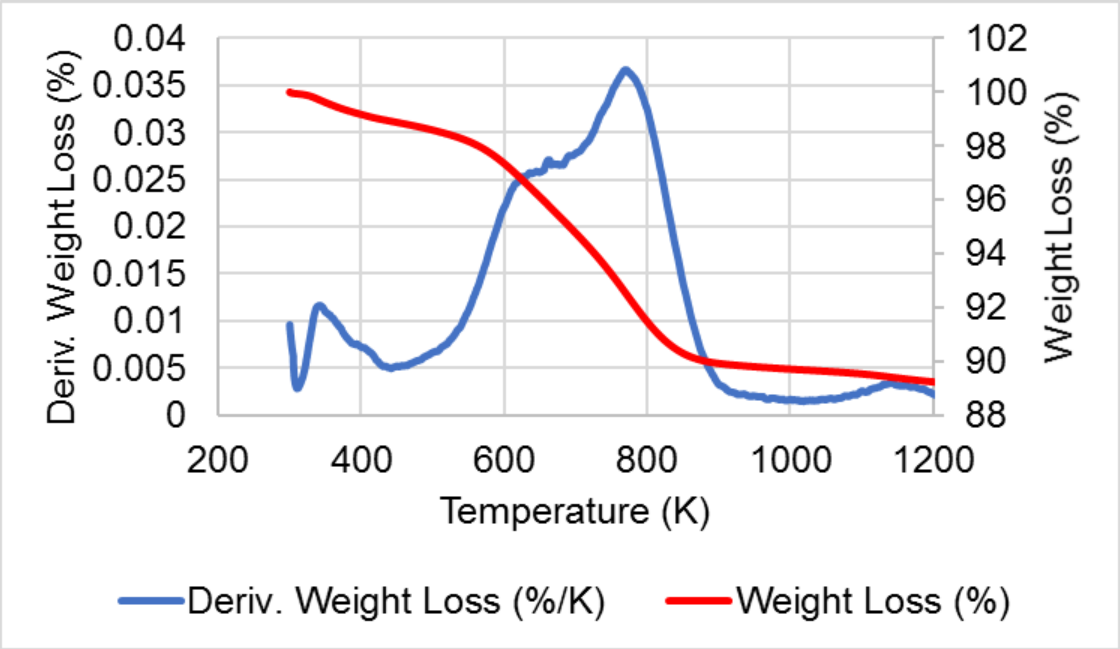

Figure 79 TPO of spent Al_2O_3 support after acetone/H_2O reaction with Kraft lignin

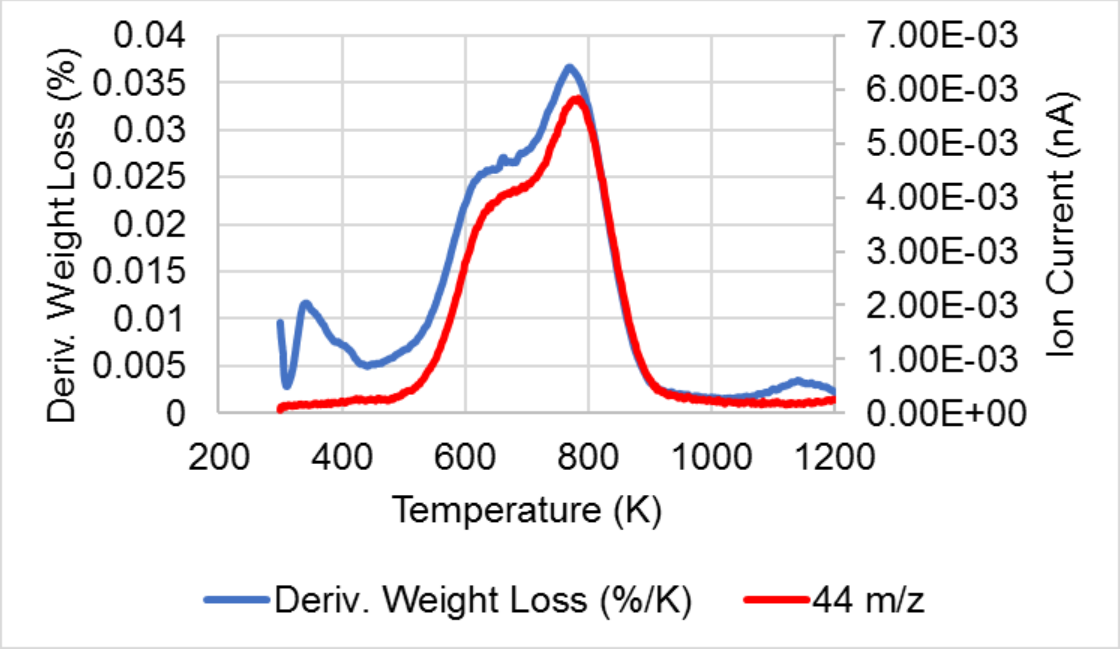

Figure 80 Derivative weight loss and CO_2 m/z 44 evolution of spent Al_2O_3 support after acetone/H_2O reaction with Kraft lignin

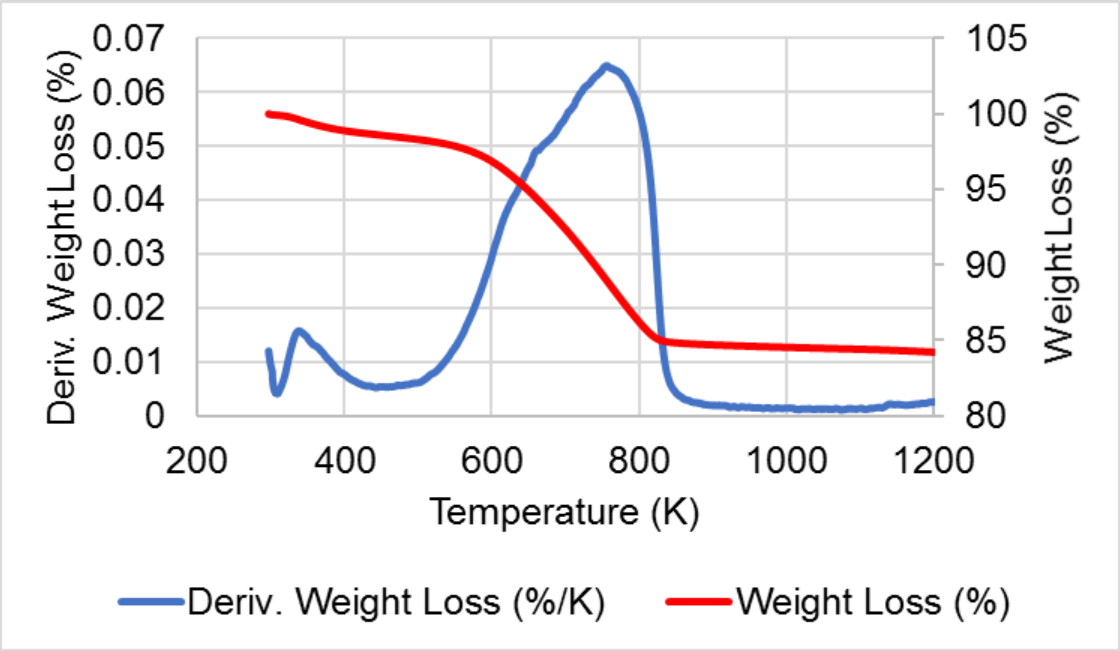

Figure 81 TPO of spent Ni/Al_2O_3 catalyst after acetone/H_2O reaction with sugar-cane lignin

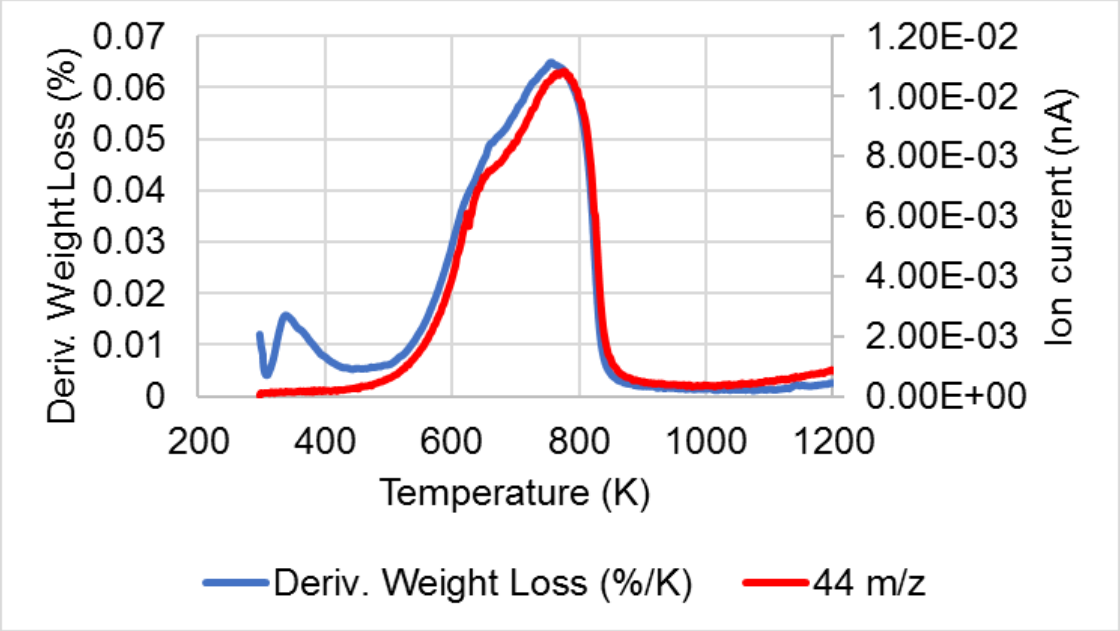

Figure 82 Derivative weight loss and CO_2 m/z 44 evolution of spent Ni/Al_2O_3 catalyst after acetone/H_2O reaction with sugar-cane lignin

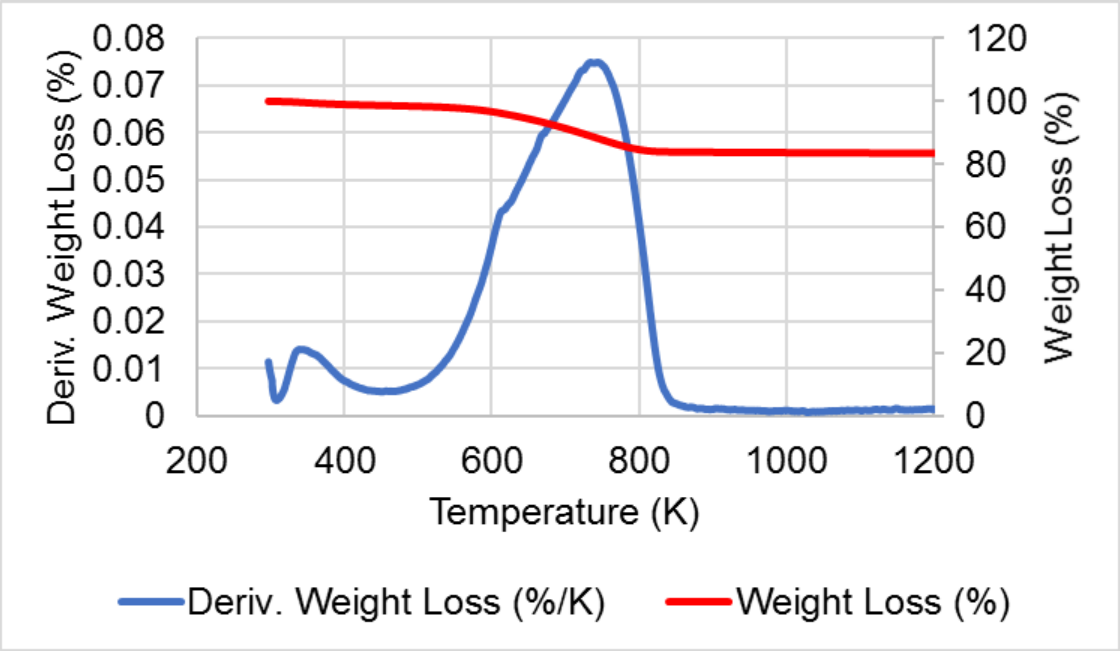

Figure 83 TPO of spent Ni/Al_2O_3 catalyst after acetone/H_2O reaction with birch parr-lignin

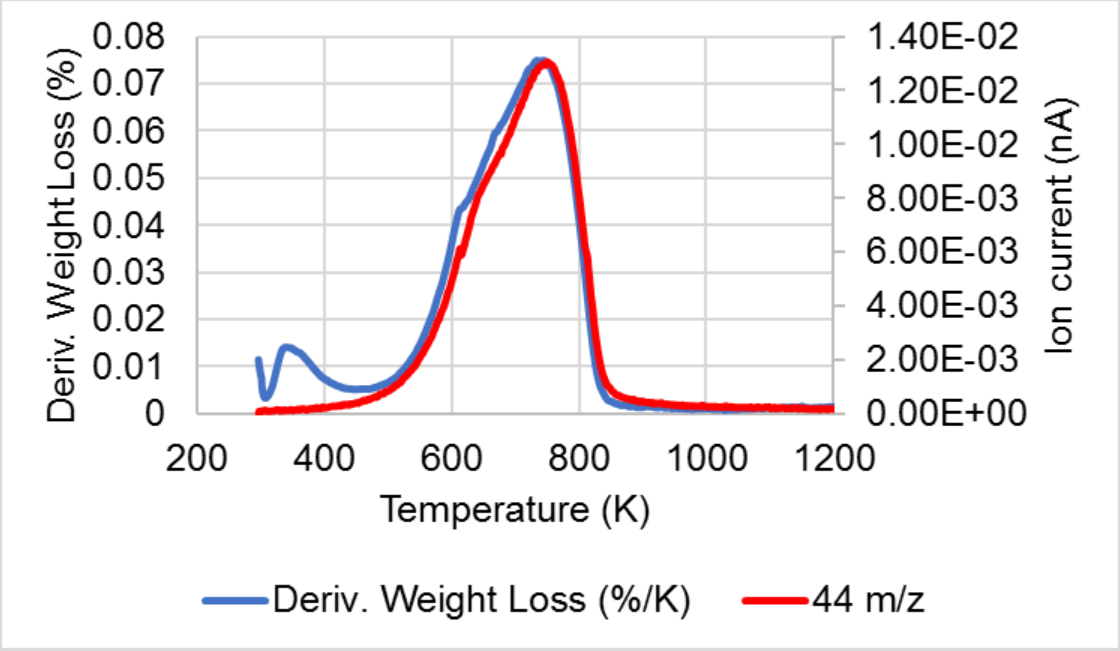

Figure 84 Derivative weight loss and CO_2 m/z 44 evolution of spent Ni/Al_2O_3 catalyst after acetone/H_2O reaction with birch parr-lignin

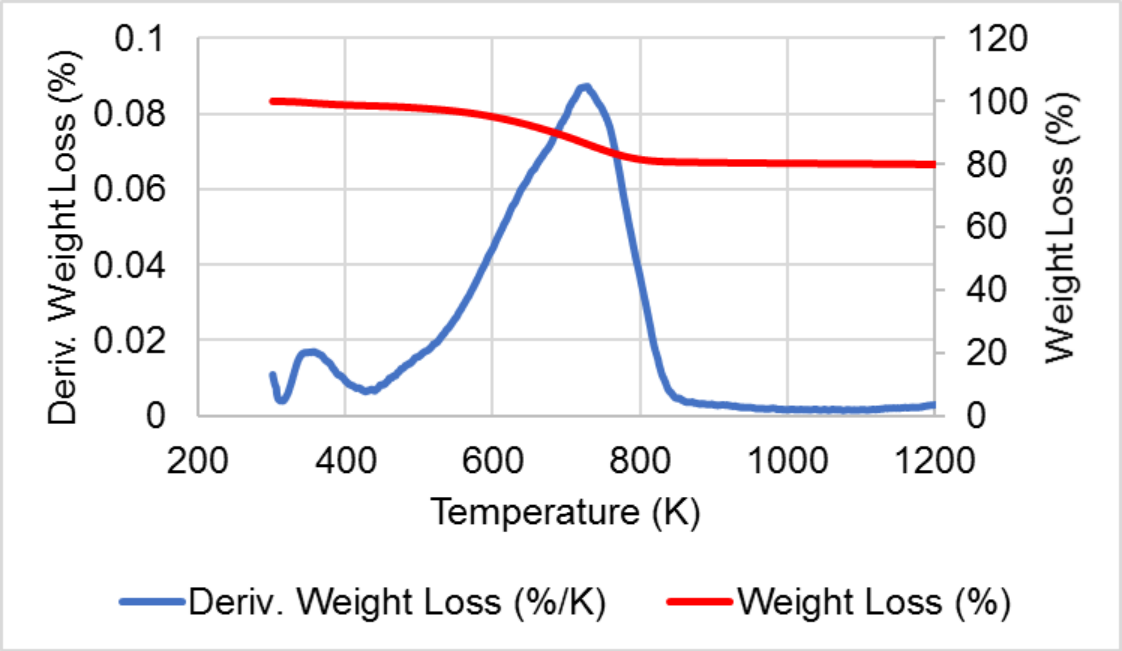

Figure 85 TPO of spent Ni/Al_2O_3 catalyst after acetone/H_2O reaction with oak parr-lignin

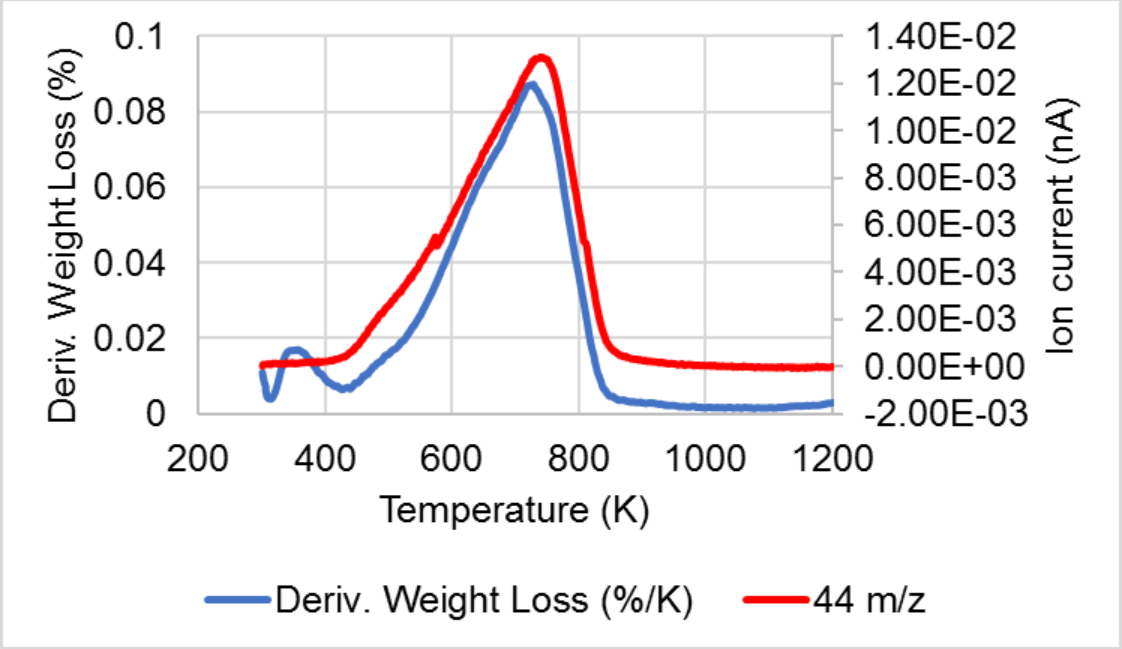

Figure 86 Derivative weight loss and CO_2 m/z 44 evolution of spent Ni/Al_2O_3 catalyst after acetone/H_2O reaction with oak parr-lignin

Combining the TGA and DTA techniques, more information about the material adsorbed onto the catalyst surface can be obtained. The DTA can inform if heat was absorbed or evolved, at the point which the transformation studied took place. The catalysts analysed showed similar DTA profiles, with a broad exothermic peak between ~500 K-900 K, as represented by Figure 87 and Figure 88. However, some plots showed slight differences.

These are shown in Figure 89, Figure 90, Figure 91, Figure 92 and Figure 93. The DTA profile of spent Pt/Al_2O_3 catalyst for oak and birch parr-lignin with acetone/water (Figure 89 and Figure 90), had a typical broad exothermic peak between ~500 K-900 K and a difference in shape at ~600 K-780 K. The spent Pt/Al_2O_3 for Kraft acetone, ethanol and IPA reactions (Figure 91, Figure 92 and Figure 93) differed to the others due to a small peak at about 450 K. These differences can be associated to the complexity of desorbed species, which caused slight differences in the energy involved in the species evolution.

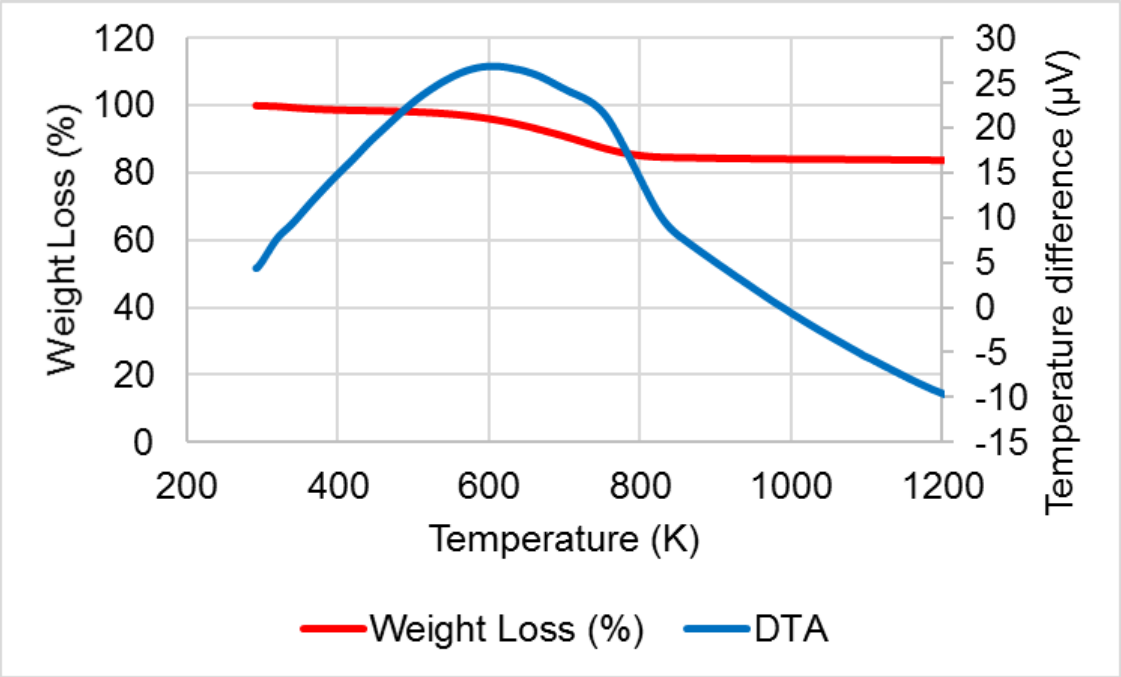

Figure 87 TPO/DTA profile of spent Pt/Al_2O_3 in acetone/H2O 50:50 v/v sugar-cane lignin reaction

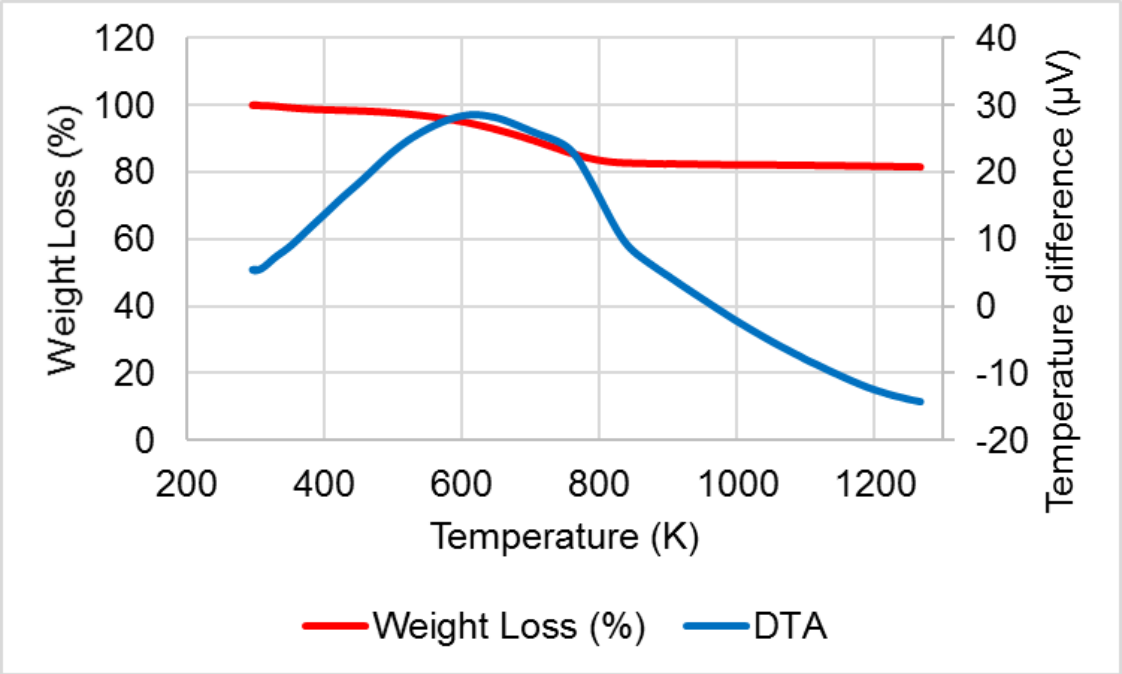

Figure 88 TPO/DTA profile of spent Pt/Al_2O_3 in fully deuterated Kraft lignin reaction

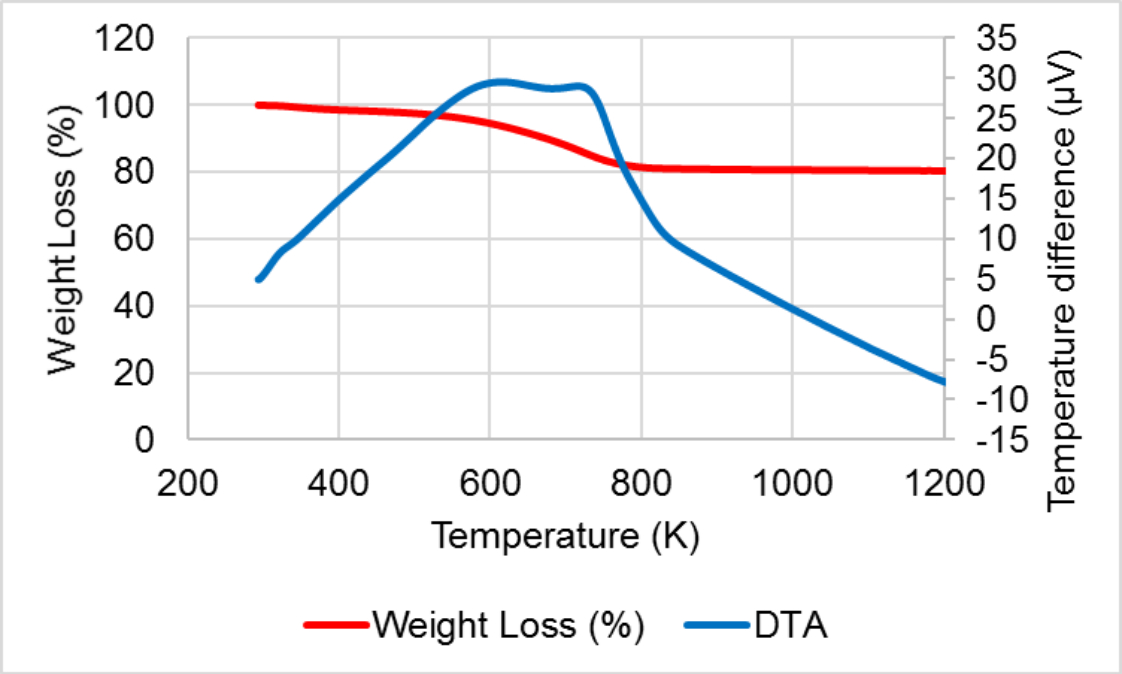

Figure 89 TPO/DTA profile of spent Pt/Al_2O_3 in acetone/H_2O 50:50 v/v oak parr-lignin

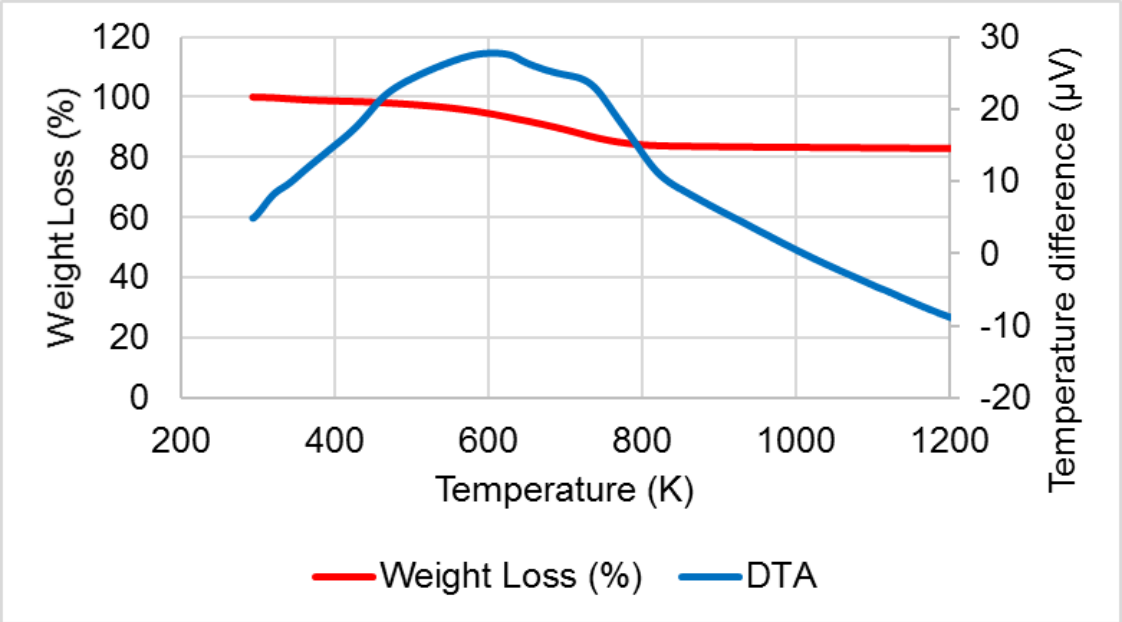

Figure 90 TPO/DTA profile of spent Pt/Al_2O_3 in acetone/H_2O 50:50 v/v birch parr-lignin

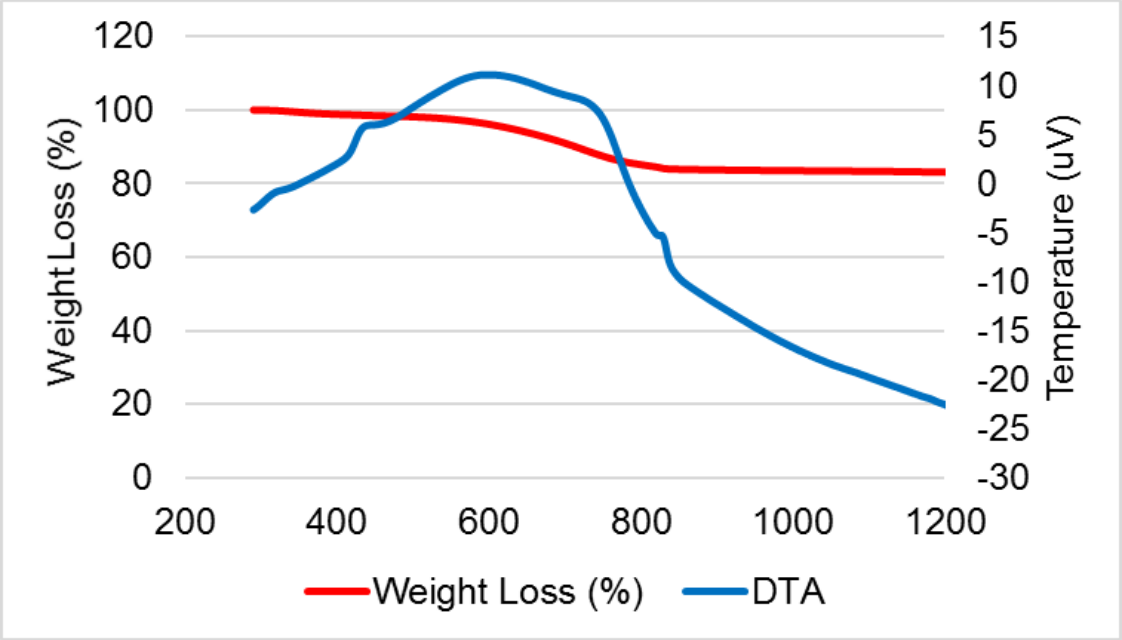

Figure 91 TPO/DTA profile of spent Pt/Al_2O_3 in acetone/H_2O 50:50 v/v Kraft lignin reaction

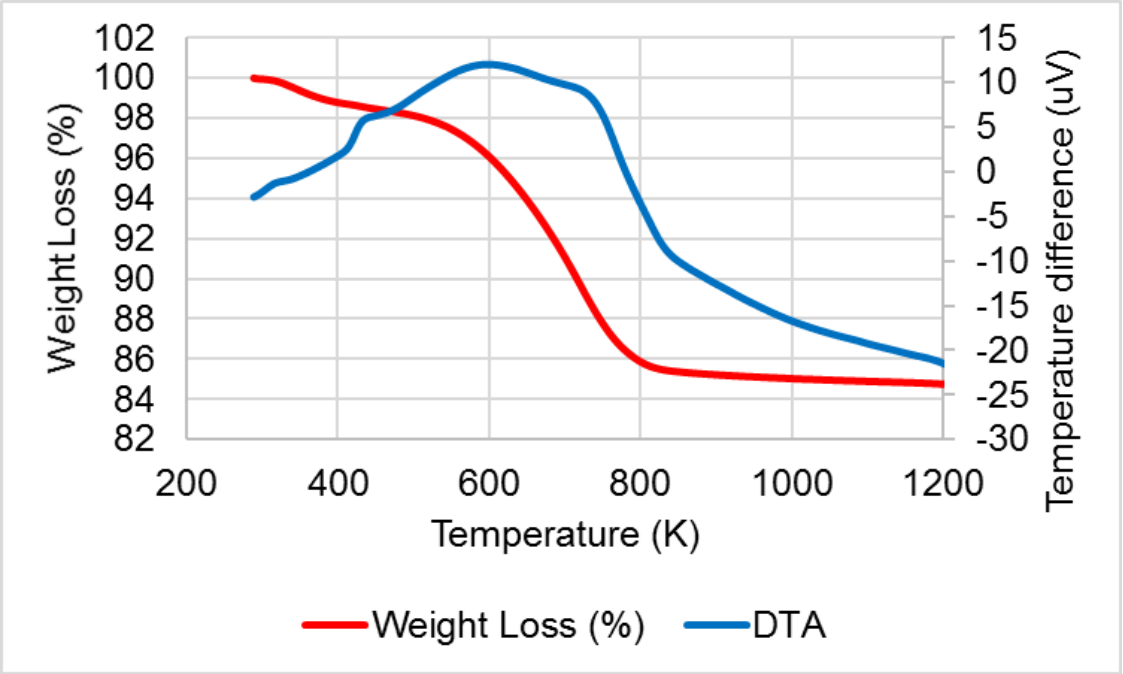

Figure 92 TPO/DTA profile of spent Pt/Al_2O_3 in IPA/H_2O 50:50 v/v Kraft lignin reaction

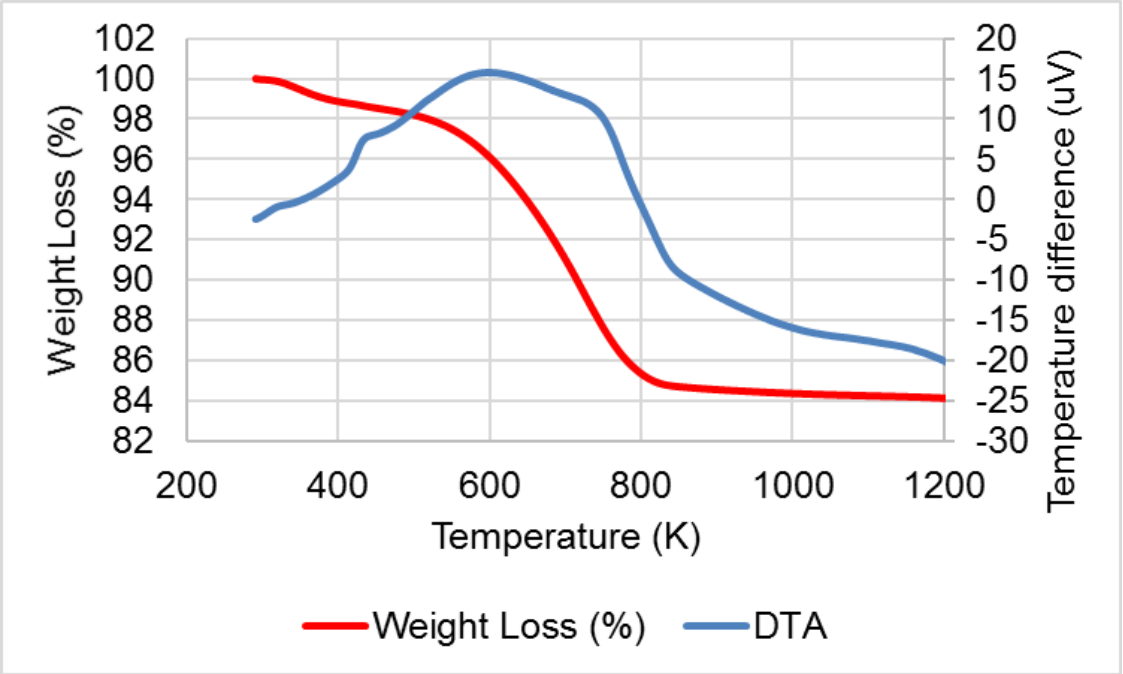

Figure 93 TPO/DTA profile of spent Pt/Al_2O_3 in $EtOH/H_2O$ 50:50 v/v Kraft lignin reaction

4.2.2 CHN analysis

The catalysts analysed by this technique were the same studied in the TPO section (Section 4.2.1). The elemental analysis of post reaction catalysts confirmed the presence of carbon in all samples. Hydrogen and nitrogen were also present in very small contents. As shown in Section 5.1, all the lignins had nitrogen in their composition. Therefore, the traces of nitrogen found in the samples can be from the lignins. This data is presented in Table 9.

Table 9 CHN analysis of post reaction catalysts

Type of reaction	C (%)	H (%)	N (%)
Spent Al_2O_3 catalyst support			
Kraft Acetone/H_2O	11.9	1.3	Not detected
Birch Acetone/H_2O	7.2	0.7	0.05
Oak Acetone/H_2O	12.5	1.2	0.04
Sugar-cane Acetone/H_2O	8.9	0.9	0.08
Spent Pt/Al_2O_2			
Kraft EtOH/H_2O	8.9	0.9	Not detected
Kraft IPA/H_2O	8.4	1.0	0.03
Kraft Acetone/H_2O	9.3	1.1	0.03
Kraft Partially deuterated	8.7	0.9	0.04
Kraft Fully deuterated	9.2	0.9	0.03
Sugar-cane Acetone/H_2O	8.3	0.8	0.05
Birch Acetone/H_2O	8.2	0.9	0.05
Oak Acetone/H_2O	10.6	0.9	0.01
Birch IPA/H_2O	8.0	1.0	0.04
Oak IPA/H_2O	10	0.8	0.02
Spent Ni/Al_2O_3 catalyst			
Oak Acetone/H_2O	10.9	0.9	0.06
Birch Acetone/H_2O	8.8	0.8	0.05
Sugar-cane acetone/H_2O	10.7	1.0	0.05

4.2.3 BET analysis

The catalysts analysed were the same studied in the TPO (Section 4.2.1) and CHN analyses (Section 4.2.2). They had an increase in their surface area and decrease in their pore volume after reaction compared to the initial values. The changes were more significant in the Al_2O_3 support; however, most values obtained were very similar with different lignins, except of sugar-cane that gave the smallest variation.

Initially, surface area (m^2/g), pore volume (cm^3/g) average pore diameter (Å) for Al_2O_3 was 104 m^2/g, 0.5 cm^3/g and 116 Å, for Pt/Al_2O_3: 124 m^2/g, 0.6 cm^3/g and 146 Å, and for Ni/Al_2O_3 106 m^2/g, 0.5 cm^3/g and 126 Å. The difference of average pore diameter was not significant, remaining very similar to the initial values.

Table 10 BET analysis of post reaction catalysts

Type of reaction	S_{BET} (m^2/g)	V_p(cm^3/g)
Spent Al_2O_3		
Kraft Acetone/H_2O	118	0.3
Birch Acetone/H_2O	119	0.3
Oak Acetone/H_2O	119	0.3
Sugar-cane Acetone/H_2O	110	0.3
Spent Pt/Al_2O_3		
Kraft EtOH/H_2O	140	0.4
Kraft IPA/H_2O	130	0.4
Kraft Acetone/H_2O	128	0.4
Kraft Partially deuterated	132	0.4
Kraft Fully deuterated	129	0.4
Sugar-cane Acetone/H_2O	140	0.4
Birch Acetone/H_2O	137	0.4
Oak Acetone/H_2O	134	0.4
Birch IPA/H_2O	128	0.3
Oak IPA/H_2O	131	0.4
Spent Ni/Al_2O_3		
Oak Acetone/H_2O	112	0.4
Birch Acetone/H_2O	108	0.3
Sugar-cane acetone/H_2O	106	0.3

4.2.4 XRD analysis of post-reaction catalysts

Figure 94 presents the Al_2O_3 in birch lignin reaction and acetone/water 50:50 v/v while Figure 95 shows the Pt/Al_2O_3 after Kraft lignin EtOH, IPA and acetone reactions (solvent/H_2O 50:50 v/v). The XRD patterns of the spent alumina catalysts showed that there

was no boehmite peaks and the support did not change from its initial pattern, confirming that hydration did not take place in the reactions affecting Al_2O_3 stability even with different solvent mixtures.

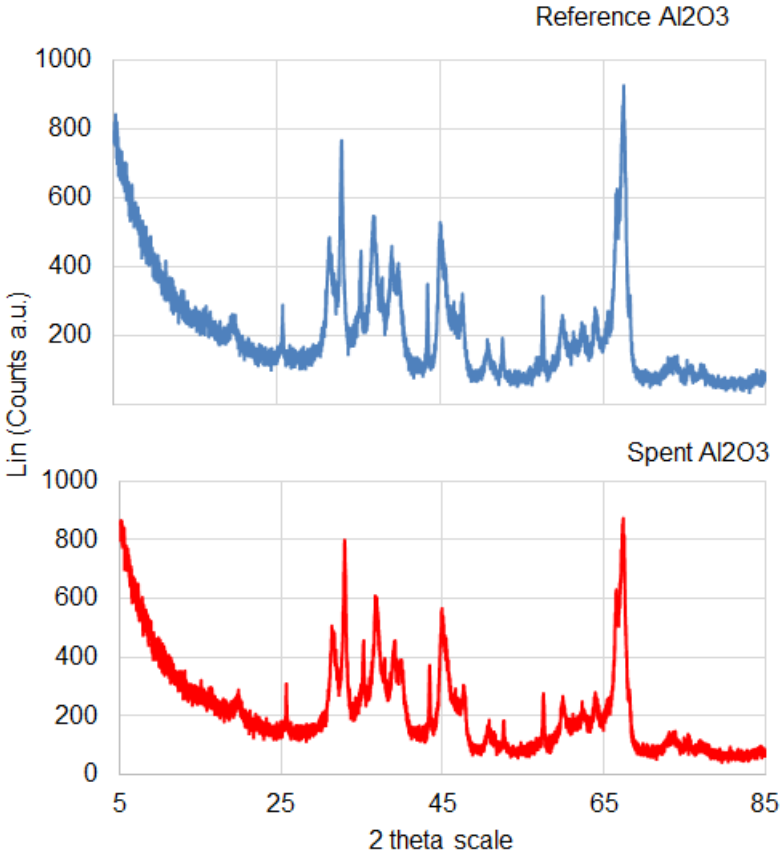

Figure 94 XRD patterns of post reaction Al_2O_3 support

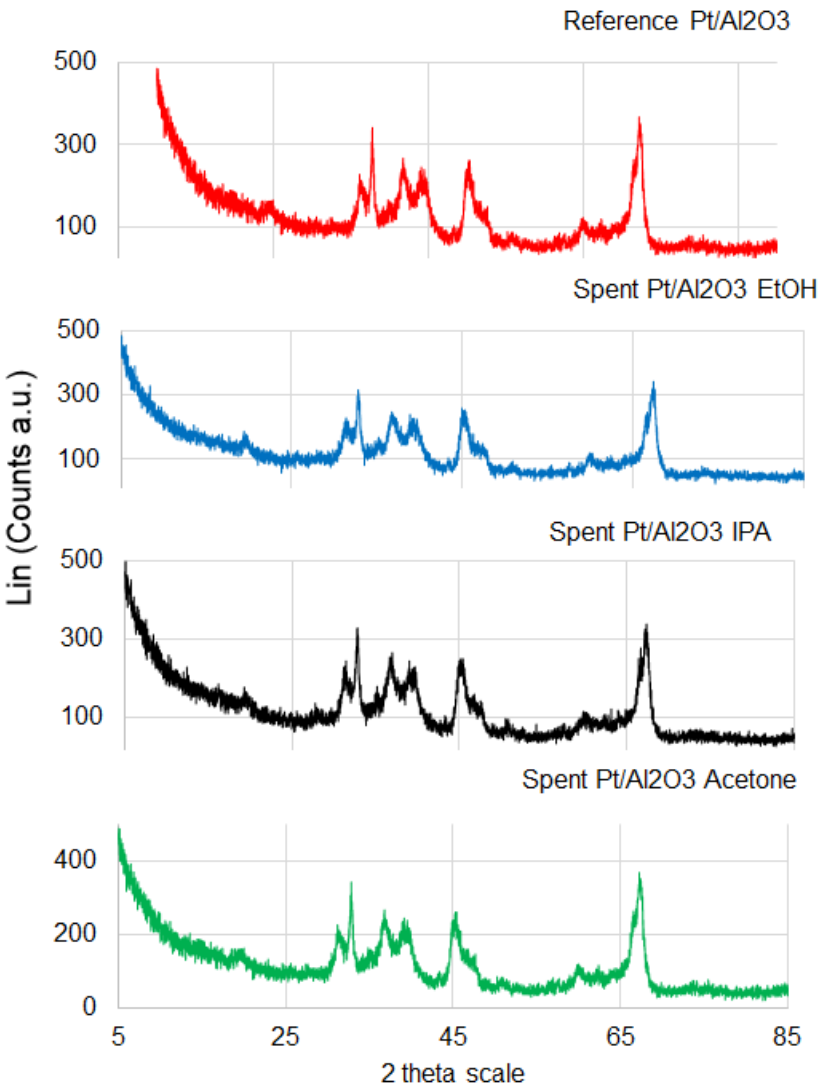

Figure 95 XRD patterns of post reaction Pt/Al_2O_3 catalysts

In order to evaluate if the zirconia support could be affected in the reaction medium by the solvent and presence of water, the ZrO_2 support from the experiment with birch lignin and acetone/water (50:50 v/v) was recovered and as showed in Figure 96, there were no changes in this support, remaining the same monoclinic zirconia after the experiment.

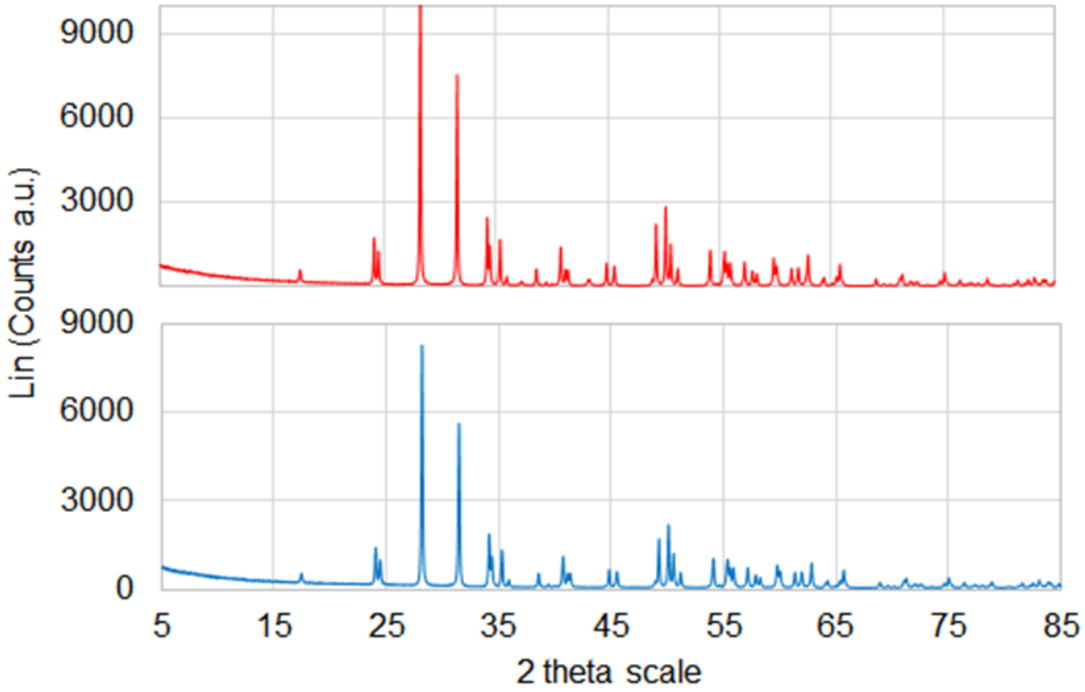

Figure 96 XRD patterns of post reaction ZrO_2 support

4.2.5 Raman analysis

Raman Analysis was performed on the spent catalysts (Al_2O_3, Pt/Al_2O_3 and Ni/Al_2O_3) to obtain more information about surface carbon. Carbonaceous material can cause fluorescence in the analysis and overwhelm the Raman signal. To avoid this issue as much as possible, UV radiation was used. It has been reported that UV radiation significantly contributed to the study of heavy coke material deposited on catalyst surface, considerably decreasing fluorescence [91]–[93]. In the Figures below there were two bands with broad peaks with maxima at ~ 1380 cm^{-1} and ~ 1600 cm^{-1}, which corresponded to coke deposition [94] related to disordered graphite (D band) and graphitic carbon (G band) [95].

The D/G ratio (Table 11) for the reactions with spent Pt/Al_2O_3 were detected as follows: Kraft EtOH, Kraft IPA and Kraft acetone (Figure 97) were similar, sugar-cane lignin < birch parr-lignin and oak parr-lignin (Figure 98). This data shows that sugar-cane lignin in reaction with Pt/Al_2O_3 presented the lower D/G ratio value.

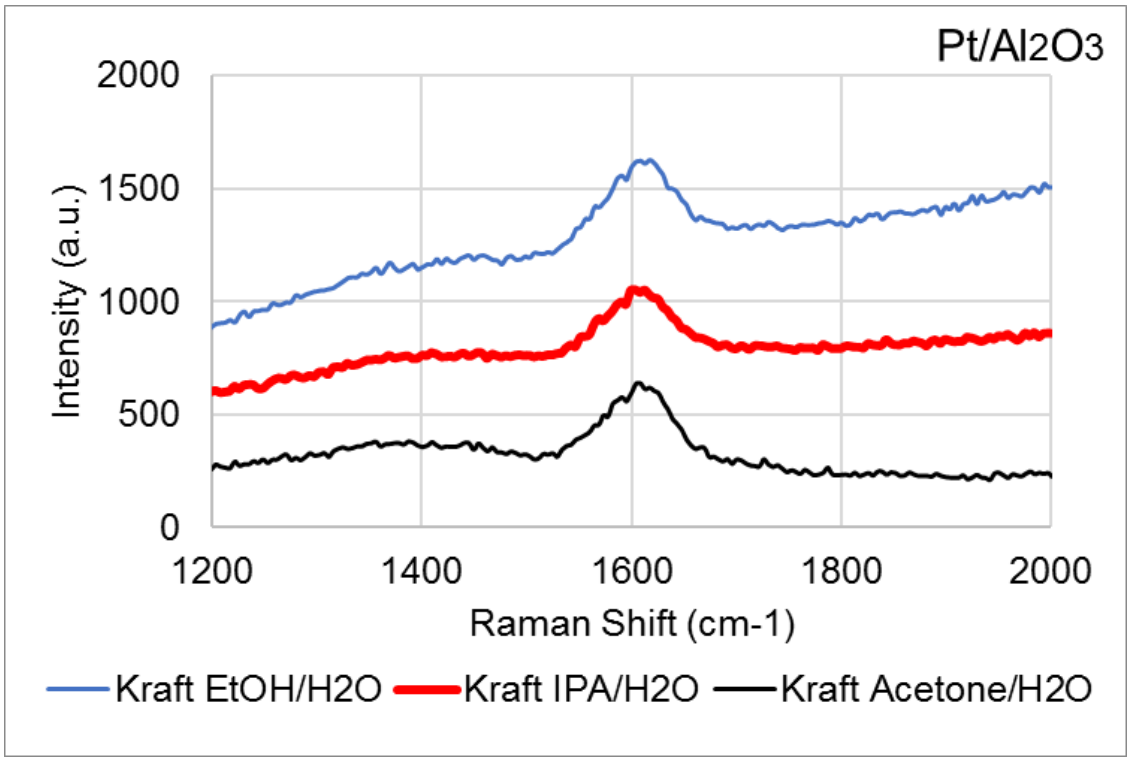

Figure 97 Raman spectra for spent Pt/Al_2O_3 catalyst used in Kraft lignin depolymerisation with acetone, ethanol, IPA (solvent/H_2O 50:50 v/v) solvent mixture

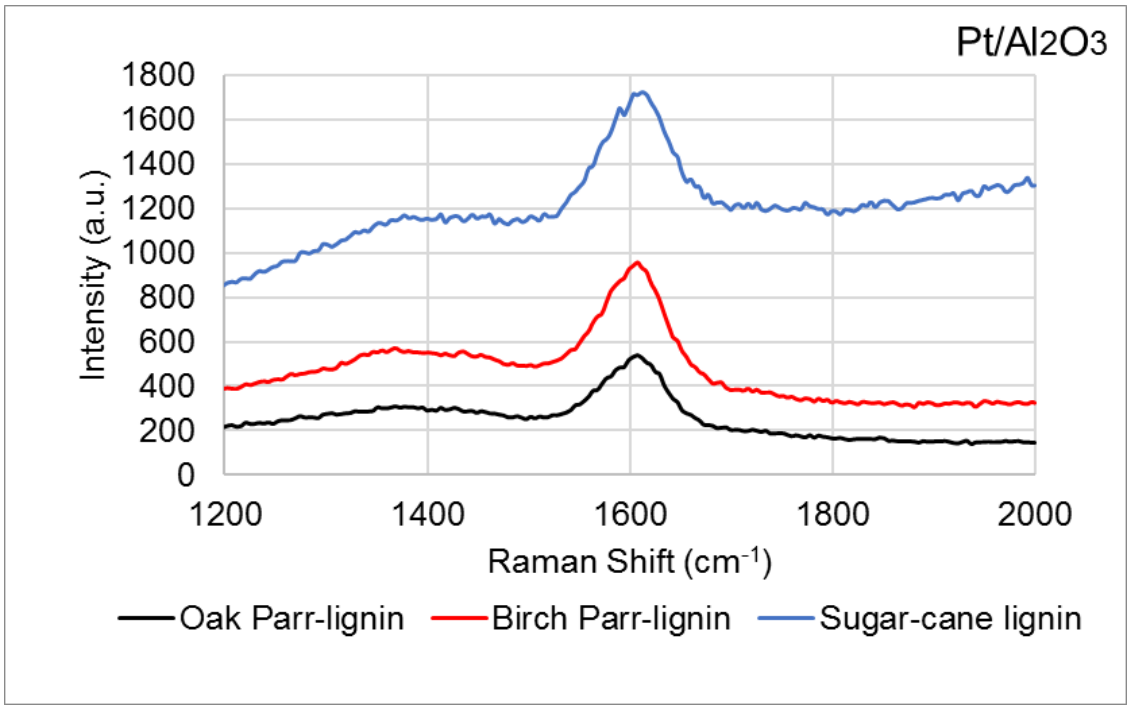

Figure 98 Raman spectra for spent Pt/Al_2O_3 catalyst used in sugar-cane, oak and birch parr-lignins depolymerisation with acetone/H_2O 50:50 v/v solvent mixture.

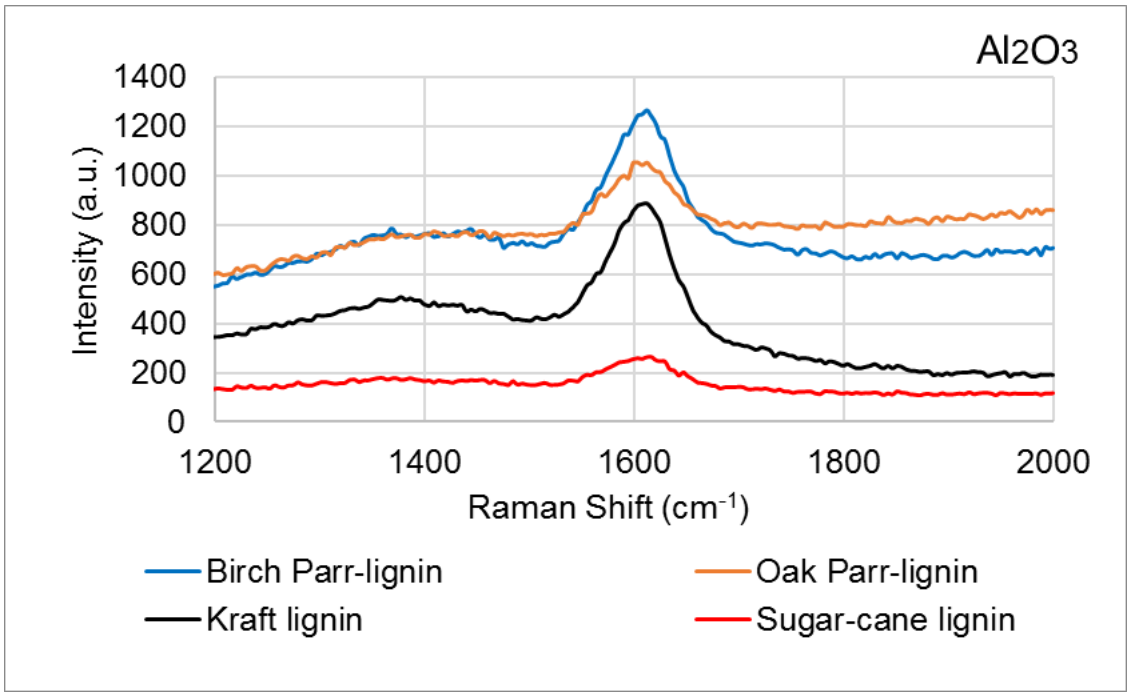

Figure 99 Raman spectra for spent Al_2O_3 support used in sugar-cane, Kraft, oak and birch parr-lignins depolymerisation with acetone/H_2O 50:50 v/v solvent mixture.

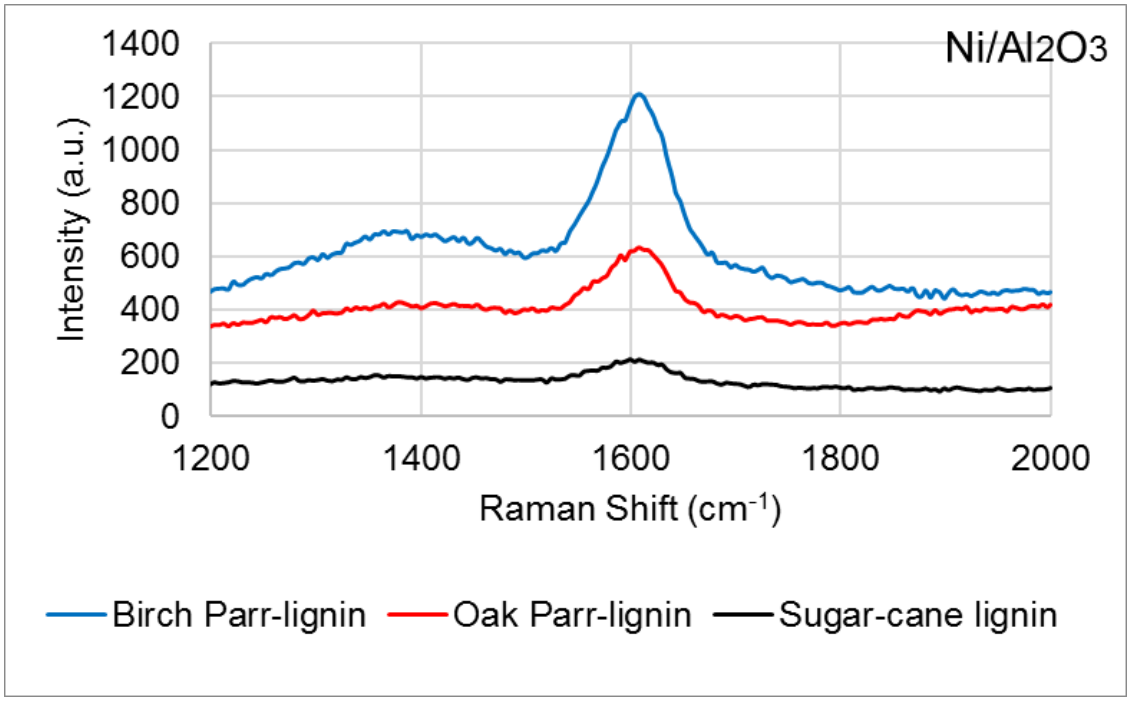

Figure 100 Raman spectra for spent Ni/Al_2O_3 catalyst used in sugar-cane, oak and birch parr-lignins depolymerisation with acetone/H_2O 50:50 v/v solvent mixture.

D bands (~1380) were not detected as well-defined peaks in the samples and did not show high intensities. They were detected for Pt/Al_2O_3 catalyst in reactions with Kraft EtOH, IPA and acetone (Figure 97), oak, birch parr-lignins and sugar-cane (Figure 98), Al_2O_3 and Kraft lignin (Figure 99), Ni/Al_2O_3 and birch parr-lignin (Figure 100). The D:G ratios are displayed in Table 11. The values obtained were very similar, indicating that these samples have similarities in the type of ordered carbon deposited

Table 11 D:G ratios determined from the Raman analysis for spent Al_2O_3, Pt/Al_2O_3 and Ni/Al_2O_3 catalysts

Type of reaction	D:G ratio
Al_2O_3 support	
Kraft Acetone/H_2O	0.27
Birch Acetone/H_2O	0.17
Oak Acetone/H_2O	0.22
Pt/Al_2O_3 catalyst	
Kraft EtOH/H_2O	0.30
Kraft IPA/H_2O	0.22
Kraft Acetone/H_2O	0.25
Sugar-cane Acetone/H_2O	0.11
Birch Acetone/H_2O	0.24
Oak Acetone/H_2O	0.24
Ni/Al_2O_3 catalyst	
Birch acetone/H_2O	0.28
Oak Acetone/H_2O	0.24

5 Characterisation of Kraft and isolated lignins

The Kraft and isolated lignins were characterized using Gel Permeation Chromatography (GPC), CHN analysis, and a 2D HSQC NMR technique.

5.1 CHN analyses

The elemental analyses showed the percentage of C, H and N in the Kraft and isolated lignins. Previous characterisation of the Kraft lignin studied in this research showed that it also had oxygen (28 %) and sulfur (3 %) [26]. The results are presented Table 12.

Table 12 CHN analysis of Kraft Lignin

Lignin	C (%)	H (%)	N (%)
Kraft	62	5.9	0.6
Sugar-cane	54	5.6	0.9
Birch parr-lignin	64	6.3	0.3
Oak parr-lignin	62	5.6	0.3

5.2 Gel permeation chromatography

The GPC was able to provide general information about molecular weight distribution (Mw), molecular number (Mn) and polydispersity (Ip) of Kraft and the isolated lignins. As shown in Table 13, the Mw of Kraft lignin corresponded to 4973 g/mol, also the Mn and Ip were typical high values of a lignin obtained from softwoods [96]. The sugar-cane and parr-lignins presented a lower Mw compared to the highly condensed Kraft lignin.

Table 13 GPC analysis of Kraft Lignin

	Molecular Weight (Mw, g/mol)	Molecular Number (Mn, g/mol)	Polydispersity (Ip)
Kraft lignin	4973	1236	4.0
Sugar-cane	2292	731	3.0
Birch parr-lignin	2987	977	3.0
Oak parr-lignin	2707	1029	2.6

Figure 101 displays the molecular weight distribution plot of Kraft lignin. In the graph, the Mw decreases from the left to the right. There was a main peak around 12 minutes, which could be assigned to an abundant condensed fraction while the peaks from ~ 13 minutes may correspond to lower molecular weight fragments.

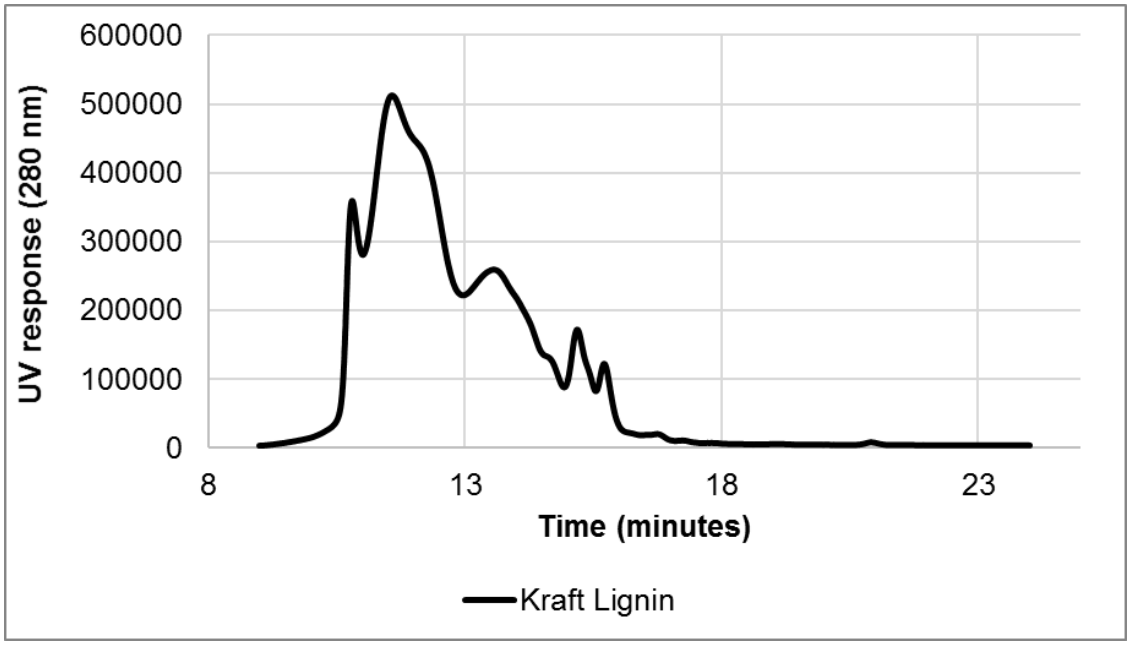

Figure 101 GPC profile of Kraft lignin

Figure 102 displays the molecular weight distribution plot for sugar-cane lignin. The highest intense peak eluting at ~ 15 min was related to the solvent used (THF). The graph shows a peak at ~ 12 min, which was related to highest molecular weight fractions, as in the GPC the separation of the polymer occurs according to the molecular size as a function of time. The heavier molecules appear first, while the smaller afterwards. From ~ 13 min the intensity decreased, and no high peaks were found, which can be attributed to smaller lignin fractions.

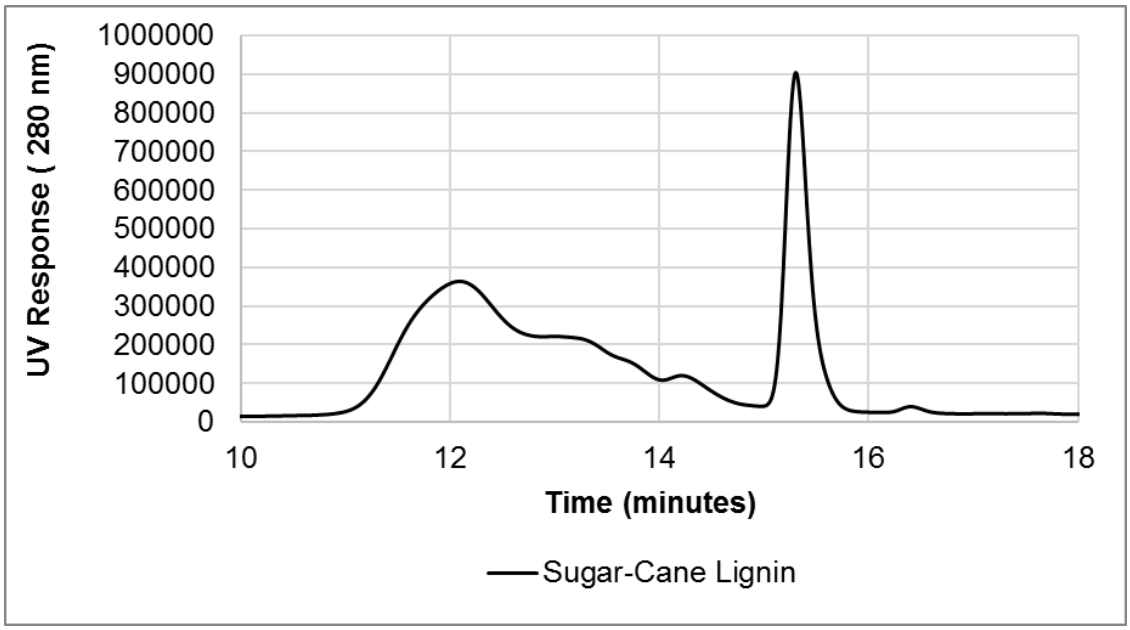

Figure 102 GPC profile of sugar-cane lignin

The molecular weight distribution plot is presented in Figure 103 GPC profile of birch parr-lignin. There was a small peak ~ 11 min and the highest peak ~ 12 min related to heavier molecules, the following peaks ~ 13 min are related to smaller fractions and solvent.

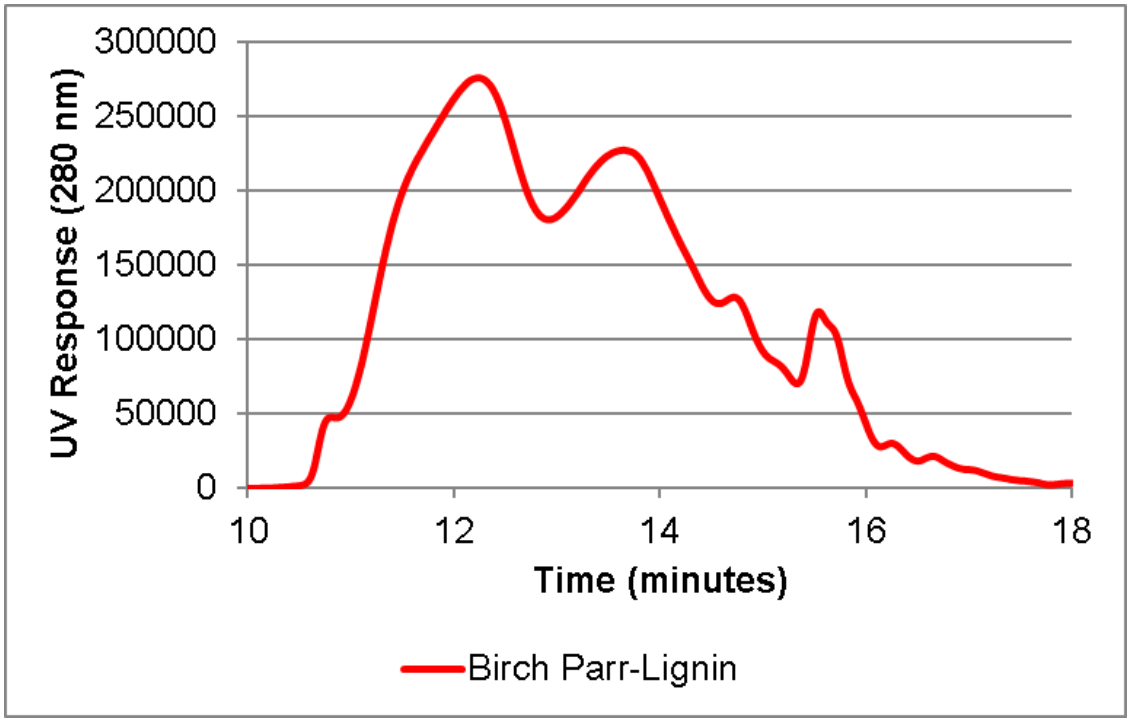

Figure 103 GPC profile of birch parr-lignin

The molecular weight distribution plot is presented in Figure 104. There was a main peak ~ 12 min and the smaller at ~ 13 min related to smaller fractions.

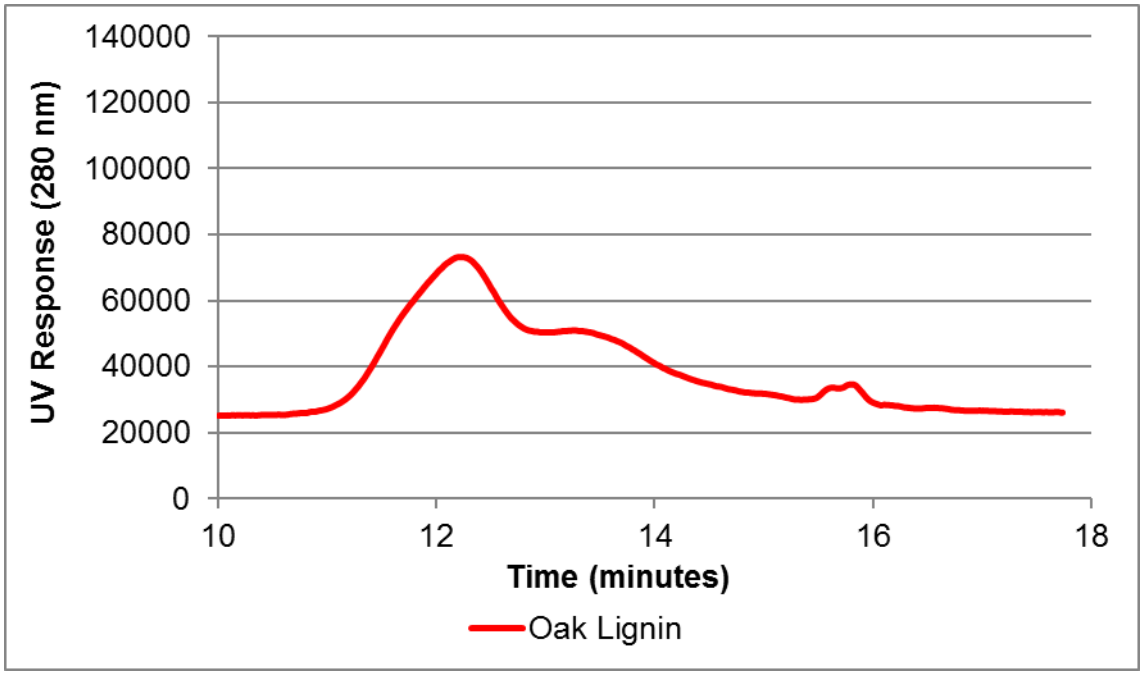

Figure 104 GPC profile of oak parr-lignin lignin

5.3 NMR analysis

This technique provided information about the bonds in lignin structure, monomer proportions (G: guaiacyl , S: syringyl and H: p-hydroxyphenyl) and the calculation of linkage percentages.

The samples were run in triplicate and the standard deviations calculated. In Figure 106 and Figure 107, the HSQC NMR spectrum of Kraft, sugar-cane and birch parr-lignins are shown. Chemical structures were colour coded according to the linkage they were associated to. Orange: H unit, blue: G unit and red: S unit.

5.3.1 Kraft lignin

It was found that only G units were present in the molecule and linkages such as β-β, β-5 and β-O-4. The linkages percentage is presented in Table 14 and Figure 105 presents the NMR spectrum.

Table 14 Kraft Lignin linkage content identified by 2D NMR. Standard deviation for β-O-4, β- β and β -5, 0.9, 0.4 and 0.4, respectively

Kraft lignin linkages		
β-O-4 (%)	**β-β (%)**	**β-5 (%)**
11	4.5	4.4

Figure 105 shows the HSQC NMR spectrum of Kraft lignin. Chemical structures are colour coded according to the linkage they are associated to. Orange: H unit, blue: G unit and red: S unit.

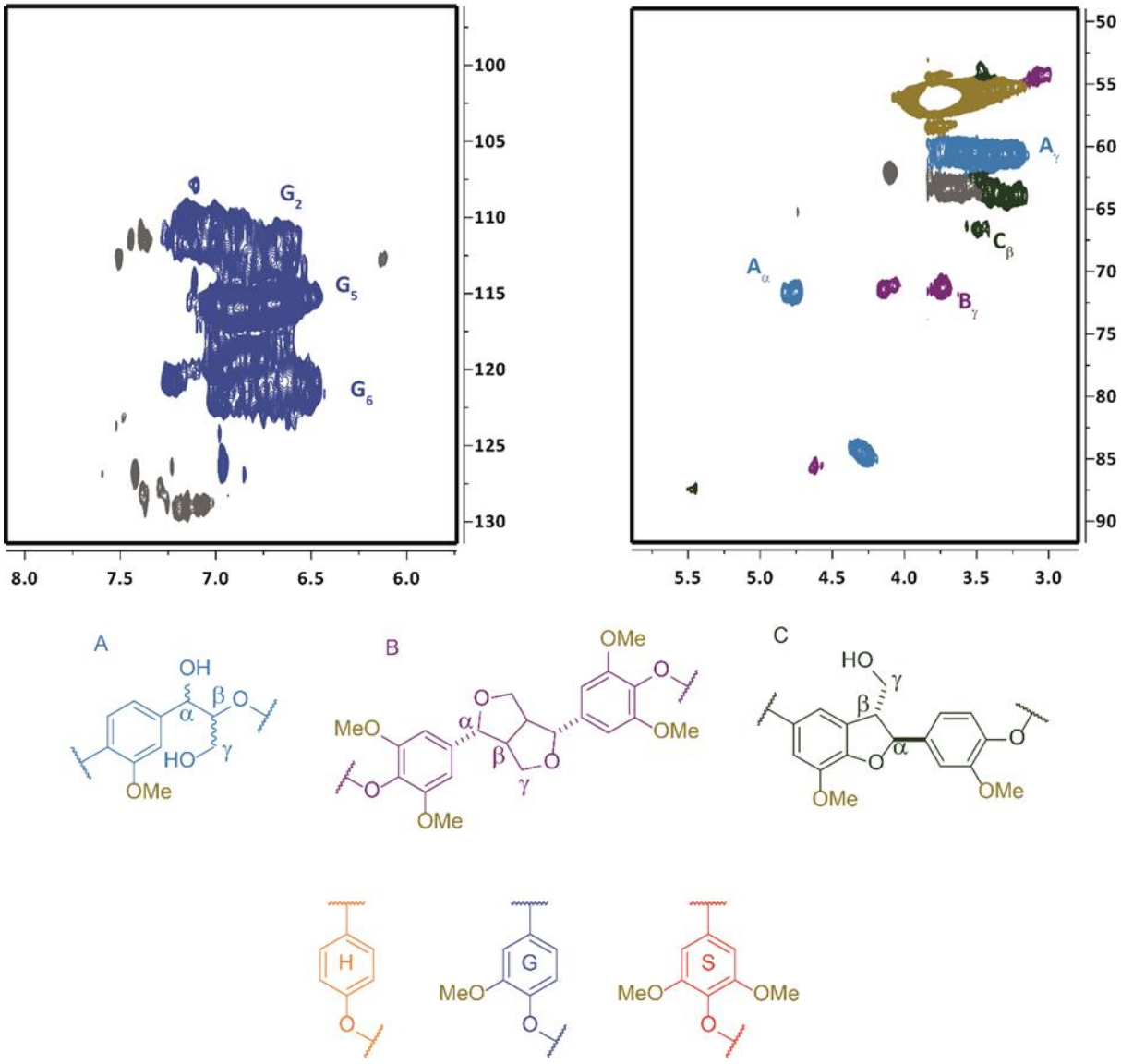

Figure 105 Regions from the 2D HSQC NMR spectra of the Kraft Lignin. Linkages identified: β-O-4, β-β and β-5

5.3.2 Sugar-cane lignin

It was found that this lignin had S, G and H units, and β-O-4, β-5 bonds and β-O-4(Et) linkages. This last linkage is typical of lignins extracted with ethanol, where the ethyl group can go to the molecule structure in the repolymerisation process (Section 7.1.2). Table 15 shows all linkages percentage and Figure 106 shows the HSQC NMR spectrum of sugar-cane lignin.

Table 15 Sugar-cane lignin units and linkage content identified by 2D NMR. Samples were analysed in triplicates. Standard deviation for units S, G and H were 0.16, 0.2, 0.3 and for β-O-4, B-O-4(Et) and B-5 1.1, 0.16, 0.22, respectively

Lignin unit			Linkage		
S (%)	**G (%)**	**H (%)**	**β-O-4 (%)**	**β-O-4 (Et) (%)**	**β-5 (%)**
73.6	17	9.4	37	7.0	5.0

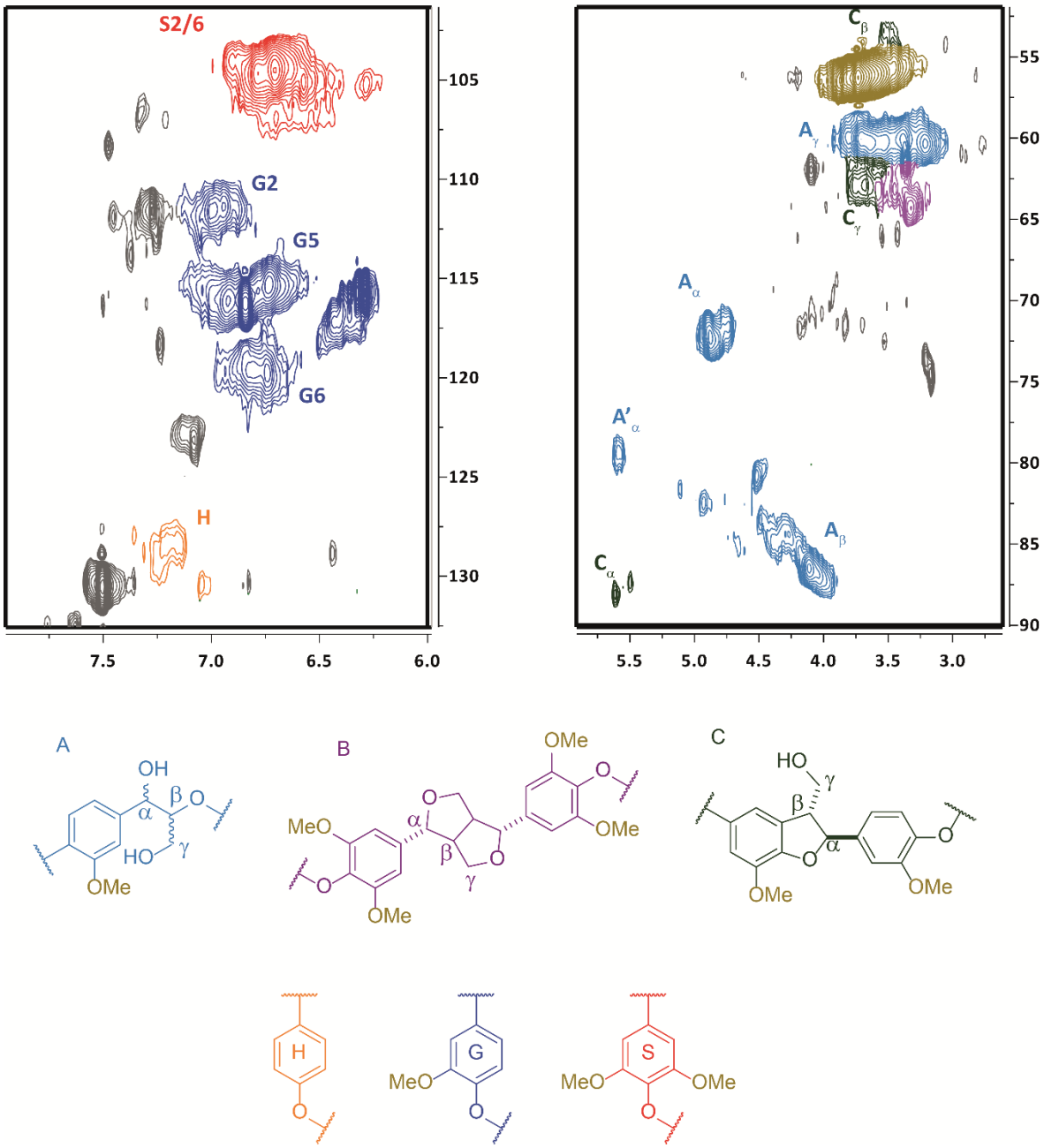

Figure 106 Regions from the 2D HSQC NMR spectra of the sugar-cane Lignin. Linkages identified: β-O-4, β-O-4(Et) and β-5.

5.3.3 Birch parr-lignin

The type of units and linkages in this lignin were identified and it had β-O-4, β-β and β-5 bonds, G and S units. These data are presented in Table 16.

Fraction 2 of Pt/Al_2O_3 catalysed reaction of birch parr-lignin was re-reacted to check if the reutilisation of Fraction 2 is advantageous in terms of fine chemicals obtainment. Before reaction, solvent was vapored off from Fraction 2 and the solid material was submitted to NMR analysis to see how it changed after reaction. Figure 108 shows that compared to the original lignin (Figure 107) the linkages were no longer present.

Table 16 Birch parr-lignin units and linkage content identified by 2D NMR. Samples were analysed in triplicates. Standard deviation for units S and G were 0.25, 0.25 and for β-O-4, β-5 and β-β 0.27, 0.41 and 0.40, respectively

Lignin Unit		Linkage		
S (%)	G (%)	β-O-4 (%)	β-5 (%)	β- β (%)
90	10	26	5	10

Figure 107 shows the HSQC NMR spectrum of birch parr-lignin. Chemical structures were colour coded according to the linkage they are associated to. Orange: H unit, blue: G unit and red: S unit.

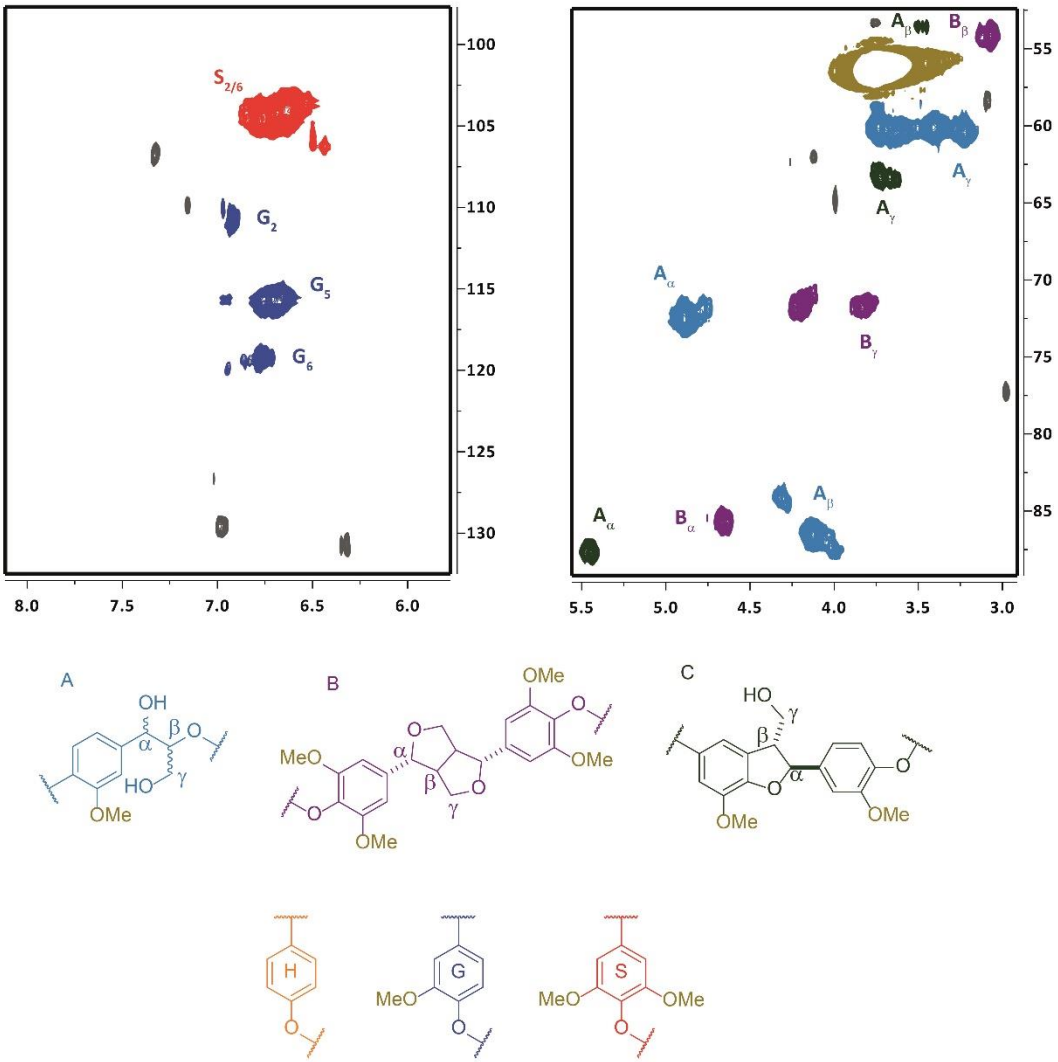

Figure 107 Regions from the 2D HSQC NMR spectra of the birch parr-lignin. Linkages identified: β-O-4, β-β and β-5.

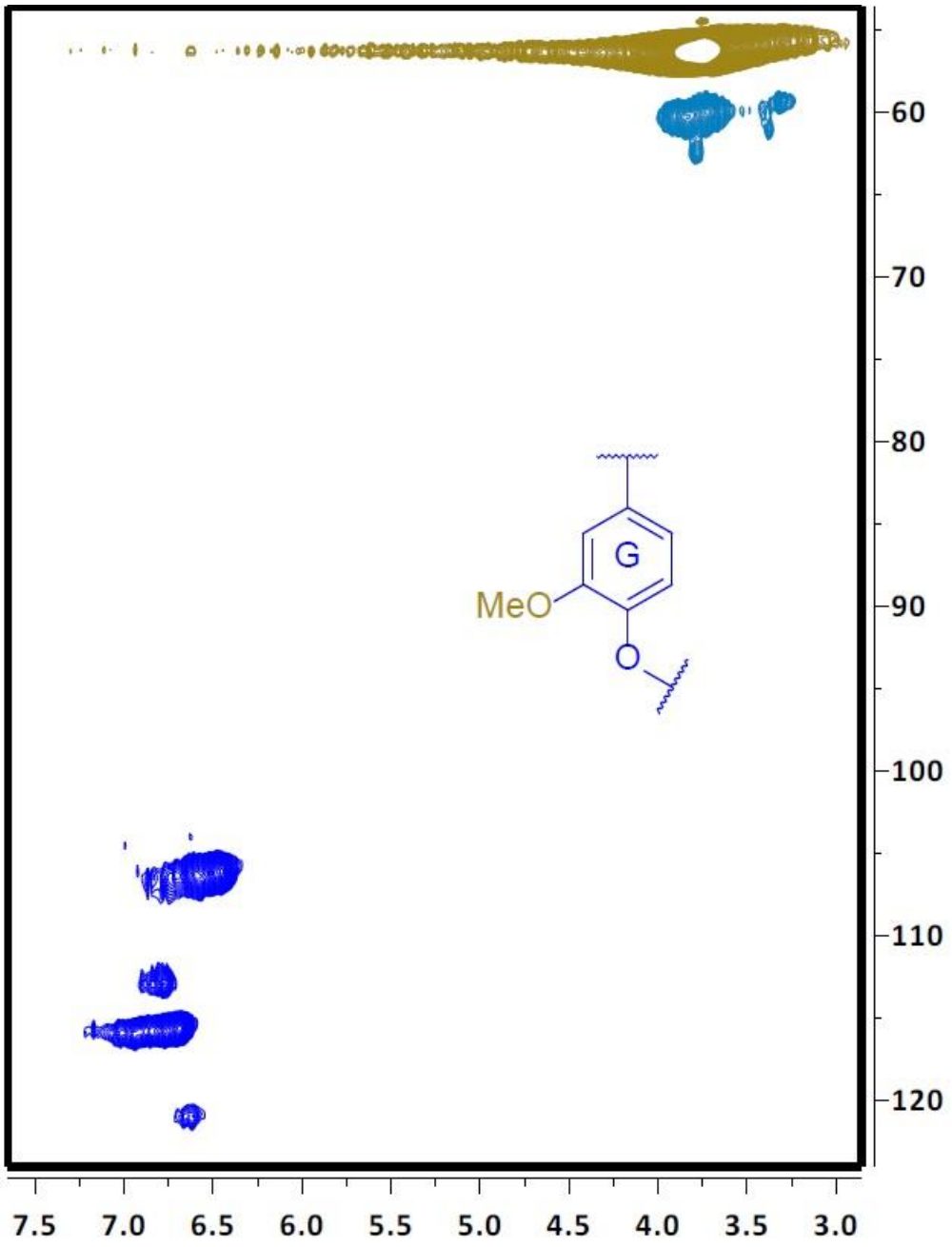

Figure 108 Regions from the 2D HSQC NMR spectra of the HF birch parr-lignin. There were no linkages identified.

6 Depolymerisation reactions of Kraft and isolated lignins

6.1 Kraft lignin

The pre-treatment used to obtain Kraft lignin can cause depletion of the original bonds in the native molecule, leading to the formation of linkages harder to cleave [97]. Therefore, reactions such as hydrogenolysis may require harsher conditions, such as high temperature and pressure. Previous studies at The University of Glasgow, showed that at 573 K and 20 bar of hydrogen using a Parr Autoclave reactor, heterogeneous catalysts and alcoholic solvents in mixture with water, resulted in different reaction yields of monomeric compounds (fine chemicals) from Kraft lignin depolymerisation. The research also presented that an increase in temperature or stirring did not affect dramatically the overall yields of the products. The reaction conditions of 573 K, 20 bar of hydrogen and 1000 rpm were the most reasonable for these experiments [26].

Hence, the following sections show the results of Kraft lignin depolymerisation at high temperature and pressure, in the presence of different solvent mixtures (ethanol, isopropanol, acetone and water) and alumina supported catalysts (Pt/Al_2O_3 and Rh/Al_2O_3).

The reaction products were identified by GC-MS and are labelled in the Figures as follows: (1) 2-methoxyphenol, (2) 4-methyl-2-methoxyphenol (3) 4-ethyl-2-methoxyphenol, (4) 4-propyl-2-methoxyphenol, (5) 1,2-dihydroxybenzene, (6) 4-ethylbenzene-1,2-diol, (7) 4-(3-hydroxypropyl)-2-methoxyphenol (8) 4-(3-methoxypropyl)-2-methoxyphenol.

6.1.1.1 Non-catalytic depolymerisation of Kraft lignin

It has been reported that Kraft lignin can depolymerise resulting in alkyl phenolic compounds in the presence of solvent, at high hydrogen pressure and temperature [26][2].

Initially, it was of interest of this research to study the effects of different solvent mixtures in various proportions with water (acetone/H_2O, EtOH/H_2O and IPA/H_2O, 25:75, 50:50, 75:25 v/v), hydrogen (20 bar) and temperature (573 K) without a catalyst.

Figure 109 shows the reactions in the presence of EtOH/H_2O mixtures (25/75, 50:50, 75:25 v/v). The overall yields were 9, 9.5 and 11.5 g/100 g, respectively. Alkyl phenolic compounds were generated in this solvolysis and the increase of ethanol in the solvent

mixture resulted in more products being obtained. Compound 1 presented the higher yields in all experiments while compound 7 the lower values. Different reaction mixtures did not show identical products distribution. The EtOH/H_2O 50:50 v/v had higher yield for compound 5, although EtOH/H_2O 75:25v/v produced more of compounds 1, 4 and 8.

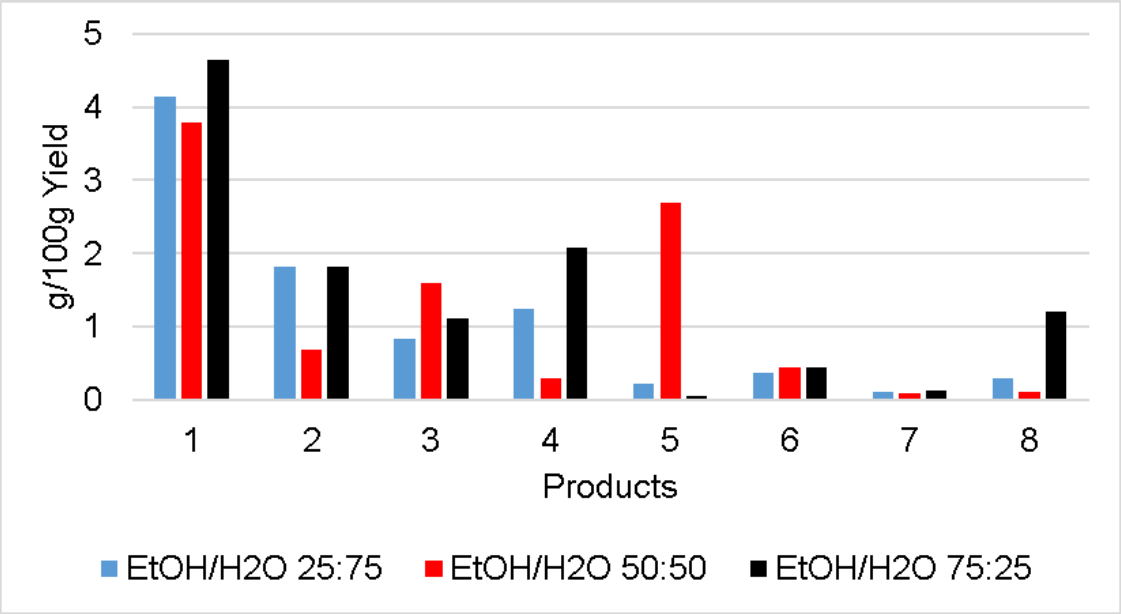

Figure 109 Kraft lignin depolymerisation in the presence of EtOH/H_2O mixture in different proportions (25:75, 50:50, 75:25 v/v).

Figure 110 presents the results with IPA/H_2O mixtures (25:75, 50:50, 75:25 v/v). The overall yields were 9.6, 5.6 and 6.4 g/100 g. In these reactions, 2-methoxyphenol (1) also showed the major yields. The 25:75 v/v mixture was the best solution, as all compounds were in higher quantities, especially 2-methoxyphenol (1) and 4-methyl-2-methoxyphenol (2). Comparing the mixtures with 50 % and 75 % of IPA, just two showed a significant difference in yield.

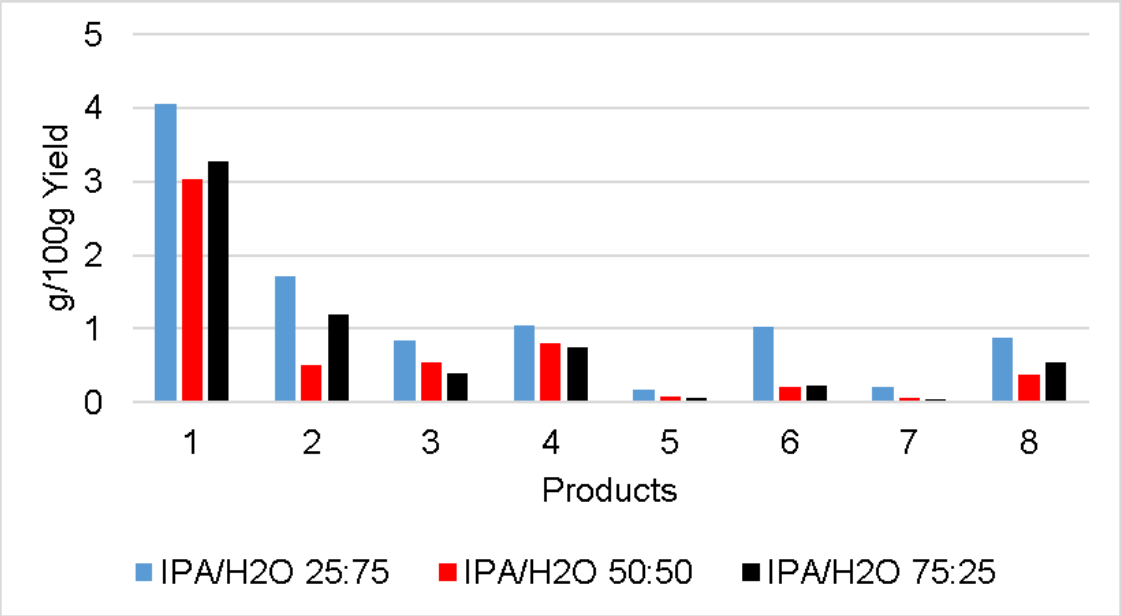

Figure 110 Kraft lignin depolymerisation in the presence of IPA/H_2O mixture in different proportions (25:75, 50:50, 75:25 v/v).

The reactions in the presence of acetone/H_2O (25:75, 50:50, 75:25 v/v) are shown in the Figure below. The overall yields were 10.5, 8.6, 8.9 g/100 g. Compounds 1, 2 and 4 had better results, especially the 2-methoxyphenol (1) with 25:75 v/v acetone mixture. Compounds 5, 6 and 7 had the lowest values for all reactions. For the other products, the change in acetone percentage did not affect dramatically the molecules generation, as there were no significant high yields.

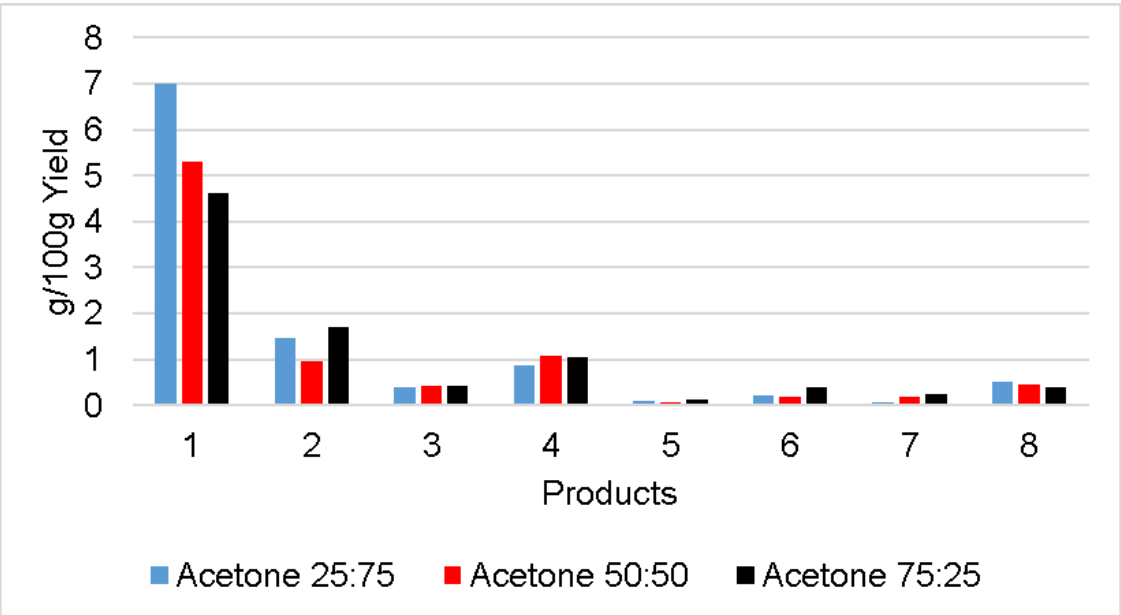

Figure 111 Kraft lignin depolymerisation in the presence of acetone/H2O mixture in different proportions (25:75, 50:50, 75:25 v/v).

6.1.1.2 Catalytic depolymerisation of Kraft lignin

Literature shows the relevance of precious metals (especially Rh and Pt) supported on alumina, for lignin depolymerisation. They affected product distribution and overall yields of reactions [4]. Therefore, the influence of Pt/Al_2O_3 and Rh/Al_2O_3 catalysts in the hydrogenolysis of Kraft lignin was investigated using the reference solutions and the same reaction conditions.

6.1.1.3 Effect of alumina support

In order to analyse if the alumina support was participating in the reactions, the $EtOH/H_2O$, IPA/H_2O and $Acetone/H_2O$ 50:50 v/v solutions were used in the presence of Al_2O_3 support and Kraft lignin. The overall yields were 9.7, 6.9 and 8.7 g/100 g, respectively. Figure 112, Figure 113 and Figure 114 show product distribution and includes the reference reactions for comparison.

According to Figure 112, parallel to the reference experiment, the yields of compounds 4, 7 and 8 significantly increased with Al_2O_3. The 4-(3-hydroxypropyl)-2-methoxyphenol (7) had the major yield and 4-ethylbenzene-1,2-diol (6) the lowest, moreover, 1, 3 and 5 generation was not favoured by the support. Figure 113 shows that the addition of Al_2O_3 in the reaction increased the yields of compounds 1, 2, 3 and 4 while the other molecules did not show considerable changes. Lastly, in Figure 114 the addition of support improved the production of 3, 4 and 6. Compounds 5 and 7 had the lowest yields and the Al_2O_3 practically did not affect the values. The highest yields were related to 2-methoxyphenol (1) in most reactions.

Different solvent mixtures showed different product distributions not only in the reference reactions (Section 6.1.1.1), but also in the presence of Al_2O_3. Depending on the experiment, the support increased the yield of individual molecules. Hence, this data pointed out that the alumina support presented catalytic activity and it was not inert in the reactions of Kraft lignin depolymerisation.

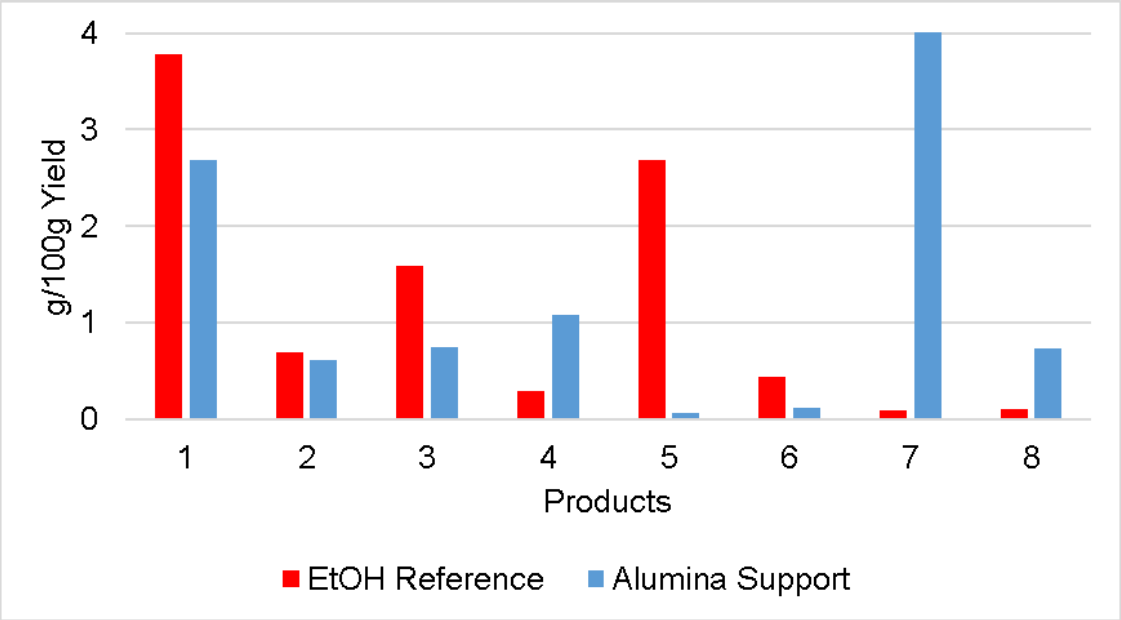

Figure 112 Depolymerisation of Kraft lignin in the presence of Al_2O_3 support and EtOH/H_2O mixture (50:50 v/v).

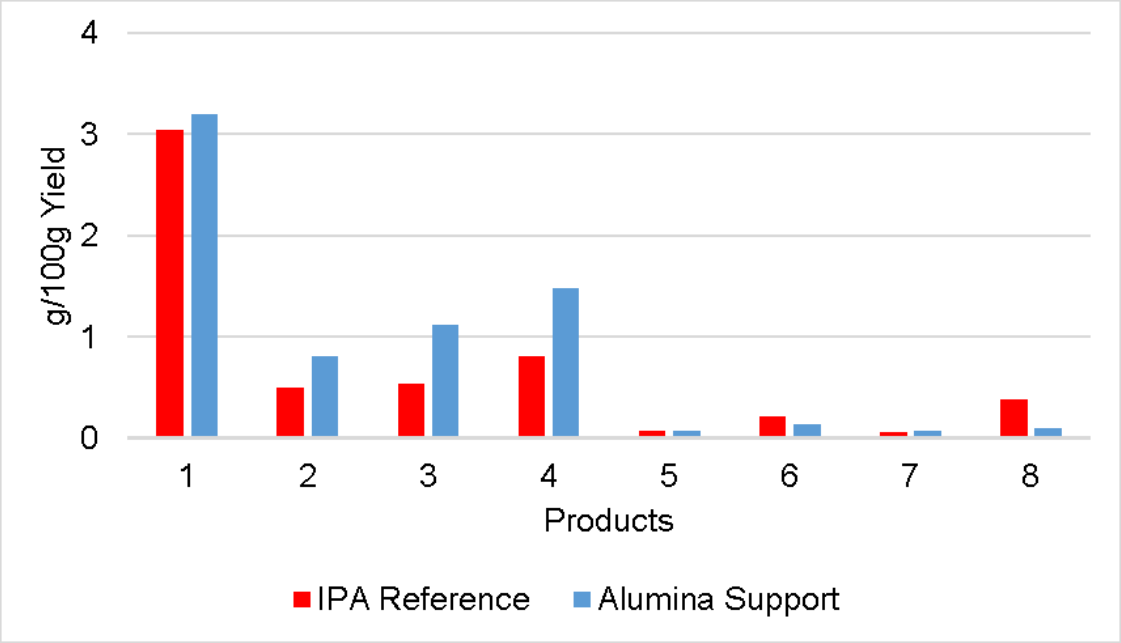

Figure 113 Depolymerisation of Kraft lignin in the presence of Al_2O_3 support and IPA/H_2O mixture (50:50 v/v).

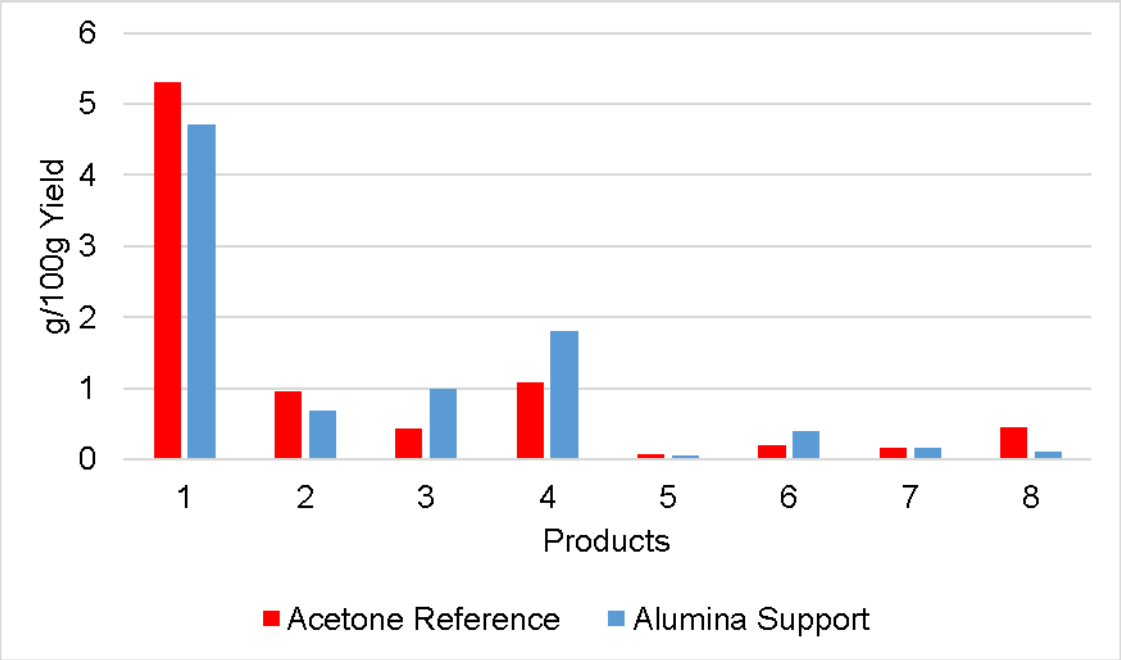

Figure 114 Depolymerisation of Kraft lignin in the presence of Al_2O_3 support and Acetone/H_2O mixture (50:50 v/v).

6.1.1.4 Reactions in the presence of Pt/Al_2O_3

The effects of Pt/Al_2O_3 in the hydrogenolysis of Kraft lignin are presented in this section. For all reactions, 2-methoxyphenol was the major product.

Figure 115 displays the product distribution of EtOH/H_2O (25:75, 50:50, 75:25 v/v) catalysed reactions. The overall yields were 7.9, 6.8, 8.5 g/100 g, respectively. Compounds 1, 2, 3 and 5 showed an increase in yield with 75 % of EtOH in solution and for most products, the 25 and 50 % mixtures did not cause high changes in yields, apart from compound 2. Comparing with the reference (Figure 109), the addition of Pt/Al_2O_3 changed product distribution. Molecule 6 had its yield increased with catalyst, while Compound 4 and 8 only for mixtures with 25 and 50 % of ethanol.

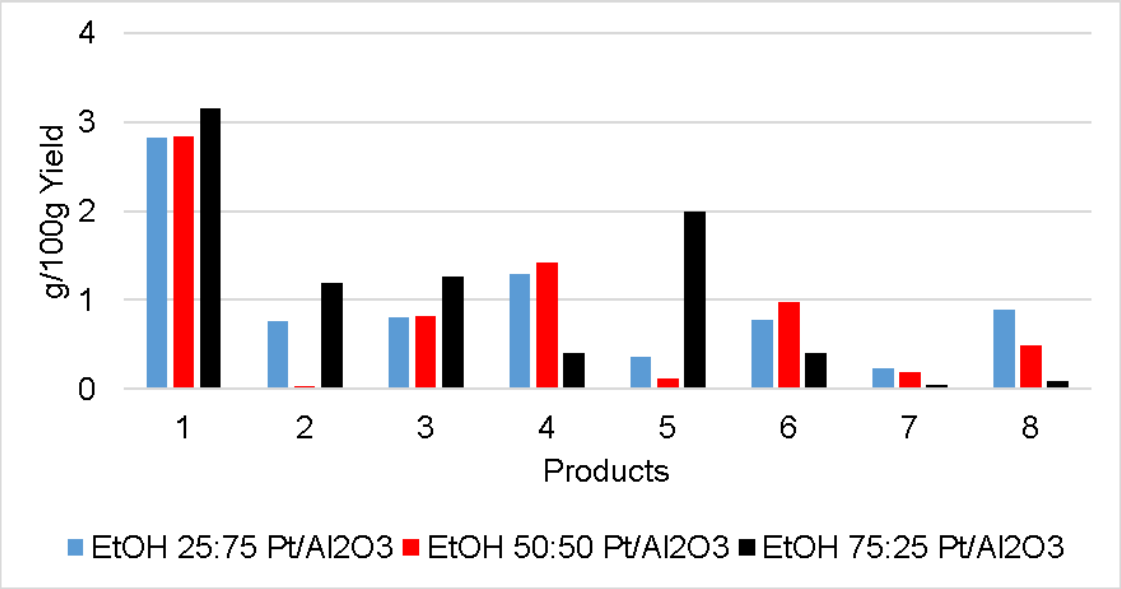

Figure 115 Pt/Al_2O_3 Catalysed depolymerisation of Kraft lignin in the presence of various EtOH/H_2O mixtures (25:75, 50:50, 75:25 v/v).

Figure 116 shows results of IPA catalysed reactions. The overall yields were 8.5, 5.6 and 6.5 g/100 g. Compounds 1, 2, 3 and 5 with 25 % IPA presented the higher yields while 7 had the lowest. Related to the reference (Figure 110) 2-methoxyphenol (1) had slightly lower yields, however, the addition of Pt/Al_2O_3 increased the yields of 4-propyl-2-methoxyphenol (3) for all reactions and 1,2-dihydroxybenzene (5) with 25 % of IPA.

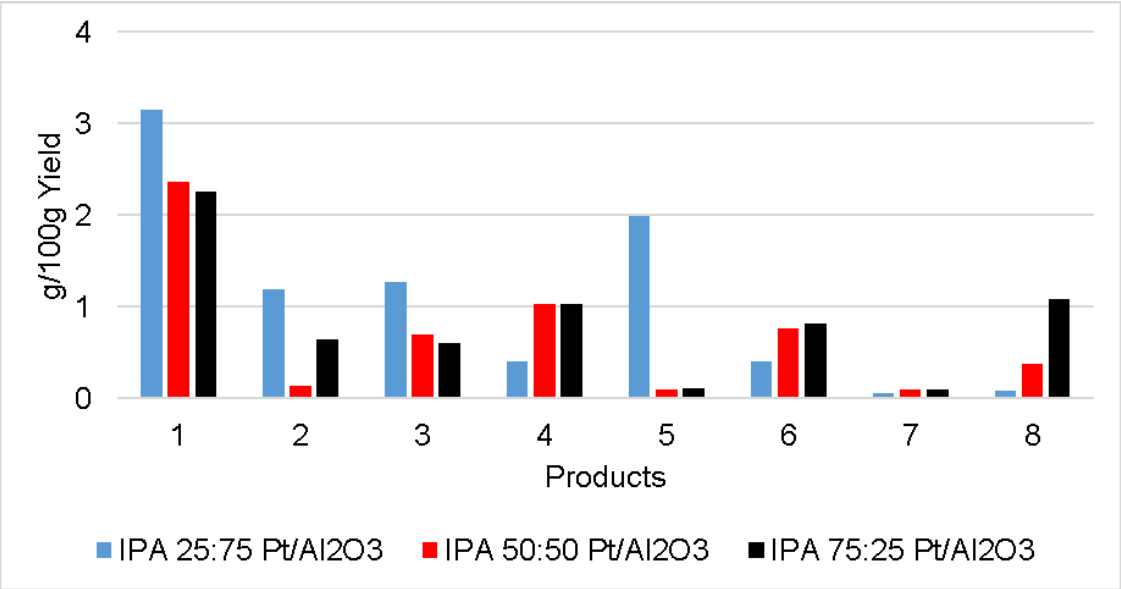

Figure 116 Pt/Al_2O_3 Catalysed depolymerisation of Kraft lignin in the presence of various IPA/H_2O mixtures (25:75, 50:50, 75:25 v/v).

Figure 117 represents the catalysed reactions for acetone/H_2O mixtures. The overall yields were 7.1, 7, and 9.7 g/100 g. The 2-methoxyphenol (1) was the major product and the reaction in the presence of 25 % acetone influenced more in its generation. The 25 and 50 % solutions, did not affect considerably most products. For all other molecules, 75 % acetone contributed to an intensification in their yields. This data showed that the decrease in water in the solution favoured more product generation. Compared to the reference (Figure 111), the addition of Pt/Al_2O_3 influenced product distribution. It enhanced the yields of molecules 4, 6 in all reactions and 8 with 75 % acetone, whereas, for 5 and 7 the catalyst did not show significant influence in the values.

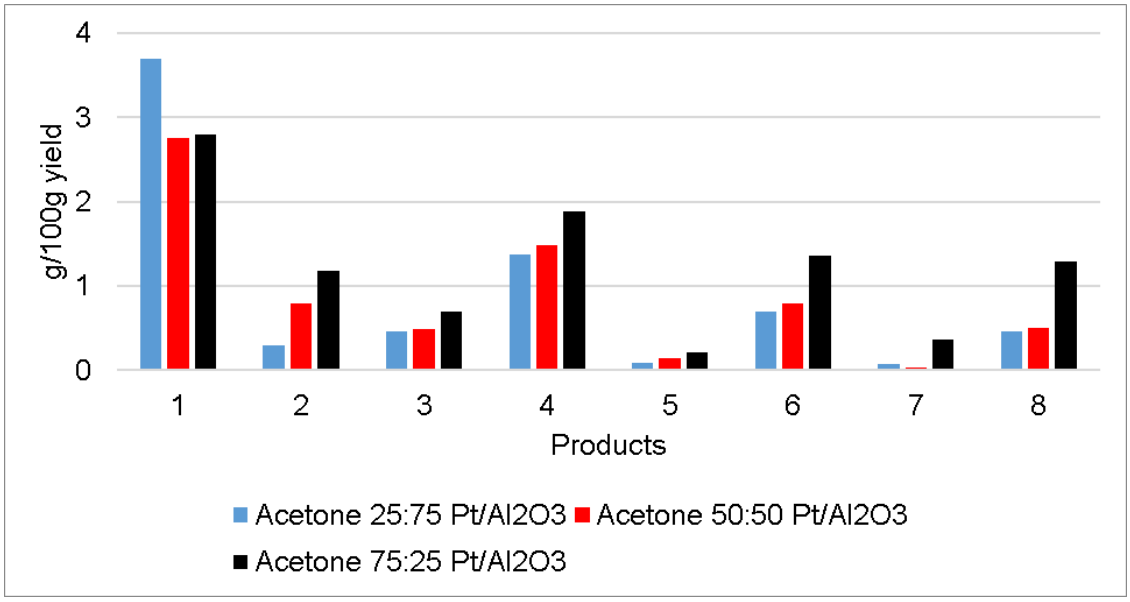

Figure 117 Pt/Al_2O_3 Catalysed depolymerisation of Kraft lignin in the presence of various Acetone/H_2O mixtures (25:75, 50:50, 75:25 v/v).

6.1.1.5 Reactions in the presence of Rh/Al_2O_3

In Figure 118, compound 1 and 4 showed higher yields with 50 % of EtOH, while products 2 and 8 with 75 % of alcohol. Compared to the reference reactions (Figure 109) compound 4 and 8 increased their yields with Rh/Al_2O_3 and 50 % of EtOH. The overall yields were 6.5, 7.3 and 6.6 g/100 g.

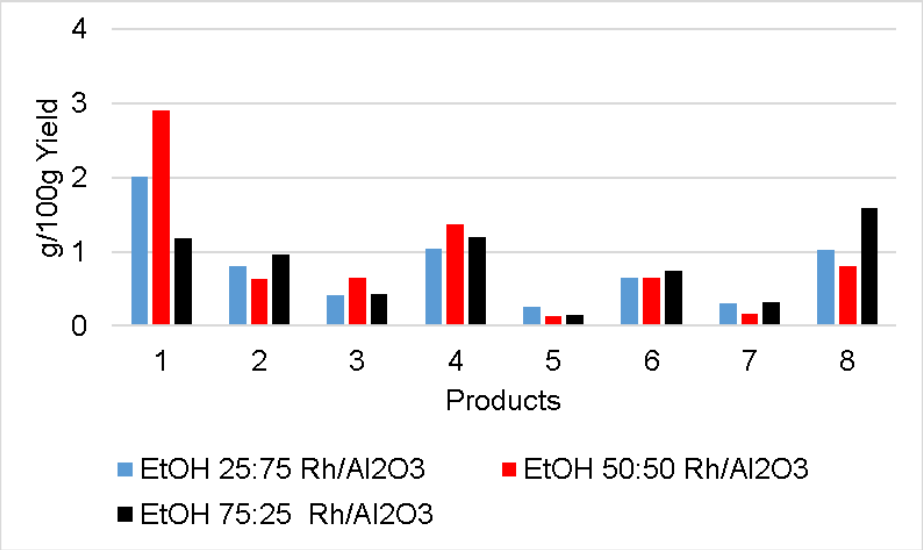

Figure 118 Rh/Al_2O_3 Catalysed depolymerisation of Kraft lignin in the presence of various $EtOH/H_2O$ mixtures (25:75, 50:50, 75:25 v/v).

Figure 119 shows the reactions with IPA/H_2O solutions. The overall yields were 6.5, 10.2 and 7.3 g/100 g. Products 1, 4 and 6 were favoured in the presence of 50 % IPA mixture, while compound 5 had higher yield with 75 % IPA. Apart from compound 2, the 25 % isopropanol reactions did not show significant changes in the products yields. Compared to the reference (Figure 110) molecules 3, 4, 5, 6 and 8 were favoured in terms of yields by the addition of catalyst.

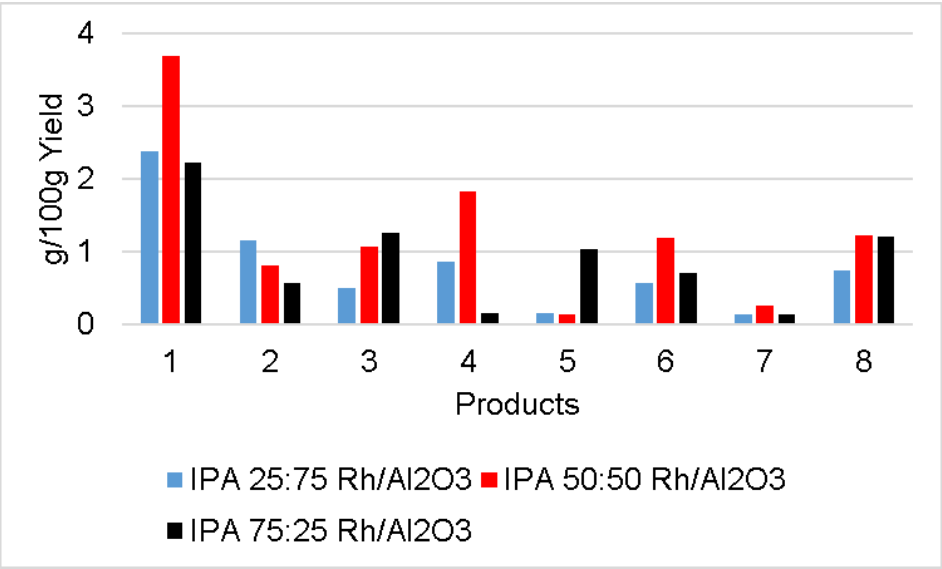

Figure 119 Rh/Al2O3 Catalysed depolymerisation of Kraft lignin in the presence of various IPA/H2O mixtures (25:75, 50:50, 75:25 v/v).

The experiments with acetone/water solutions are shown in Figure 120. 2-methoxyphenol (1) reached the highest yields with 50 % acetone mixture, followed by 6 and 8 with 75 % acetone. The products 5 and 8 could not be detected when 50 % solution was used and 6 and 7 were produced in very low quantities. The overall yields were 9.4, 9.7 and 6.2 g/100 g.

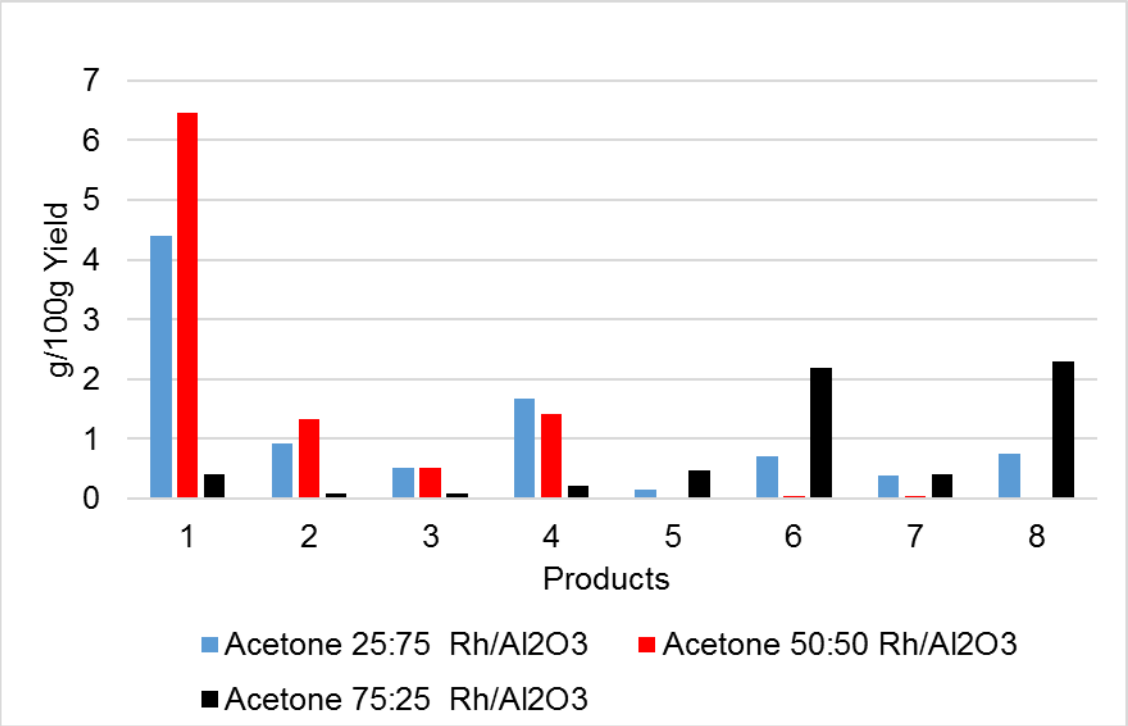

Figure 120 Rh/Al_2O_3 Catalysed depolymerisation of Kraft lignin in the presence of various Acetone/H_2O mixtures (25:75, 50:50, 75:25 v/v).

Despite some solutions with higher content of solvent (proportion solvent/water 75:25 v/v) providing considerable yields for some catalysed and non-catalysed reactions, it is still not a viable process. The reason for this conclusion is that after the completion of the reaction, the high amount of char formation made catalyst recovery not possible, the residues with the catalyst were attached in the reactor vessel and stirrer making it difficult to remove. It may be related to part of the lignin fragments reacting and, the other part polymerising during the experiment in contrast to dissolving into solution.

6.1.1.6 GPC characterisation of reactions

In order to analyse the changes in Mw, Mn and Ip after depolymerisation of lignin, a selection of six experiments were studied. They were in the presence of EtOH/H_2O, IPA/H_2O and Acetone/H_2O 50:50 v/v with and without Pt/Al_2O_3 and compared to the original Kraft lignin. The values can be found in Table 17 and Figure 121, Figure 122 and Figure 123 show the GPC profile for these experiments.

Table 17 GPC analysis for Kraft lignin reactions

Reaction type		Molecular Weight (Mw)	Molecular Number (Mn)	Polydispersity (Ip)
A	Kraft lignin	4973	1236	4.0
B	EtOH/H_2O Reference	1296	589	2.2
C	EtOH/H_2O Catalysed	1390	650	2.1
D	IPA/H_2O Reference	1155	584	1.9
E	IPA/H_2O Catalysed	1029	571	1.8
F	Acetone/H_2O Reference	879	458	1.9
G	Acetone/H_2O Catalysed	968	510	1.8

Table 17 shows that compared to the original Kraft lignin, the Mw, Mn and Ip values for the reactions were considerably lower. This was expected as the depolymerisation of Kraft lignin by a solvent or a metal based catalyst can provide the total or partial cleavage of C-O-C or C-C bonds in the molecule [98], hence changing these properties. Comparing reference and catalysed experiments for each solvent mixtures, there were not dramatic differences in values. In Table 17, the lowest Mw was for reaction F and the higher for C while Mn had the smallest values for F and major for C. In addition, the Ip did not change significantly.

In Figure 121, Figure 122 and Figure 123 the Kraft lignin Mw profile was included. The exact compounds or fragments related to the peaks could not be detected due to fluctuations in peak width and discrepancy of UV responses between the molecules. In order to identify and quantify compounds, a GC-MS was used. Therefore, the information obtained from GPC was the estimative of Mw distribution and not of specific compounds. For the reactions, all figures were shifted to the right, which is related to lower molecular weight products. This

was presumed as in Table 17 the Mw values dropped for the reactions. The decrease in Mw is also indicated by the lower peak intensity of the high Mw fraction at 13-14 min in Figure 121 and Figure 123, especially in catalysed reactions, with the exception of a relative abundance of the Mw fraction eluting at 13-14 min in the catalysed IPA reaction.

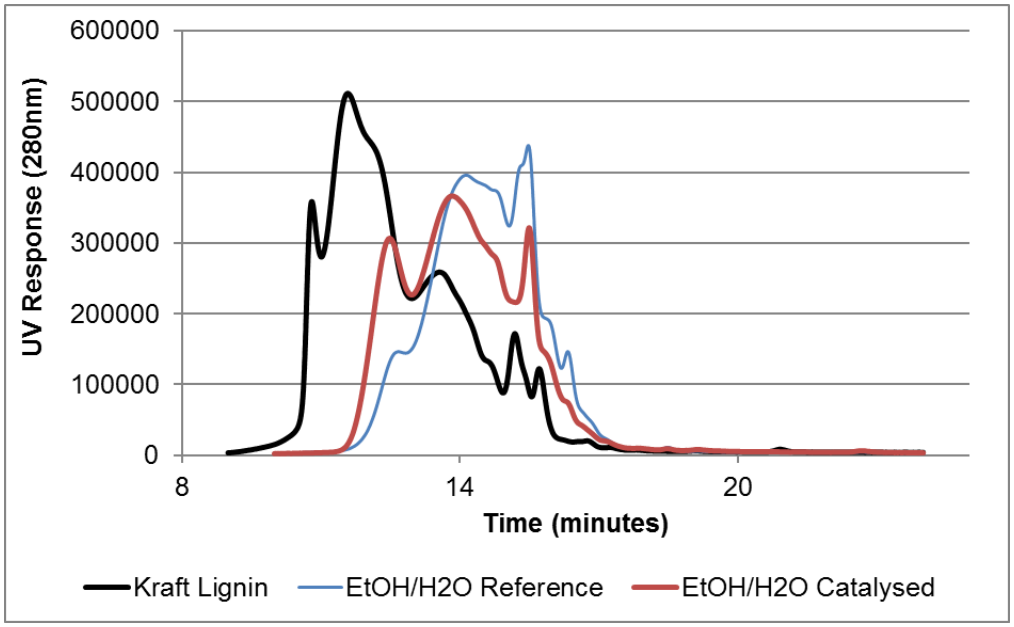

Figure 121 GPC profile for Kraft lignin, EtOH/H_2O reference and catalysed reactions.

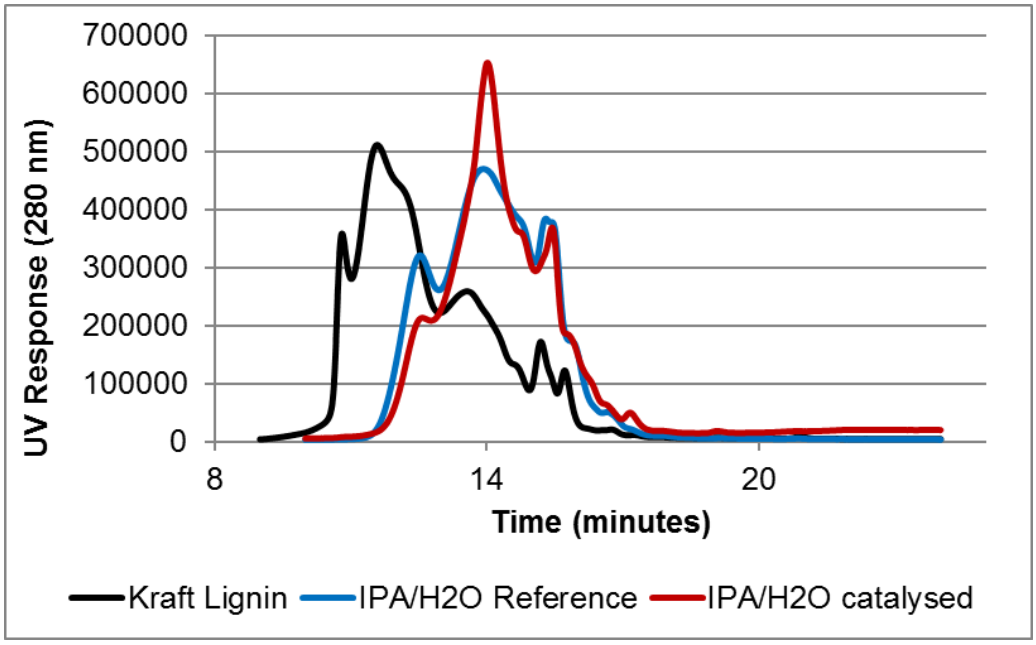

Figure 122 GPC profile for Kraft lignin, IPA/H_2O reference and catalysed reactions.

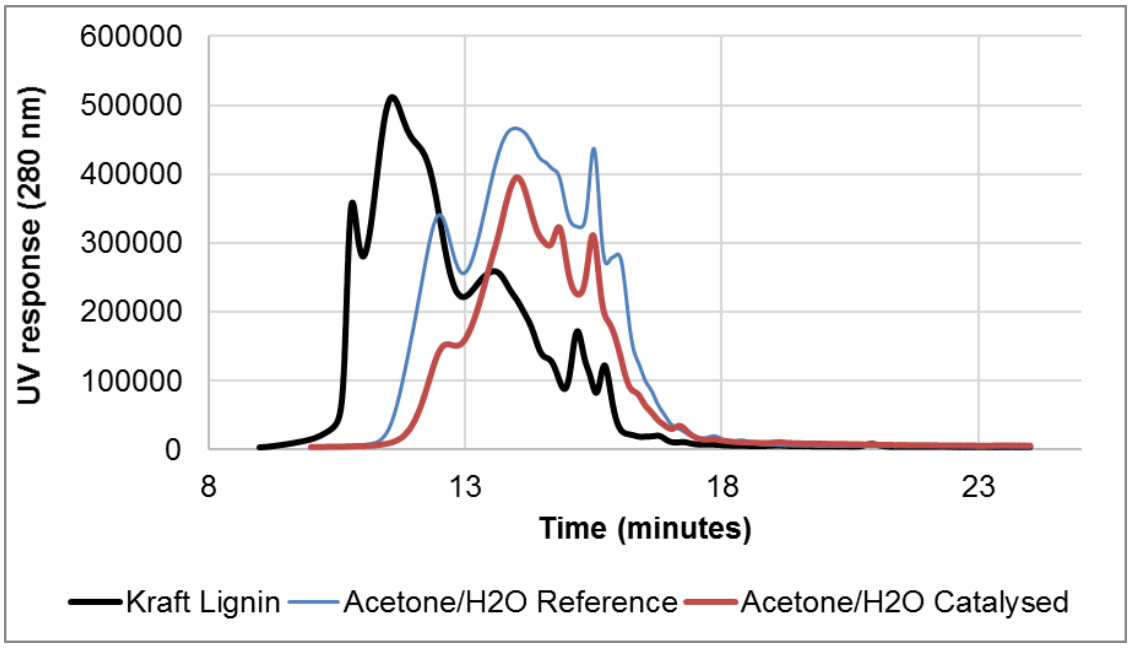

Figure 123 GPC profile for Kraft lignin, Acetone/H_2O reference and catalysed reactions.

6.1.1.7 Isotopic labelling studies of Kraft lignin

Section 6.1.1.1 and 6.1.1.2 presented the effects of solvent and catalyst addition in Kraft lignin depolymerisation. They showed that just the use of solvent resulted in the production of fine chemicals. Despite the similarity in overall yields between catalysed and non-catalysed reactions, the addition of catalyst in the system affected product distribution and yields of individual compounds. Therefore, each catalyst influenced the reaction differently depending on the type of solvent mixture used.

In general, the KIE values, obtained when the isotopic label is in the solvent, may signify three different situations: 1) Positive kinetic isotopic effect (PKIE), $K_H/K_D>1$, where the solvent could be acting as a reactant, 2) Inverse kinetic isotopic effect (IKIE), with solvent not directly involved in products formation, $K_H/K_D<1$, and 3) Non-kinetic isotopic effect, $K_H/K_D=1$, which the solvent was not involved in the compound generation [99].

In the literature, solvent effects (methanol/water 50:50 v/v) and gas (H_2) were evaluated in Kraft lignin depolymerisation by using their deuterated forms and Pt/Al_2O_3 catalyst. The study showed that the monomeric products can present values of PKIE or IKIE, indicating that the reaction mechanism is not simple and different steps can be involved in products formation [26].

Continuing the work of Dr. McVeigh (2016), this research shows a systematic study on the Kinetic Isotopic effect, evaluating a non-alcoholic solvent (acetone) in mixture with water (50:50 v/v), gas (H_2, 20 bar) and catalyst (Pt/Al_2O_3) involvement in Kraft lignin depolymerisation. The study consisted in a fully deuterated catalysed experiment (FDC), which solvent and gas were in their deuterated forms, a partially deuterated catalysed experiment (PDC), where hydrogen was kept as H_2 (g), and a fully deuterated non-catalysed experiment (FDNC) with all components in their deuterated forms without catalyst. These results could provide information about mechanistic pathways involved in the obtainment of fine chemicals from Kraft lignin.

The experimental procedure for the isotopic reactions were the same as that used for protiated experiments (Section 3.3.2).

The results of the isotopic reactions are described in Figure 124 and Table 18.

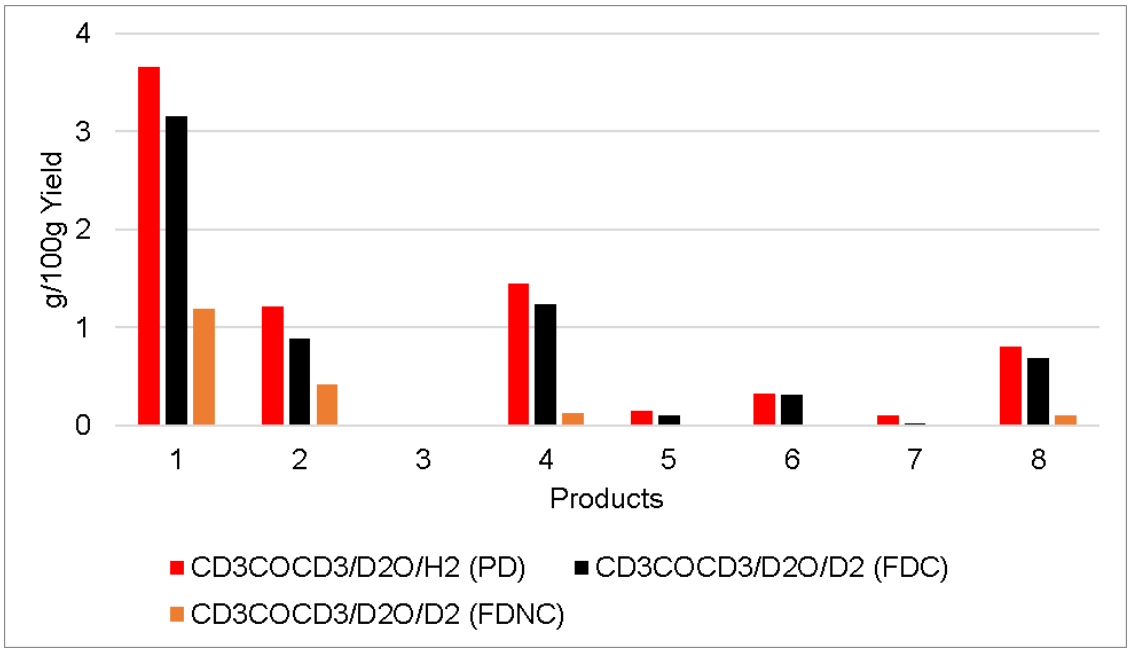

Figure 124 Partially protiated and fully protiated experiments in the presence of Pt/Al_2O_3 catalyst.

Figure 124 shows the yields for each molecule after PDC, FDC and FDNC experiments. The overall yields were 7.7, 6.4 and 1.9 g/100 g. Compound 3 was not identified among the products of PDC and FDC, while 3, 5, 6 and 7 could not be detected in the FDNC experiment.

It was found that the increase in yield of most aromatic monomers was given as PDC >FDC > FDNC. 2-methoxphenol (compound 1) had the highest yield, especially in a PDC experiment. The absence of catalyst in the FDNC significantly decreased the compounds yields. This resulted in high PKIE values (Table 18). However, when the catalyst was in the system (FDC) these yields increased.

After the experiments, all products had deuterium (D) incorporated to the molecules. Table 18 presents the number of incorporated D atoms (NIDA) identified by MS in each product. The NIDA does not change from a partially deuterated to the fully deuterated reactions. The position of each deuterium atom in the molecules 2-methoxyphenol and 4-(3-hydroxypropyl)-2-methoxyphenol could be identified and are shown in Figure 125. In these two molecules, the deuterium was found in the ring. However, in certain compounds, the deuterium position can be identified in the alkyl groups (Section 7.4).

Table 18 summarises the Kinetic Isotopic Effect of each individual compound and the number of incorporated deuterium atoms. The non-detected compounds were labelled as ND.

Table 18 KIE and NIDA values for partially deuterated (PDC), fully catalysed deuterated (FCD) and fully non-catalysed deuterated (FNCD) reactions of Kraft lignin. Non-detected compounds (ND).

	Experiment			
	PDC	FDC	FDNC	
Monomer	KIE values			NIDA
1	0.8	0.8	4.4	2
2	0.7	1	ND	4
3	ND	ND	8.3	5
4	1.0	1.2	ND	5
5	1.0	1.3	2.3	7
6	2.4	2.5	ND	5
7	0.4	1.7	4.2	7
8	0.6	0.7	ND	1

According to Table 18, for all reactions, most molecules presented different KIE. In the PDC reaction, compounds 1, 2 and 8 showed very similar values of IKIE, compound 7 showed a high IKIE, while 4 and 5 did not present any KIE.

In the FDC experiment, D_2 gas was added to the system. Comparing to PDC, molecules 7 changed from IKIE to PKIE and 2 did not show KIE. The variations in the values for the other molecules were not significantly high.

The FDNC values for KIE were considerably different of FDNC and PDC reactions. Four molecules were not identified among products (2, 4, 6 and 8) and there were high values of positive kinetic isotopic effects for all other molecules, especially 4-ethyl-2-methoxyphenol (3), which shows the high involvement of solvent in the rate determining step of their formation. Hence, the catalysed and non-catalysed reactions pursue different reaction mechanisms. The simple change in solvent, gas or the addition of catalyst affected the rate-determining step of products formation.

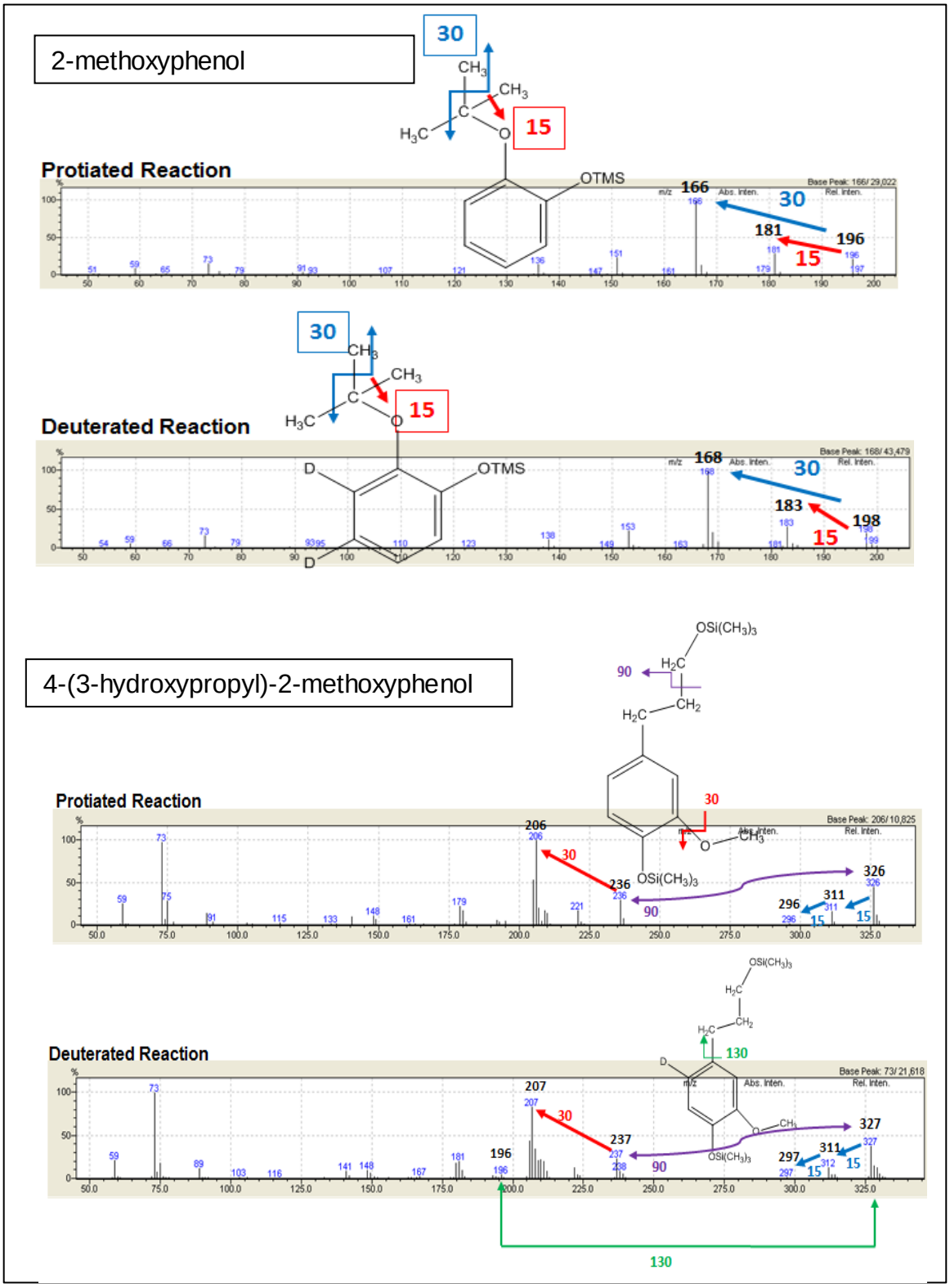

Figure 125 Added deuterium atoms onto 2-methoxyphenol and 4-(3-hydroxypropyl)-2-methoxyphenol.

6.2 Sugar-cane lignin

Due to the minor amount of sugar-cane lignin available for the experiments, only the non-alcoholic solvent (acetone) in mixture with water (50:50 v/v) along with the alumina supported catalysts (Pt/Al_2O_3, Rh/Al_2O_3, Ni/Al_2O_3 and Fe/Al_2O_3) were selected for hydrogenolysis. The choice of this solvent was especially because the use of alcohols in lignin extraction methods or depolymerisation reactions has been widely investigated over the past years. This allows exploring other alternative solvent. In addition, the alumina catalysts were selected since they could be recovered, in contrary to the carbon and zirconia materials.

6.2.1 Non-catalytic and catalytic depolymerisation

A reaction using only the solvent mixture, high temperature and gas was performed as a reference reaction. The experiment was also carried out in the presence of Al_2O_3 with the aim of investigating if the alumina support presented catalytic activity. Figure 126 shows the results and includes the reference reaction for comparison. For the reference experiment, compound 7 had the highest yield while compounds 2, 8 and 15 were not detected among products.

In the presence of Al_2O_3, the molecules 2A and 14 were not observed, however, 9 could be detected. Molecules 1, 4 and 11 showed a slight increase, with 1 having the highest yield. This data shows that compared to the solvolysis, the addition of alumina did not present significant differences. The overall yields were 3.9 and 3.4 g/100 g, for the reference and Al_2O_3 reactions, respectively.

The reaction products for sugar-cane lignin reactions were identified by GC-MS and are labelled in the figures as follows: (1) 2-methoxyphenol, (2) 4-methyl-2-methoxyphenol, (2A) 4-ethylphenol, (3) 4-ethyl-2-methoxyphenol, (4) 4-propyl-2-methoxyphenol, (5) 1,2-dihydroxybenzene, (6A) 2,6-dimethoxyphenol, (7) 4-(3-hydroxypropyl)-2-methoxyphenol, (8) 4-(3-methoxypropyl)-2-methoxyphenol, (9) 4-methyl-2,6-dimethoxyphenol, (10) 4-(2-hydroxyethyl)-2,6-dimethoxyphenol, (11) 4-ethyl-2,6-dimethoxyphenol, (12) 4-propenyl-2,6-dimethoxyphenol, (13) 4-(2-hydroxyethyl)-2-methoxyphenol, (14) 4-propyl-2,6-dimethoxyphenol, (15) 4-(1-hydroxy-2-methyl-pent-3-enyl)-2,6-dimethoxyphenol.

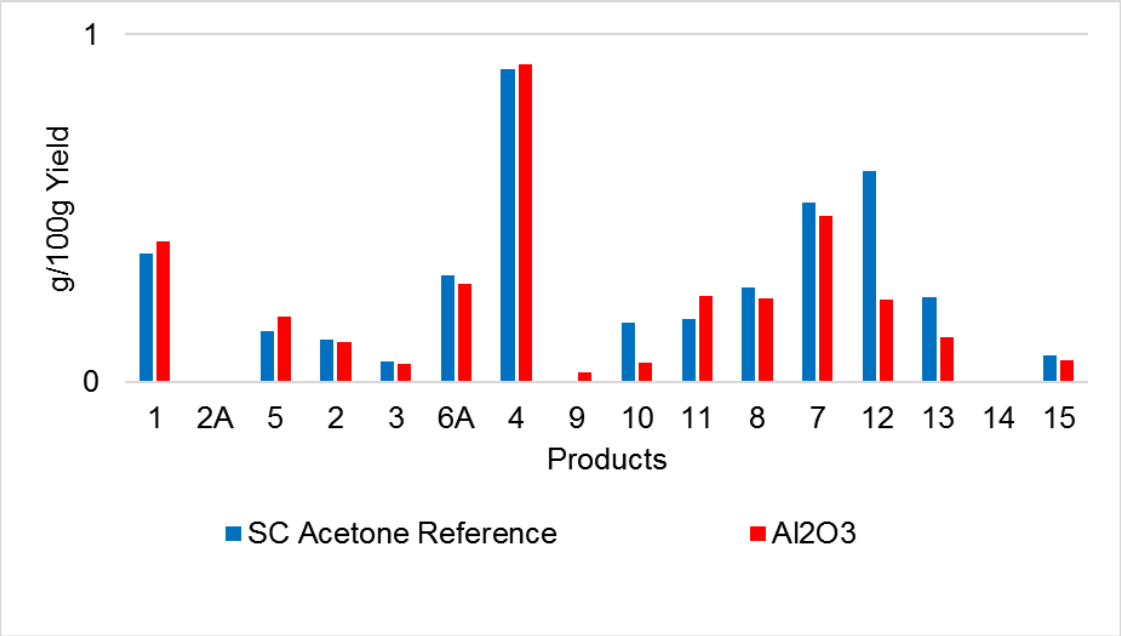

Figure 126 Depolymerisation of sugar-cane lignin in the presence of Al_2O_3 support and Acetone/H_2O mixture (50:50 v/v).

Figure 127 presents the product distribution of reference and Pt/Al_2O_3 catalysed reactions. All 16 products were generated with catalyst. The majority of compounds showed an increase in yield with Pt/Al_2O_3, especially 2A, 6A, 11 and 14. Comparing with the reference, the addition of catalyst changed product distributions and it showed a high selectivity for compound 2A. The overall yield was 11.4 g/100 g.

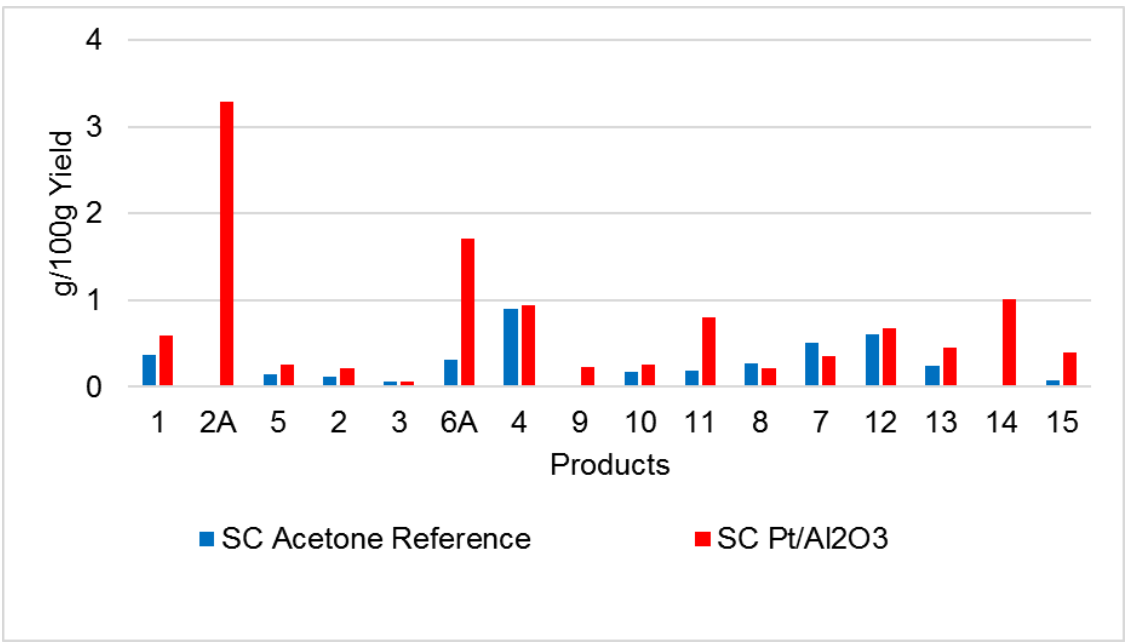

Figure 127 Depolymerisation of sugar-cane lignin in the presence of Pt/Al_2O_3 support and Acetone/H_2O mixture (50:50 v/v).

Figure 128 shows results of reference and Rh/Al_2O_3 catalysed reactions. All 16 products were generated in the presence of catalyst. Related to the reference, the addition of Rh/Al_2O_3 considerably increased yields for almost all products (except for 4), especially compounds 2A, 6A, 10, 11, 12, 13, 14 and 15. As the Pt/Al_2O_3, the Rh/Al_2O_3 showed a high selectivity for product 2A. The overall yield was 12.9 g/100 g,

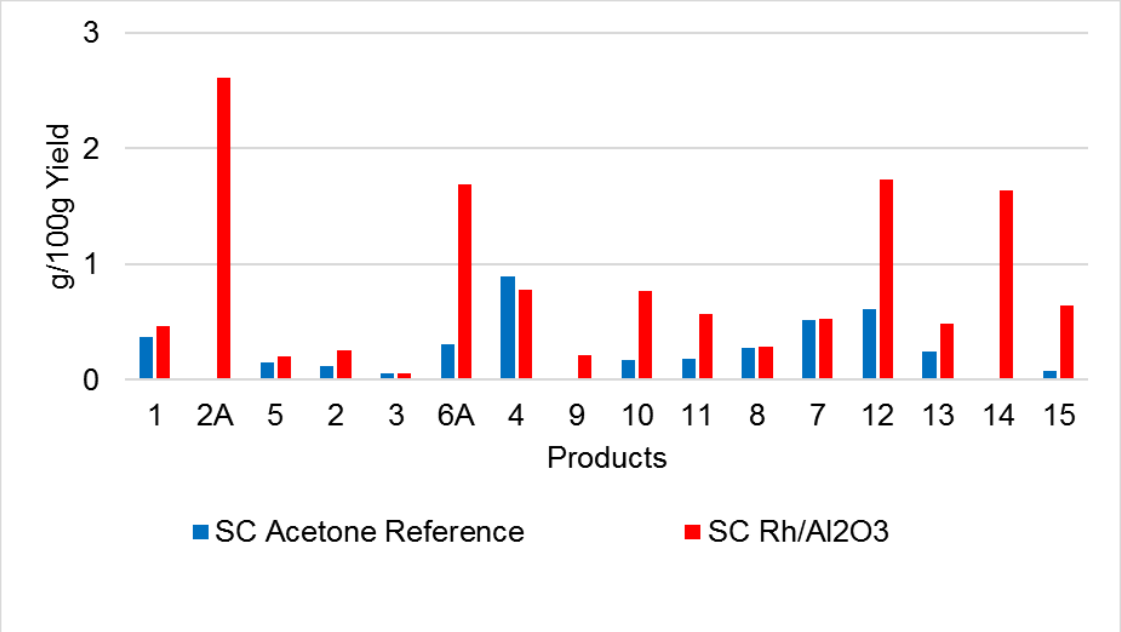

Figure 128 Depolymerisation of sugar-cane lignin in the presence of Rh/Al_2O_3 support and Acetone/H_2O mixture (50:50 v/v).

The results of reference and Ni/Al_2O_3 catalysed reactions are displayed in Figure 129. All 16 products were generated in the presence of catalyst, except compound 10. Related to the reference, the addition of Ni/Al_2O_3 increased yields for products 1, 2A, 5, 6A, 4, 11 and 14. Similar to the noble metal catalysts, Ni/Al_2O_3 showed highest selectivity for compound 2A. The overall yield was 8.3 g/100 g.

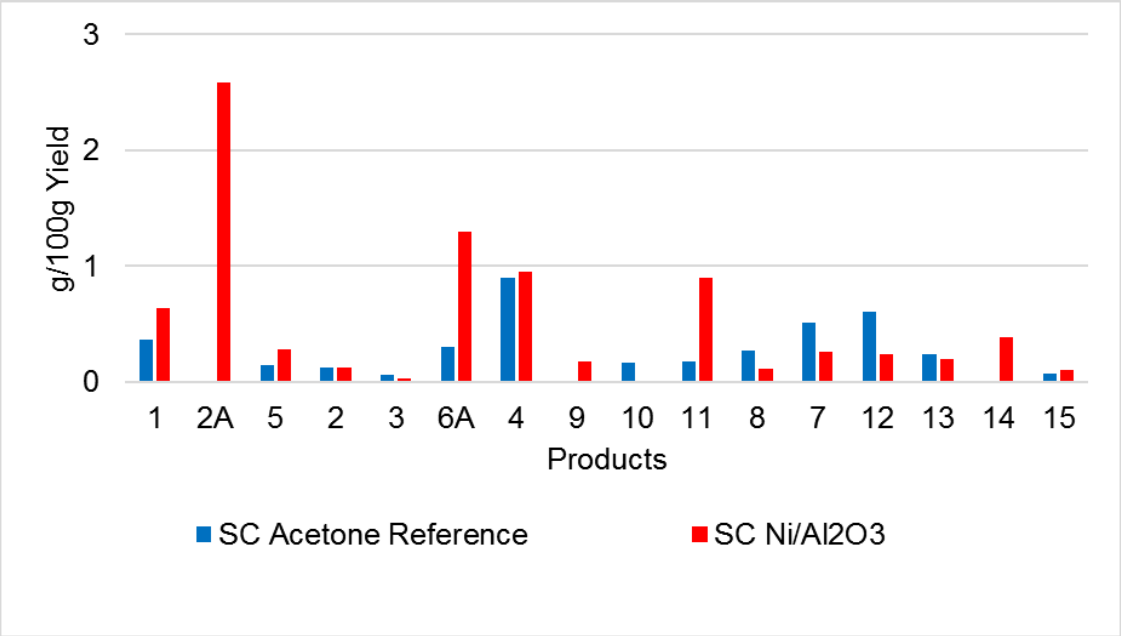

Figure 129 Depolymerisation of sugar-cane lignin in the presence of Ni/Al_2O_3 support and Acetone/H_2O mixture (50:50 v/v).

The results of reference and Fe/Al_2O_3 catalysed reactions are displayed in Figure 130. Compared to the previous reactions, this catalyst showed poorer performance. Related to the reference, the addition of Fe/Al_2O_3 increased yields for products 1, 2A, 5, 3, 10 and 11, while for 6A, 4, 8, 7, 12 and 13 the solvolysis was more effective. Fe/Al_2O_3 also showed a high selectivity for compound 2A. The overall yield was 6.6 g/100 g.

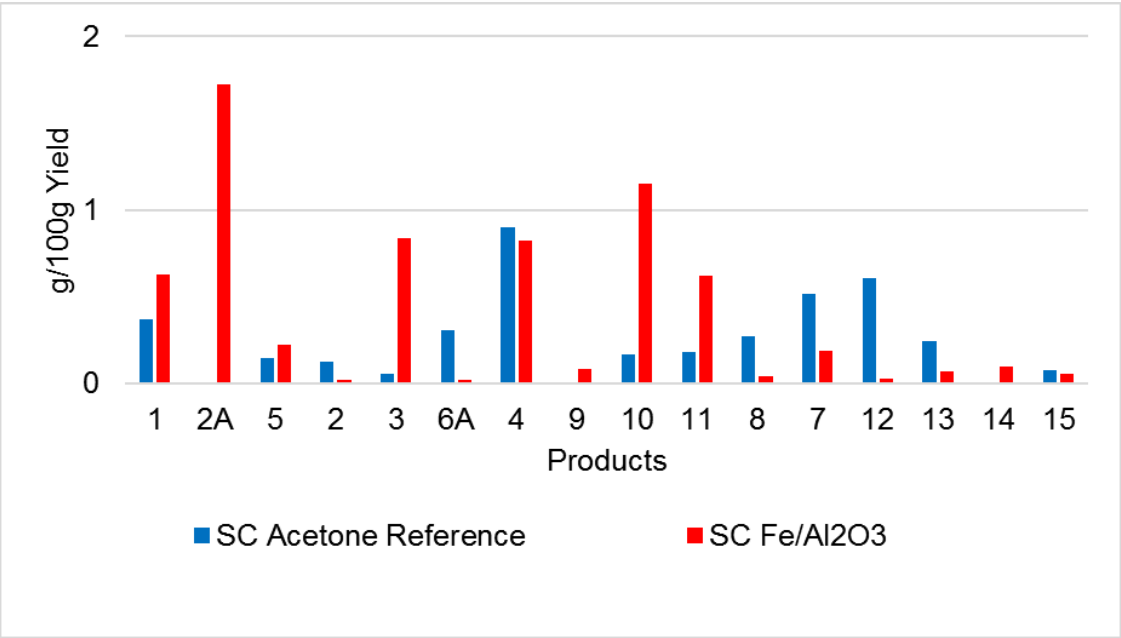

Figure 130 Depolymerisation of sugar-cane lignin in the presence of Fe/Al_2O_3 support and Acetone/H_2O mixture (50:50 v/v).

6.3 Parr-lignins

The parr-lignins studied were extracted according to method described in Section 3.1. The wood sources were birch and oak, both hardwoods.

The Kraft chapter (Section 6.1) provided a systematic study of solvent effect and the influence of catalysts (Pt/Al_2O_3 and Rh/Al_2O_3) in these reactions. It was found that the amount of char formation was reduced when a solvent/water 50:50 v/v mixture was present in the reactions. Hence, solvent/water 50:50 v/v was used as standard for the sugar-cane and parr-lignin reactions.

In order to explore alternative solvents, acetone and IPA solutions with water (solvent/water 50:50 v/v) were used with the parr-lignins. This section describes the study of different catalytic systems, analysing how the depolymerisation, product distribution and selectivity were affected by the metal and support in the parr-lignins. The catalysts that were involved in the reactions were based on platinum, rhodium, nickel and iron. Different supports such as alumina, zirconia and carbon were used, and the results are described in the following sections.

6.3.1 Depolymerisation of birch parr-lignin

Reactions with birch parr-lignin were performed using Acetone/H_2O and IPA/H_2O mixtures. Alumina support, Pt/Al_2O_3, Rh/Al_2O_3, Ni/Al_2O_3, Fe/Al_2O_3, carbon support, Ni/C, Fe/C, zirconia support, Ni/ZrO_2 and Fe/ZrO_2 were used as catalysts.

6.3.1.1 Effects of acetone solution and alumina-based catalysts in the depolymerisation of birch parr-lignin

The following reactions were performed with acetone/H_2O mixture. In the interest of studying if the alumina support was participating in the reactions, the solvent solution was used in the presence of Al_2O_3 support and birch parr-lignin. In addition, the solvolysis was also performed. The overall yields were 3.2 and 4.6 g/100 g, respectively. Figure 131 shows product distribution. Paralleled to the reference experiment, the support showed catalytic activity increasing the yields of compounds 1, 5, 2, 3, 6A, 9, 8, 7, 14 and 15A, and especially product 6A which had the major yield. All 14 products were formed in the presence of solvent mixture, however, compounds 10 was not generated with support.

The reaction products for birch parr-lignin reactions were identified by GC-MS and are labelled in the figures as follows: (1) 2-methoxyphenol, (2) 4-methyl-2-methoxyphenol, (3) 4-ethyl-2-methoxyphenol, (5) 1,2-dihydroxybenzene, (6A) 2,6-dimethoxyphenol, (7) 4-(3-hydroxypropyl)-2-methoxyphenol, (8) 4-(3-methoxypropyl)-2-methoxyphenol, (9) 4-methyl-2,6-dimethoxyphenol, (10) 4-(2-hydroxyethyl)-2,6-dimethoxyphenol, (11) 4-ethyl-2,6-dimethoxyphenol, (12) 4-propenyl-2,6-dimethoxyphenol, (13) 4-(2-hydroxyethyl)-2-methoxyphenol, (14) 4-propyl-2,6-dimethoxyphenol, (15A) 4-(3-hydroxypropyl)-2,6-dimethoxyphenol.

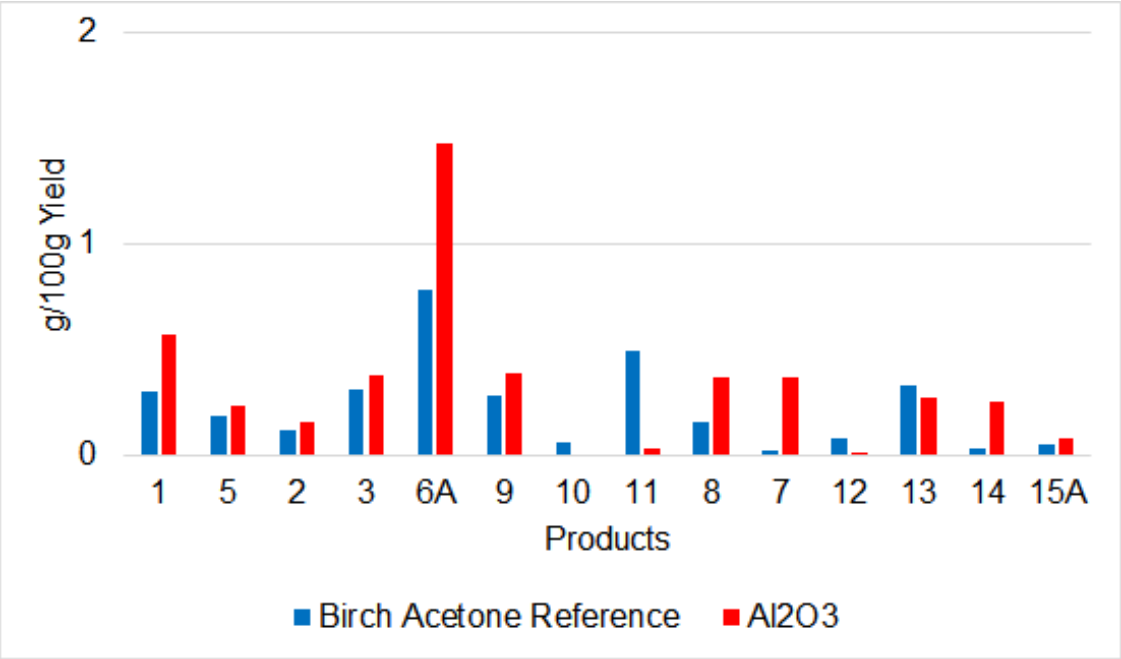

Figure 131 Depolymerisation of birch parr-lignin in the presence of Al_2O_3 support and Acetone/H_2O mixture (50:50 v/v).

Figure 132 shows the results of Pt/Al_2O_3 experiment. Comparing to the reference, the addition of catalyst considerably affected product yield. With the exception of compound 13, all other products showed an increase in yield with Pt/Al_2O_3. This catalyst showed a high selectivity for molecules 6A, 11 and, especially, 8. The overall yield was 9.8 g/100 g.

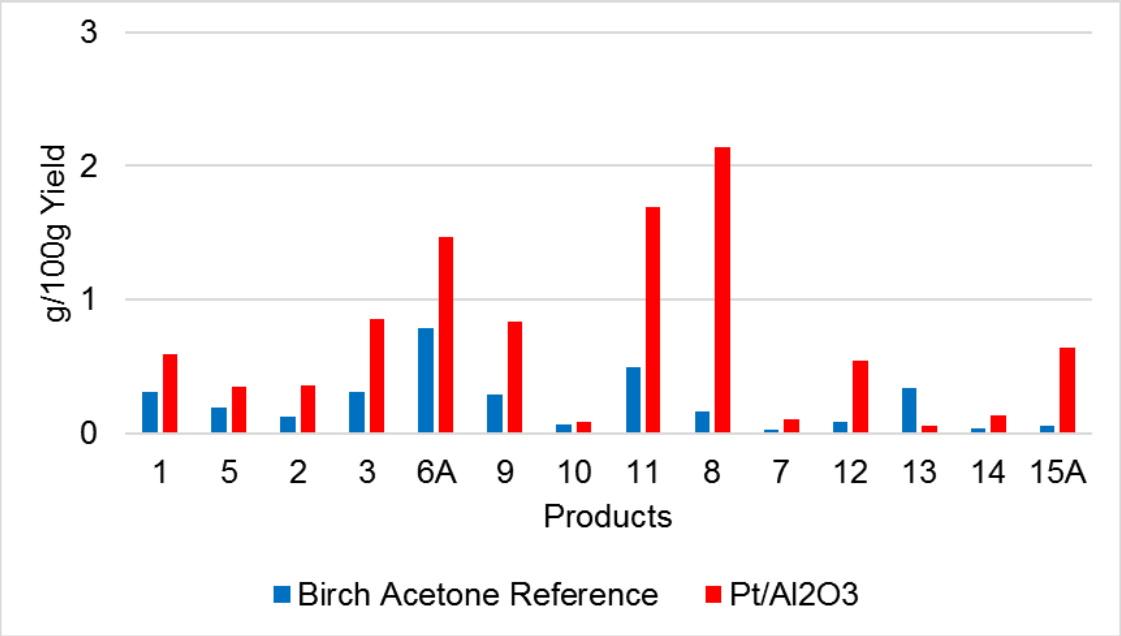

Figure 132 Depolymerisation of birch parr-lignin in the presence of Pt/Al_2O_3 and Acetone/H_2O mixture (50:50 v/v).

The Pt/Al_2O_3 used in the previous reaction (Figure 132) was recovered and re-reacted with fresh birch parr-lignin in typical reaction conditions. This enabled the verification of whether the catalyst lost activity after reaction and if the re-use was advantageous. Figure 133 shows a comparison between non-catalysed, catalysed and re-used Pt/Al_2O_3 reactions. The main product 8, had its yield significantly decreased, while compounds 7 and 10 increased considerably their values. For 1 and 13 there was a slight increase while all other products had their yields decreased with the re-use of catalyst. In general, the catalytic activity was affected resulting in a drop of individual and overall yields. The value was 7.3 g/100 g, compared to 3.2 and 9.8 g/100 g for non-catalysed and catalysed reactions.

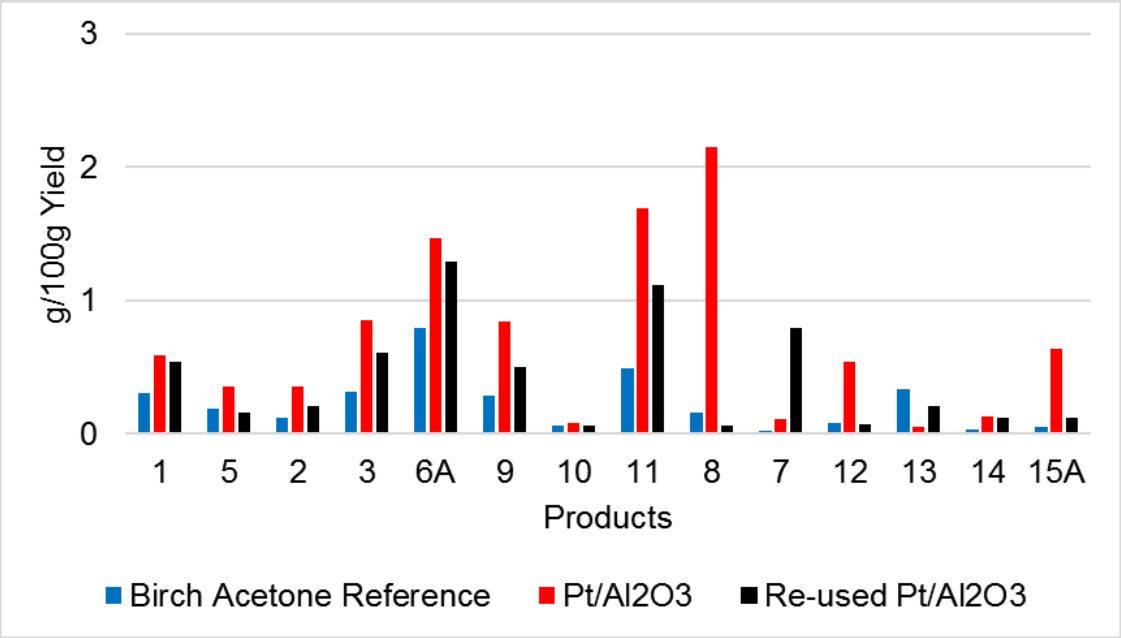

Figure 133 Depolymerisation of birch parr-lignin in the presence of re-used Pt/Al_2O_3 and Acetone/H_2O mixture (50:50 v/v).

The products obtained from reaction over Rh/Al_2O_3 is described in Figure 134. The overall yield was 8 g/100 g. Relating to the reference, the addition of catalyst affected products yield. Rh/Al_2O_3 showed catalytic activity increasing the yields of compounds 1, 2, 7, 8, 9, 10, 11, 14 and 15A. This catalyst had a high selectivity for molecules 8, 9 and, especially, 7.

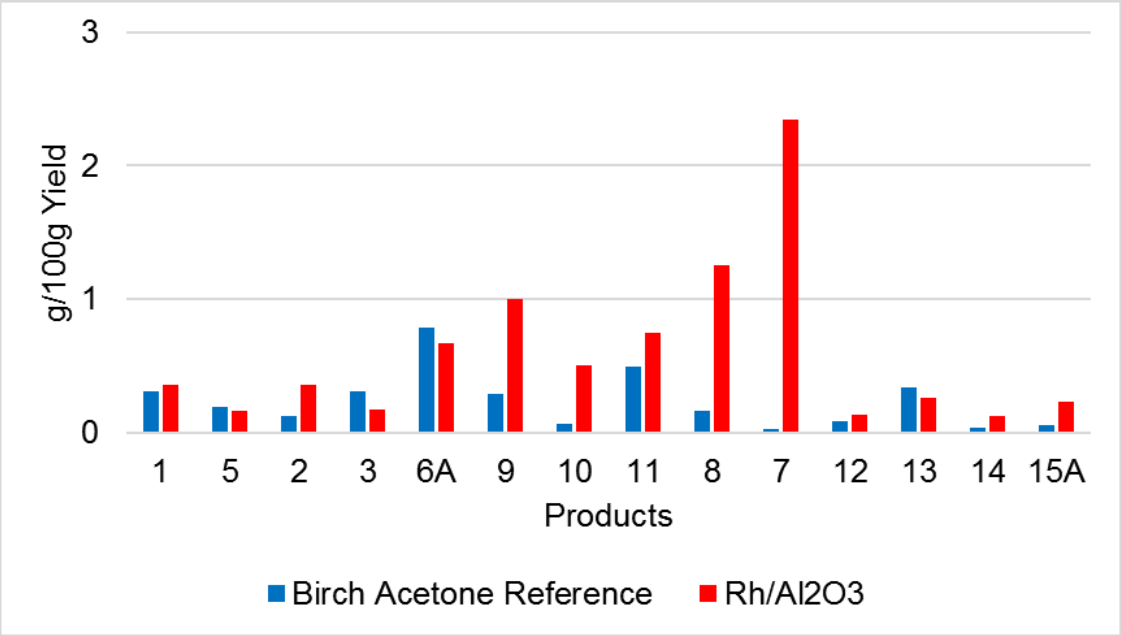

Figure 134 Depolymerisation of birch parr-lignin in the presence of Rh/Al_2O_3 and Acetone/H_2O mixture (50:50 v/v).

The results from the Ni/Al_2O_3 experiment are presented in Figure 135. The overall yield was 7.6 g/100 g. The catalyst showed a good performance affecting products yield. In the presence of Ni/Al_2O_3, excepting compound 13, all other molecules had their yields increased. In addition, it showed a high selectivity for products 6A, 8 and 11. In terms of individual products, this metal had a better performance than the noble metal platinum (Figure 132).

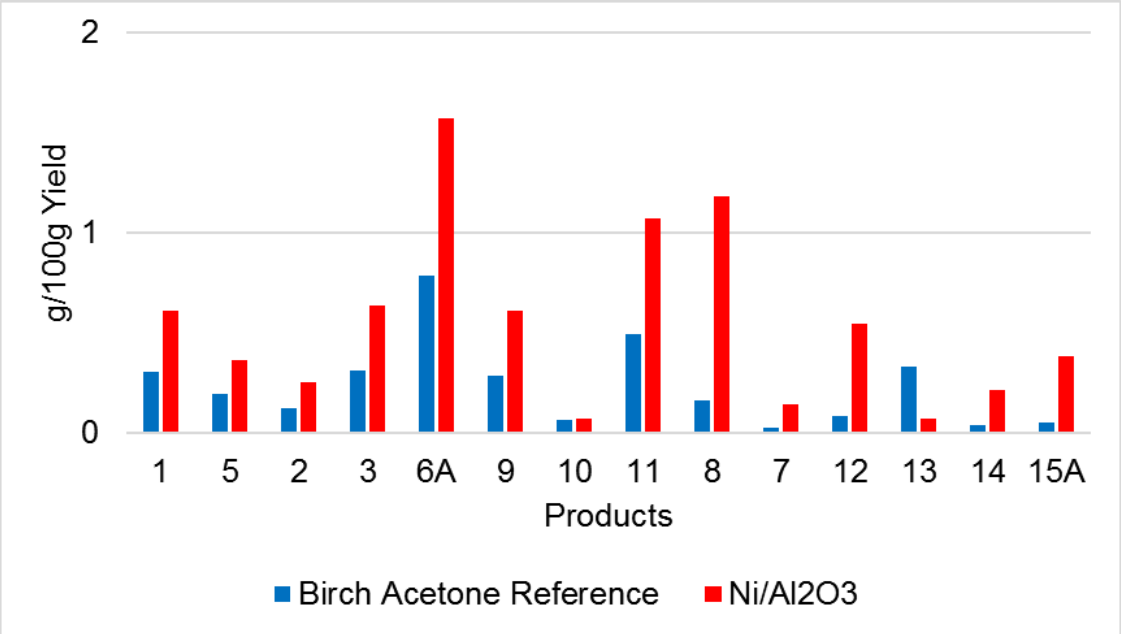

Figure 135 Depolymerisation of birch parr-lignin in the presence of Ni/Al_2O_3 and Acetone/H_2O mixture (50:50 v/v).

The Ni/Al_2O_3 used in the previous reaction (Figure 135) was recovered and re-reacted with fresh birch parr-lignin in typical reaction conditions. This enabled the verification of whether the catalyst lost activity after reaction and if the re-use was advantageous. Figure 136 shows a comparison between non-catalysed, catalysed and reaction with re-used Ni/Al_2O_3. The main product, 6A, had its yield decreased, while compounds 7 and 10 increased considerably their values. For 13, 14 and 15A there was a slight increase. However, all other products had their values decreased with the re-use of catalyst. Despite of the catalytic activity being slightly affected, the overall yield did not change dramatically comparing with the fresh Ni/Al_2O_3 previously reported. The overall yield was 7g/100 g.

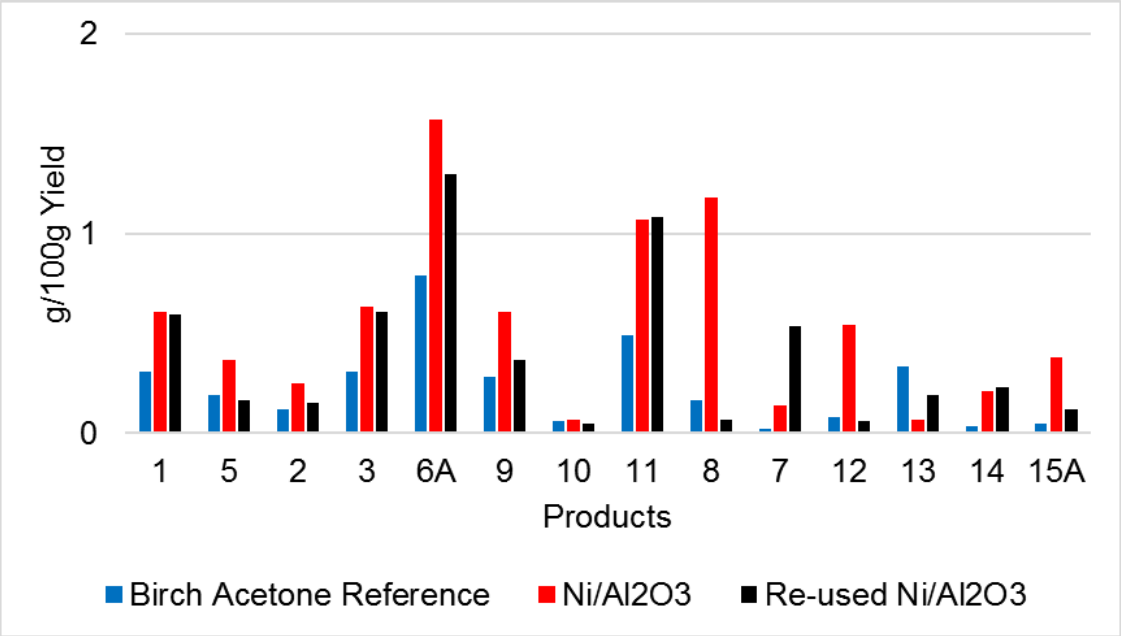

Figure 136 Depolymerisation of birch parr-lignin in the presence of re-used Ni/Al_2O_3 support and Acetone/H_2O mixture (50:50 v/v).

The results obtained over Fe/Al_2O_3 catalysed reaction are described in the Figure below. Relating to the reference, the addition of catalyst did not significantly affect products' yield. Compounds 1, 6A, 8, 10, 11, 12 and 14 had their yields slightly increased in the presence of Fe/Al_2O_3. The overall yield was 3.8 g/100 g.

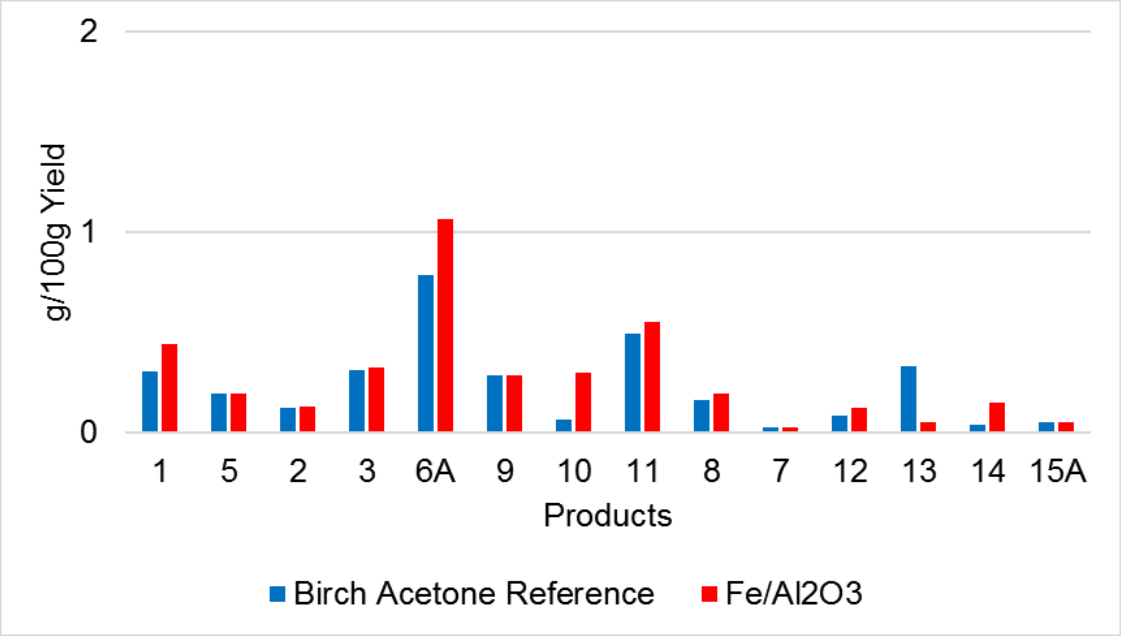

Figure 137 Depolymerisation of birch parr-lignin in the presence of Fe/Al_2O_3 support and Acetone/H_2O mixture (50:50 v/v).

6.3.1.2 Effects of carbon-based catalysts in the depolymerisation reactions of birch parr-lignin

The effect using a carbon support (C) in the depolymerisation was studied. The overall yield was 6.8 g/100 g. Figure 138 shows the product distribution. Parallel to the reference experiment, the support was not inert and showed catalytic activity increasing the yields of most products, especially 6A, 8 and 11.

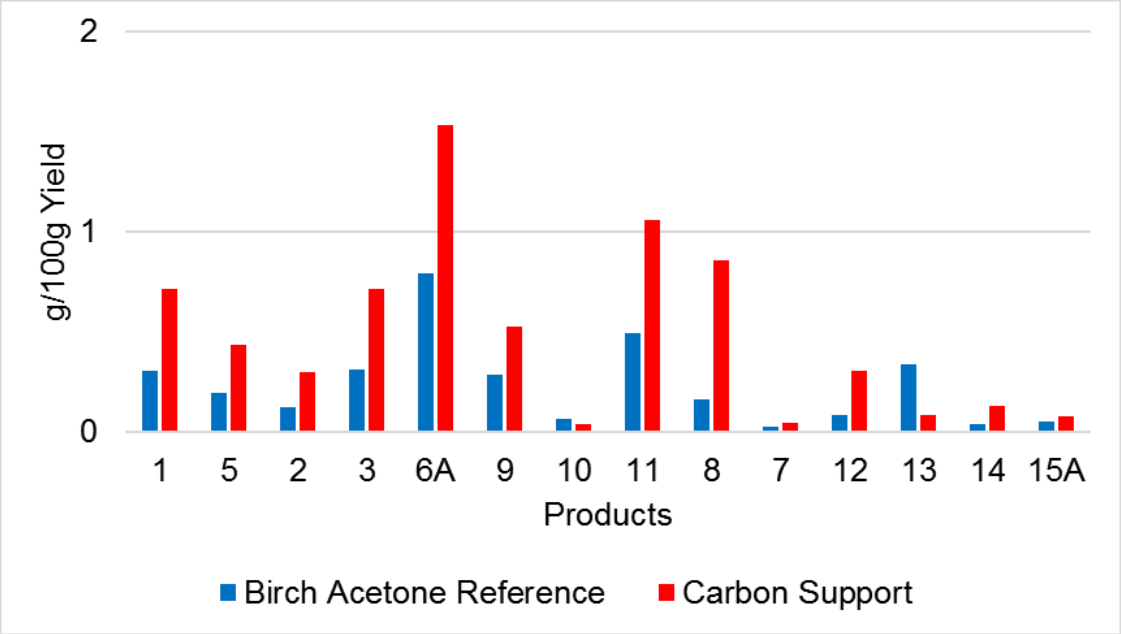

Figure 138 Depolymerisation of birch parr-lignin in the presence of carbon support and Acetone/H_2O mixture (50:50 v/v).

Figure 139 shows the results with Ni/C. Compared to the reference, the addition of catalyst changed product yield. The overall yield was 5 g/100 g. With the exception of compounds 8 and 13, all other products showed an increase in yield with Ni/C. This catalyst showed good selectivity for product 6A.

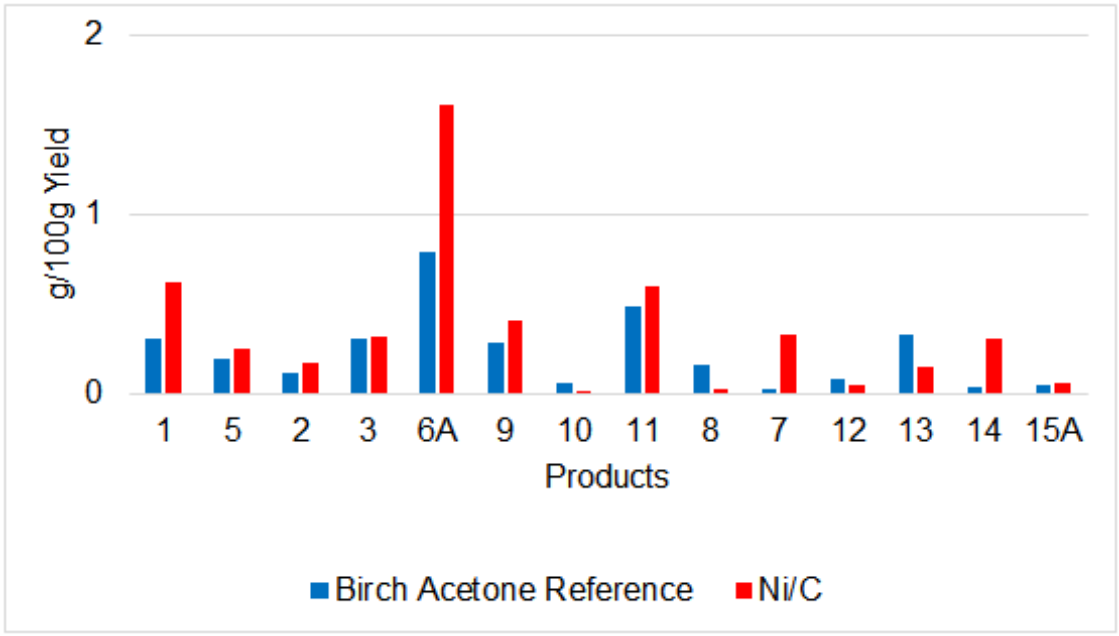

Figure 139 Depolymerisation of birch parr-lignin in the presence of Ni/C and Acetone/H_2O mixture (50:50 v/v).

Figure 140 shows the results over Fe/C. The addition of catalyst did not significantly affect the yield of most products. However, the presence of Fe/C contributed significantly for the generation of products 3 and 10, while 1, 8, 12, 14 and 15A slightly increased. For the other compounds, the solvolysis was more effective. The overall yield was 3.4 g/100 g.

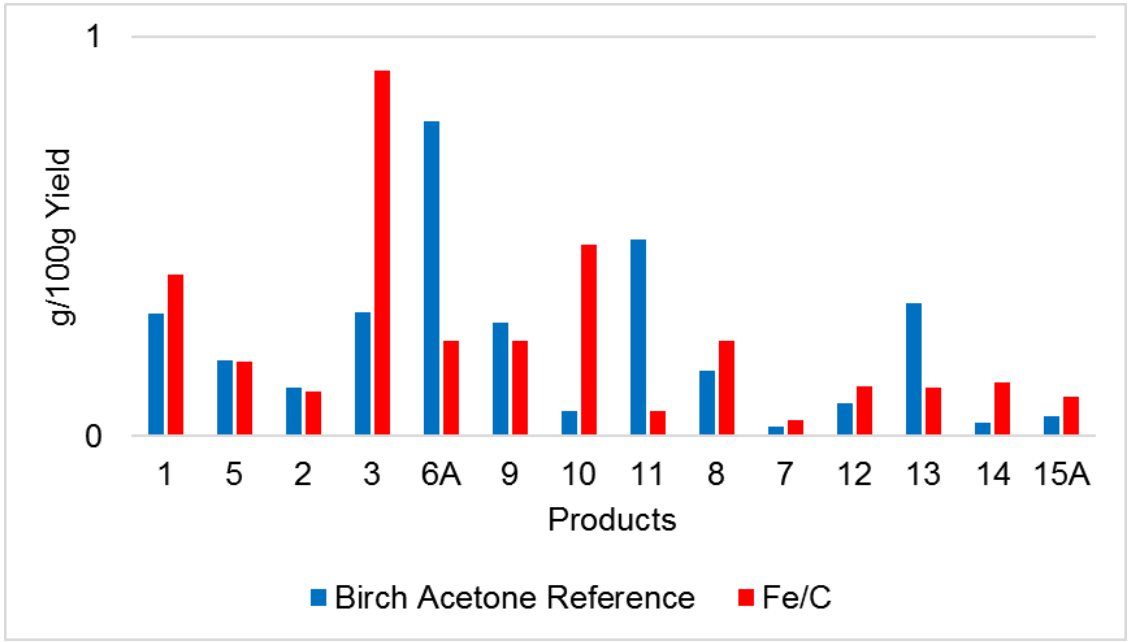

Figure 140 Depolymerisation of birch parr-lignin in the presence of Fe/C and Acetone/H_2O mixture (50:50 v/v).

6.3.1.3 Effects of zirconia-based catalysts in the depolymerisation reactions

The influence of zirconia support (ZrO_2) in the depolymerisation reaction was evaluated. The graph below shows that the ZrO_2 only slightly increased the generation of products 6A and 15A, contrariwise, all other compounds generation was more effective with solvolysis. The overall yield was 2 g/100 g.

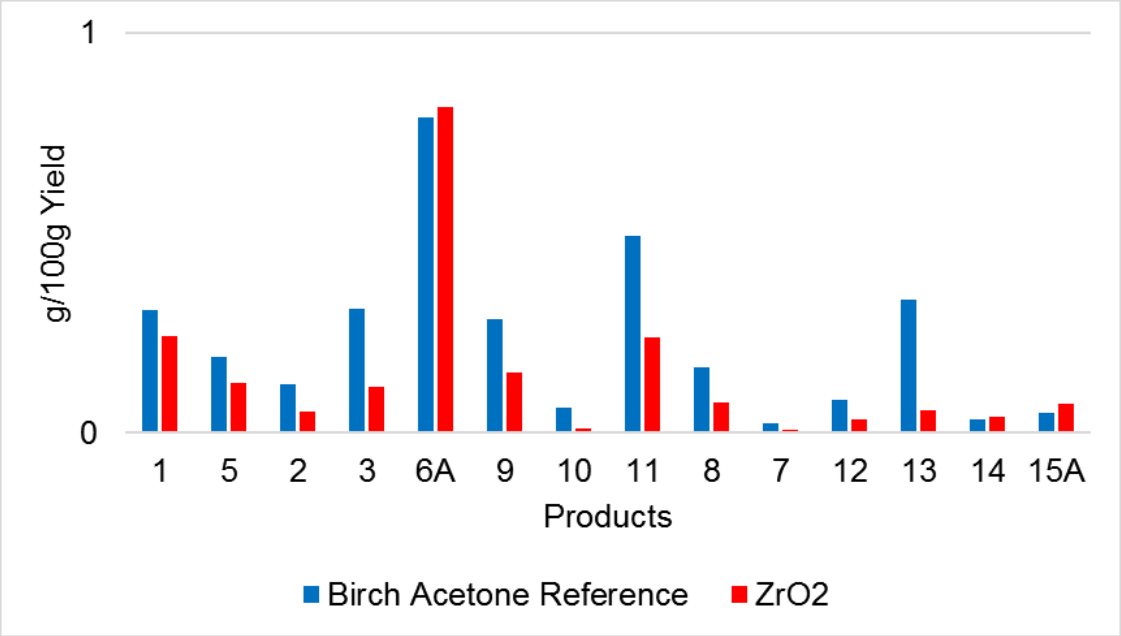

Figure 141 Depolymerisation of birch parr-lignin in the presence of ZrO_2 support and Acetone/H_2O mixture (50:50 v/v).

Figure 142 shows the results over Ni/ZrO_2. In the catalytic run, nickel did not affect the yields of products 5 and 9, while 13 was favoured by solvolysis. The other products increased with Ni/ZrO_2. Related to the previous reaction with only support (Figure 141), the metal affected the reaction, changing product distribution and increasing molecule yield. The overall yield was 4 g/100 g.

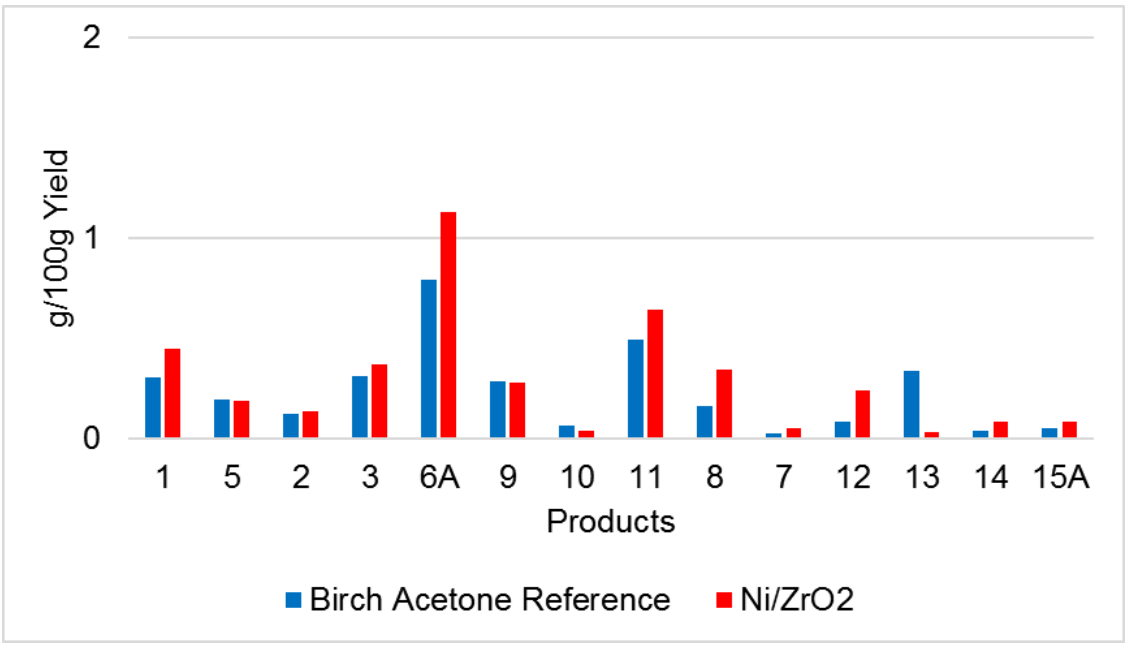

Figure 142 Depolymerisation of birch parr-lignin in the presence of Ni/ZrO_2 support and Acetone/H_2O mixture (50:50 v/v).

The Fe/ZrO_2 catalysed reactions are shown in the Figure below. The catalyst did not affect products yields to any great extent. Except for compound 13 that was favoured by solvolysis, all other molecules showed very similar yields between catalysed and non-catalysed experiments. In this case, iron was slightly better than the zirconia support (Figure 141), but it did not show an improvement in the alkyl phenolics yields as the nickel previously described (Figure 142). The overall yield was 2.7 g/100 g.

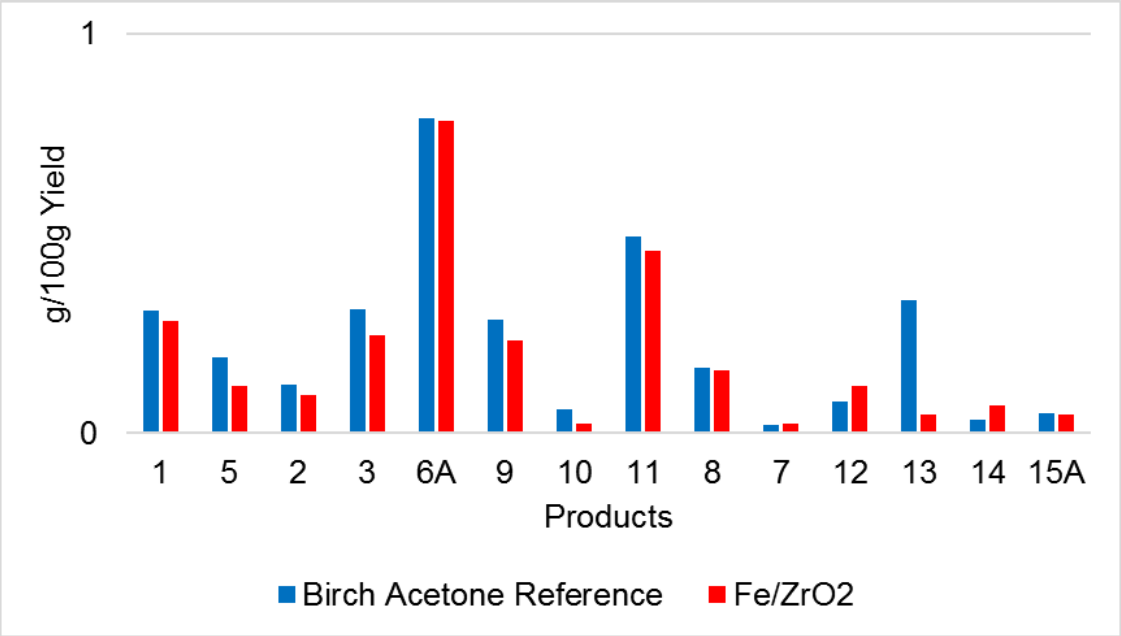

Figure 143 Depolymerisation of birch parr-lignin in the presence of Fe/ZrO_2 support and Acetone/H_2O mixture (50:50 v/v).

6.3.1.4 Effects of isopropanol solution and alumina-based catalysts in the depolymerisation of birch parr-lignin

The following reactions were performed with IPA/H_2O mixture. The effects of solvent mixture and alumina support (Al_2O_3) in the reactions with birch parr-lignin are displayed in Figure 144. The overall yields were 3.9 and 7 g/100 g, respectively. The support showed more catalytic activity in the presence of this solvent enhancing the yields of most compounds, especially 6A and 13.

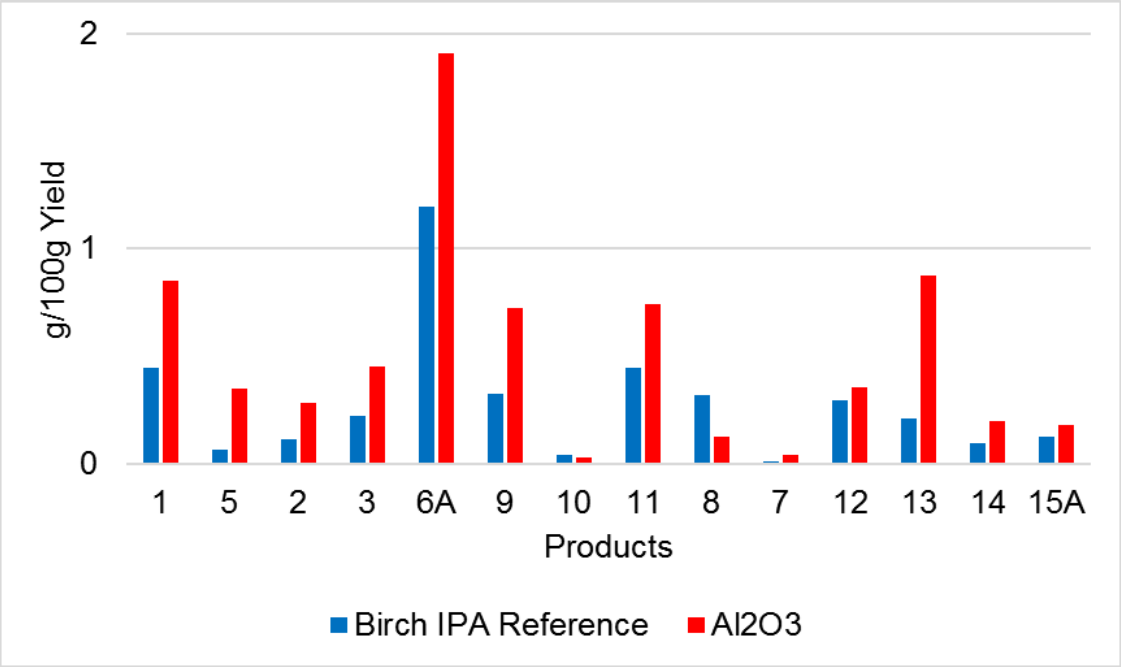

Figure 144 Depolymerisation of birch parr-lignin in the presence of Al_2O_3 support and IPA/H_2O mixture (50:50 v/v).

Figure 145 shows the results over Pt/Al_2O_3. Compared to the reference, the addition of catalyst considerably increased the yield of most products. With the exception of compounds 3, 6A, 13 and 15A, all other products showed an increase in yield with Pt/Al_2O_3. This catalyst had high selectivity for molecules 9, 11 and, especially, 8. The overall yield was 6.8 g/100 g.

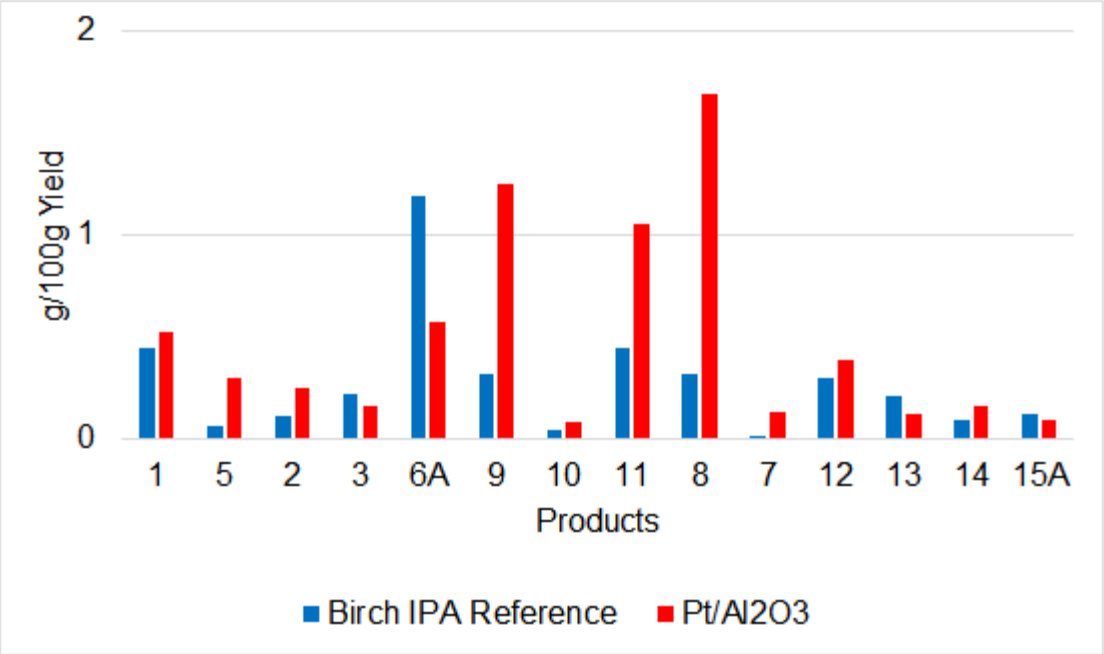

Figure 145 Depolymerisation of birch parr-lignin in the presence of Pt/Al_2O_3 and IPA/H_2O mixture (50:50 v/v).

The results of the reaction over Rh/Al_2O_3 are presented in Figure 146. The overall yield was 6 g/100 g. The catalyst favoured some products. Apart from compounds 1, 6A, 9, 11 and 12, all other products showed better yields with Rh/Al_2O_3. In contrast to Pt/Al_2O_3, this catalyst had a high selectivity for molecules 10 and, especially, 7. Product 8 was also benefited.

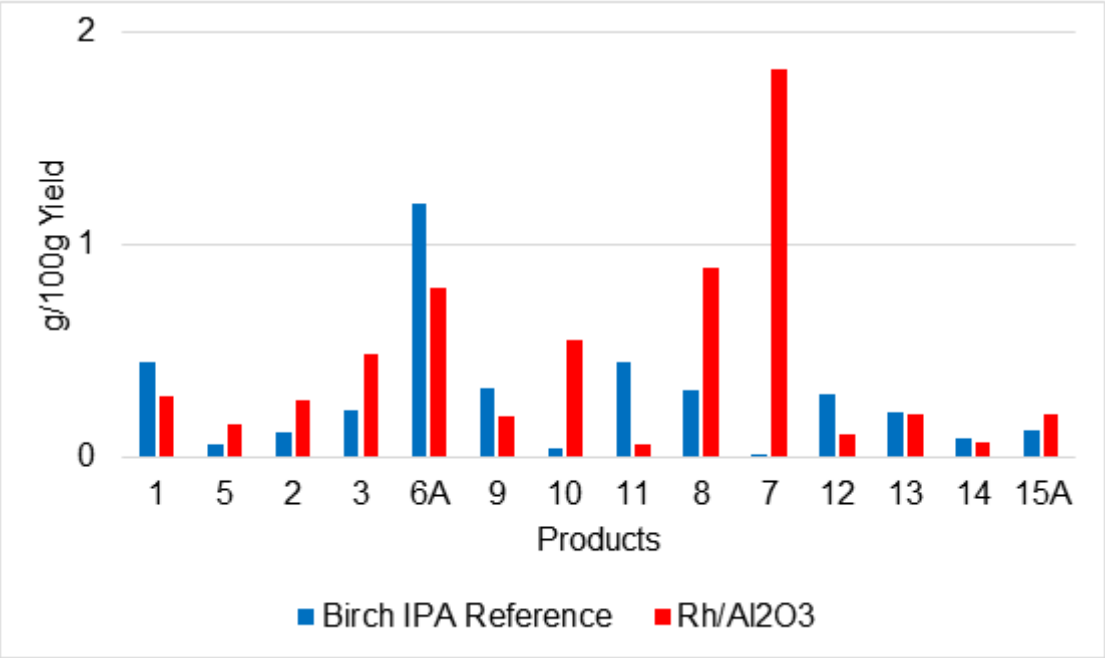

Figure 146 Depolymerisation of birch parr-lignin in the presence of Rh/Al_2O_3 and IPA/H_2O mixture (50:50 v/v).

Ni/Al_2O_3 experiments are presented in Figure 147. The overall yield was 9 g/100 g. Overall, nickel had better activity than the noble metal catalysts (Figure 145 and Figure 146), as it augmented the yields of all individual products. In addition, it presented a high selectivity for compounds 6A, 8, 9 and11.

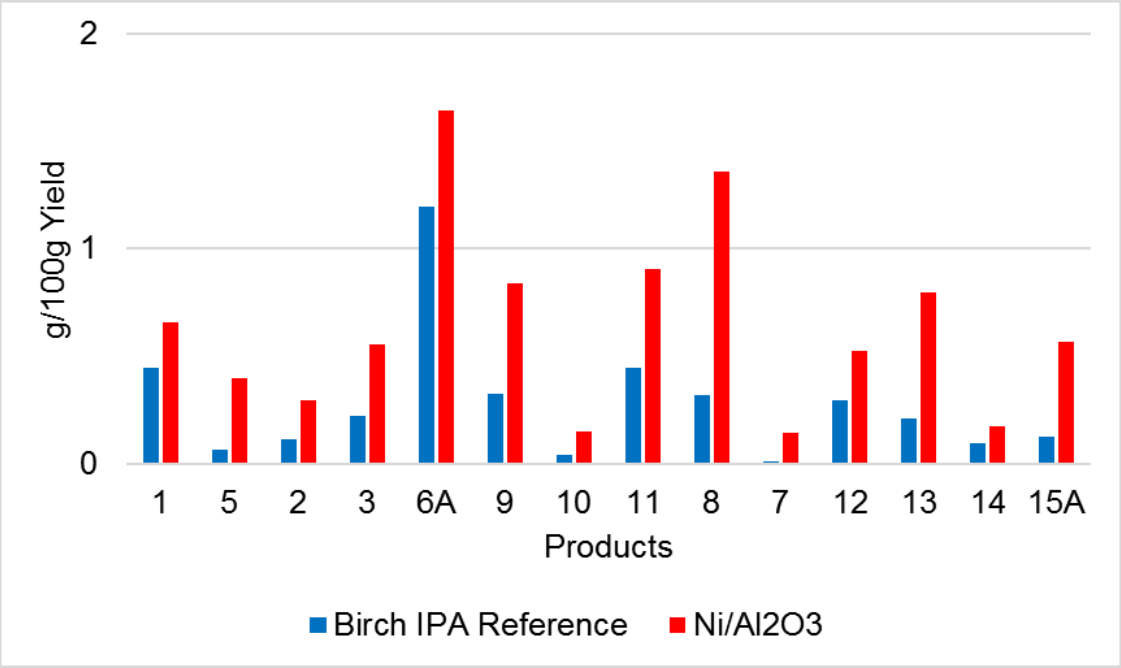

Figure 147 Depolymerisation of birch parr-lignin in the presence of Ni/Al_2O_3 and IPA/H_2O mixture (50:50 v/v).

The Fe/Al_2O_3 catalysed reactions are shown in the Figure below. This metal did not have a large effect on product yield. Compound 12 was to some extent more favoured by solvolysis, though 10, 13 and 15A were more influenced by Fe/Al_2O_3. The other alkyl phenolics had their values just slightly increased with catalyst. The overall yield was 6.3 g/100 g.

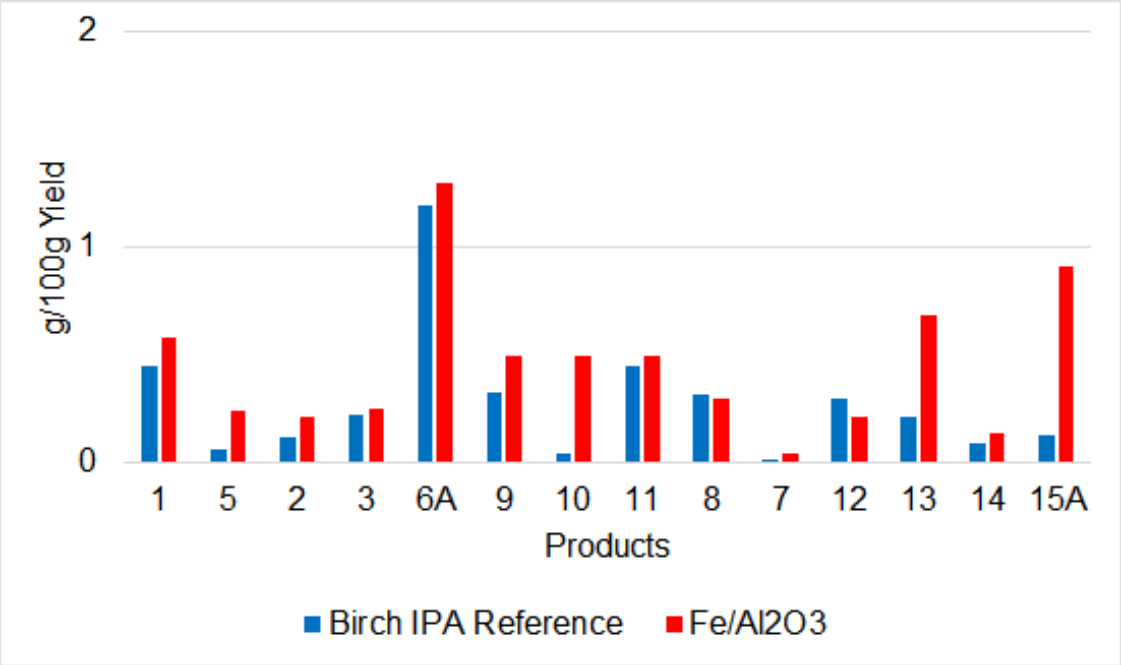

Figure 148 Depolymerisation of birch parr-lignin in the presence of Fe/Al_2O_3 and IPA/H_2O mixture (50:50 v/v).

6.3.1.5 Effects of carbon-based catalysts in the depolymerisation reactions

The effect of carbon support (C) in the depolymerisation was studied. The overall yield was 5.4 g/100 g. Figure 149 illustrates product distribution. Parallel to the reference experiment, the support had catalytic activity increasing the yields of most products, especially 6A and 13. Inversely, 1, 3, 5 and 11 were more favoured by solvolysis.

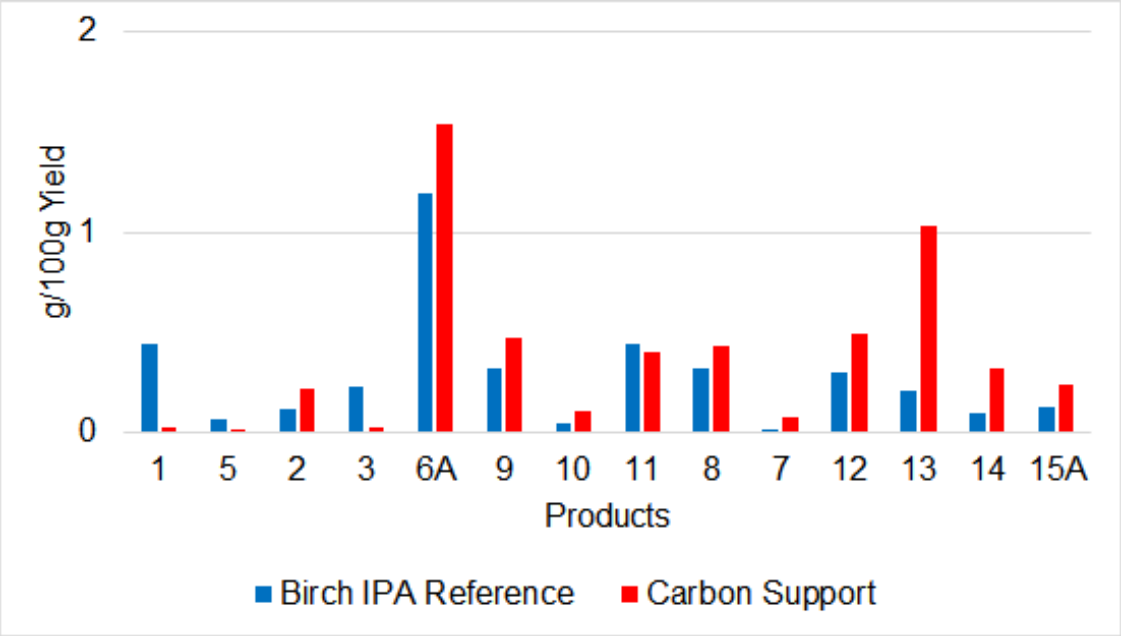

Figure 149 Depolymerisation of birch parr-lignin in the presence of carbon support and IPA/H_2O mixture (50:50 v/v).

Figure 150 shows results of reference and Ni/C catalysed reactions. The overall yield was 8.4 g/100 g, respectively. Compound 6A and 8 with Ni/C presented the highest yields while 7 and 10 the lowest. Product 3 was more favoured by solvolysis while all others significantly by the presence of Ni/C.

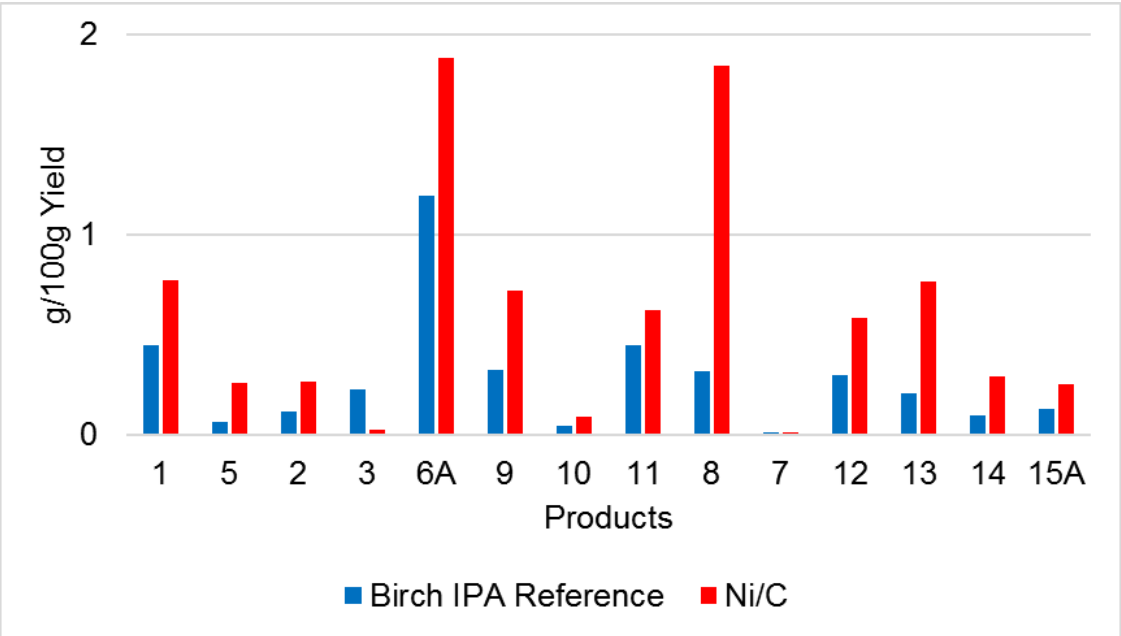

Figure 150 Depolymerisation of birch Parr-lignin in the presence of Ni/C and IPA/H_2O mixture (50:50 v/v).

Figure 151 shows the reaction with Fe/C. This catalyst showed a high selectivity for product 15A and contributed to the generation of 7 and 14. However, compounds 1, 2, 3, 5, 9 and 10 just slightly increased in yield with catalyst. The other alkyl phenolics were not favoured by the presence of Fe/C. The overall yield was 6.7 g/100 g.

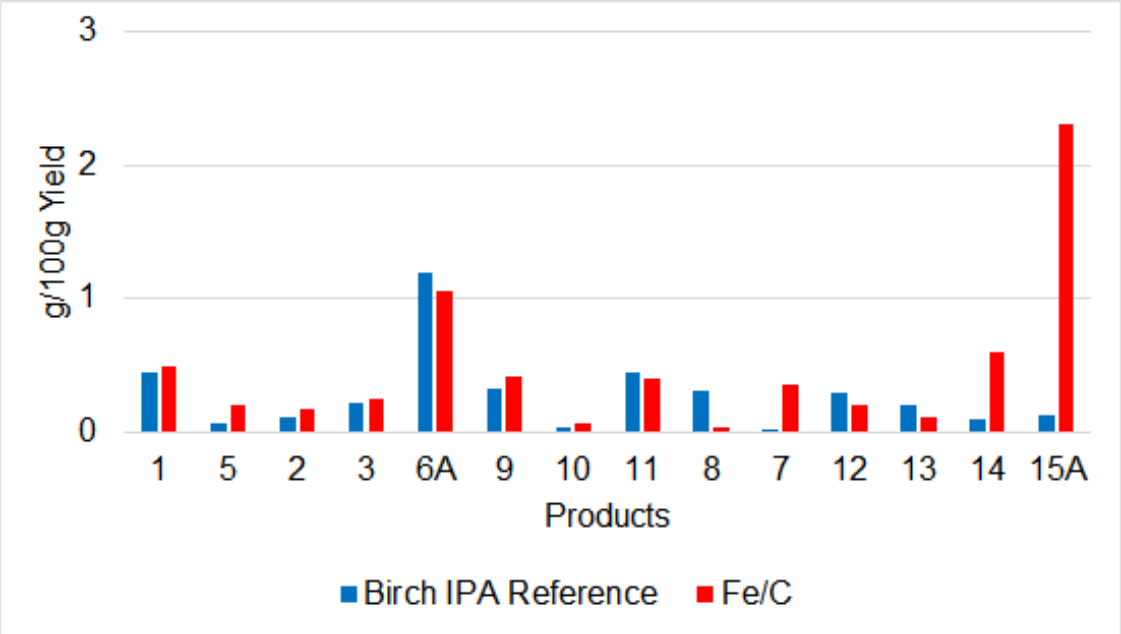

Figure 151 Depolymerisation of birch Parr-lignin in the presence of Ni/C and IPA/H_2O mixture (50:50 v/v).

6.3.1.6 Effects of zirconia-based catalysts in the depolymerisation reactions

The influence of zirconia support (ZrO_2) in the hydrogenolysis with IPA/H_2O solution was studied. Figure 153 shows that the ZrO_2 changed the product distribution. The highest yield was achieved with product 9 and the lowest 7. The generation of 1, 5, 2, 10, 11, 13 and 14 were also favoured by the support. All other compound generation was more effective with solvolysis. The overall yield was 5 g/100 g.

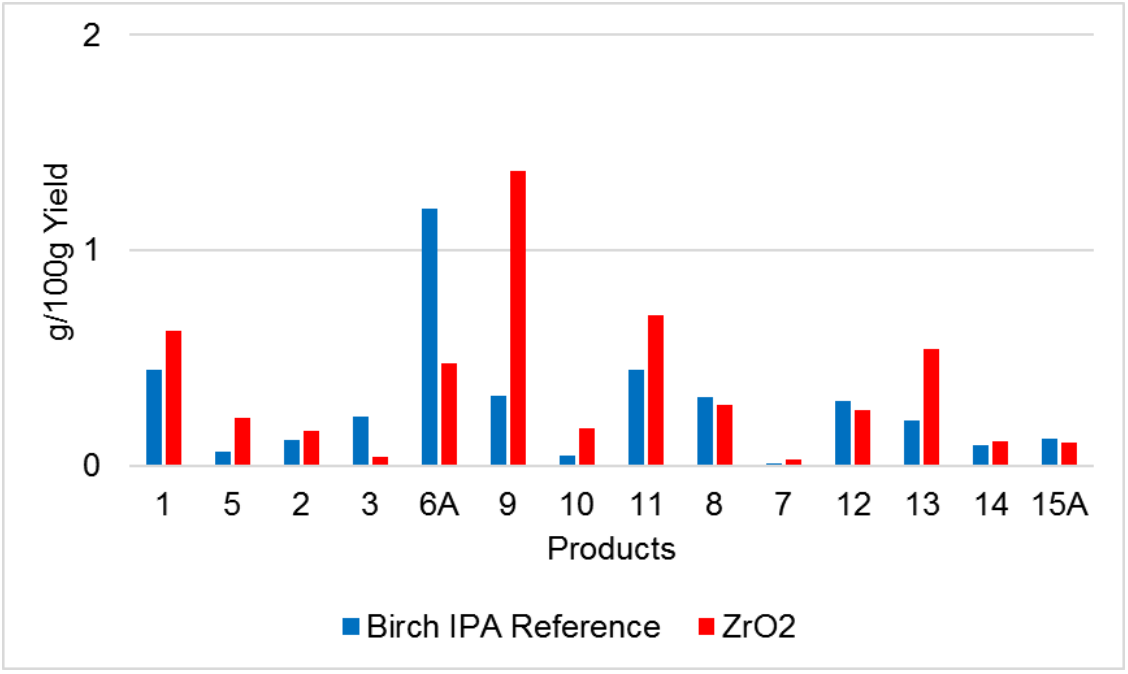

Figure 152 Depolymerisation of birch parr-lignin in the presence of ZrO_2 and IPA/H_2O mixture (50:50 v/v).

The hydrogenolysis with Ni/ZrO_2 is shown below. This catalyst did not show a significant influence in products yields. Most compounds had yields very similar to the solvolysis. Compared to the reference, molecule 13 was the most favoured with the presence of nickel. The overall yield was 4.8 g/100 g.

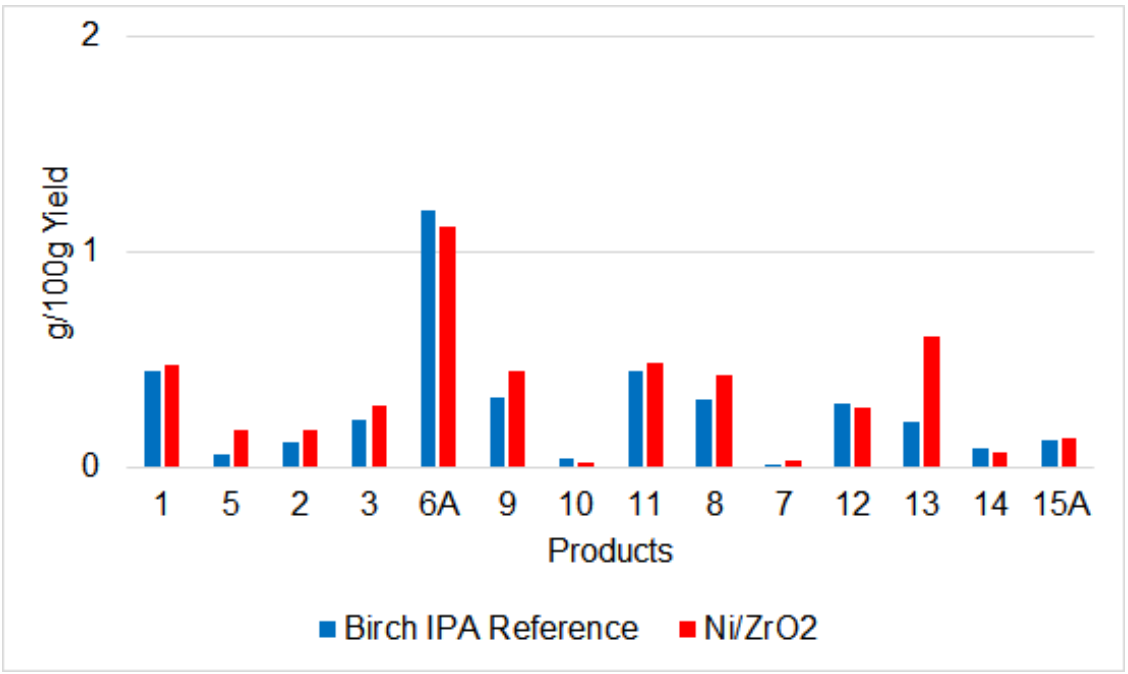

Figure 153 Depolymerisation of birch parr-lignin in the presence of Ni/ZrO_2 and IPA/H_2O mixture (50:50 v/v).

The hydrogenolysis with Fe/ZrO_2 is shown in the Figure below. Similar to the Ni/ZrO_2 (Figure 153), this catalyst did not have a significant influence on product yields. Most compounds had yields very similar to the solvolysis. In this case, molecule 15A was the most favoured with the presence of iron. The overall yield was 4 g/100 g.

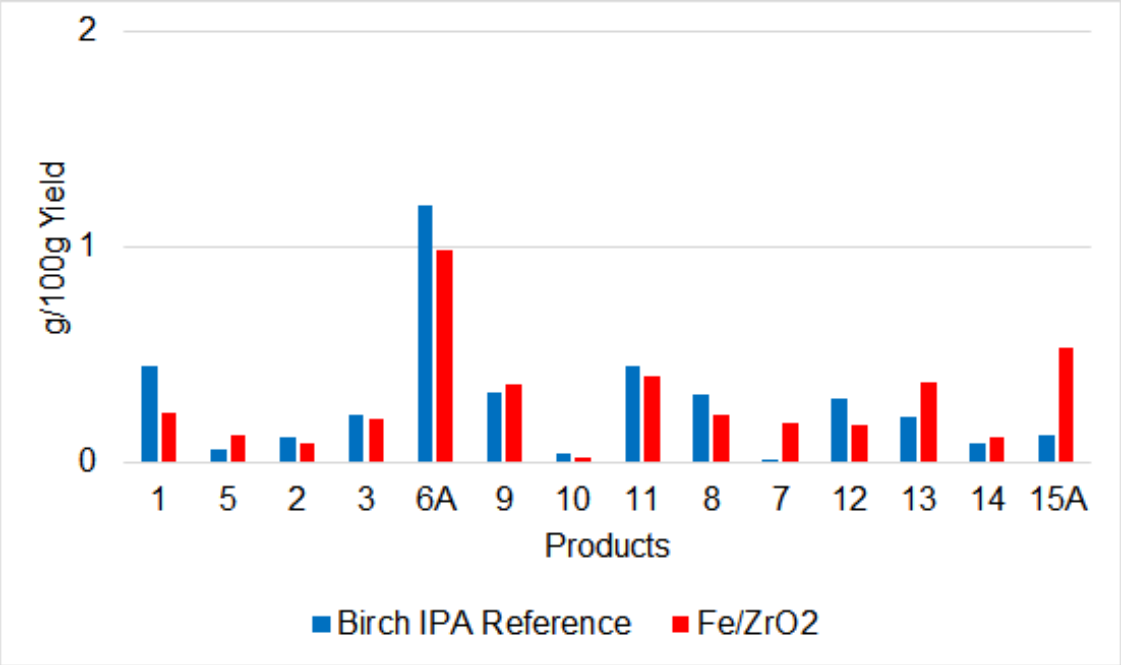

Figure 154 Depolymerisation of birch parr-lignin in the presence of Fe/ZrO_2 and IPA/H_2O mixture (50:50 v/v).

6.3.1.7 Effect of Pt/Al_2O_3 in the Fraction 2

The Fraction 2 (lignin post reaction residues solubilised in acetone, details Section 3.3.2) of Pt/Al_2O_3 experiment (Figure 132) was re-reacted in the presence of fresh catalyst (Pt/Al_2O_3). Figure 155 shows a comparison between the reference, the Pt/Al_2O_3 hydrogenolysis of birch parr-lignin and Fraction 2 reactions. The hydrogenolysis resulted in very low yields of all molecules even in the presence of a noble metal catalyst. In addition, compound 13 was not detected. This signifies that the Fraction 2 is composed by a highly condensed molecule with bonds that are harder to break.

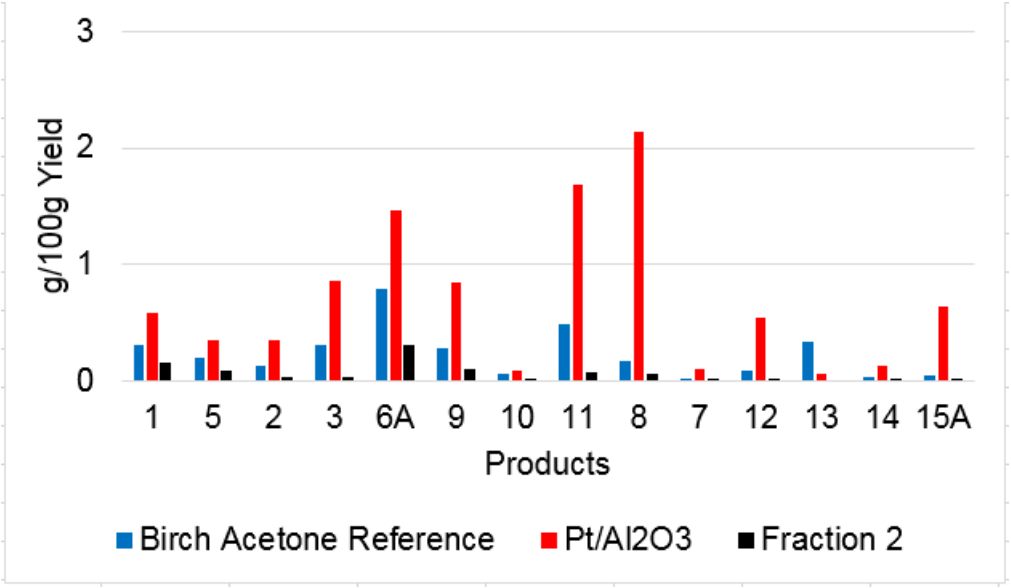

Figure 155 Comparison between reference, the Pt/Al_2O_3 hydrogenolysis of birch parr-lignin and Fraction 2 reactions.

6.3.2 Depolymerisation of oak parr-lignin

Depolymerisation of oak parr-lignin was performed using Acetone/H_2O and IPA/H_2O mixtures. Alumina support, Pt/Al_2O_3, Rh/Al_2O_3, Ni/Al_2O_3, Fe/Al_2O_3, carbon support, Ni/C, Fe/C, zirconia support, Ni/ZrO_2 and Fe/ZrO_2 were used as catalysts.

6.3.2.1 Effects of acetone solution and alumina-based catalysts in the depolymerisation of oak parr-lignin

The following experiments were carried out with acetone/H_2O mixture. To analyse if the alumina support was presenting catalytic activity, the reference solution was used in the presence of Al_2O_3 support and oak parr-lignin. The overall yields were 3.9 and 12.3 g/100 g, respectively. Figure 156 shows product distribution. Paralleled to the reference experiment, the support showed activity increasing the yields of all compounds. Product 6A had the major yield, followed by 11, 1 and 5 while 8 had the lowest values.

The reaction products for oak parr-lignin reactions were identified by GC-MS and are labelled in the figures as follows: (1) 2-methoxyphenol, (2) 4-methyl-2-methoxyphenol, (3) 4-ethyl-2-methoxyphenol, (5) 1,2-dihydroxybenzene, (6A) 2,6-dimethoxyphenol, (7) 4-(3-hydroxypropyl)-2-methoxyphenol, (8) 4-(3-methoxypropyl)-2-methoxyphenol, (9) 4-methyl-2,6-dimethoxyphenol, (10) 4-(2-hydroxyethyl)-2,6-dimethoxyphenol, (11) 4-ethyl-2,6-dimethoxyphenol, (12) 4-propenyl-2,6-dimethoxyphenol, (13) 4-(2-hydroxyethyl)-2-

methoxyphenol, (14) 4-propyl-2,6-dimethoxyphenol, (15A) 4-(3-hydroxypropyl)-2,6-dimethoxyphenol.

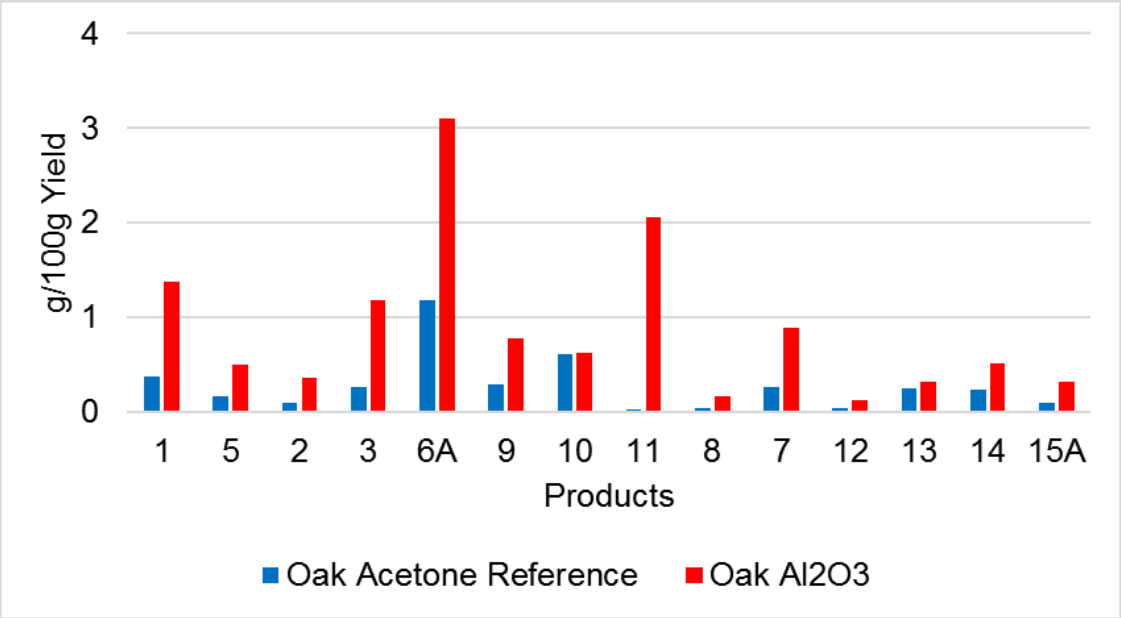

Figure 156 Depolymerisation of oak parr-lignin in the presence of Al_2O_3 support and Acetone/H_2O mixture (50:50 v/v).

Pt/Al_2O_3 catalysed reactions are displayed in Figure 157. Pt/Al_2O_3 influenced the product yield. The overall yield was 8.4 g/100 g. Except for compounds 10, 13 and 14, all other products increased in yield with Pt/Al_2O_3. Similar to the birch parr-lignin reaction, Pt/Al_2O_3 showed a high selectivity for molecules 6A and 11 but, also, compound 7 was favoured by this catalyst.

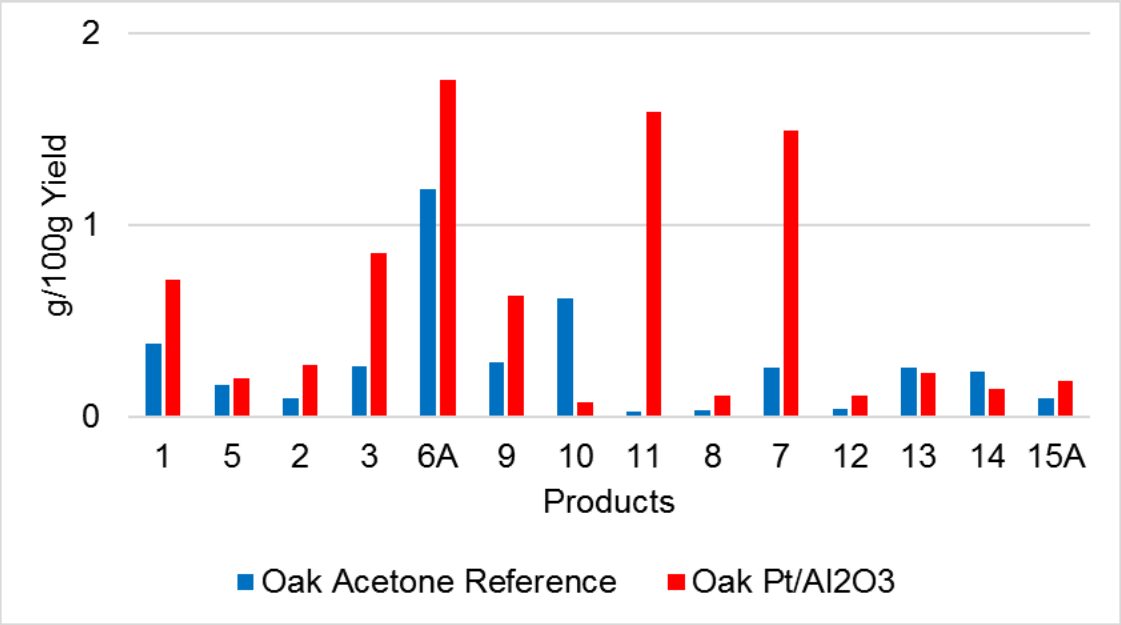

Figure 157 Depolymerisation of oak parr-lignin in the presence of Pt/Al_2O_3 support and Acetone/H_2O mixture (50:50 v/v).

The reaction with Rh/Al_2O_3 is described in Figure 158. The overall yield was 12.2 g/100 g. Rh/Al_2O_3 had good catalytic activity increasing the yields of almost all products (except 10 and 14). This metal showed a better performance than platinum (Figure 157). It had high selectivity for molecules 6A, 11 and, especially 7.

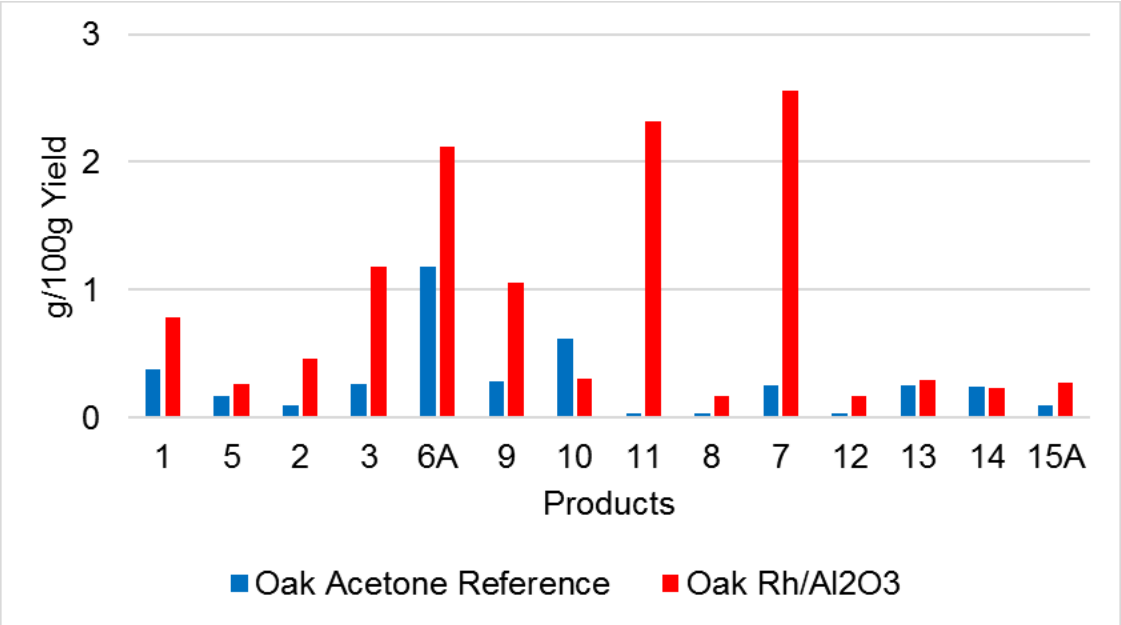

Figure 158 Depolymerisation of oak parr-lignin in the presence of Rh/Al_2O_3 support and Acetone/H_2O mixture (50:50 v/v).

The reactions with Ni/Al_2O_3 are shown in Figure 159. The overall yield was 5.8 g/100 g. Nickel had a high selectivity for product 11 as it considerably increased its yield. Nevertheless, the presence of Ni/Al_2O_3 in the reaction did not augment the values of compounds 5, 10, 13, 14 and 15A and the other products did not have their yields significantly increased. Hence, nickel did not show as good a performance in product yields as the noble metals (Figure 157, Figure 158) with this lignin.

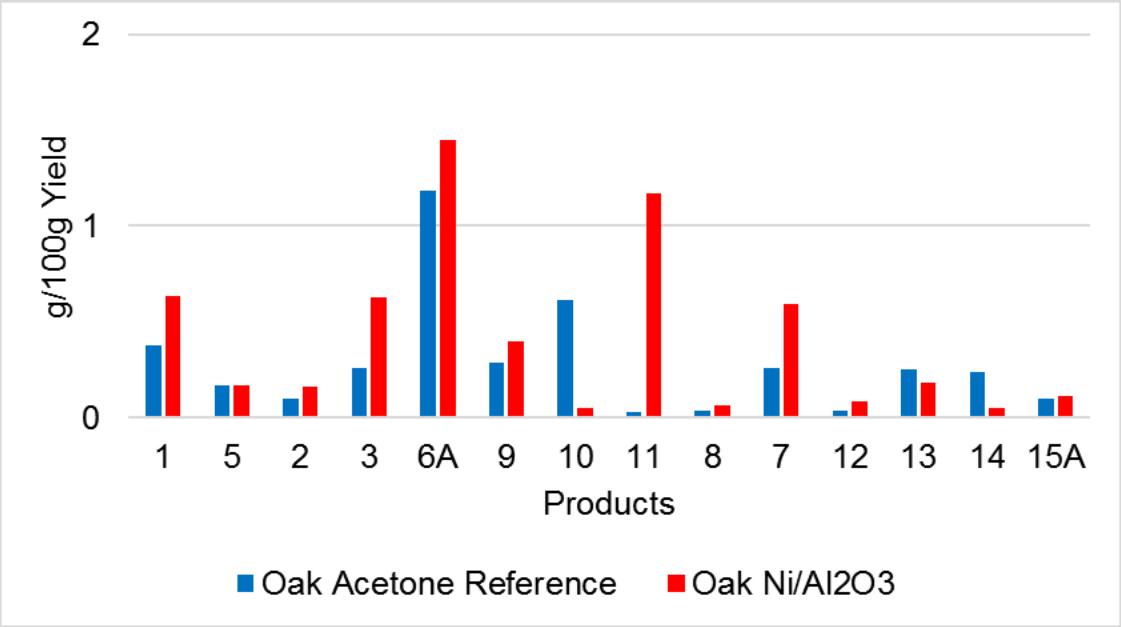

Figure 159 Depolymerisation of oak parr-lignin in the presence of Ni/Al_2O_3 support and Acetone/H_2O mixture (50:50 v/v).

The Fe/Al_2O_3 catalysed reaction is shown in the Figure below. Similar to the birch and sugar-cane lignins (Figure 130 and Figure 137), this material did not affect the product yield significantly. In addition, some molecules such as 1, 3, 6A, 10 and 14 were more favoured by solvolysis. Compounds 5, 8, 9, 11, 12, 13 and 15A had their yields slightly increased with catalyst. The overall yield was of 3.9 g/100 g.

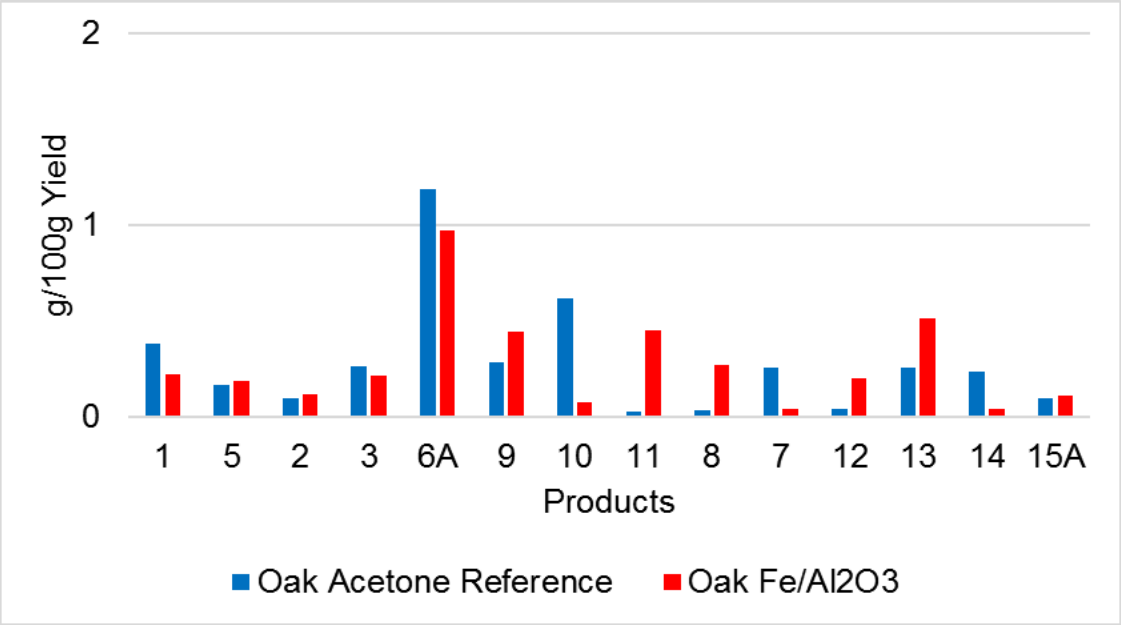

Figure 160 Depolymerisation of oak parr-lignin in the presence of Fe/Al_2O_3 support and Acetone/H_2O mixture (50:50 v/v).

6.3.2.2 Effects of carbon-based catalysts in the depolymerisation of oak parr-lignin

The effect of carbon support (C) in the depolymerisation was studied. Acetone/H_2O 50:50 v/v solution was used in the presence of C and oak parr-lignin. The overall yields were 3.9 and 13.3 g/100 g, respectively. Figure 161 shows product distribution. Paralleled to the reference experiment, the support showed high catalytic activity increasing the yields of most products, especially 1, 6A, 11 and 7. Hence, the carbon support was not inert in the mechanism of product formation.

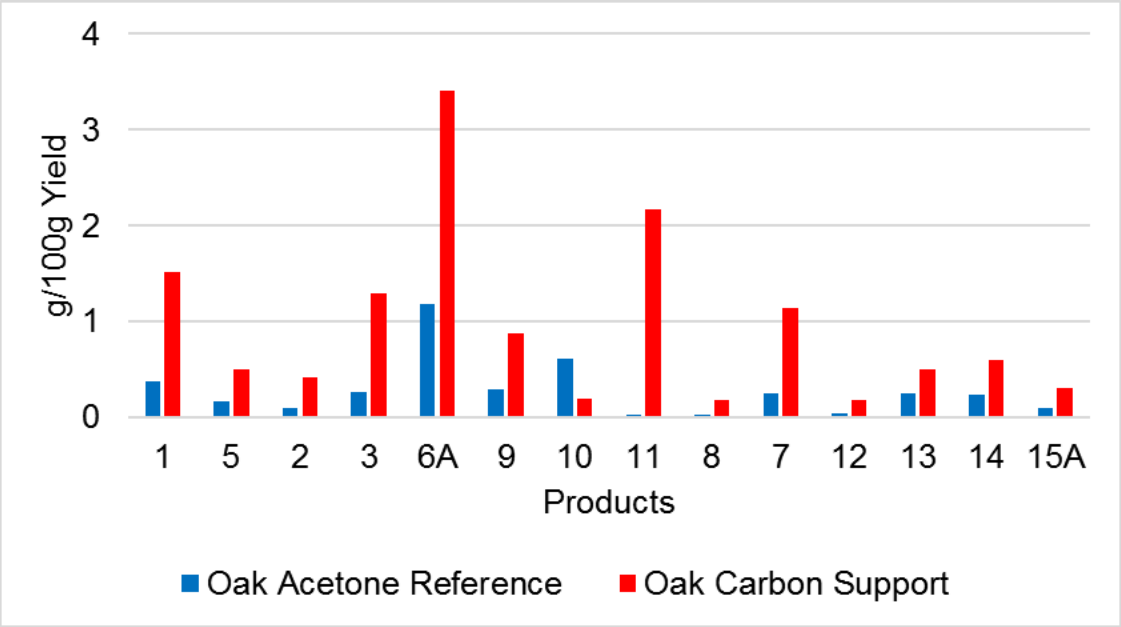

Figure 161 Depolymerisation of oak parr-lignin in the presence of carbon support and Acetone/H_2O mixture (50:50 v/v).

Figure 162 shows the results with Ni/C. With the exception of compound 10, all other products showed an increase in yield with Ni/C. This catalyst had high selectivity for product 6A. Although it had a catalytic activity similar to the carbon support, the Ni/C had highest yields for molecules 7 and 11. The overall yield was 13 g/100 g.

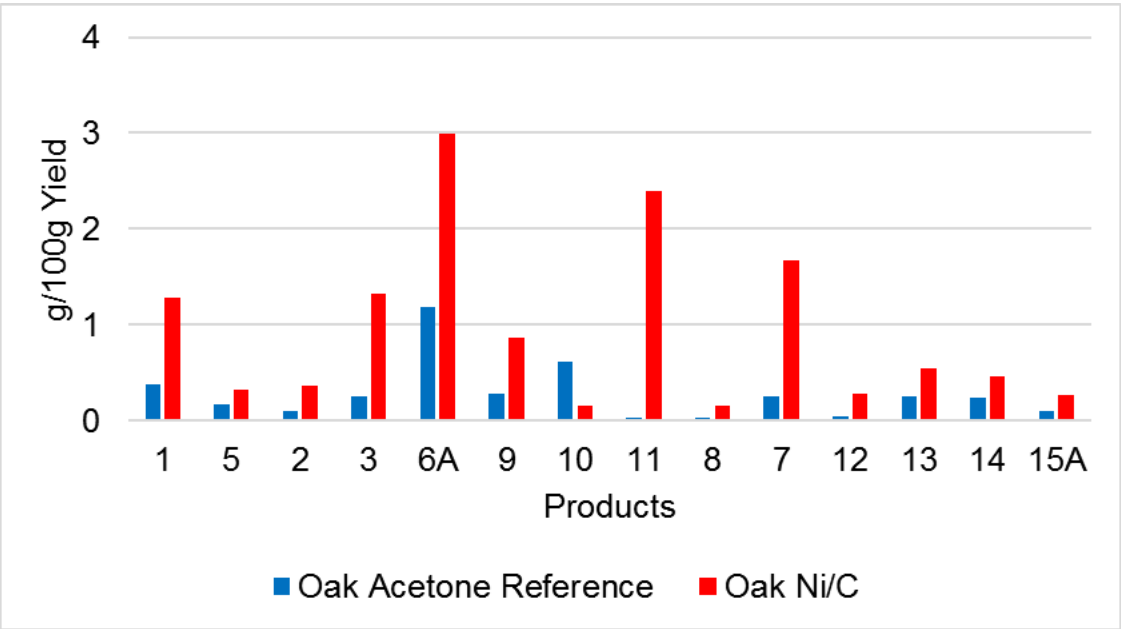

Figure 162 Depolymerisation of oak parr-lignin in the presence of Ni/C and Acetone/H_2O mixture (50:50 v/v).

Figure 163 shows the results with Fe/C. This mostly contributed for the generation of products 1 and 11 while 5, 3, and 9 slightly increased. For the others, solvolysis was more effective. The overall yield was 3.3 g/100 g.

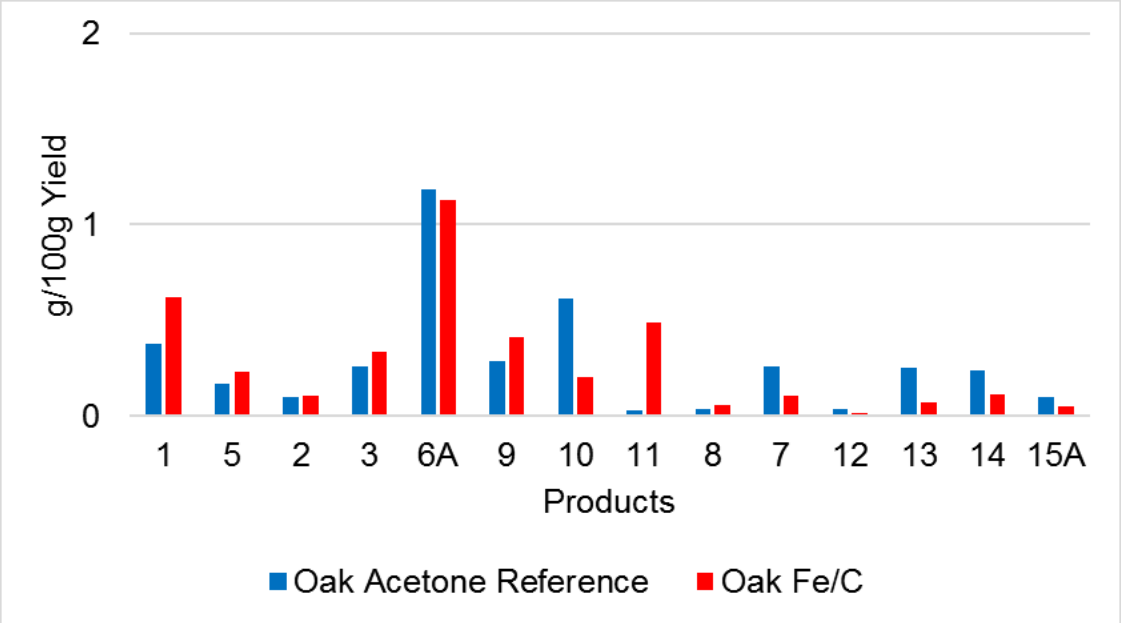

Figure 163 Depolymerisation of oak parr-lignin in the presence of Fe/C and Acetone/H_2O mixture (50:50 v/v).

6.3.2.3 Effects of zirconia-based catalysts in the depolymerisation reaction of oak parr-lignin

The depolymerisation reaction was studied in the presence of zirconia support. Acetone/H_2O 50:50 v/v solution was used in the presence of ZrO_2 and oak parr-lignin. In Figure 164, it was found that the support had a very bad performance. Only compound 11 had an increase in yield in the presence of this support. The overall yield was 3 g/100 g.

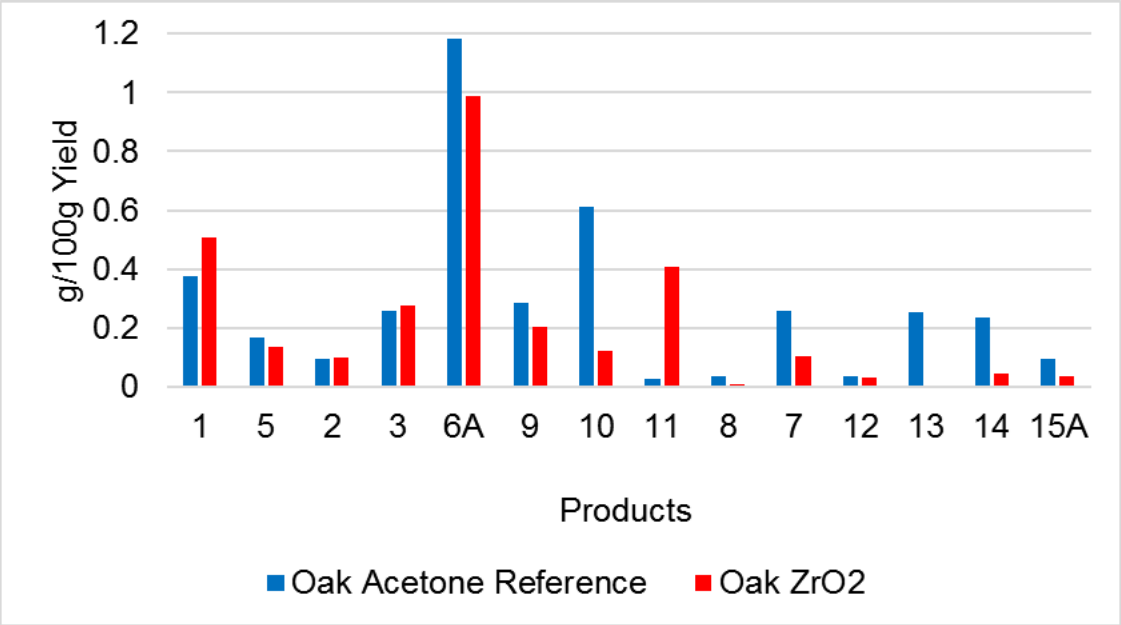

Figure 164 Depolymerisation of oak parr-lignin in the presence of zirconia support and Acetone/H_2O mixture (50:50 v/v).

The depolymerisation reaction using Ni/ZrO_2 is displayed in Figure 165. The presence of nickel in the support, changed product distribution improving the yields of compounds 1, 2, 3, 8, 11 and 12. Despite high selectivity for product 11, this catalyst did not show a substantial contribution in individual product yields as eight of the fourteen products (5, 6A, 9, 10, 7, 13, 14 and 15A) had their values favoured by the solvolysis. The overall yield was 3.8 g/100 g.

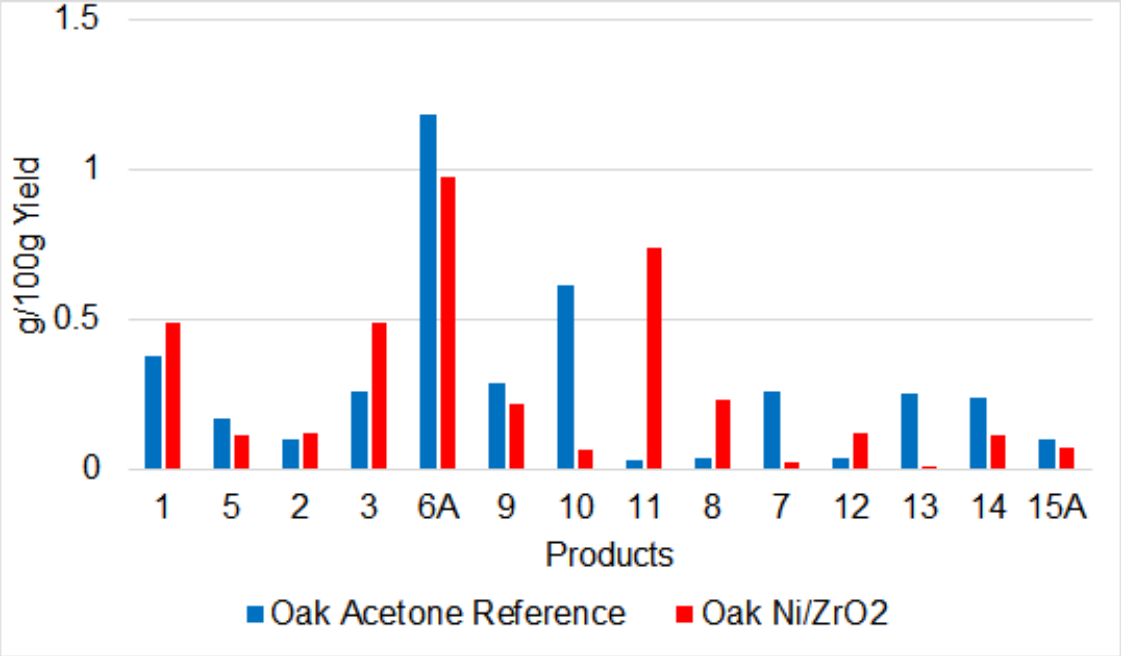

Figure 165 Depolymerisation of oak parr-lignin in the presence of Ni/ZrO_2 and Acetone/H_2O mixture (50:50 v/v).

The reaction with Fe/ZrO_2 is shown in the Figure below. The presence of iron also changed product distribution and showed a better performance than the support (ZrO_2) and Ni/ZrO_2 (Figure 164 and Figure 165). This catalyst increased yields for compounds 3, 9, 11, 12, 13 and 15A. Like the Ni/ZrO_2, this material also had high selectivity for product 11. The overall yield was 4.6 g/100 g.

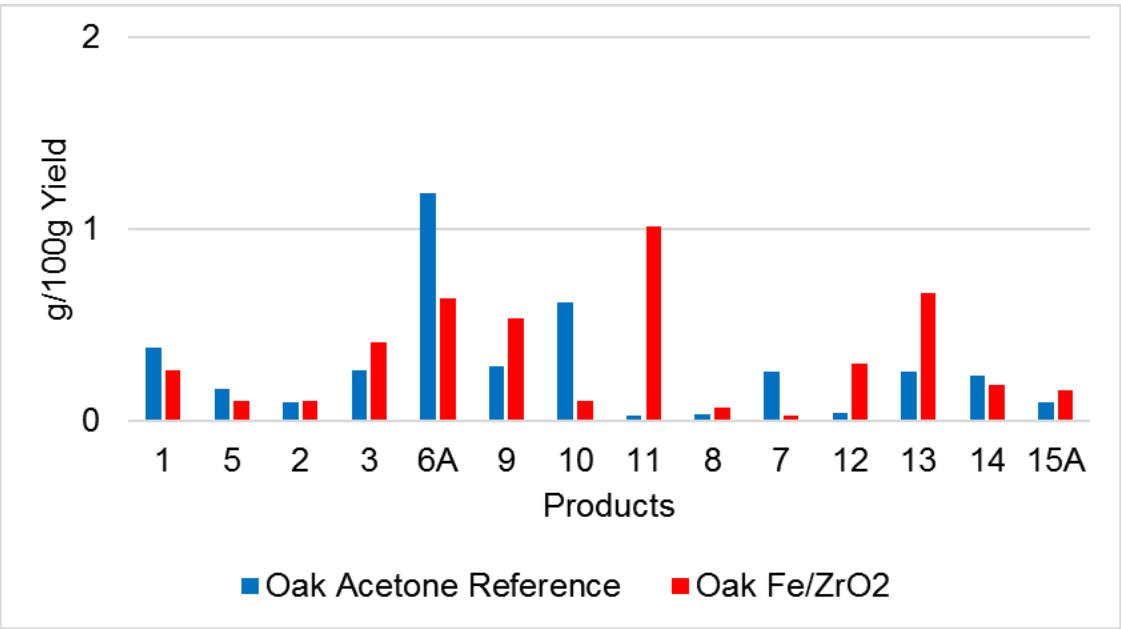

Figure 166 Depolymerisation of oak parr-lignin in the presence of $Fe//ZrO_2$ and Acetone/H_2O mixture (50:50 v/v).

6.3.2.4 Effects of isopropanol solution and alumina-based catalysts in the oak parr-lignin depolymerisation

The following experiments were carried out with IPA/H_2O mixture. The solvolysis of oak parr-lignin in the presence of IPA/H_2O solution and the reaction in the presence of Al_2O_3 support are described in Figure 167. The overall yields were 4.7 and 5.7 g/100 g, respectively. The support showed some catalytic activity slightly increasing the yields of most compounds. Nevertheless, products 3, 10, 12 and 15A were produced in highest quantities with solvent.

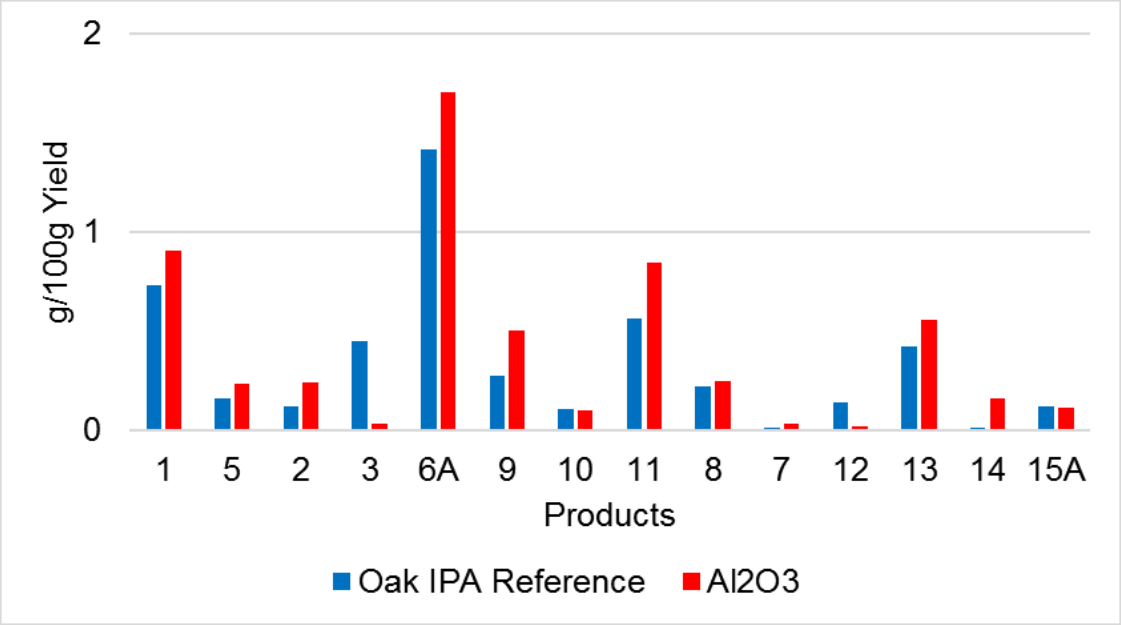

Figure 167 Depolymerisation of oak parr-lignin in the presence of Al_2O_3 and IPA/H_2O mixture (50:50 v/v).

Pt/Al_2O_3 catalysed reactions are displayed in Figure 168. The overall yield was 5.2 g/100 g. Related to the reference and the reaction with Al_2O_3 support, the presence of platinum resulted in the selectivity of products 2,8, 9 and 11, augmenting their individual yields. Compounds 5, 7, and 14 just had a slight increase in the values while all other products were promoted by solvent.

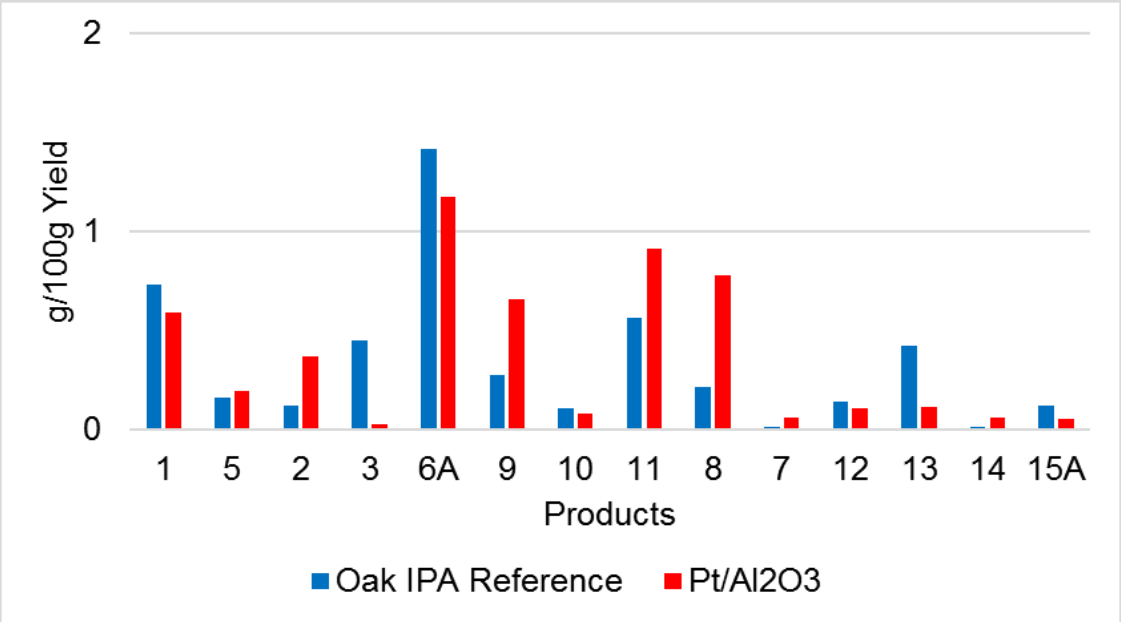

Figure 168 Depolymerisation of oak parr-lignin in the presence of Pt/Al_2O_3 and IPA/H_2O mixture (50:50 v/v).

The reaction with Rh/Al_2O_3 is showed in Figure 169. The overall yield was 4.9 g/100 g. The catalyst showed a high selectivity for product 9. Similar to the Pt/Al_2O_3 catalysed reaction (Figure 168), the Rh/Al_2O_3 influenced individual product yields (2, 9, 10, 8, 7, 12 and 14) but the IPA/H_2O mixture also had high selectivity in the production of certain compounds, such as 1, 6A, 11 and 13.

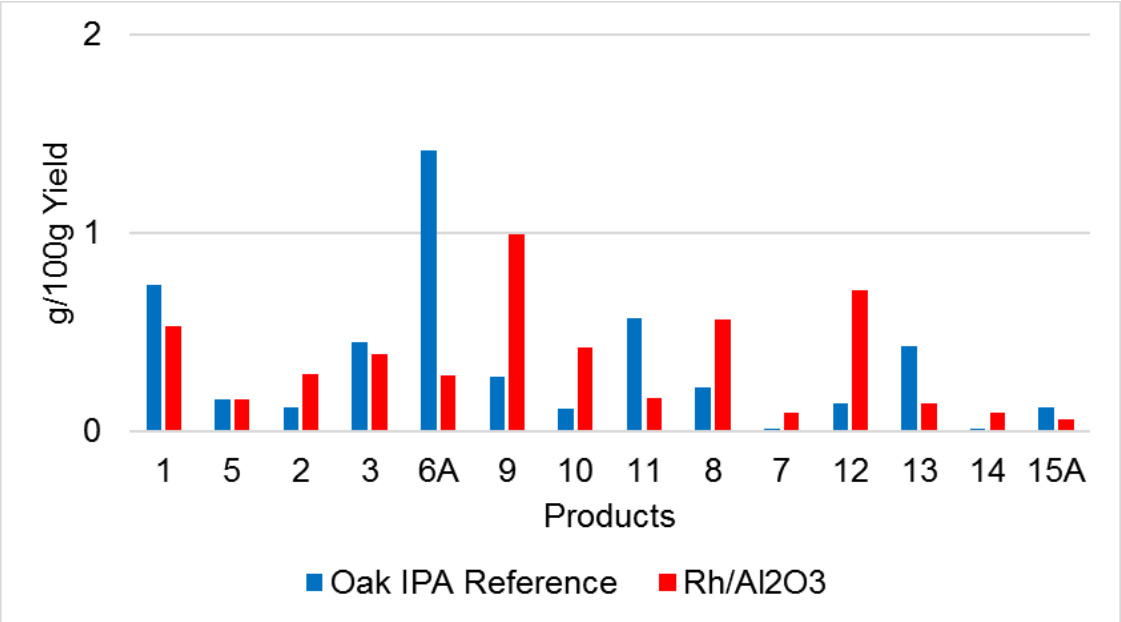

Figure 169 Depolymerisation of oak parr-lignin in the presence of Rh/Al_2O_3 and IPA/H_2O mixture (50:50 v/v).

The depolymerisation experiments with Ni/Al_2O_3 are shown in Figure 170. The overall yield was 7.4 g/100 g. The nickel showed a better performance compared to noble metals supported on alumina (Figure 168 and Figure 169). It had the highest overall yield and increased the production for all individual compounds (except 10) and with high selectivity for 6A and 9.

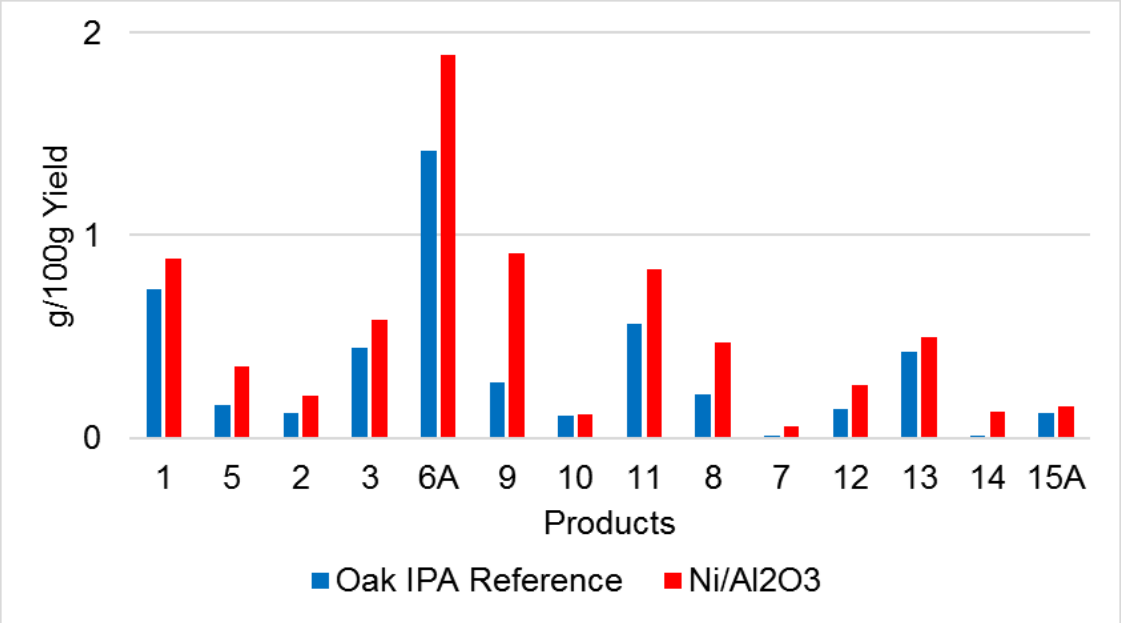

Figure 170 Depolymerisation of oak parr-lignin in the presence of Ni/Al_2O_3 and IPA/H_2O mixture (50:50 v/v).

The Fe/Al_2O_3 catalysed reaction is shown in the Figure below. Overall, the Fe/Al_2O_3 catalyst did not show a great performance. For certain products the solvolysis was better (1, 5, 2, 3, 6A, 8, 11 and 12), however, the presence of iron brought a high selectivity towards 9 and 7. In addition, molecules 10, 12, 14 and 15A had their values slightly increased. The overall yield was 4.1 g/100 g.

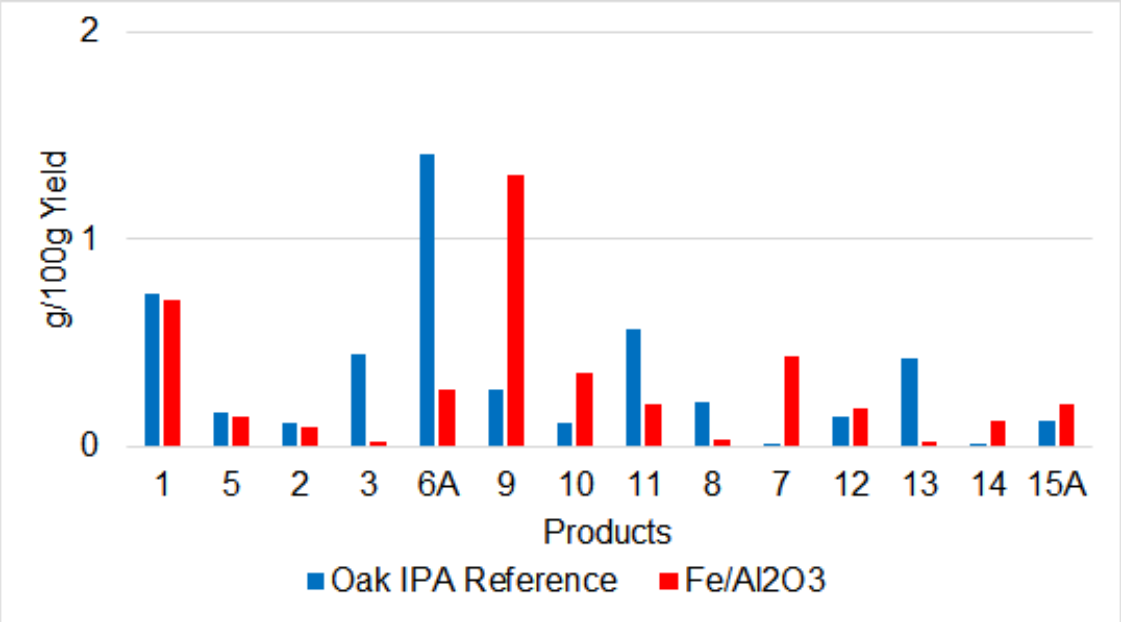

Figure 171 Depolymerisation of oak parr-lignin in the presence of Fe/Al_2O_3 and IPA/H_2O mixture (50:50 v/v).

6.3.2.5 Effects of carbon-based catalysts in the depolymerisation of oak parr-lignin

Carbon support was used in an IPA reference reaction in order to evaluate if it would present catalytic activity. The overall yield was 5.6 g/100 g. Figure 172 shows product distribution. The support showed relative catalytic activity increasing the yields of products 2, 7, 8, 9, 10, 12, 14 and 15A. Hence, the carbon support was not inert but not as active as in the presence of acetone solution (Figure 161).

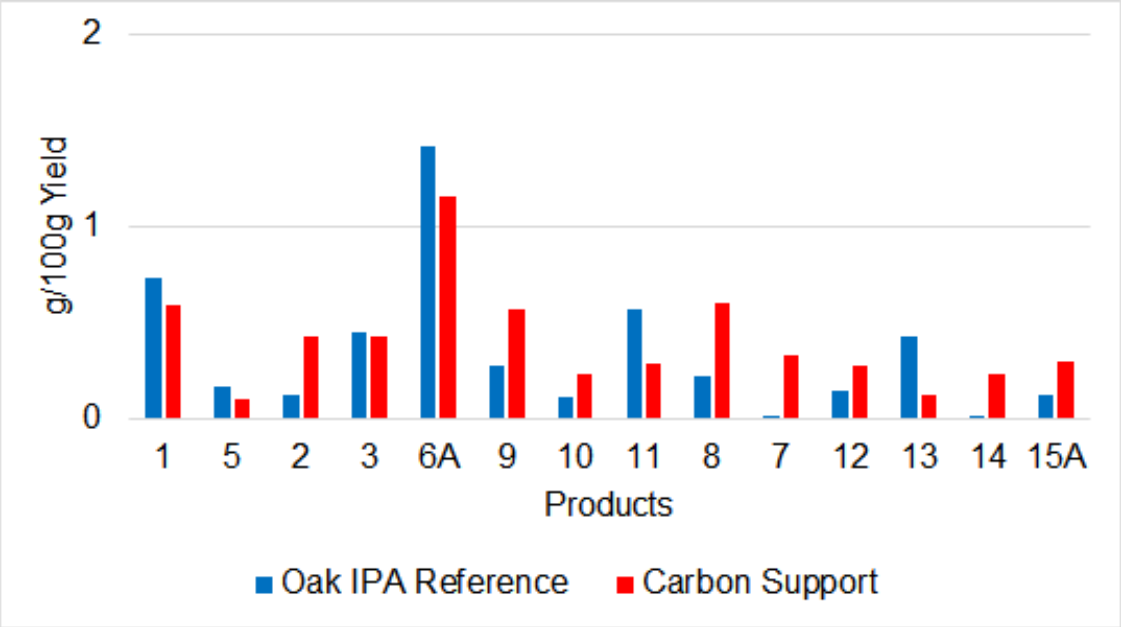

Figure 172 Depolymerisation of oak parr-lignin in the presence of carbon support and IPA/H_2O mixture (50:50 v/v).

Figure 173 shows the results for Ni/C catalysed reactions. The overall yield was 6.3 g/100 g. Apart from compounds 5, 3 and 10, all other products showed an increase in yield with Ni/C. Hence, related to the reaction with support (Figure 172) the presence of nickel on the support, increased the yields towards individual compounds, mainly 9, 8 and 11.

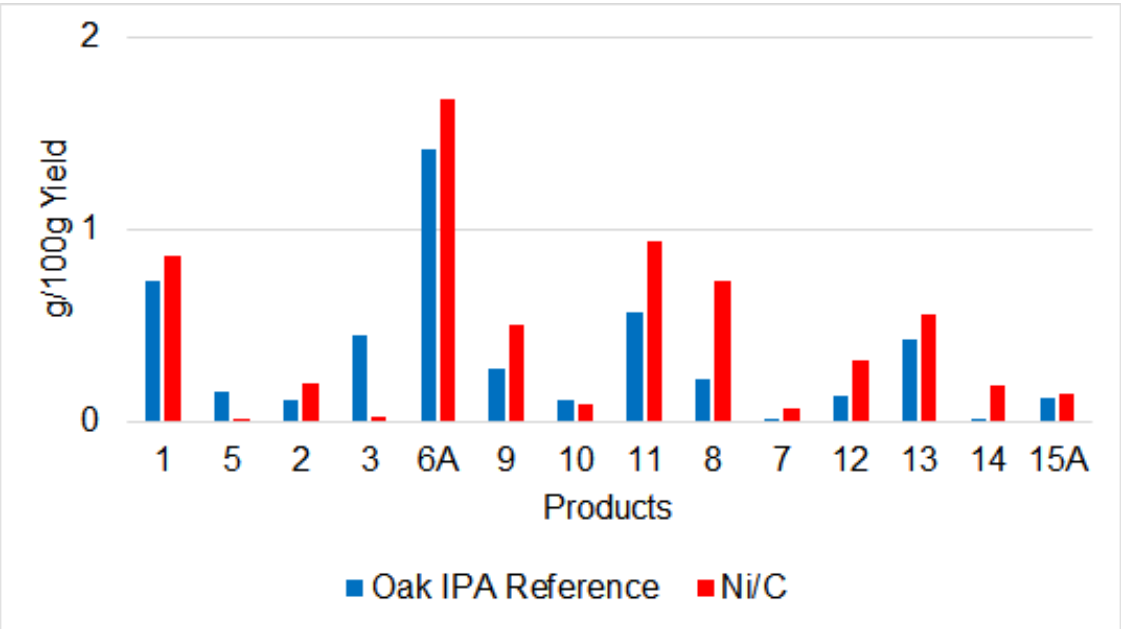

Figure 173 Depolymerisation of oak parr-lignin in the presence of Ni/C and IPA/H_2O mixture (50:50 v/v).

The reaction with Fe/C is presented in Figure 174. Addition of Fe/C did not significantly affect most products yields. This catalyst contributed compounds for 9, 14 and 15A generation. The overall yield was 4.7 g/100 g.

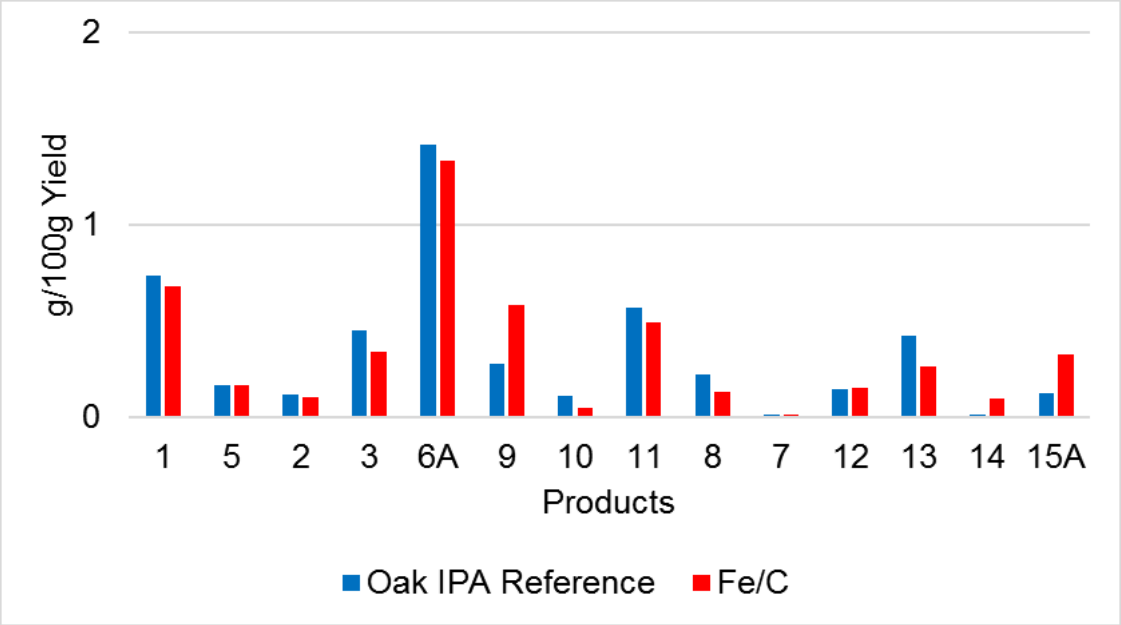

Figure 174 Depolymerisation of oak parr-lignin in the presence of Fe/C and IPA/H_2O mixture (50:50 v/v).

6.3.2.6 Effects of zirconia-based catalysts in the oak parr-lignin depolymerisation

The effect of zirconia support was studied in the reaction with IPA solution. As presented in the Figure below, the addition of ZrO_2 to the reference reaction did not bring considerable changes. The support affected to some extent products 9, 11, 14 and 15A, however, for other molecules, their values with ZrO_2 were similar to the reference experiment. The overall yield was 4.5 g/100 g.

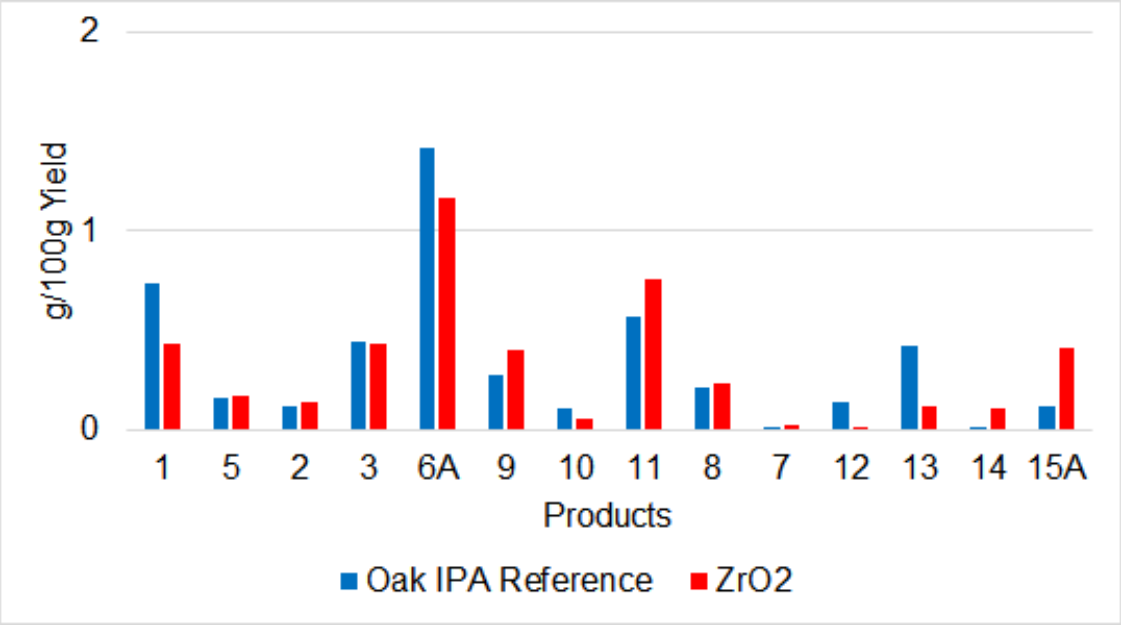

Figure 175 Depolymerisation of oak parr-lignin in the presence of ZrO_2 support and IPA/H_2O mixture (50:50 v/v).

The Ni/ZrO_2 depolymerisation reaction is described in Figure 176. The overall yield was 4.8 g/100 g. The presence of nickel in the support did not show significant variations. It was found a small increase in yields for products 2, 8, 9,11,12, 14 and 15A. Compounds 8 and 12 were slightly favoured by the presence of metal.

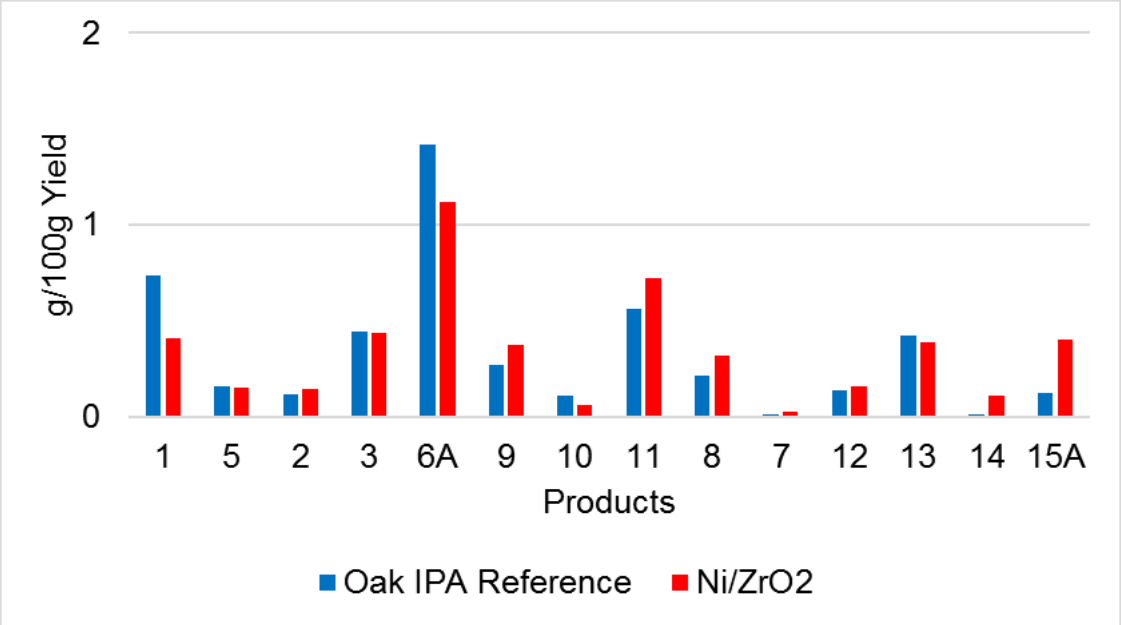

Figure 176 Depolymerisation of oak parr-lignin in the presence of Ni/ZrO_2 support and IPA/H_2O mixture (50:50 v/v).

The reaction with Fe/ZrO_2 is presented in Figure 177. The presence of iron resulted in better yields than the experiments with ZrO_2 and Ni/ZrO_2 (Figure 175 and Figure 176). This catalyst slightly increased most yields (5, 2, 3, 9, 8, 7, 12, 13, 14 and 15A). The other molecules were slightly better produced with solvolysis. This material had high selectivity for product 8. The overall yield was 6 g/100 g.

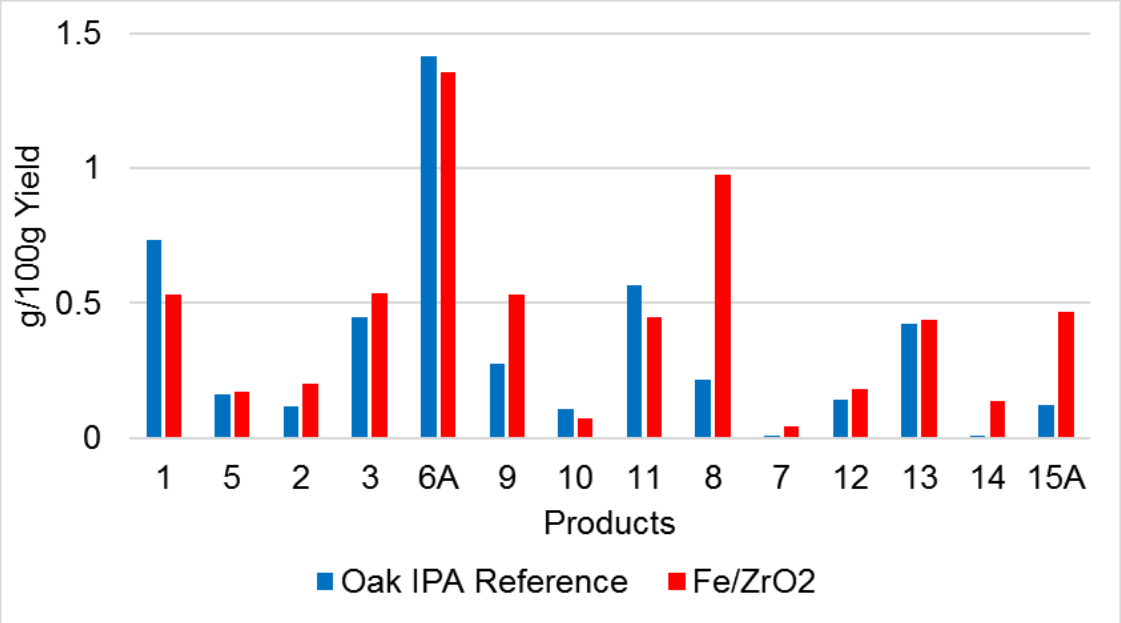

Figure 177 Depolymerisation of oak parr-lignin in the presence of Fe/ZrO_2 support and IPA/H_2O mixture (50:50 v/v).

6.3.2.7 GPC analysis of depolymerised lignins

In this section, a selection of reactions was used to demonstrate the change in molecular weight distribution, molecular number and polydispersity after a depolymerisation reaction in the presence and absence of Pt/Al_2O_3. In general, these lignins showed a much lower molecular weight compared to the Kraft lignin. All Mw and Mn values reduced after depolymerisation reactions. Table 19 shows the changes in Mw, Mn and Ip for these experiments. Compared to the starting materials, all lignins showed in the GPC plot a shift to the right from ~12 to ~ 14 min which was regarded to lower molecular weight products in these samples. For sugar-cane lignin, birch and oak parr-lignin, acetone reference and catalysed (Pt/Al_2O_3) experiments were used.

Table 19 GPC analysis of sugar cane, birch and oak Parr-lignins for catalysed and non-catalysed reactions.

Reaction type		Molecular Weight (Mw, g/mol)	Molecular Number (Mn)	Polydispersity (Ip)
A	**SC Lignin (SC)**	2291	731	3.0
B	Acetone/H_2O Reference (SC)	1355	541	2.5
C	Acetone/H_2O Catalysed (SC)	1179	517	2.27
D	**Birch parr-lignin (BP)**	2987	977	3.0
E	Acetone/H_2O Reference (BP)	863	528	1.6
F	Acetone/H_2O Catalysed (BP)	1208	566	2.1
H	**Oak parr-lignin (OP)**	2707	1029	2.6
I	Acetone/H_2O Reference (OP)	1605	605	2.6
J	Acetone/H_2O Catalysed (OP)	1199	594	2.0

Figure 178 shows the molecular weight distribution plot for the sugar-cane lignin reactions presented in Table 19. Original lignin was included in the graph for comparison. Catalytic and non-catalysed reactions had similar profiles. Hence, this data alone showed that the catalyst did not make a dramatic change in the reaction. However, Table 19 showed that the Mw values obtained were not exactly in the same region. The starting sugar-cane lignin reduced from 2291 to 1355 g/mol (~ 40 %) without catalyst and 1179 g/mol (~ 49 %) with catalyst in the reaction. The Ip values revealed that the reference provided slightly less uniform fragments (2.5) when related to the catalytic run (2.27).

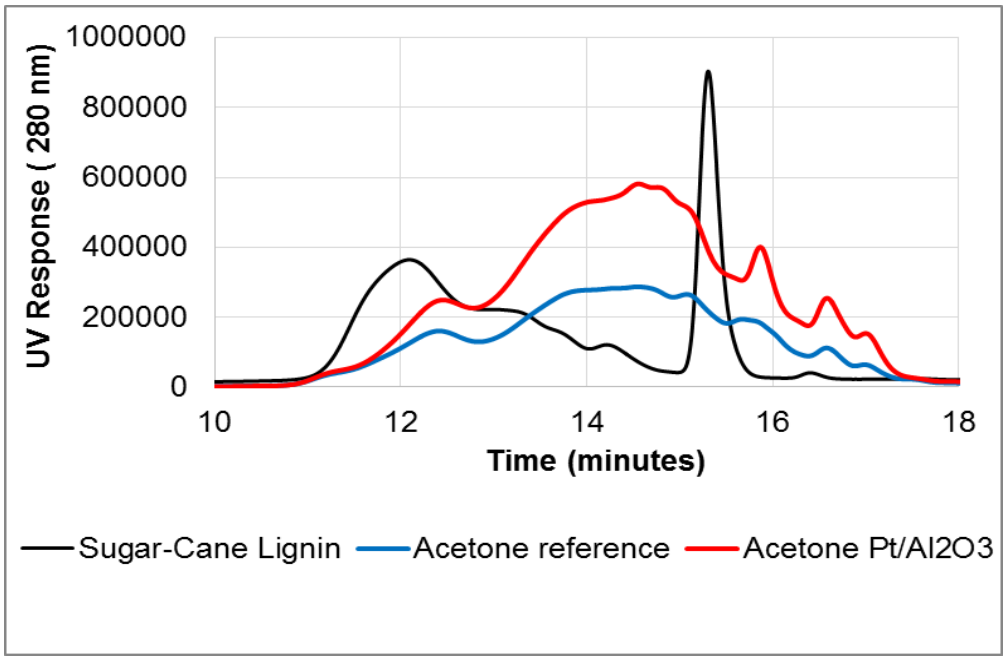

Figure 178 GPC profile of sugar-cane lignin, acetone non-catalysed and Pt/Al_2O_3 catalysed depolymerisation.

For the reactions involving birch parr-lignin, acetone and Pt/Al_2O_3, the resultant GPC plots in Figure 179 were not very similar. Table 19 shows that the Ip was 1.6 compared to 2.1 for the catalytic run, hence, the solvolysis resulted in less complex polymer formation. However, in terms of reaction, Table 19, showed an increase in the depolymerisation for the catalytic run as the starting birch lignin reduced its Mw in ~ 60 % with the presence of Pt/Al_2O_3.

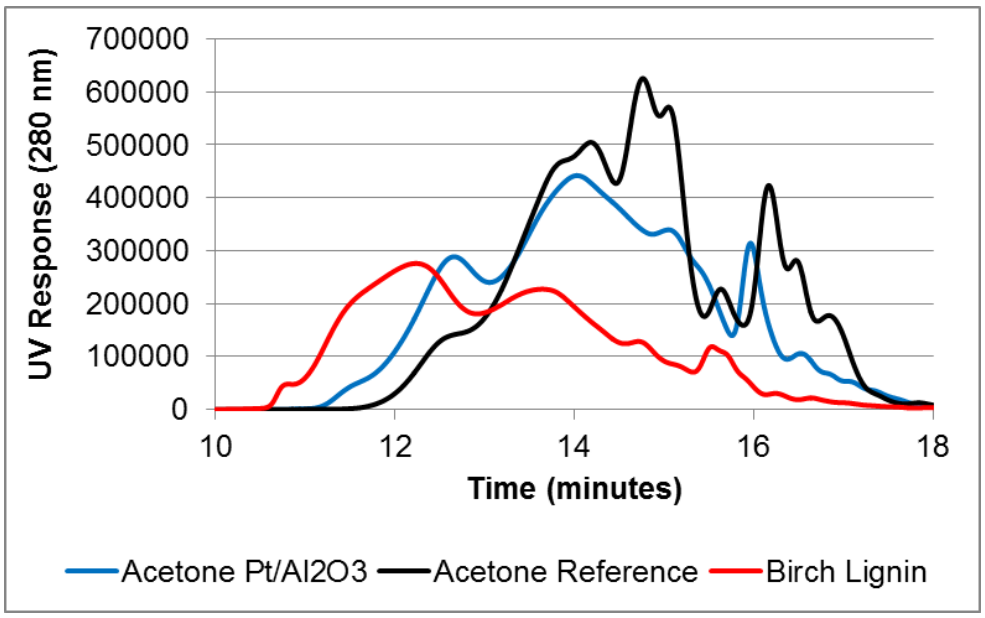

Figure 179 GPC profile of birch parr- lignin, acetone non-catalysed and Pt/Al_2O_3 catalysed depolymerisation.

According to Table 19, for acetone reference and catalysed experiments, oak lignin reduced from 2707 Da to 1605 Da (~40 %) and 1199 Da (~56 %), respectively. Therefore, this lignin was able to convert up to 56 % of its original weight in these reaction conditions. According to the Ip, the catalytic run had more uniform molecule fragments (Ip value of 2), while the solvolysis showed molecules complexity similar to the original lignin (Ip value of 2.6), probably due to fragments formed in the repolymerisation process. Figure 180 shows the GPC profile of oak parr-lignin with acetone/H_2O solution (50:50 v/v) in non-catalysed and catalysed reactions.

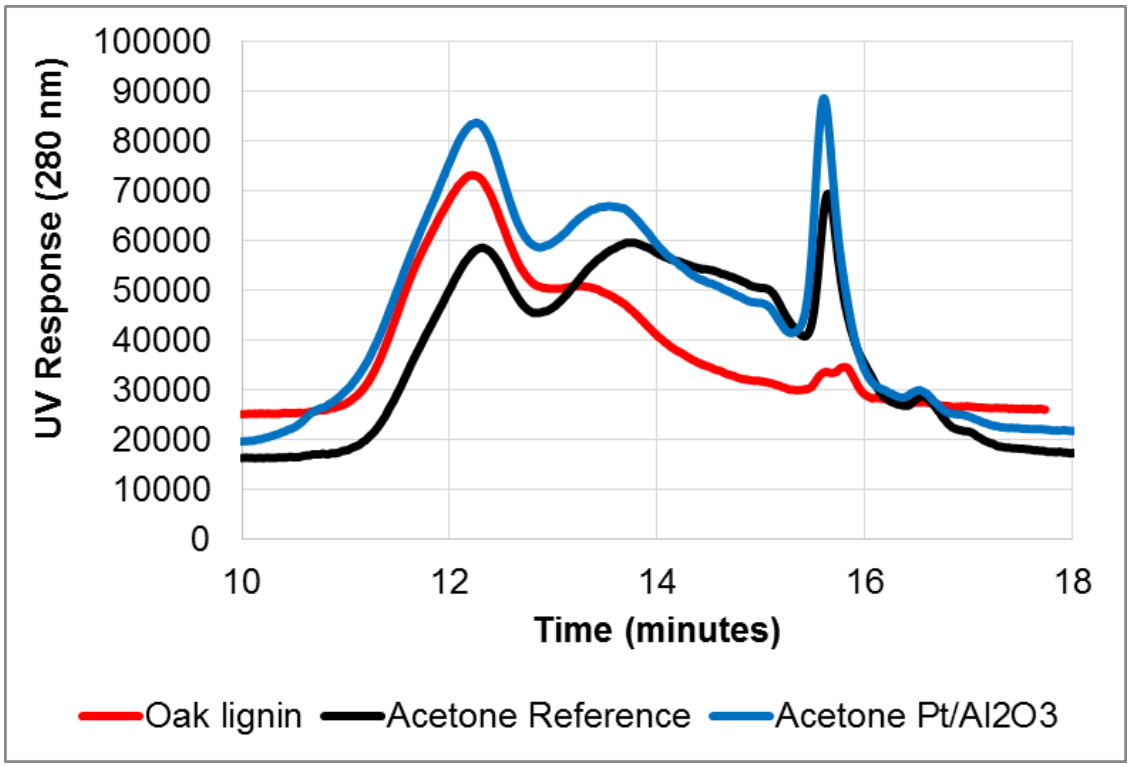

Figure 180 GPC profile of oak parr- lignin, acetone non-catalysed and Pt/Al_2O_3 catalysed depolymerisation.

7 Discussion

7.1 Solvent effects in Kraft and isolated lignin depolymerisation

The lignins studied in this project had different wood sources and extraction pre-treatments. As a result, a variety of linkages such as β-O-4, β-O-4(Et), β-5 and β-β were detected by NMR (Section 5.3). Such bonds are essential in lignin depolymerisation. GPC analysis showed different molecular weight, molecular number and polydispersity, revealing the degrees of condensation on these materials. In depolymerisation of lignin, a wide range of products can be formed in the gas, solid and liquid phase. The compounds discussed in this study were those detected in the liquid phase.

Depolymerisation happened in Kraft, sugar-cane and parr-lignins in the presence of solvent mixtures and hydrogen at 573 K. The same product yield was not found for different lignins in equivalent solvent proportions, signifying that the action of the solvent in the generation of phenolic monomers depended on the type of lignin studied. Reactions were conducted at high pressure and high temperature. These thermochemical experiments were to some extent similar to pyrolysis. However, the use of solvents allowed the transformation of solid (lignin) into liquid products (aromatics) with less char formation. Despite various researchers including the use of solvents in lignin depolymerisation, there is a lack of detailed information about their role in the reaction mechanism. Clarifying how solvents cause product formation in the presence or absence of catalysts is still a challenge. However, it was possible to analyse the influence of solvents in these reactions.

7.1.1 The behaviour of pure substances and mixtures

Amphiphiles are substances that present hydrophilic and lipophilic characteristics [100]. Examples are the alcohols and acetone used in this research. The polar aspect of these molecules can interact with water through hydrogen bonds, while the non-polar can induce a hydrophobic behaviour, resulting in the same molecule causing deviations from ideal solutions and Raoult's law in water. Some of the physical properties that can be affected in these type of solutions are viscosity, density, dieletric constant and surface tension [101].

In non-azeotropic mixtures, the components have different boiling points (BP) and the most volatile (with lower BP) evaporates first [102]. Azeotropic mixtures evaporate and condense at a constant temperature, at a certain pressure. In addition, the composition of the vapour is

the same as in the liquid mixture [103]. The alcohol/water solutions used in this work were examples of azeotropic mixtures. For water/ethanol and water/IPA solutions, the azeotrope boiling points are 351.2 K [104] and 353.57 K [105], respectively. However, acetone/water solution was non-azeotropic as the components have considerably different boiling points (water and acetone, BP 373 K and 329 K, respectively). However, despite those solutions being non-azeotropic and zeotropic, these concepts of BP behaviour could not be fully extended to the system used in this research. Distillation was not of interest and the experiments were carried out in a closed system, which could prevent the mixture from boiling, enhancing the possibility of supercritical fluids formation.

At room pressure and temperature, substances can be in the solid, liquid or gas phase depending on how strong their intermolecular forces are. However, changes in pressure (P) and temperature (T) can cause phase transitions. Figure 181 illustrates these changes in a water phase diagram. The vertical lines represented the coexistence curves. The vapour state of water is found in the point 1, followed by an equilibrium between solid-vapour at point 2. At point 3, water is converted into solid while at point 4 solid-liquid coexist. For point 5, water was only in the liquid phase. By changing T and P, water becomes solid at point 6, however, keeping P constant and increasing T, water became a liquid again at 7. Triple point is represented by C, which was end of the liquid-vapour coexistence curve [106].

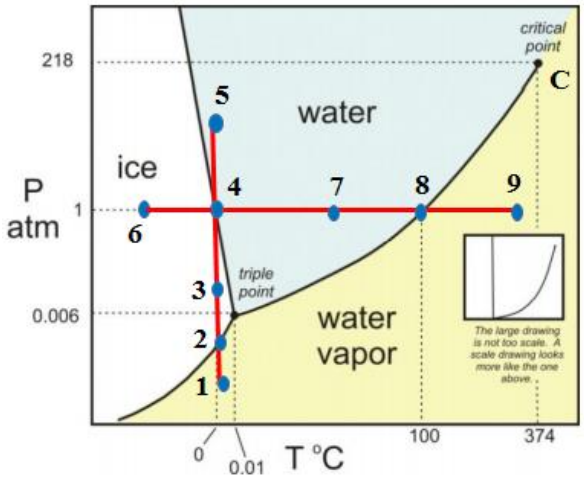

Figure 181 Phase diagram of water. Adapted from reference [107]**.**

For a pure substance, a critical point (CP) is characterised by the absence of phase boundaries at specific critical temperature and critical pressure. Consequently, it is the end of a phase equilibrium curve [108]. One of the most common examples is the critical point of liquid-vapour. As shown in Figure 181 point C was the end of the curve that had the conditions for

coexistence of two phases. In a closed system, the vapour density increases until it reaches the CP, at this point, its density become equal to the liquid density and they turn out to be indistinguishable [108]. Above the CP, supercritical fluids can exist. These substances have changes in their properties and they become simultaneously similar to liquids and gases. This is represented by variations in aspects such as density, viscosity and diffusion coefficient [109].

The CP of substances was a relevant topic for this research as this work was performed at high temperature and pressure in a closed system. Table 21 summarises the values of individual critical points for water, ethanol, isopropanol and acetone. Water was the only substance that in its pure state would not reach the critical point in the reaction conditions used in this work. However, the pressures reached during the reactions (Table 20) would be enough for the other solvents (if they were in their pure state) to pass their critical points. One important consideration was that the experiments were carried out with solvent mixtures and not with pure substances. In solutions of miscible components, intermolecular interactions are broken and new ones formed, and this varied according to the type of solvent or proportion in the mixture used. Phase diagrams of mixtures can be very different compared to a pure substance. Ethanol and water, for example, boil at 351 K and 373 K, respectively. However, in a mixture of EtOH and H_2O the boiling point appears at 351.2 K. The IPA solutions behaviour at high temperature and pressure were not assumed to be equal to the ethanol, but neither very different, because, in general, the BP of these azeotrope mixtures is similar (EtOH/H_2O, 351.2 K and IPA/H_2O, 353.57 K). In our experiments, for acetone, the pressure and temperature used were much higher than its critical point. Acetone-water mixtures had different values for individual critical temperatures (CT) (acetone CT < water CT). Thus, the lower CT represented the phase separation temperature. Intermolecular interactions can be broken with increase in temperature, and the increase in the positive entropy effect would result in $\Delta G < 0$ [110], favouring acetone to leave the liquid phase. In this case, this solvent could be in a supercritical state (SC) and a complex system of SC acetone and water in phases equilibrium was also considered to exist. SC conditions of alcohols is highly studied in the literature [111]–[114] and these systems are not simple to describe, as they form an azeotropic mixture with water. In addition, the solutions in this work were not identical (various proportions with water were used) adding more challenge for understanding. According to Table 20, it was found that the increase in solvent content, enhanced the pressure of the system during the reaction. Indicating that the alcohols were passing to the vapour phase, possibly achieving supercritical state.

It was important to consider that the reactions carried out in this project involved solvent mixtures, hydrogen and the lignin mostly dissolved in all solvent solutions. There were various intermolecular interactions occurring that could have affected the critical points. Hence, this was not a simple binary system that could be directly compared to pure substances or ideal mixtures. In addition, due to technical limitations, the system could not be accessed during the reactions and its exact behaviour at 573 K could not be described.

After the experiment, when the reactor had returned to room temperature, there was no significant pressure variation (+/- 2 bar) compared to the initial (20 bar). Hence, gas formation was not considered in this study. Firstly, because if gaseous products were formed, the quantity was low and, lastly, there were technical limitations to detect and quantify gases.

Table 20 Pressure at 573 K for all solvent mixtures in the presence of Kraft lignin and 20 bar of hydrogen

Solvent Mixture	Pressure (bar)
EtOH/H_2O 25:75 v/v	120
EtOH/H_2O 50:50 v/v	140
EtOH/H_2O 75:25 v/v	150
IPA/H_2O 25:75 v/v	125
IPA/H_2O 50:50 v/v	135
IPA/H_2O 75:25 v/v	145
Acetone/H_2O 25:75 v/v	115
Acetone/H_2O 50:50 v/v	135
Acetone/H_2O 75:25 v/v	150

Table 21 Temperature and pressures of the critical points of water [106], ethanol [115], isopropanol [116] and acetone [117].

Solvent	Temperature (K)	Pressure (bar)
Water	647	218
Ethanol	514	63
Isopropanol	509	49
Acetone	508	48

7.1.2 Possible solvent reaction pathways in lignin depolymerisation

Water in subcritical or supercritical conditions has been widely studied in lignin depolymerisation, including settings at various pressures, temperatures, lignin-H_2O proportion and time [50], [118], [119]. In conditions close to critical point, water can present valuable characteristics, such as low viscosity and capacity to mix with organic compounds. In these conditions, hydrolysis can be favoured due to the presence of more H^+ and OH^-, as well as acid or base catalysed reactions [120]. In our reactions, hydrolysis could not be prevented as all solutions were in mixture with water. It was assumed as part of the mechanism of product formation. Figure 182 shows possible hydrolysis pathways and typical products from lignin depolymerisation in water.

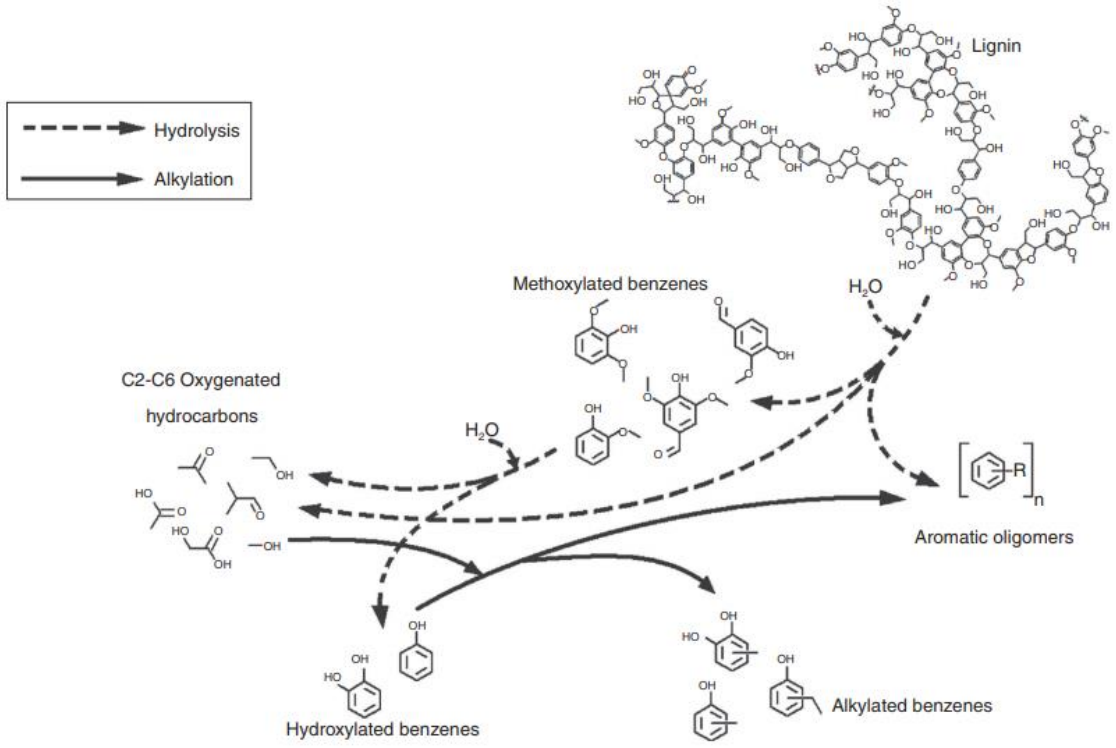

Figure 182 Possible reaction products from solvolysis of lignin [67]

In the literature, lignin depolymerisation was revealed to happen in supercritical water in the absence of catalyst. However, the yields usually were not high and there was considerable char formation. These effects were then minimised by the addition of phenol to the system [114]. Phenol could act by promoting homogeneity and minimizing condensation problems [121], highlighting the relevance of solvent mixtures. Organosolv lignin depolymerisation was investigated in the presence of supercritical acetone, methanol and ethanol. It was found

that acetone was the best solvent to be used. In addition, less condensed lignins were more suitable for the generation of monomeric products in these reactions [112].

Nielsen and co-authors studied the effect of different alcohols (ethanol, methanol, 1-propanol and 1-buthanol) in the supercritical state for the depolymerisation of lignin [122]. They found that, for some reason still not clear, methanol was the solvent with the poorest performance while the others had similar oil yield. They suggested a sequence of pathways by which the depolymerisation could occur (Figure 183). They included some transformations of the alcohols themselves, described as follows: a) polymerisation of solvent leading to the formation of light organics b) Decarbonylation generating gas c) reaction of solvent with lignin with possible combination of the alcohol chain in the bio oil d) polymerisation of light organics formed in path b, becoming part of the final bio-oil e) gas formation from bio oil and previous alcohol incorporation f) decomposition of light organics to gas.

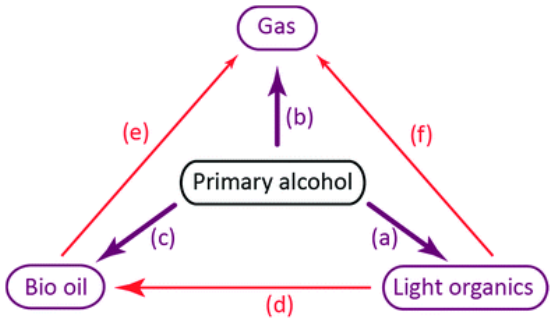

Figure 183 Pathways that alcohols can take under supercritical conditions [122]

These paths showed that not only the cleavage of lignin linkages happened in the supercritical state, but these solvents could undergo side reactions. This highlights the complexity of the system studied in this project and that additional aspects involving solvent consumption could be involved. However, because most of the tests in this work were performed using mixtures, interpretation of the results is not as simple as in homogenous systems. How exactly our solvents were behaving compared to Figure 183 during the experiment conditions is still unknown. However, if these alcohols went supercritical at some extent, compounds from the above diagram could also be in the reaction.

Researchers showed the incorporation of alcohol solvents in lignin after reaction by examining H:C molar ratios. It was found that the increase in the H:C ratio was directly related to alcohol chain length [122]. This could correspond to the incorporation of alcohol

in the bio oil. The presence of alkyl groups from alcohols in depolymerised lignins were mainly confirmed by NMR analysis and many reaction pathways were suggested. The following two main routes were considered in Figure 184: (a) Homolytic cleavage followed by a scavenger alcohol radical incorporating into the molecule, minimising condensation issues. (b) Cleavage of ether bonds by solvolysis (transesterification) [122].

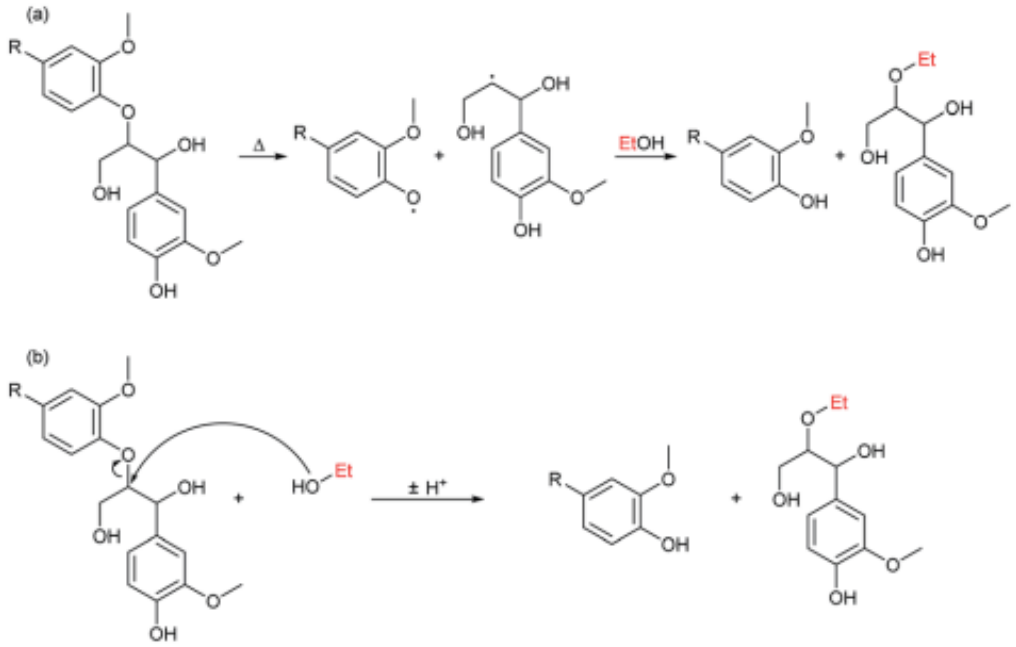

Figure 184 Reaction pathways in the presence of alcohol [122]

7.1.3 Solvolysis of Kraft lignin

As discussed in the previous sections, several investigations considered the role of solvents in lignin depolymerisation. One of the main points was the reductive depolymerisation of lignin due to the alcohols' capacity in promoting the cleavage of ether linkages, hydrogen donor effects and their contribution in decreasing recondensation. Most researchers have focused on the performance of individual solvents with knowledge of solutions of variable composition used in depolymerisation very limited. This project investigated various solvent mixtures with water, adding new information to this area of study. In this subsection, an understanding of how different compositions of non-alcoholic and alcoholic solvents can influence Kraft lignin depolymerisation will be discussed.

For Kraft lignin, the combination of various solvent/water mixtures resulted in different selectivities of guaiacol-type products. This lignin was originally from softwoods, and the absence of syringyl products was consistent with the lignin nature. The overall yields of the

reactions were not very different as shown in Table 22. The highest value, 11.5 g/100 g, was achieved with EtOH/H_2O mixture 75:25 v/v and the lowest yield, 5.6 g/100 g, with IPA/H_2O 50:50 v/v. It was thought that the increase in solvent content in the mixture could favour lignin dissolution and become a valuable tool for the depolymerisation, however the overall yields did not confirm this (due to the similarity in values). Deoxygenated aromatics were not observed in the reactions, but the products had different substitution patterns with methyl, ethyl or propyl groups in the rings, indicating that alkylation may have occurred.

Table 22 Overall yield of Kraft lignin solvolysis

Solvent/H_2O mixture used v:v	Reference reaction Yield g/100 g
IPA/H_2O 25:75	9.6
IPA/H_2O 50:50	5.6
IPA/H_2O 75:25	6.4
EtOH/H_2O 25:75	9.0
EtOH/H_2O 50:50	9.5
EtOH/H_2O 75:25	11.5
Acetone/H_2O 25:75	10.5
Acetone/H_2O 50:50	8.6
Acetone/H_2O 75:25	8.9

The products detected from Kraft lignin reactions were (1) 2-methoxyphenol, (2) 4-methyl-2-methoxyphenol (3) 4-ethyl-2-methoxyphenol, (4) 4-propyl-2-methoxyphenol, (5) 1,2-dihydroxybenzene, (6) 4-ethylbenzene-1,2-diol, (7) 4-(3-hydroxypropyl)-2-methoxyphenol (8) 4-(3-methoxypropyl)-2-methoxyphenol.

EtOH solutions enhanced individual product yield more effectively than the other mixtures, as shown in Figure 185. The reactions generated mainly compounds 1, 2, 4 and 5 and the lowest yield was related to product 7. With the exception of product 5, all had alkyl chains attached to the ring. The overall yield was favoured with an increase of ethanol concentration in the solution. Therefore, more EtOH resulted in better general results. However, when this data was evaluated in more detail, the 75 % EtOH was not necessarily the best solution. Each mixture showed different selectivities, enhancing a specific compound's yield. According to Figure 185, EtOH at 50 % and 75 % in solution, favoured dealkylation, increasing the yield of 1,2-dihydroxybenzene (5) and 2-methoxyphenol (2), respectively. It was reported that depolymerisation of a high condensed lignin (soda lignin) with ethanol showed that this alcohol worked as a capping agent stabilizing reaction intermediates by O-alkylating the hydroxyl groups and C-alkylating the aromatic rings [111]. This can be related to the

increase of individual yields for certain compounds with more ethanolic solutions. It was also considered that steps such as hydrolysis (Figure 182) and synergistic effects between water and solvent were simultaneously occurring.

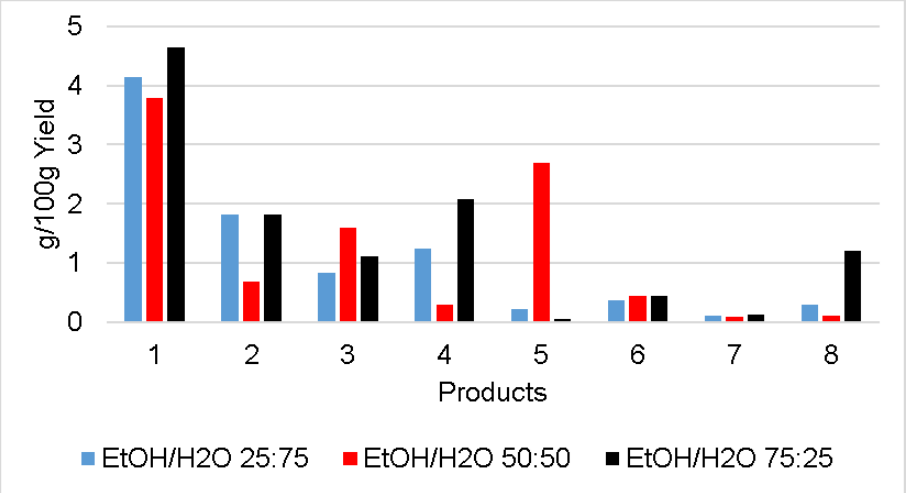

Figure 185 Kraft lignin depolymerisation in the presence of EtOH/H_2O mixture in different proportions (25:75, 50:50, 75:25 v/v).

The change in solvent mixture to IPA/H_2O produced similar yields of products in comparison to ethanol. IPA with 25 % in concentration increased the generation of all individual products. This indicated that IPA had less influence in product generation compared to EtOH. The higher content of water increased product yields, signifying that depolymerisation via hydrolysis was the main reaction pathway. In addition, 2-methoxyphenol (1) was the major product, indicative that dealkylation was also favoured.

It has been reported that acetone at high temperatures (e.g. 873 K) could decompose to methane and ketene (CH_2=C=O) [123]. However, the reactions of acetone involved in this project were run with water and at 573 K. It was difficult to establish the exact behaviour of acetone as it was used in various proportions with water. It could achieve supercritical state but not necessarily generate these compounds (methane and ketene). It was reported that supercritical acetone has high acidity, can behave as a reactant, solvent and even catalyst [124]. Studies involving degradation of polymers [125] and dehydration of carbohydrates [126] are areas that were explored using acetone in its supercritical state. For our reactions with acetone, there were similarities in overall yields with the other solvent mixtures (Table 22) but the main products generated changed. The units with alkyl chains in the ring were not as favoured as with the other solvents. Highest selectivity was towards 2-methoxyphenol (1) which indicated that dealkylation was enhanced. 25 % concentration of acetone in

solution gave ~ 7 g/100 g of this product. 25 % IPA also increased product 1 yield, but the value was much lower compared to acetone (~ 4 g/100 g). These solutions have in common more water in their composition, confirming that 2-methoxyphenol (1) generation was favoured by hydrolysis mechanisms in those mixtures. Acetone could act in mainly two ways: 1) initially contributing to the dissolution of lignin, minimising resistance to the mass transfer and favouring rate formation of product 1 and 2) acting as a catalyst increasing the presence of H^+ in the medium, as its acidity could change via keto-enol tautomerism in similar reaction conditions (Figure 186) [124]. There was no significant selectivity for any product other than compound 1. For 1,2-dihydroxybenzene (5), similarly to the IPA reactions, very low yields were found, indicating that the generation of this product was selective to the presence of 50 % EtOH in the reaction.

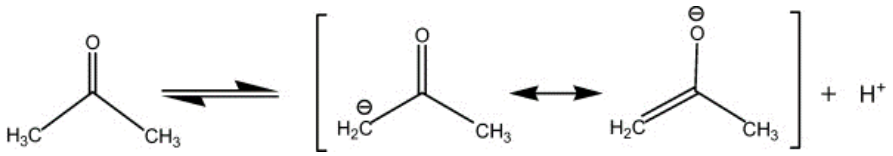

Figure 186 Enhanced acidity of acetone due to keto-enol tautomerism [124]**.**

For any type of solvent used (ethanol, isopropanol or acetone), in all experiments, 2-methoxyphenol was the main product. As mentioned previously, its generation was mainly promoted by hydrolysis in the case of acetone and IPA solutions. Studies involving hydrolytic depolymerization of hydrolysis lignin showed that the reasonable performance of water can be a consequence of lower dielectric constant and capacity of solubilise organic compounds in reactions with high temperature and pressure, compared to water under ambient conditions [119].

In the Kraft lignin various bonds types were detected, e.g. C-O-C bond (β-O-4,11 %) and C-C bonds (β-β, 4.5 % and β-5, 4.4 %). Linkages such as β-β and β-5 are in positions in the lignin structure that make them very difficult to cleave (Figure 187). In contrast, the ether bonds are labile bonds in lignin and the energy required to break them is considerably less than that for the C-C bonds (Section 1.5.1.1). As 2-methoxyphenol was produced as a major product in all reactions, it was suggested that this product was generated by the cleavage of these weaker bonds. A possible reaction pathway for this product formation was the solvolytic cleavage of β-O-4 with elimination of formaldehyde. This is shown in Figure 188. A γ-methylol group was lost as formaldehyde (HCHO) and the enol ether (2) was hydrolysed

resulting in the cleavage of the ether bonds and 2-methoxyphenol as one of the products [127].

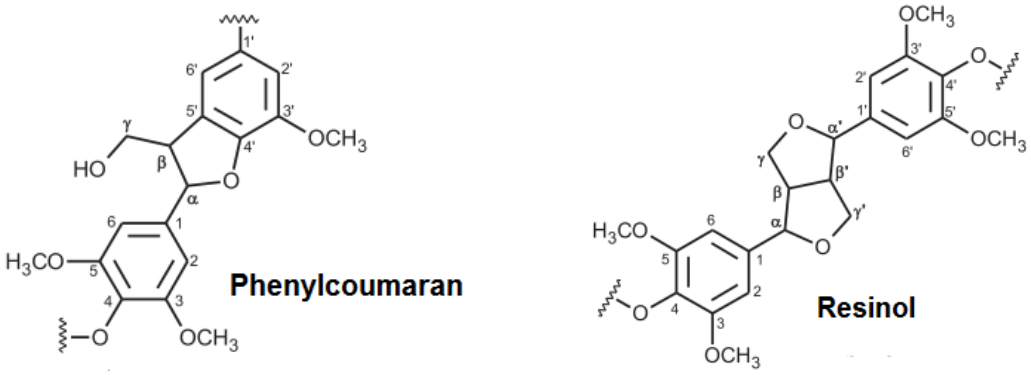

Figure 187 β-5 and β-β linkages in Kraft lignin [25]**.**

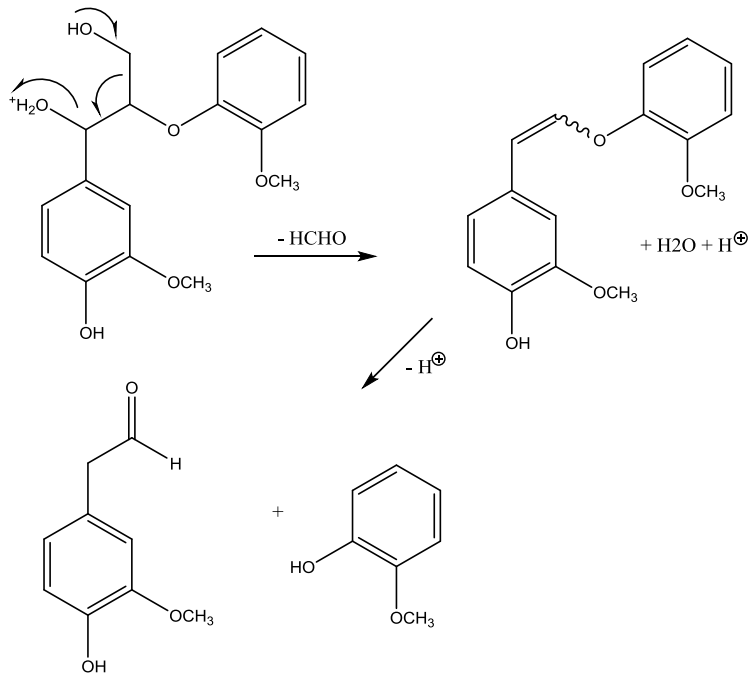

Figure 188 Reaction mechanism of solvolysis in a lignin model compound [127]**.**

Another possible explanation for this high selectivity to 2-methoxyphenol (guaiacol), was that the Kraft lignin (KL) depolymerisation included ferulic acid (FA) reactions. Kumar and co-authors reported KL degradation by β-proteobacterium and one of the intermediates detected (2-methoxy-4-vinylphenol) indicated degradation of FA [128]. Another study showed thermal degradation of FA with radical generation and compounds such as 4-

vinylguiacol (not detected in our reactions) as the main product, followed by guaiacol, ethyl guaiacol and vanillin (not detected). The mechanism is shown in Figure 189.

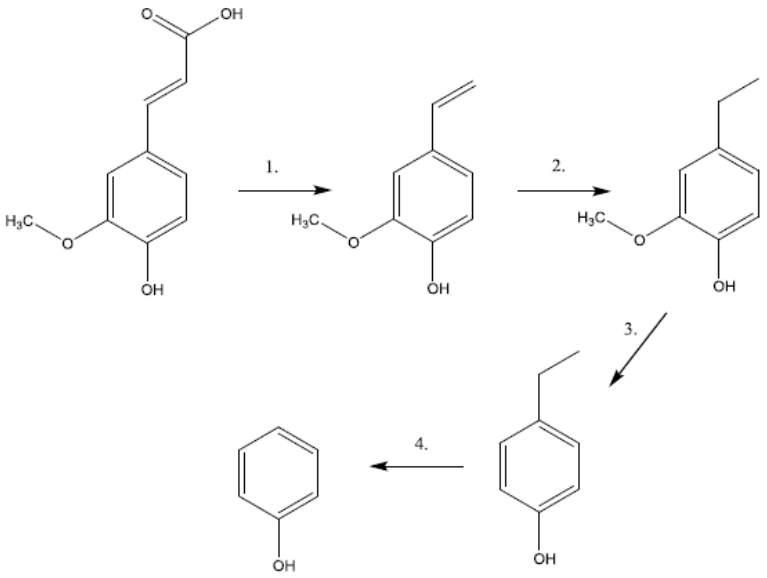

Figure 189 Reaction mechanism for ferulic acid thermal degradation [26]

A relevant point to consider in these experiments is the low overall yields. This characteristic can be associated with the poor content of labile bonds, making the solvolysis difficult or re-polymerisation processes favoured. One of the main issues regarded to lignin depolymerisation is the condensation of reaction intermediates. Mainly because it results in char formation with highly condensed post reaction materials. One of the ways which recondensation could occur is illustrated in Figure 190. The reaction resulted in heterolytic cleavage C-O bond, followed by condensation [26], [42].

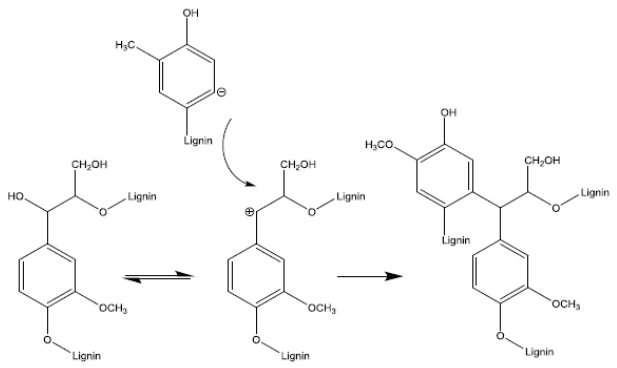

Figure 190 Condensation reaction pathway for lignin [26][42]

From the GPC analysis, despite the possibility of repolymerization reactions occurring with highly condensed materials formed, under our conditions of temperature, pressure and solvent mixtures, the molecular weight distribution for all shown reactions (Section 6.1.1.6), decreased. Compared to the original lignin, the Mw after reaction decreased by 74 %, 77 % and 82 % for reactions using EtOH/H_2O, IPA/H_2O and acetone/H_2O (50:50 v/v), respectively. It was expected that fracture of phenolic ether linkages may have happened altering Kraft lignin molecular weight. The changes in Mn were also expected. In the literature the conversion of one molecule into others resulted in lower molecular number for linear or branched polymers [129].

7.1.4 Solvolysis of sugar-cane (SC) and parr-lignins (PL)

Sugar-cane and parr-lignin solvolysis were run under the same conditions as Kraft lignin (at 573 K and 20 bar hydrogen). The solvent mixtures were 50 % acetone or IPA with water. The results presented gave similar overall yields, with values only up to 4.7/100 g. Compared to Kraft lignin, the other lignins had less condensed linkages and G, H or S units (see Section 5.3). In the products both guaiacyl and syringyl monomer types were detected. The solvolysis was able to form products that maintained the alkyl chain with various functional groups in the ring.

The origin of SC lignin was herbaceous crops in contrast to birch and oak lignins that were from hardwoods. SC lignin had not only 37 % of β-O-4 bonds but also 7 % β-O-4(Et). This last linkage was related to the incorporation of the ethyl group during the extraction process with ethanol. As a result, among all lignins studied, SC was the less condensed material. Selective cleavage of C-O-C bonds was reported to be promoted especially by noble metal catalysts [2]. Hence, as expected, the solvolysis was not very effective, resulting in low yield (3.9 % of products). The results showed a specific selectivity towards 4-propyl-2-methoxyphenol. Other main products were 2-methoxyphenol, 4-ethylphenol, 4-(3-hydroxypropyl)-2-methoxyphenol, 4-propenyl-2,6-dimethoxyphenol. In all products, the presence of various type of alkyl chains in the ring indicated that dealkylation was not favoured by solvolysis as it was for Kraft lignin, and the complexity of certain products suggested that they could be formed from a lignin fragment stabilised in the reaction medium, not following re-polymerisation. Also, the incorporation of solvent into the structure, could be involved resulting in added functionality. Three compounds were not identified, 4-ethylphenol, 2,6-dimethoxy-4-methylphenol and 1-propyl-3,5-dimethoxyphenol. Nevertheless, they were detected in catalysed reactions, evidencing that a

higher activation energy for the breakage of certain linkages was present and it was overcome by catalyst addition. This topic was discussed in more detail in the next section.

Birch parr-lignin (β-O-4 content of 26 %) was less condensed than Kraft but more than SC lignin. In the solvolysis with IPA and acetone solutions, as expected the yields were not high. This proposes that, similar to Kraft lignin, water was promoting hydrolysis and this was the favoured route. Both experiments had 2,6-dimethoxyphenol as the main product. The G:S ratio for this lignin showed that S units were more abundant (Section 5.3.3), therefore, product 6A as the main product was consistent with this lignin composition. Moreover, considerable low yields were regarded to compounds 7, 10, 12, 14 and 15A. Similarly to the SC lignin, dealkylation was not preferred and molecules with various alkyl chains and functional groups bonded to the ring were found. Even with the main product being based on a S unit, according to the yields of the other individual products, there was no obvious trend for other compounds selectivity towards S units.

Oak parr-lignin in reaction with acetone and IPA solutions had overall yields of 3.9 and 4.7 g/100 g, respectively. The presence of the same products in oak and birch parr-lignins suggested that these lignins had similarities in their chemical structure. In both experiments, 2,6-dimethoxyphenol was the main product. With IPA, products from the guaiacyl unit had better yields, especially compounds 1, 11 and 13 while acetone favoured two syringyl-type products, they were 1 and 10. The presence of alcohol slightly favoured more depolymerisation than acetone. These revealed different selectivities for the solutions and hydrolysis was not predominating in the mechanism. The reason why the solutions effect was different compared to birch Parr-lignin and sugar-cane may be associated with the lignin nature.

The GPC analysis data (Section 5.2) of sugar-cane and parr lignins confirmed their less condensed nature compared to Kraft, due to their lower molecular weight. In addition, the Mw values for the solvolysis showed that solvent had the capacity of breaking down these lignin linkages producing monomers and other lignin fragments. The lignins were converted into various molecules and condensed fragments, consequently, the molecular weight changed, decreasing compared to the original lignins.

7.1.5 Summary of lignin depolymerisation by solvolysis

This project focused on the catalytic depolymerisation of lignin to fine chemicals. As the catalysed reactions were run in the presence of solvent solutions, it was of interest to first analyse the influence of these solvents and, especially, if they would not only be dissolving lignin but also participating in the reaction, promoting depolymerisation. It was revealed that solvolysis happened and its effect depended on the type of lignin involved. A more condensed lignin (Kraft) was more affected by thermal degradation with solvents while uncondensed lignins showed inferior overall yields. This indicated that the lignin nature affected depolymerisation.

For the solvolysis of Kraft lignin, 2-methoxyphenol was the main product with acetone/water 25:75 v/v showing the highest selectivity. In the generation of the other individual compounds, the solvent mixtures affected product generation differently, and no obvious trend was found. Thus, it was not possible to establish what was the best solution. Deoxygenation did not occur while 2-methoxyphenol and 1,2-dihydoxybenzene were products revealing dealkylation mechanisms.

Solvolysis of sugar-cane and parr-lignins had a variety of guaiacyl and syringyl product-types, but it was not successful. The overall yields were lower than Kraft, most reactions did not change product selectivity considerably with the change in solvent, indicating pyrolysis and hydrolysis mechanisms with char formed by polymerisation of lignin intermediates. These experiments resulted in more complex alkyl-phenolics than Kraft lignin. The presence of 2-methoxyphenol and 2,6-dimethoxyphenol revealed dealkylation and 1,2 dihydroxybenzene indicated C-O cleavage in the methoxy group by the solvents.

BTX compounds were not detected. This data is in agreement with similar reactions in the literature [26]. The low yields in these reactions indicated high degrees of re-condensation issues. Despite of monomeric products being obtained in these experiments, most products seemed to be produced from hydrolysis or thermal degradation.

7.2 Catalytic depolymerisation of Kraft and isolated lignins

This section aims to discuss the effect of heterogeneous catalysts in lignin depolymerisation. Various supports (alumina, carbon and zirconium dioxide) and metals (platinum, rhodium, nickel and iron) were explored. The solvent mixtures used in these reactions contributed to the dissolution of solid lignin and facilitated its contact with the heterogeneous catalysts. In addition, the conditions used could promote solvents to supercritical state and enhance hydrogen diffusion. According to studies in lignin model compounds, the active sites in heterogeneous catalysts for lignin depolymerisation were expected to promote selective cleavage of C-C and C-O-C bonds [2], [49], [130], [131].

Diffusion and adsorption processes are critically relevant for experiments using heterogeneous catalysts [132]. An optimal exchange rate of product molecules over the surface of the catalyst is required for active sites to be available for more reactant adsorption and formation of new compounds [133]. The reactions involved in this project had liquid/solid/gas interfaces. This multiphase system added complexity for the reactions, hindering evaluation of the relative contribution of each component, and especially to specify what was happening in the pores of the catalysts.

Mass transport is the motion of the components in a system, and diffusion, driven by entropy, is one of the ways which this movement can occur [134]. If in an experiment the reaction rate is not affected by changes in stirring, it is not diffusion-limited [135]. Previous work in this topic was carried out by McVeigh (2016). The study [26] involved the same reaction conditions adopted in this project, ammonia lignin and stirring speeds of 500, 1000 and 1500 rpm. The values of monomeric compounds obtained were 6.7, 16.4 and 15.9 %, respectively. It was revealed that the increase in stirring enhanced product yields. The difference in values from 500-1000 rpm indicated that the reaction at that point was diffusion limited, however, the similarities in values between 1000-1500 rpm suggested that from this point it underwent kinetic control. Despite the increase in yields of the products, the char formation considerably augmented with stirring speed, revealing undesired condensation reactions [26]. This work provided relevant information for this research, contributing to the choice of 1000 rpm as the stirring speed for the reactions.

Most of the products found in the solvolysis were detected also in the catalysed reactions. The changes were mostly due to enhancement or decrease in their yields. Each reaction

reported in this chapter showed complex behaviour and behaved in unique ways. Hence, lignin depolymerisation will be mostly discussed individually, but similarities, when they exist, will be highlighted. The next subsections discuss in detail how the presence of heterogeneous catalysts affected depolymerisation of Kraft, sugar-cane and parr-lignins. The type of products detected in these experiments are summarised in Table 23.

Table 23 Products detected by GC-MS for Kraft, sugar-cane, oak and birch parr-lignin reactions

Monomer code	Monomer name
(1)	2-methoxyphenol
(2)	4-methyl-2-methoxyphenol
(2A)	4-ethylphenol
(3)	4-ethyl-2-methoxyphenol
(4)	4-propyl-2-methoxyphenol
(5)	1,2-dihydroxybenzene
(6)	4-ethylbenzene-1,2-diol
(6A)	2,6-dimethoxyphenol
(7)	4-(3-hydroxypropyl)-2-methoxyphenol
(8)	4-(3-methoxypropyl)-2-methoxyphenol
(9)	4-methyl-2,6-dimethoxyphenol
(10)	4-(2-hydroxyethyl)-2,6-dimethoxyphenol
(11)	4-ethyl-2,6-dimethoxyphenol
(12)	4-propenyl-2,6-dimethoxyphenol
(13)	4-(2-hydroxyethyl)-2-methoxyphenol
(14)	4-propyl-2,6-dimethoxyphenol
(15)	4-(1-hydroxy-2-methyl-pent-3-enyl)-2,6-dimethoxyphenol
(15A)	4-(3-hydroxypropyl)-2,6-dimethoxyphenol

7.2.1 Effect of alumina catalysts in lignin depolymerisation

7.2.1.1 Al_2O_3 support and noble metals

The alumina support used in this study was mostly composed of θ- and δ- phases. Boehmite is a mineral that has aluminium, oxygen and hydrogen in its composition AlO(OH) [136]. Thermal dehydration at high temperatures produces γ-alumina, δ-alumina, θ-alumina and α-alumina, respectively [137]. However, as shown in Section 4.2.4, there was no change in the alumina structure and the temperature used in the reactions (573 K) was not high enough for phase transitions. In the depolymerisation of the lignins, Al_2O_3 was not inert. The versatility of its chemical structure was reported to present catalytic behaviour in oxidation and reduction reactions. Alumina has Lewis acidity attributable to aluminium cations and Bronsted acidity due to the proton donor capacity [138]. Hence, alumina has been used in this project because of its mechanical resistance, high surface area, and the possibility of it acting as a catalyst [138].

As previously discussed, the use of solvent solutions promoted different degrees of depolymerisation depending on the type of lignin used. Alumina support was tested to evaluate if it would affect the depolymerisation of these lignins. Table 24 summarised the overall yields of reactions with alumina support.

Table 24 Overall yield of Kraft, sugar-cane and parr-lignins reactions involving Al_2O_3 support. Solvent/water 50:50 v/v.

Reaction Type	Overall yield (g/100 g)	
	Solvolysis	Al_2O_3
Kraft lignin EtOH/H_2O	9.5	9.7
Kraft lignin IPA/H_2O	5.6	6.9
Kraft lignin Acetone/H_2O	8.6	8.7
Sugar-cane lignin Acetone/H_2O	3.9	3.4
Birch parr-lignin Acetone/H_2O	3.2	4.6
Birch parr-lignin IPA/H_2O	3.9	7.0
Oak parr-lignin Acetone/H_2O	3.9	12.3
Oak parr-lignin IPA/H_2O	4.7	5.7

7.2.1.2 Kraft and sugar-cane lignins depolymerisation

As shown in Table 24, the overall yield for alumina reactions with Kraft lignin compared to solvolysis, only varied significantly for the IPA reaction, which had its value enhanced with the presence of alumina. Al_2O_3 had similar selectivity to the solvent solution but increased yields of 2-methoxyphenol, 4-methyl-2-methoxyphenol, 4-ethyl-2-methoxyphenol and 4-propyl-2-methoxyphenol. According to these results, the presence of alumina favoured more alkylated products. These *para*-substituted phenols were reported to be produced by acid catalysed etherification of the γ-OH group in lignin [139] but also, decarboxylation of the side chains can result in ethyl-substituted monomers [139]. In addition, some parallel reactions could have occurred with the alcohol. IPA at this temperature (573 K) can dehydrate forming propylene over Al_2O_3 [140]. Indeed, in the presence of alumina their dehydration can occur even at temperatures of 513 K and 613 K [140]. This signified that side products possibly formed from IPA, could have contributed to Kraft lignin depolymerisation. In this specific case, this may have influenced the solubility of lignin or even intermediates stabilisation, decreasing condensation issues.

The results of Kraft lignin reactions over Pt/ and Rh/alumina catalysts showed that selectivity depended on the type of catalyst used and solvent mixture. In the literature, it was reported that heterogeneous catalysts and high hydrogen pressure can favour deoxygenation [141]–[143], however, this was not confirmed from the products detected. Rh/Al_2O_3 gave, for most solvent mixtures, the main products 2-methoxy-4-propylphenol (4), 4-ethylbenzene-1,2-diol (6) and 2-methoxy-4-(3-methoxypropyl)phenol (8). Rh showed that in most cases even by changing the solvent mixture, these compounds had their yields enhanced, exhibiting selective cleavage of lignin bonds caused by Rh. Reactions with IPA favoured also the generation of compounds 3 and 5, this higher selectivity to alkylated products was possibly due to the hydrogen donor capacity of IPA [144]. However, in reactions with 50 % of acetone, compounds 5 and 8 were not generated. This showed that depending on the type of catalyst, a certain composition of solvent mixture can lead to selectivity and affect product formation. For Pt/Al_2O_3 experiments, no trend was found, as it was for Rh. While EtOH and acetone mixtures gave as main products 4-ethylbenzene-1,2-diol (6) and 2-methoxy-4-(3-methoxypropyl)phenol (8), IPA favoured the yields of 4-ethyl-2-methoxyphenol (3) and 1,2-dihydroxybenzene (5). By changing solvent mixture the type of main products also changed with IPA favouring slightly more dealkylation (more compound 5 formation). Pt also favoured 2-methoxy-4-propylphenol generation. These main products indicated that

different bonds were broken and the hydrogenolysis promoted by Pt was influenced by solvent differently than Rh, as the main products changed with change in solvent solution.

The noble metal catalysts, despite enhancing some individual yields, did not show promising results. One possible explanation for the low overall yields and their overall poor performance could be that the sulfur content in Kraft lignin poisoned the catalysts and decreased their activity. In addition, after the reaction, the catalysts turned black, confirming char/coke formed and deposited onto the catalyst surface. The carbonaceous material detected could act to decrease active sites for hydrogenolysis and affect selectivity. Hence, the alumina support gave more promising results.

For the experiments involving sugar-cane lignin, while alumina had similar performance as the non-catalysed experiment, Pt/Al_2O_3 and Rh/Al_2O_3 reactions gave overall yields of 11.4 and 12.9 g/100 g respectively. Both catalysts had superior activity than only Al_2O_3 or solvolysis. Pt and Rh are known as good catalysts for lignin C-O-C bond cleavage [1], [2] and the main products found were principally dimethoxyphenols with different substituted groups attached to the ring. sugar-cane lignin had the higher content of β-O-4 bonds and less condensed lignins were reported as more susceptible to hydrogenolysis [2]. New compounds (2A, 6A and 14) were detected in the presence of these metals, revealing selectivity in their formation and an energy barrier overcome by the addition of catalyst.

In these reactions, most products were alkylated phenols, however the higher selectivity was towards product 2A. Two possible reaction paths are shown in Figure 191 and Figure 192 for this monomer formation. As sugar-cane lignin had H units, it is suggested that a fragment similar to p-coumaryl alcohol (2) was generated from the lignin (1) by hydrogenolysis (a). This was followed by decarboxylation (b) giving 4-vinylphenol (3) and hydrogenation (c) producing 4-ethylphenol (4). The other route (Figure 192) is that compound 2A was generated via demethoxylation of 4-ethyl-2-methoxyphenol (5).

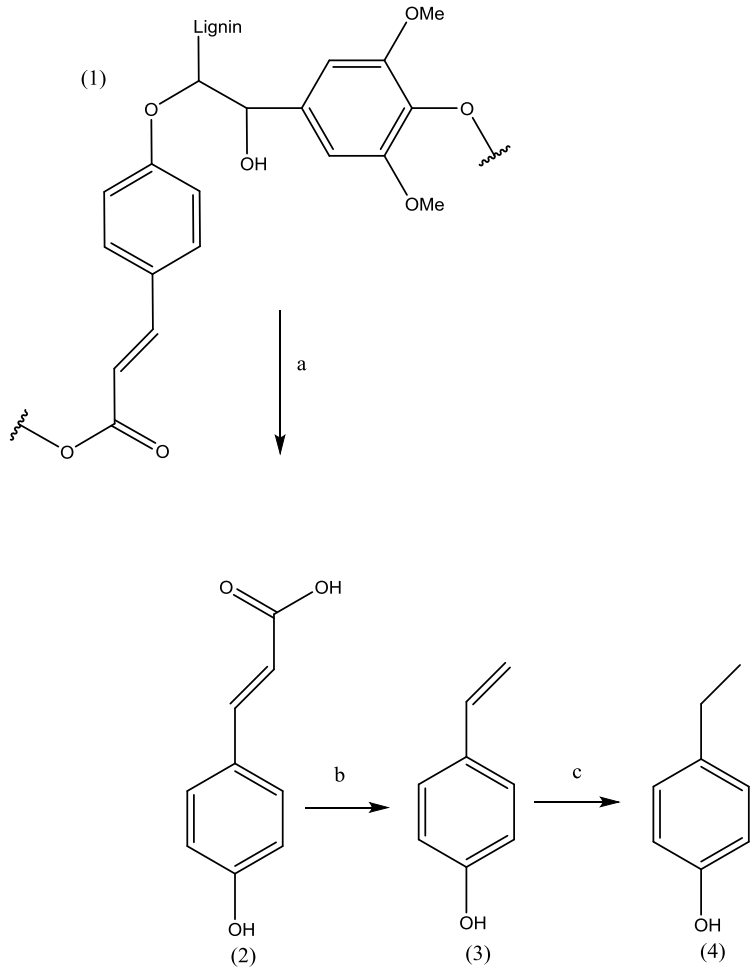

Figure 191 Reaction pathway for the generation of 4-ethylphenol from p-coumaryl alcohol fragment.

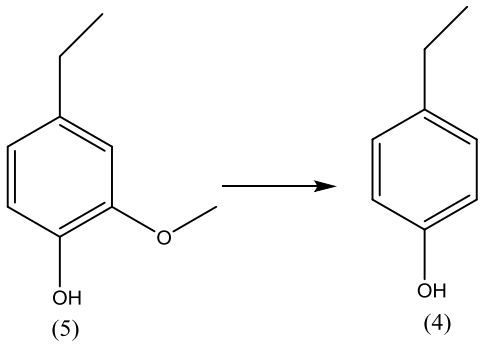

Figure 192 Reaction pathway for the generation of 4-ethylphenol from 4-ethyl-2-methoxyphenol.

Solvolysis and Al_2O_3 reactions had the molecule 4-(2-hydroxyethyl)-2,6-dimethoxyphenol as the main product. The presence of platinum and rhodium changed this selectivity to molecules, 2,6-dimethoxyphenol, 4-propenyl-2,6-dimethoxyphenol and 4-propyl-2,6-dimethoxyphenol. This showed that noble metals also increased products with functionality and small alkyl chains. These results may be related to the type of linkages susceptible for hydrogenolysis in this lignin. For example, it was reported that the amount of β-O-4 linkages was associated to higher alkyl-phenolic products (propyl phenolic in particular) in depolymerisation [26]. Sugar-cane lignin had in its constitution predominantly S units (NMR analysis, Section 5.3.2), therefore, the enhancement in the generation of syringyl type of products was expected.

7.2.1.3 Birch and oak parr-lignins depolymerisation

Birch parr-lignin experiments with acetone or IPA and alumina catalysts gave the same main products, consisting of phenols with alkyl chains and methoxy groups attached to the ring (compounds 6A, 8 and 7). This signified that dealkylation was not the only route and water was highly involved in the reaction mechanism, possibly via hydrolysis (as the change in solvent did not affect their generation. Solvent/water 50:50 v/v). Al_2O_3 support, Ni/Al_2O_3 and Fe/Al_2O_3 gave 2,6-dimethoxyphenol as the main product. Ni and Fe may not have altered the mechanism, suggesting that dealkylation was promoted mainly by the acidic sites of alumina and enhanced by the presence of the metals via hydrogenolysis. Pt gave 4-(3-methoxypropyl)-2-methoxyphenol and Rh gave 4-(3-hydroxypropyl)-2-methoxyphenol as the main products, respectively. They also had high selectivities to many other products such as compounds 9, 8, 12 and 15A. Therefore, the presence of the noble metals changed compound selectivity compared to the support and Ni. The chemical structure of these molecules indicated that dealkylation was not as favoured and there was effective cleavage of C-O-C bonds from a more complex lignin fragment via hydrogenolysis.

The other products detected had their yield affected by the type of solvent mixture used. Consequently, the overall yield also changed. Acetone gave more syringyl type molecules, while IPA was roughly the same proportion between syringyl and guaiacyl alkyl-phenolics. Figure 193 shows the total yield from birch parr-lignin reactions. These results were superior to solvolysis, emphasizing the relevance of the catalysts to generation of monomers. Noble metals gave highest yields with acetone in solution, while Al_2O_3, Ni and Fe catalysts performed better with IPA. These differences may be due to IPA transformations over the

catalysts. Possibly, the adsorption of IPA was higher in the noble metals, increasing competition for active sites.

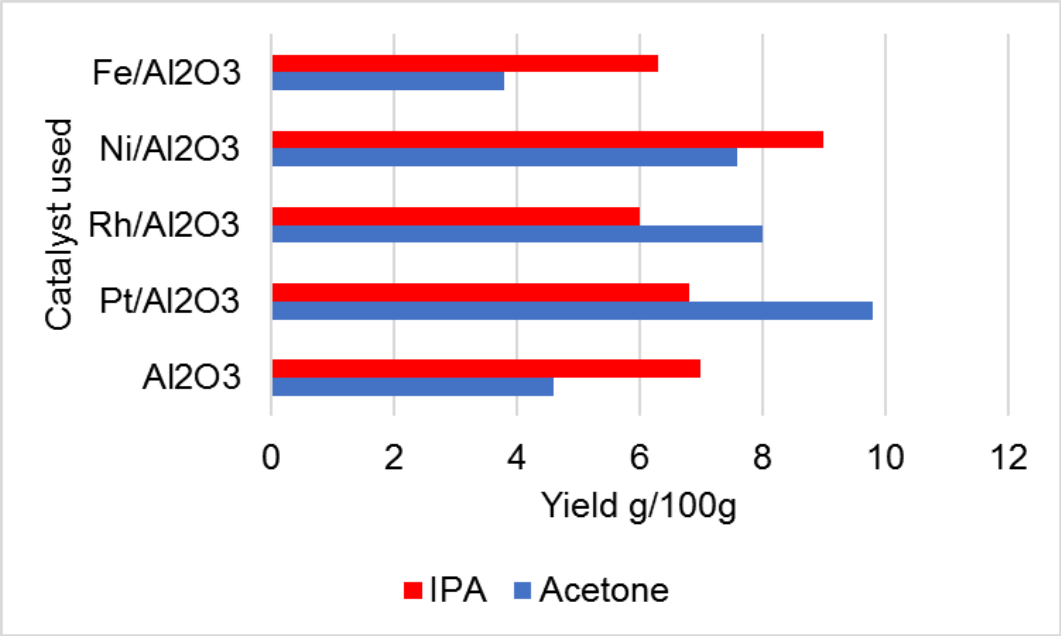

Figure 193 Comparison of overall yields for birch parr-lignin reactions. Solvent/water 50:50 v/v

Contrary to sugar-cane lignin, iron did not highly contribute to the depolymerisation of birch lignin. This was associated to condensation issues. Interestingly, Ni/Al_2O_3 showed as good a performance as Pt and Rh (for both solvents), increasing considerably the yields of the majority of products. In reaction with IPA, it gave high selectivity towards 2,6-dimethoxyphenol, 4-ethyl-2,6-dimethoxyphenol and 2-methoxy-4-(3-methoxypropyl)phenol, indicating that cleavage of lignin subunits was efficiently promoted by nickel and IPA. These results were not a surprise. As previously mentioned, IPA could have contributed with its hydrogen donor capacity. Zhu and co-authors revealed that using benzyl phenyl ether as a model compound, nickel favoured α-O-4 cleavage, forming radical intermediates. In the reaction, the presence of hydrogen and Ni-H species allowed recombination and production of stable monomers [145]. Also, studies involving various model compounds (benzyl phenyl ether, phenethyl phenyl ether and diphenyl ether) showed a trend regarding metal and generation of aromatic compounds, as follows: Ni > Pd > Ru. Hence, not only in model compounds but also with lignin molecules, nickel showed good performance as a catalyst for depolymerisation.

A different scenario was found regarding oak parr-lignin with acetone or IPA and alumina catalysts. The change in solvent changed the main products. While with acetone, the main

products were 6A, 7 and 13, for IPA they were 6A, 11 and 9. It was noticeable that with both solvents, Al_2O_3 and Ni/Al_2O_3 gave mainly 2,6-dimethoxyphenol, similar to birch lignin. This data suggests that the mechanism for this product formation involved dealkylation of similar lignin fragments (for birch and oak), mainly caused by alumina acidic sites and enhanced by the presence of nickel. Products 4-(3-hydroxypropyl)-2-methoxyphenol and 4-(2-hydroxyethyl)-2-methoxyphenol had more complex structures, indicating hydrogenolysis of the C-O-Ar bonds in lignin promoted by rhodium, iron and radical intermediates were more stabilised with acetone. Products 4-ethyl-2,6-dimethoxyphenol and 4-methyl-2,6-dimethoxyphenol had less functionality and their formation was favoured by Pt, Rh and iron. Even though these metals did not have the same product distribution.

The change of solvent affected product distributions and yield, but acetone and IPA gave roughly the same proportion of syringyl and guaiacyl alkyl-phenolics. However, the performance of the catalysts considerably changed. Figure 194 shows the total yield of reactions involving oak parr-lignin. The selectivity to aromatic monomers with acetone increased in the following order: Al_2O_3 > Rh > Pt > Ni > Fe while for IPA it was Ni > Al_2O_3 > Pt > Rh > Fe. For both solvents, iron had the worst performance and the change in solvent actually did not dramatically effect selectivity. Acetone assisted depolymerisation more efficiently, possibly due to better solubilisation of lignin and stability of intermediates. IPA decreased the overall yield for most reactions. Isopropanol could favour hydrogen availability, lignin dissolution and intermediates stability, resulting in higher products yield. However, an inverse effect was found and the overall yields decreased. This could be attributed to the lignin nature which was not the same as birch.

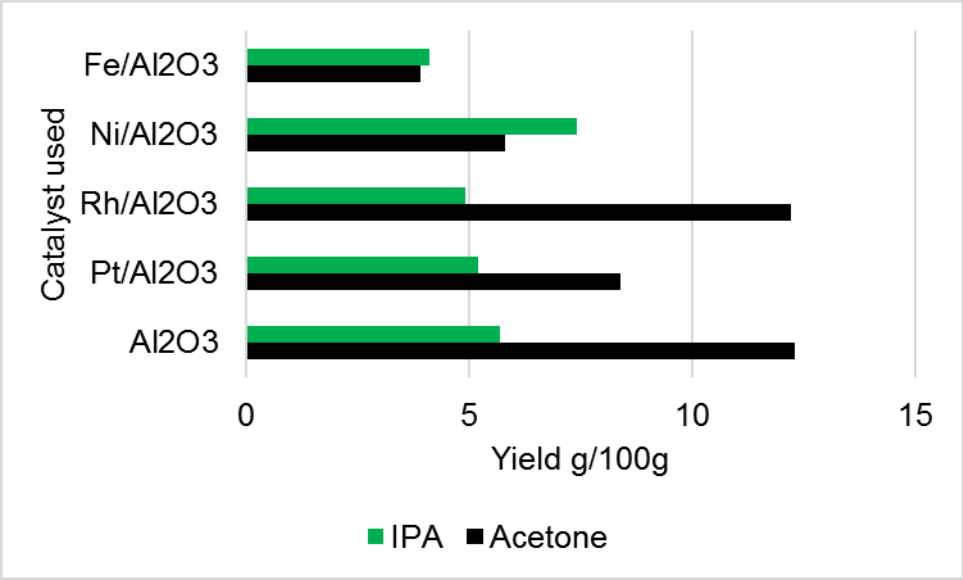

Figure 194 Comparison of overall yields for oak parr-lignin reactions. Solvent/water 50:50 v/v

7.2.1.4 Sugar-cane lignin depolymerisation

Sugar-cane lignin was reacted in acetone solution over Ni/Al_2O_3 and Fe/Al_2O_3. The presence of these catalysts gave overall yields of 8.3 and 6.6 g/100 g, respectively. These values were superior to solvolysis and reaction with only support, showing that the metals enhanced depolymerisation. Both catalysts generated compound 2A with high selectivity. For Ni/Al_2O_3, 2,6-dimethoxyphenol and 4-ethyl-2,6-dimethoxyphenol were the other major products while the other compounds had similar yields to solvolysis. For Fe/Al_2O_3, 4-ethyl-2-methoxyphenol and 4-(2-hydroxyethyl)-2,6-dimethoxyphenol were the other main products. Nickel enhanced dealkylation as the two main products were 2A and 6A, which was not the case with iron. This reaction step seems less favoured with iron, because despite also contributing to the formation of compound 2A, the other main products (10 and 11) had alkyl chains with various functional groups attached to the aromatic ring. Product 10 was not generated with Ni/Al_2O_3, while Fe/Al_2O_3 generated all products, being a less selective catalyst. The differences in product distribution and selectivities showed that these metals were depolymerising lignin through different reaction pathways. For these experiments, the presence of nickel and iron in the reactions resulted in higher catalytic activity than the support.

7.2.1.5 Summary of lignin depolymerisation over alumina catalysts

In general, it was found that for Kraft, sugar-cane and parr-lignins alumina reactions produced two main compounds, 2-methoxyphenol and 2,6-dimethoxyphenol. However, there were also alkylated molecules with considerable yields, depending on the experiment. To summarise the main products obtained from these reactions, Figure 195 shows a schematic of the main compounds from the reductive depolymerisation over Al_2O_3 catalysts.

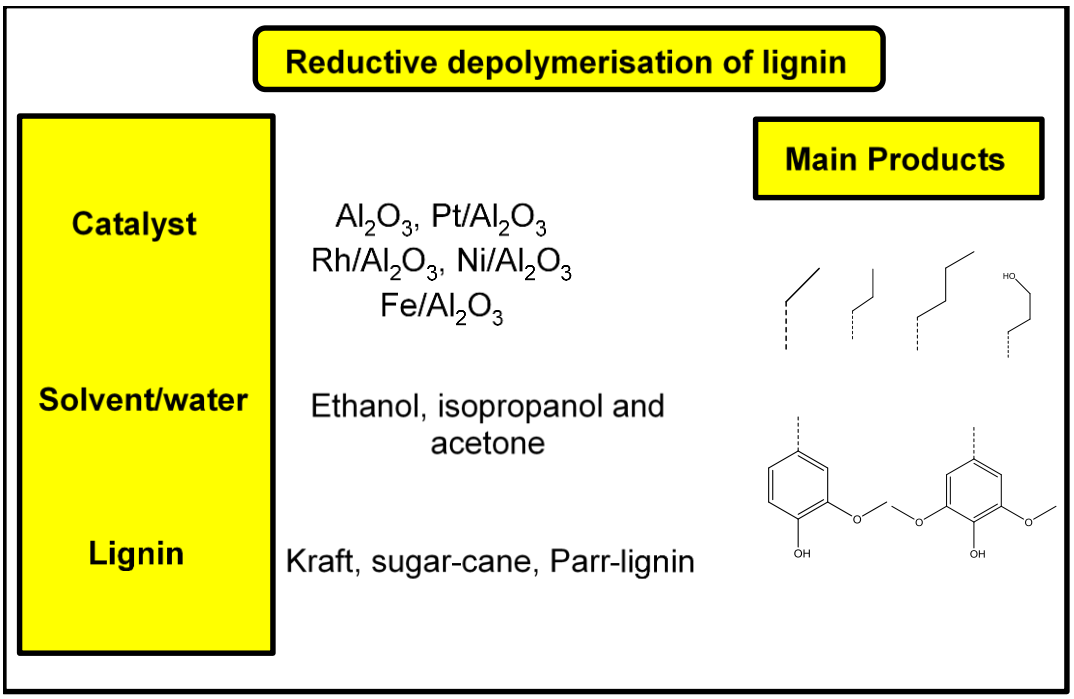

Figure 195 Main products generated from hydrogenolysis of lignins. Kraft products were only G unit-type compounds

It was noticeable that for almost all reactions with alumina support, the same main product (non-alkylated phenolic), was also found in the solvolysis reaction. Indicating that the main reaction promoted by this support was to enhance dealkylation. However this mechanism was different for sugar-cane lignin, as 4-propyl-2,6-dimethoxyphenol and 4-propyl-2-methoxyphenol were the main molecules. One of the main routes for 2-methoxy-4-propylphenol generation is the cleavage of β-O-4 linkage [26], suggesting that the C-O-C bond rupture was favoured by Al_2O_3.

Another important aspect in alumina catalyst experiments was that 2-methoxyphenol, 2,6-dimethoxyphenol and 1,2-dihydroxybenzene were produced in these reactions. Figure 197 shows the yield of these compounds in the reactions with Al_2O_3 catalysts, acetone and IPA.

Clearly, 2-methoxyphenol was not the main product for sugar-cane and parr-lignins. However, it was for Kraft, implying that the type of lignin affected product distribution. Alumina and rhodium showed the highest selectivity (Rh/Al_2O_3 >Al_2O_3 support) for this product and changes between acetone and IPA did not result in dramatic changes in yield. These results showed that the reaction was promoted mainly by alumina and enhanced by the presence of metal via hydrogenolysis.

1,2-dihydroxybenzene's yield was not significantly effected by solvent or catalyst, nevertheless there was some variation. Acetone promoted larger variations in yield, being a more suitable solvent for dealkylation. This may be due to a higher solubility of lignin and intermediates stabilisation. In terms of catalyst, Al_2O_3 gave better results than the noble and non-noble metals, as oak parr-lignin with acetone and Kraft with IPA promoted the highest yields in the presence of this support. Two main routes could be considered for this product formation. One is the dealkylation and O-CH_3 cleavage of an alkyl methoxyphenol or, as shown in Figure 196, hydrogenolysis of C_β-O or C_α-$C_{aromatic}$ bond of a lignin fragment (1) resulting in 2-methoxyphenol (2) followed by O-CH_3 cleavage and 1,2-dihydroxybenzene formation.

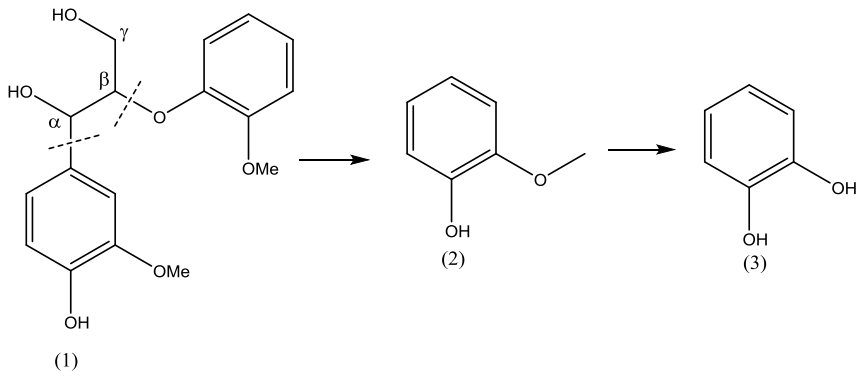

Figure 196 Possible mechanism for 1,2-dihydroxybenzene formation

For 2,6-dimethoxyphenol, the change in solvent also affected its yield. For sugar-cane lignin, platinum/rhodium and nickel/iron gave similar yields. In contrast for birch parr-lignin alumina had similar behaviour compared to platinum and nickel. Like birch, oak gave the highest yield with Al_2O_3 and nickel had a good performance being directly comparable with the noble metals.

Though the yield of 2-methoxyphenol, 2,6-dimethoxyphenol and 1,2-dihydroxybenzene varied, selective dealkylation was found for alumina catalysts and it depended on the

following two aspects: a) type of lignin b) type of solvent used with the respective catalyst. Therefore, if it is desired to produce any of these compounds, type of catalyst, lignin and solvent mixture need to be considered carefully.

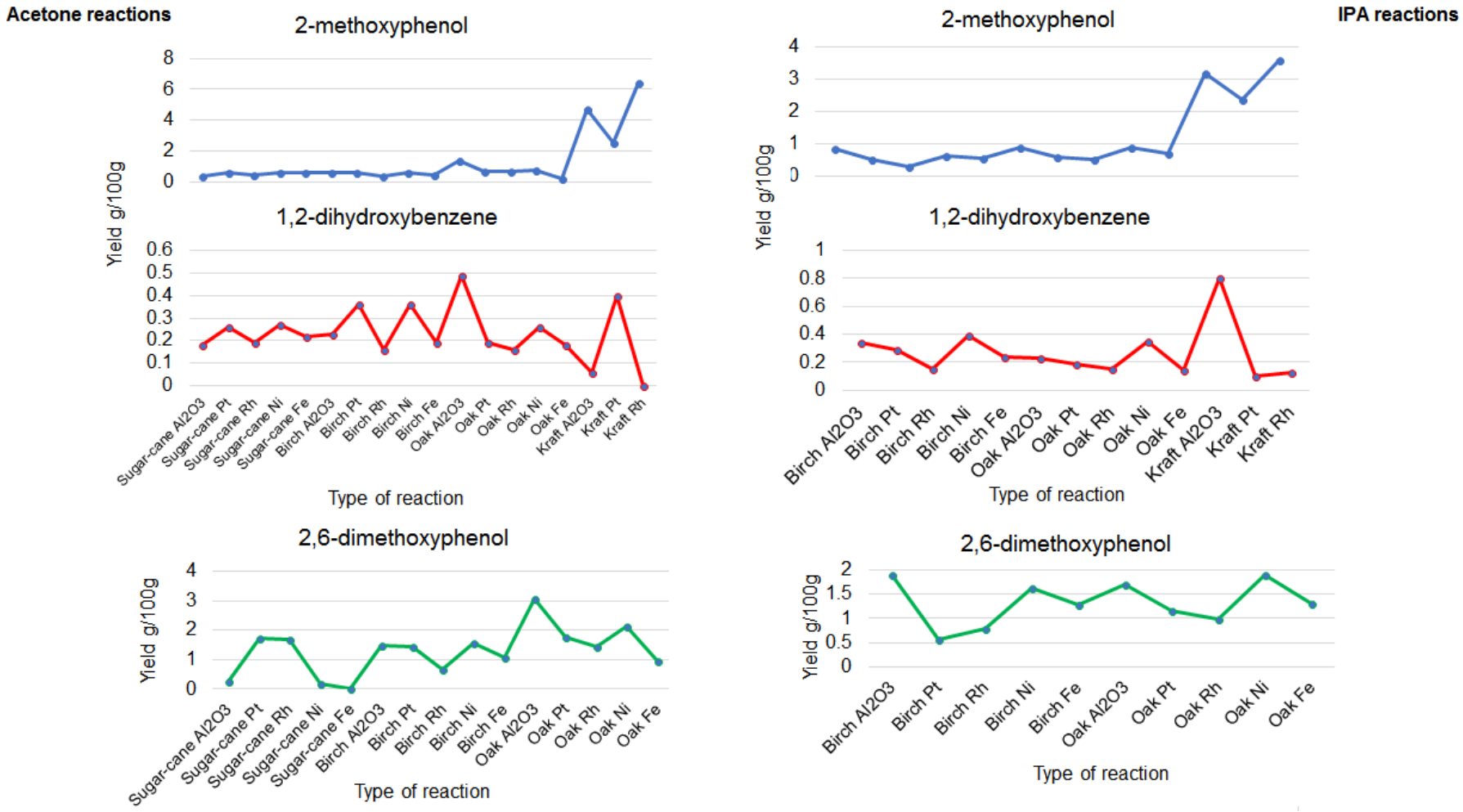

Figure 197 Yield of 2-methoxyphenol, 1,2-dihydroxybenzene and 2,6-dimethoxyphenol in reactions over Al_2O_3, Pt/Al_2O_3, Rh/Al_2O_3, Ni/Al_2O_3 and Fe/Al_2O_3 catalysts. Solvent/water 50:50 v/v.

7.2.2 Effect of carbon catalysts in lignin depolymerisation

Carbon is a support that has been explored in reactions of biomass transformation such as hydrogenation, hydrodeoxygenation and hydrolysis [146]–[149]. It has a range of valuable characteristics regarding its surface area, porosity and electron conductivity [150]. There are many types of carbon with different hybridization and surface functionalities. Figure 198 summarises the allotropes of carbon. Amorphous carbon can be obtained via pyrolysis of polymers (~ 1773 K), generating carbon black [150].

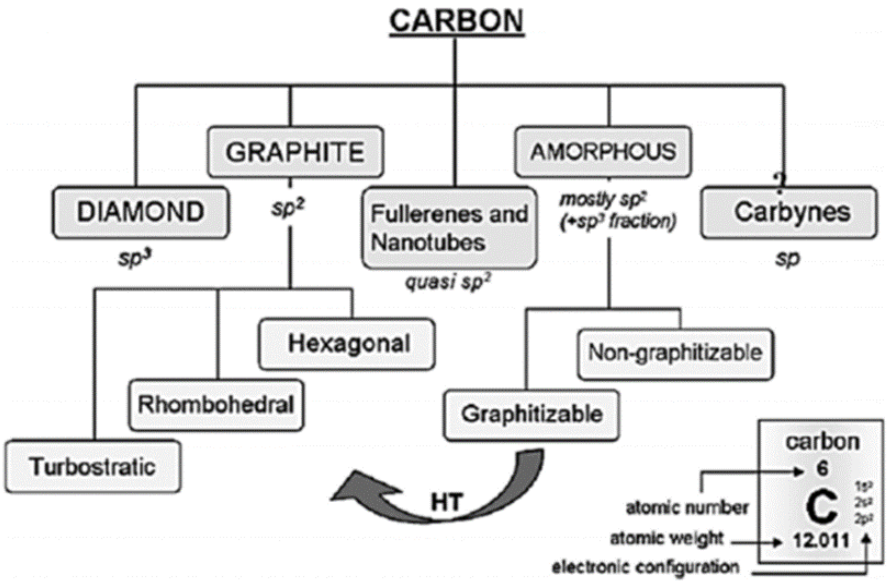

Figure 198 Types of carbon and their hybridization[150]

Graphite is a naturally occurring form of carbon. Amorphous carbon has a disordered structure, with imperfect aromatic sheets while graphite has a well-defined crystalline planar structure with unsaturated carbon in covalent bonds [151], [152]. The individual layers composing graphite are named graphene [153], [154]. Porosity is around 0.7-2 cm^3/g and surface areas in the range of 500-3000 m^2/g are found for porous carbon types [150]. The support used in this work was a mixture of amorphous and graphite carbon (Section 4.1.3). It was not possible to characterise the type of groups present on the surface of the carbon used. However, it is known that it was a neutral type of carbon and the surface area was in the range of porous carbon, in agreement with the literature [150] (Section 4.1.2). Depending on the type of chemical treatment used, various surface groups such as COOH, SO_3H and OH could be present in amorphous carbon. This results in Bronsted acidity and the capacity of carbon to promote acid-catalysed reactions [150]. Figure 199, illustrated the presence of various surface groups over the carbon surface. Neutral carbons have a balance between

acidic and basic groups over the surface, hence the support used in this work had basic and acidic character.

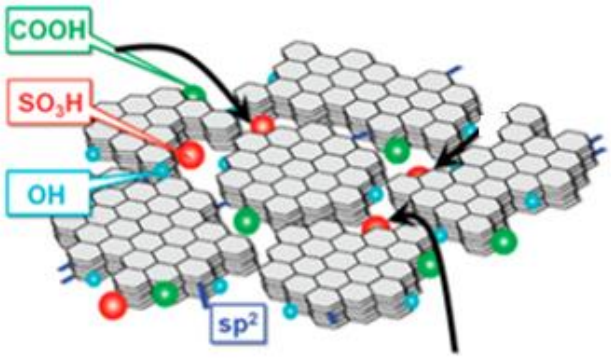

Figure 199 Hybridization and possible surface groups over carbon surface. Adapted from reference [150]

7.2.2.1 Birch and oak parr-lignins depolymerisation

It was found that the carbon support was active in birch parr-lignin depolymerisation reactions. Compared to the reference experiments, almost all individual compounds enhanced their yields. For carbon and Ni/C the main product was 2,6-dimethoxyphenol in acetone and IPA reactions. This was also the main product for Ni on the alumina experiments. As the change in solvent did not highly affect this monomer yield, it was suggested that it was initially formed by thermolysis or hydrolysis of C-O-C linkage, followed by dealkylation, the support stabilising the intermediates, avoiding re-condensation and increasing the yield. Carbon in reaction with acetone showed selectivity towards compounds 1, 8 and 11 and the presence of nickel changed selectivity to product 7. Slightly more char production was generated with IPA and changes in selectivity for the other products were found compared to acetone. However, these effects can not be only attributed to the solvent as the support could be catalysing acid-base reactions due to its surface characteristics.

The presence of iron in the catalyst with both solvents was not as effective as with nickel but the same solvent effects were not found. Selectivity changed with change of the solution. In acetone, compounds 3 and 10 had their yields increased using the iron catalyst, while the main product was 4-ethyl-2-methoxyphenol while for IPA it was 4-(3-hydroxypropyl)-2,6-dimethoxyphenol. This signified that Fe favoured more cleavage of aryl-alkyl bonds in lignin

than dealkylation. However, its poor performance suggested that this catalyst had catalysed condensation of the lignins.

Figure 200 shows the contribution of each solvent to the overall yield of the reactions. For carbon support, Ni/C and Fe/C, the type of solvent affected overall yield. For reactions with birch parr-lignin, using Ni and Fe catalysts supported on alumina and carbon, IPA performed better than acetone, improving overall yields. Acetone at 573-673 K can promote surface aldol condensation reactions and formation of acetates due to the acidic sites of alumina [155]. It is possible that acetone underwent similar side reactions with the carbon support, decreasing the availability of sites for depolymerisation or even intermediates stabilisation. In the results below the overall yield with acetone decreased as follows: C > Ni > Fe. While for IPA, it decreased as: Ni > Fe > C.

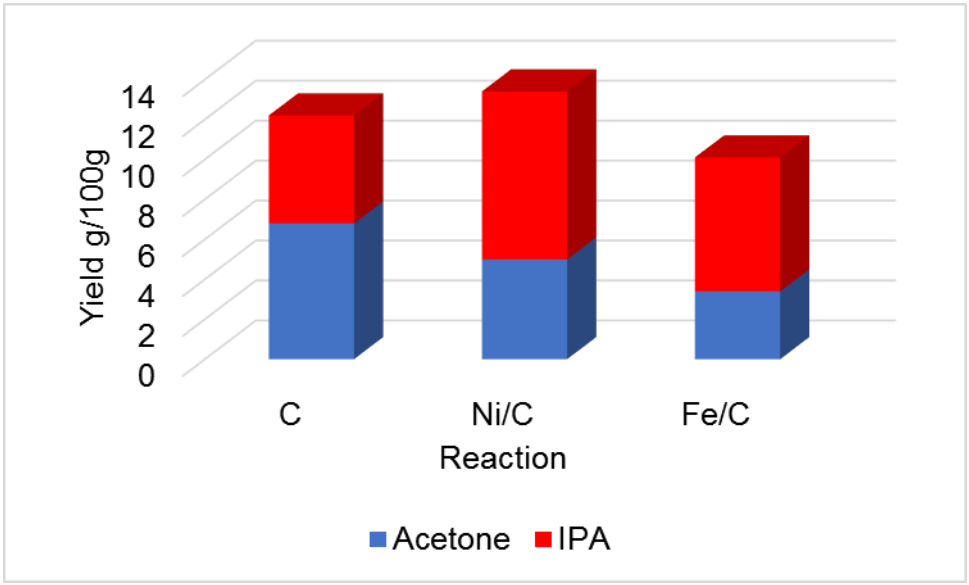

Figure 200 Contribution of acetone and IPA to the overall yield of the reactions of birch parr-lignin and carbon catalysts

The effects of carbon on oak parr-lignin reactions was different compared to birch. With acetone and the carbon support, the results were better than only solvolysis, with higher selectivity to less functionalised molecules, such as 2-methoxyphenol, 2,6-dimethoxyphenol and 4-ethyl-2,6-dimethoxyphenol. This suggested efficient cleavage of aryl-alkyl bonds in lignin by the acidic sites of carbon and acetone stabilisation of intermediates avoiding condensation. In general, the carbon support showed excellent catalytic activity in the presence of acetone with most product's yield enhanced. These results were similar to the previous reactions, showing that the acidity of a support, independent on the environment, enhances dealkylation. The reaction with Ni/C was practically identical to the experiment

with only carbon support. The presence of metal caused a slight decrease in yield, showing that the presence of metal did not affect depolymerisation considerably. However, the carbon support altered selectivity when changing solvents. With acetone, 2,6-dimethoxyphenol remained as the main product while for IPA it was 2-methoxy-4-(3-methoxypropyl)phenol. Ni/C showed better performance than only the support in the presence of IPA. Most compounds increased in yield by the presence of Ni, especially 6A, 11, 8 and 13. This may be related to more hydrogen available (from IPA) for metal hydrogenolysis reactions. Favouring bond cleavage and intermediates stabilisation. Each solvent contributed differently to product formation. While acetone favoured dealkylation, IPA increased C-O-C or C-C bond cleavage in lignin leading to alkyl-phenolics.

Fe/C showed the worst performance. The yields were very similar to solvolysis and the presence of the metal possibly affected the support catalytic activity. In the reactions with IPA, iron also had 4-(3-hydroxypropyl)-2,6-dimethoxyphenol as the main product. Suggesting similar cleavage of lignin bonds and intermediates (compared to birch). However, the change in solvent to acetone varied selectivity and 2-methoxyphenol was the main product.

Figure 201 shows the contribution of each solvent in the overall yield of the reactions. Acetone was the best solvent in reaction with oak parr-lignin.

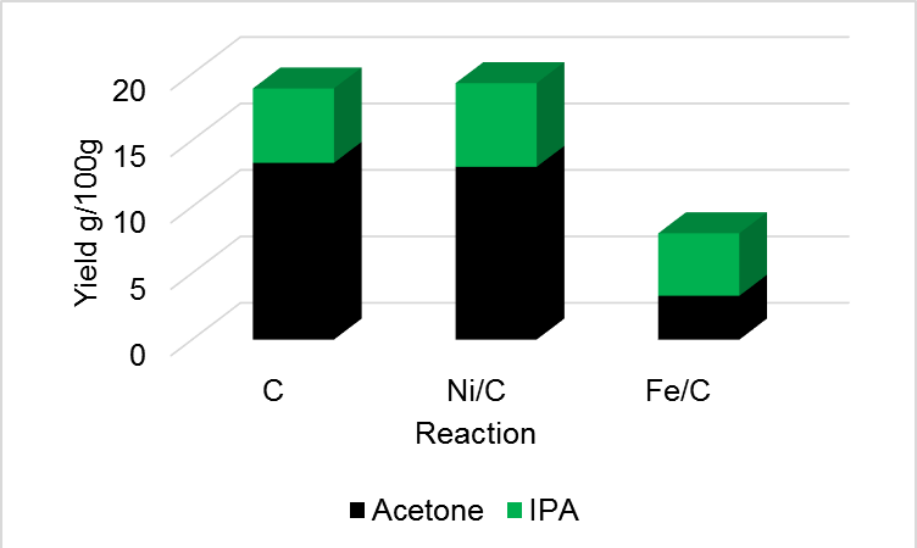

Figure 201 Contribution of acetone and IPA to the overall yield of the reactions of oak parr-lignin and carbon catalysts

7.2.3 Effect of zirconium catalysts in lignin depolymerisation

The zirconium used in this work was monoclinic. In the literature, its surface composition was characterised by the presence of hydroxyls and Lewis acidity [156]. These aspects were to some extent similar to alumina, and the interest in zirconium catalysts was attributed to possible contribution to the rupture of lignin bonds and monomer formation. In addition, a catalyst with smaller surface area could provide information about how effective this characteristic is in lignin depolymerisation.

Zirconium catalysts reactions generated the same product distribution as the previous experiments but did not show satisfactory performance compared to the other catalysts in oak and birch parr-lignins depolymerisation. The yields were very low with just a few compounds having an increase in yield (Section 6.3.1 and Section 6.3.2), but for most products solvolysis was more effective. Changes in solvent or type of lignin did not significantly alter the results, indicating that these catalysts enhanced condensation remarkably. One possible explanation is that there was a smaller surface area of Ni/ZrO_2, Fe/ZrO_2 and ZrO_2 compared to the alumina and carbon catalysts. The lignin intermediates can be relatively large molecules and if their stabilisation included adsorption over the support, it was not as efficient with zirconia.

7.2.4 Re-use of Fraction 2, Pt/Al_2O_3 and Ni/Al_2O_3 catalysts

The performance of spent Pt and Ni catalysts was evaluated in depolymerisation of birch parr-lignin. After the reaction, these catalysts could be easily separated by filtration and directly used in the subsequent cycle. The overall yields for platinum alumina, reaction with a new catalyst and recovered Pt was 3.2, 9.8 and 7.3 g/100 g, respectively. For nickel, these values were 3.2, 7.6 and 7 g/100, respectively. The results showed that there was a drop in overall yields compared to the new catalysts, with platinum more effected than nickel, decreasing the production of monomeric compounds by 2.5 g/100 g. After the reaction, these catalysts turned black in colour. This indicated char formation, which was confirmed by post reaction analysis and discussed in more detail in Section 7.5. The presence of carbon could have blocked Pt active sites more strongly than nickel, affecting its performance. In addition, it was found for both catalysts that there was a slight change in selectivity. Compounds that had low yields in the initial test with new catalysts had a small increase in yield with the re-used Pt and Ni. This may be associated to changes in surface chemistry, with slight differences in active sites in these post reaction catalysts.

The reaction of Fraction 2 (lignin post reaction residues solubilised in acetone, details Section 3.3.2) was performed to verify if it was viable to utilise the post-reaction material. The yield was very low, which brought the conclusion that the re-polymerisation of lignin produces a material that is highly condensed and not suitable for hydrogenolysis. To overcome this challenge and re-use the by-products from lignin reactions, new strategies and technologies need to be developed.

7.3 Structural analysis and reactivity towards depolymerisation of Kraft and isolated lignins

As described in Section 5.3, Kraft, sugar-cane and parr-lignins have different units (S, G and H) and linkages composition. Figure 202 shows a comparison between these lignins and the content of β-O-4 bonds. It is important to mention that the information obtained via NMR analysis were not absolute values and they were based on structural information. They were interpreted here with caution in a comparative context.

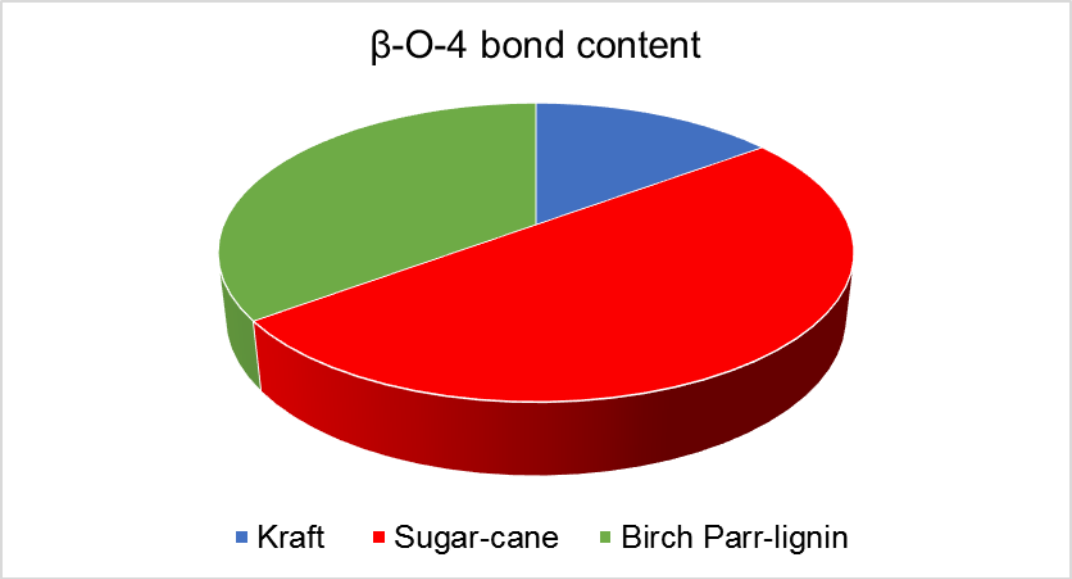

Figure 202 Comparison of β-O-4 bond abundance in Kraft, sugar-cane and parr-lignin (Section 5.3).

The extraction method employed to obtain lignin can induce different levels of modification in the chemical structure compared to a native lignin [38], [157], [158]. Based on the research that showed a relationship between β-O-4 linkages content and more generation of fine chemicals, these alterations can affect reactivity towards depolymerisation[2], [43]. This project supported this assumption as the lignins with higher content of uncondensed linkages responded more efficiently to the presence of catalysts. This highlighted the relevance of β-

O-4 linkages content to monomeric compounds generation. The NMR analysis showed other linkages (β-5 and β-β) in these lignins. It was expected that due to the highly condensed nature of these bonds, they would not be easily cleaved during the reaction and could remain intact. However, the recovered Fraction 2 (Section 5.3.3) was analysed by NMR and, surprisingly it was found that all linkages detected in the original birch parr-lignin were not detected in the Fraction 2 NMR spectra, signifying their efficient cleavage during the reaction.

Though, it is important to consider that these bonds were not the only factor that drove reactivity, the variety of units (H, S and G) in the lignins structure also resulted in a higher number of products detected with many alkyl groups and functionalities. The molecular weight distribution obtained by GPC revealed how condensed these lignins were. The values shown in Figure 203 matched with the degree of condensed bonds of these lignins obtained by NMR (based on the β-O-4 content). Overall, reducing the condensed nature of the lignin reacted with the heterogeneous catalysts, resulted in higher yields of individual products compared to the solvolysis.

Interestingly, despite of birch and oak parr-lignins coming from different feedstocks, their Mw was similar (Figure 203). This suggested that this pre-treatment did not generate highly condensed lignins compared to methods such as Kraft or soda pulping. In addition, impurities also must be considered as it may cause some influence in the depolymerisation. In the case of Kraft lignin this was clear, as the noble metal catalysts did not show a good performance, possibly due to sulfur impurities.

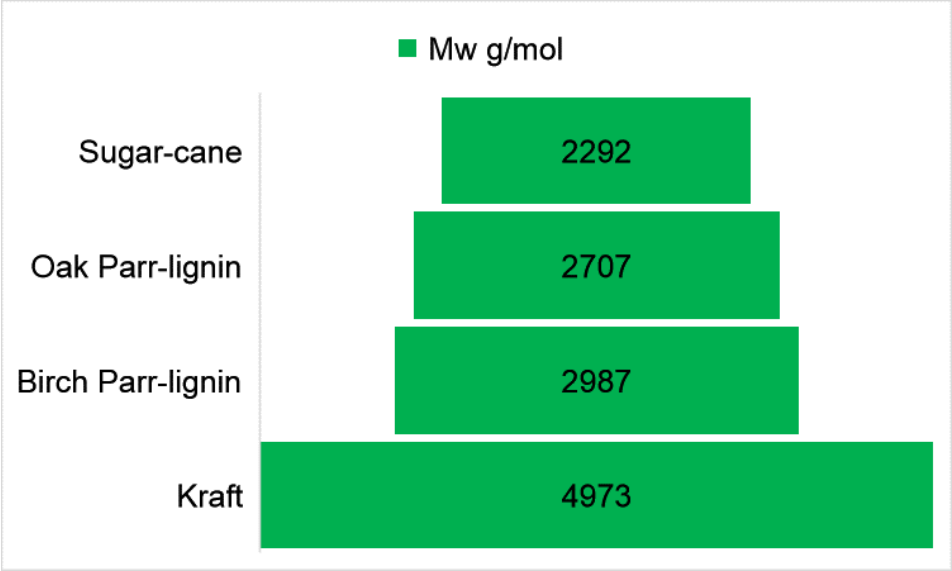

Figure 203 Mw obtained by GPC for sugar-cane lignin, oak/birch parr-lignins and Kraft lignin

The GPC analysis for the post reactions (Section 6.1.1.6 and Section 6.3.2.7) showed that compared to the original lignin the Mw and Mn values decreased. This was expected as monomeric compounds were identified in the GC-MS, confirming depolymerisation. The focus of GPC analysis was based on the changes of Mn, Mw and Ip, which could reveal degrees of depolymerisation between the reactions and compared to the original lignin polymer. The decrease in molecular number (Mn) for all lignins after reactions was expected as the conversion of one molecule into others results in lower Mn for linear or branched polymers [129]. The polydispersity is not related to only one characteristic in a polymer. It relates to microstructure, degree of chain branching, composition, etc [159]. However, the polydispersity index (Ip = Mw/Mn [159]) could not be fully understood in these experiments, because most of the structures analysed (lignins) were unknown. Nevertheless, it could be concluded that the decrease in Ip values after most reactions revealed that there were products with less chain branching and complexity than the original molecule. These results agreed with the fact that the initial lignin molecule resulted in smaller monomeric compounds and other condensed structures. For sugar-cane and parr-lignins the Mw decreased compared to the original lignin. After reaction, the Mw dropped about 40 % compared to those original Mw values for these lignins. While for Kraft, the values decreased from 4973 g/mol (original lignin weight) to the range of ~ 967.8 – 1390 g/mol after reaction, which meant a decrease up to 72 % of original weight.

It was also found that the composition of lignin varied depending on the biomass type and their products from the depolymerisation were also dependent on their nature. This was

expected as hardwoods, softwoods and herbaceous sources will have their own compositional and structural characteristics. It was not trivial to compare the extraction methods of these lignins, especially because the lignins final chemical structures were not identified and currently, there are still analytical and technical limitations to be overcome. However, this work could show that less condensed lignins can produce more monomeric compounds by hydrogenolysis. While lignins such as Kraft, responded to these reactions not very differently as to solvolysis. Hence, due to the variations in the chemical structure and impurities, the pre-treatment employed in lignin extraction is a key step to be taken in account before its depolymerisation.

7.4 Kinetic isotopic effect

This section aims to discuss isotopic labelling experiments in Kraft lignin. As presented in Section 6.1.1.7, hydrogen and solvents were changed to their deuterated forms in the presence and absence of Pt/Al_2O_3 catalyst. Experiments involving fully deuterated catalysed (FDC), partially deuterated (PDC) and fully deuterated non-catalysed (FDNC) reactions allowed analysis of how solvent and hydrogen were involved in the depolymerisation of Kraft lignin. The change in rate of a product formation when replacing H per D, showed that solvents and hydrogen influenced product formation in the solvolysis differently than in the catalysed experiment.

Reactions involving isotopic substitutions occur on the same energy surface [160]. The harmonic oscillator approximation can be used to define the vibration of a diatomic molecule [160] (Equation 11). Where h is Planck's constant, v frequency of the vibration and n the quantum number. When the molecule is in its ground state, n=0 and it can be assumed zero-point vibrational energies [160].

Equation 11 Vibrational energy levels for simple harmonic oscillator [160]

$$\boldsymbol{En = \left(n + \frac{1}{2}\right) hv}$$

Hydrogen and deuterium have the same electronic configuration, not affecting the potential energy of the system if isotopic substitution occurs. Their difference relies on their weight [161]. Consequently, the vibration of a C-H and C-D bond is not going to be the same. The equation for the stretching of a spring (Equation 12) can be used to demonstrate how the stretching frequency of the bond can be affected by deuterium compared to hydrogen [160]. As shown, v (frequency) is directly proportional to the square root of the force constant of the bond (k) and inversely proportional to the square root of the reduced mass (mr) [160].

Equation 12 Harmonic oscillator equation for fundamental vibrational frequency [160]

$$\mathbf{v = \frac{1}{2\pi}\sqrt{\frac{k}{mr}} \quad where, \; mr = \frac{m1m2}{m1 + m2}}$$

When the rate of the protiated reaction is equal to the rate of the deuterated (k_H=k_D), there is no KIE and the isotopic substitution occurred in a site other than the rate determining step

[162], [20]. If $k_H/k_D > 1$, a normal KIE takes place. It is assumed to be a positive KIE when the isotopic substitution occurred at a site that was the rate determining step of the reaction [162], [20]. For secondary KIE, the isotopic substitution occur at sites adjacent to the rate-determining step, which could be at α, β or γ position. Lastly, for $k_H/k_D<1$ an inverse KIE is assumed and the rate determining step was increased by the presence of deuterium [20].

Figure 204 illustrates a positive KIE according to the reaction coordinate[162]. The activation energy for C-D cleavage was higher compared to C-H. This revealed that the reaction occurred faster with hydrogen ($k_H/k_D>1$) and a normal KIE [162]. The magnitude of this KIE was directly related to the zero-point energy (ZPE) difference when passing from the reactant to the transition state (TS). In this case, compared to C-D, the ZPE difference of the transition state (TS) for C-H was less than the ZPE difference of the reactant, revealing a positive kinetic isotopic effect [162]. If the opposite occurs and $ZPE_{diff\text{-}TS} < ZPE_{diff\text{-}react}$, an inverse kinetic isotopic is found. Finally, if $ZPE_{diff\text{-}TS} = ZPE_{diff\text{-}react}$, there is no KIE [162]. Therefore, kinetic isotopic effects are associated to the transition state theory (TST). Hence, the activate complex and the variations of ZPE of reactants and TS determine the magnitude and occurrence of KIE [162].

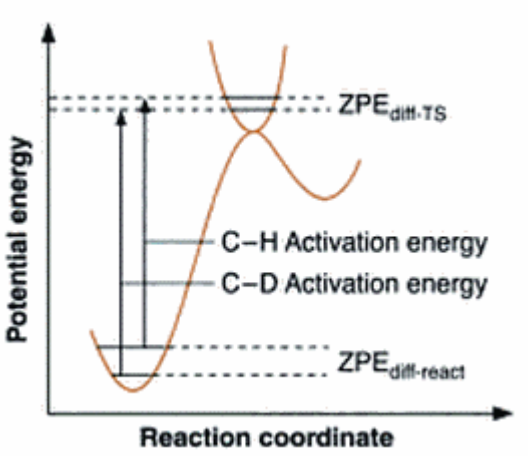

Figure 204 Reaction coordinate diagram for KIE. Adapted from reference [162].

The changes in reaction rate by the addition of deuterated solvents are classified as solvent kinetic isotopic effect (SKIE) [163]. Nevertheless, their interpretation is not always straightforward, and is associated to more than one cause. Solvents can be involved directly in the reaction mechanism, promote H/D exchange with reactants and stabilise the activated

complex by solvation [160], [162]. These effects also can be primary, secondary or normal, depending on the degree of involvement of the solvent in the reaction [160], [162], [163]. In this work, the reactions involving deuterated solvents and deuterium showed different results for the individual molecules. This signified that there was not only one reaction path and each molecule had specific mechanism of formation.

The values obtained in the reactions are summarised in Table 25. The monomers detected by GCMS were: (1) 2-methoxyphenol, (2) 4-methyl-2-methoxyphenol (3) 4-ethyl-2-methoxyphenol, (4) 4-propyl-2-methoxyphenol, (5) 1,2-dihydroxybenzene, (6) 4-ethylbenzene-1,2-diol, (7) 4-(3-hydroxypropyl)-2-methoxyphenol (8) 4-(3-methoxypropyl)-2-methoxyphenol.

Table 25 KIE for PDC, FDC and FDNC reactions. ND: non-detected compounds. PDC, partially deuterated catalysed reaction. FDC, fully deuterated catalysed, FDNC, fully deuterated non-catalysed. NIDA (number of incorporated deuterium atoms).

	Experiment			
	PDC	FDC	FDNC	
Monomer	KIE values			NIDA
1	0.8	0.8	4.4	2
2	0.7	1.0	ND	4
3	ND	ND	8.3	5
4	1.0	1.2	ND	5
5	1.0	1.3	2.3	7
6	2.4	2.5	ND	5
7	0.4	1.7	4.2	7
8	0.6	0.7	ND	1

Comparing FDC, PDC and FDNC, the number of incorporated deuterium atoms did not change (NIDA). Due to the complexity of lignin and the system investigated, it was not possible to detect reaction intermediates and to obtain a proton inventory to establish how many protons were contributing to the KIE. Therefore, the analysis was simplified to focus on the different values of KIE detected and their relationship to how the solvent/gas affected the rate (Section 3.3.3.1) of final products formation.

According to Table 25, compounds 4 and 5 did not show a KIE in the presence of the solvents, however when hydrogen was added to the system, the values slightly increased generating a secondary KIE. These values in the range of 1.2-1.3 suggested that the isotopic substitution had occurred at a site adjacent to the rate determining step [163]. In addition, it

was reported that at high temperatures, D_2O can undergo slight structural changes compared to H_2O, affecting solvation and causing secondary KIE [163]. In the case of molecules 1, 6 and 8, they had very similar values of KIE in the PDC and FDC reactions. Hence, the addition of deuterium (D_2) may have not affected the rate-determining step of these compounds formation. The high positive value obtained for 4-ethylbenzene-1,2-diol (6) indicated that the solvent was directly involved in the mechanism of this product formation. A possible mechanism for this product generation was as follows: C-C or O-CH_3 cleavage, which could be promoted by the presence of Pt/Al_2O_3 via hydrogenolysis.

For the products 2-methoxyphenol (1) and 2-methoxy-4-(3-methoxypropyl)phenol (8), the IKIE could be associated to the following aspect: stabilisation of transition state more efficiently by the presence of deuterated solvents [164], thereby decreasing condensation of lignin intermediates.

The high values of PKIE found in the FDNC reaction, confirmed that the generation of products was not simply by thermolysis. Solvents were highly involved in products 1, 3, 5 and 7 formation even in the absence of catalyst. In addition, very different values found showed that different mechanistic venues were involved in catalysed and non-catalysed experiments. The highest value for 4-ethyl-2-methoxyphenol (3) suggested that direct bond cleavage by hydrolysis happened. The high number of incorporated deuterium atoms in the FDNC experiment were the same as in the catalysed experiments. However, these results can not be associated to simple H/D exchange. It is important to highlight that deuterated acetone could be in its supercritical state and deuterated water at subcritical conditions (high temperature and pressure) may have its properties changed (dieletric constant and capacity of solubilise organic compounds). These aspects may have played a role and facilitated the exchange process.

The last paragraphs discussed general possibilities regarded to the influence of solvents and deuterium in Kraft lignin depolymerisation. However, these results can not be simplified only to these explanations. Lignin fragmentation can involve various steps and KIE were suggested to be also a sum of various effects along the reaction pathway. This was exemplified in the literature by studies involving 4-propylsyringol, CD_3OD and Ni/C, under argon, which showed H/D exchange resulting in the incorporation of deuterium in the phenol hydroxyl and in the ring [98]. In addition, birch lignin depolymerisation showed the same H/D exchange profile in the 4-propylsyringol product [98]. The mechanism of bond cleavage in the native lignin was not simple compared to the model compound. In the lignin chemical

structure, it was suggested that the hydroxyl can be in the C_α or C_γ, while C_β was involved with C-O-C linkages. Elimination of C-OH groups could be caused via β-elimination and OH lost in the form of H_2O, followed by C=C hydrogenation. In addition, heterocleavage of C-OH followed by addition of deuterium (hydrogenolysis) could occur [98]. One important consideration in the reactions studied in this project, was the presence β-O-4 bonds. A study [98] of isotopic substitutions and C-O-C bond cleavage is presented in Figure 205. According to the mechanism, cleavage of β-O-4 bonds and reactions such as hydrogenolysis, dehydration and hydrogenation can be involved in the product formation [98].

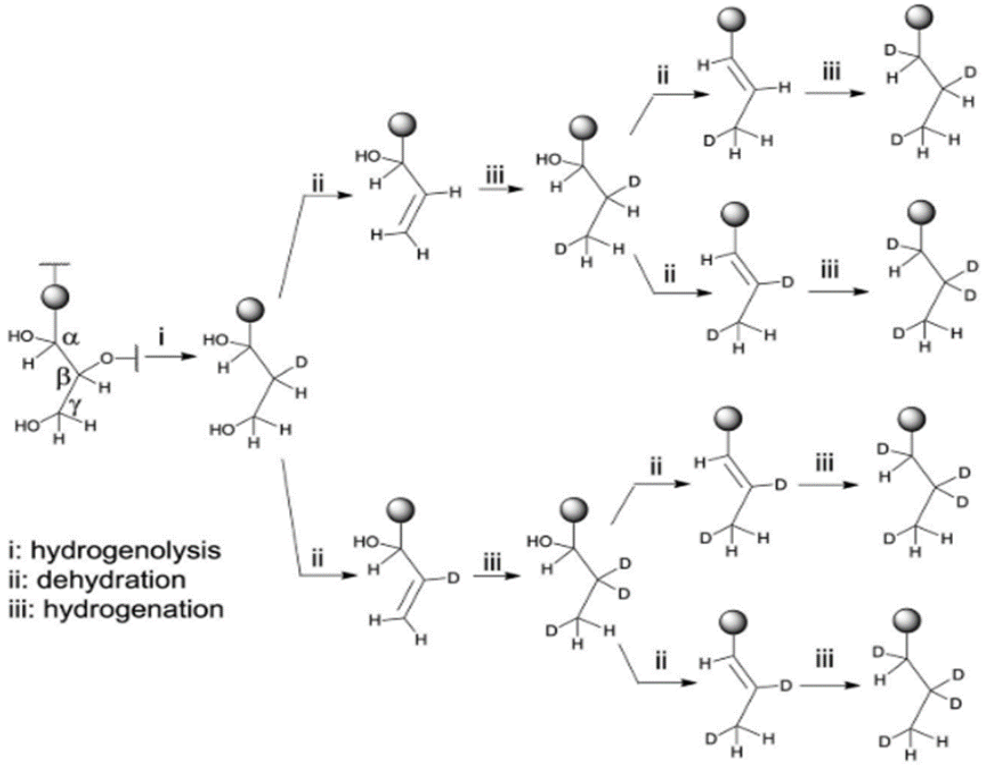

Figure 205 Lignin depolymerisation mechanism via hydrogenolysis, dehydration and hydrogenation [98]

Comparing FDC, PDC and FDNC, the number of incorporated deuterium atoms did not change. In Section 6.1.1.7, it was shown that the deuterium atoms were in the ring of the product (for FDC experiment with Pt/Al_2O_3). This was in agreement with the literature, as the presence of deuterium incorporation into the aromatic ring via H/D exchange was already reported [165], [166]. McVeigh (2016) showed that deuterium was incorporated into 4-ethyl-2-methoxyphenol molecule, depending on the type of deuterated environment. Five and six deuterium atoms were incorporated into this molecule in reaction with fully deuterated (D_2, D_2O and CD_3OD) and partially deuterated systems (D_2, D_2O and CH_3OH), respectively. These atoms were not only detected in the ring but also in the alkyl chain [26]. Compounds

2, 4, 6 and 8 were not detected among the products for FDNC while product 3 was not detected in PDC and FDNC.

This study highlighted that lignin depolymerisation does not occur via only one reaction pathway and that rate determining steps are not trivial to determine in lignin. An identified KIE can be a sum of other effects involved along the depolymerisation, showing that each reaction has particular characteristics and that generalisations of lignin depolymerisation can be a mistake. Aspects such as type of catalyst and solvent mixture determine product distribution.

7.5 Post reaction catalyst characterisation

The reactions conducted in this project were in the presence of various catalysts, solvents and complex molecules (lignins). After reaction the catalysts turned black, indicating char formation. The focus of this project was not to promote a systematic and detailed study of the carbonaceous material formed in the post reaction catalysts but it was of interest to analyse if there were direct relationships between the type of carbon on catalyst surface, with the type of lignin and solvent mixture used in the reaction: especially, because the re-used catalysts (Section 6.3.1.1) changed yield and selectivity to fine chemicals. Due to the large amount of samples, a selection of alumina catalysts were recovered as representatives for the others. This allowed us to verify if the presence of noble or non-noble metals in the Al_2O_3 support could also affect this carbonaceous material. The poor performance of zirconium catalysts did not warrant their post reaction study and the difficulties in Ni/C and Fe/C recovery were the reasons why only alumina catalysts were investigated.

Catalyst deactivation is one of the challenges in many industrial catalytic reactions [167]. Coke formation can occur at acidic sites of catalysts decreasing catalytic activity or even causing deactivation [168]. If there is carbon laydown, it can be burned off without volatilising the metals [169]. Nevertheless, high temperatures can result in sintering and affect catalyst activity, adding a further challenge to the problem [168]. As discussed in Section 6.3.1.1, the recovered Ni and Pt alumina catalysts had slight changes in selectivity compared to the new catalysts. They decreased in activity, with lower yields for most products. Even though the changes were not dramatic, it is possible that the catalyst performance varied due to coke deposition from the reaction.

XRD analysis showed that there were no structural changes in the alumina catalysts. There were no variation in terms of peak position, relative intensity or appearance of additional peaks. BET analysis revealed an increase in surface area and decrease in pore volume for most spent catalysts. These results were in agreement with other studies [26] involving lignin depolymerisation, suggesting that increase in surface area could also be a characteristic of the type of surface carbonaceous materials formed from lignin. The analysis for the Pt/Al_2O_3 catalyst used in the deuterated reactions did not show significant changes compared to the equivalent protiated experiments. There was no obvious trend for the type of lignin or reaction or the changes in surface area of the catalysts.

7.5.1 TGA-TPO and CHN analysis of the spent catalysts

The presence of carbon was confirmed by TGA-TPO and CHN analysis. The TPO-MS plots presented in Section 4.2.1, showed mass loss between ~ 400 K and 800 K which was accompanied by CO_2 evolution. Hydrocarbonaceous species could be present in these samples as it was reported [71] that weight loss at ~ 742 K can be attributed to this type of carbon material in fast combustion [71].

It is interesting to note that Al_2O_3 support in reactions of Kraft and oak parr-lignins with acetone gave the highest amount of carbon laydown (12 %, CHN analysis). Relating these results to their TPO plots (Section 4.2.1), these catalysts had similar weight loss. However, as shown in the Figure below, the TPO plot of Kraft lignin had a range of carbon species on the surface with different types combusting at ~ 620 K, at ~ 680 K and peak maxima at ~ 780 K. This signified that despite the similarities with oak parr-lignin, the type of carbon deposited was not the same. At least three carbon species were formed from the reaction with Kraft lignin and decomposed along with the rise in temperature.

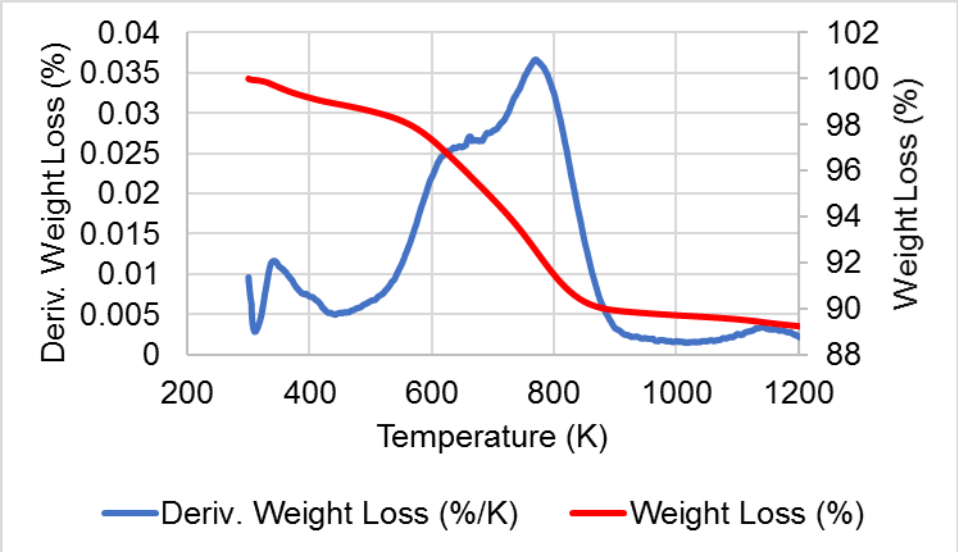

Figure 206 TPO of spent Al_2O_3 catalyst after acetone/H_2O reaction with the Kraft Lignin

The TPO plots for spent Ni/Al_2O_3 showed more similarities, even with varying lignin and solvent. However, in Pt/Al_2O_3 systems the carbon deposit had many variations dependent upon the reaction observed. Hence, the change in metal, changed the complexity of carbon deposited. This agreed with the fact that the catalysts showed different selectivities in the reactions, and therefore the interaction with the lignin would not be the same, resulting in difference in the type of deposited species.

In reactions with the Kraft and parr-lignins, the use of IPA resulted in a carbon combustion in the Pt/Al_2O_3 TPO plots at about ~ 600 K. This type of carbon species was not specific for this solvent and Pt/Al_2O_3, as it was also found with acetone with oak and birch lignins. Small combustion events at ~ 610 K and 630 K were found for Pt/Al_2O_3 in the case of sugar-cane, oak parr-lignin and Kraft, as well as for the Al_2O_3 catalyst, acetone and birch lignin. This data indicated that any change in metal, solvent or lignin had the potential to effect the type of carbon species. The TGA analysis revealed the complexity of the carbonaceous material. Based on the identified combustion events in the TPO plots, Table 26 summarises the form of carbon species considered in these catalysts. Unfortunately, it was not possible to find an obvious trend between lignin, solvent, catalyst and forms of carbon deposited. Nevertheless, it was concluded that there was interaction between lignin and the catalyst and that not only one type of carbon was deposited over the catalyst surface. In addition, the main carbon that appears at ~ 700K appears to be the same for all catalysts.

Table 26 Forms of carbon species over the catalysts by changing the solvent and lignin

Type of reaction	Forms of carbonaceous species over the catalyst
Spent Al_2O_3	
Kraft Acetone/H_2O	3
Birch Acetone/H_2O	2
Oak Acetone/H_2O	2
Sugar-cane Acetone/H_2O	3
Spent Pt/Al_2O_3	
Kraft IPA/H_2O	2
Kraft Acetone/H_2O	2
Kraft Fully deuterated	3
Sugar-cane Acetone/H_2O	3
Birch Acetone/H_2O	5
Oak Acetone/H_2O	2
Birch IPA/H_2O	2
Oak IPA/H_2O	3

The carbon was also analysed by CHN and the values detected revealed the same trend as that found with TGA. Initially, it was expected more carbon would be deposited over the Pt/Al_2O_3 surface from Kraft lignin due to its more condensed character and higher chances for re-polymerisation. Nevertheless, as shown in Figure 207, according to the CHN analysis, there was a trend for carbon deposited onto this catalyst surface and the type of lignin. It was higher for oak parr-lignin, followed by Kraft, sugar-cane and birch. This may be associated

to the lignin nature and interactions of these molecules with the respective catalyst during the reaction, and not only to condensation. Hence, the amount of carbon depended on the type of lignin. A similar tendency was found for Al_2O_3 and Ni/Al_2O_3 as presented in Figure 208. A direct correlation between the type of solvent and the amount of carbon deposited was not found.

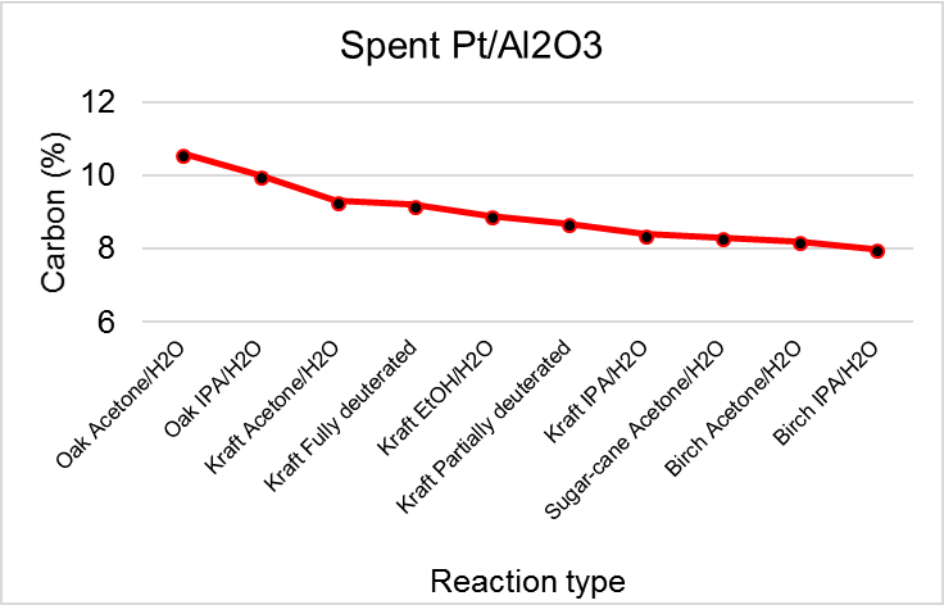

Figure 207 Carbon deposition over Pt/Al_2O_3 catalyst according to CHN analysis

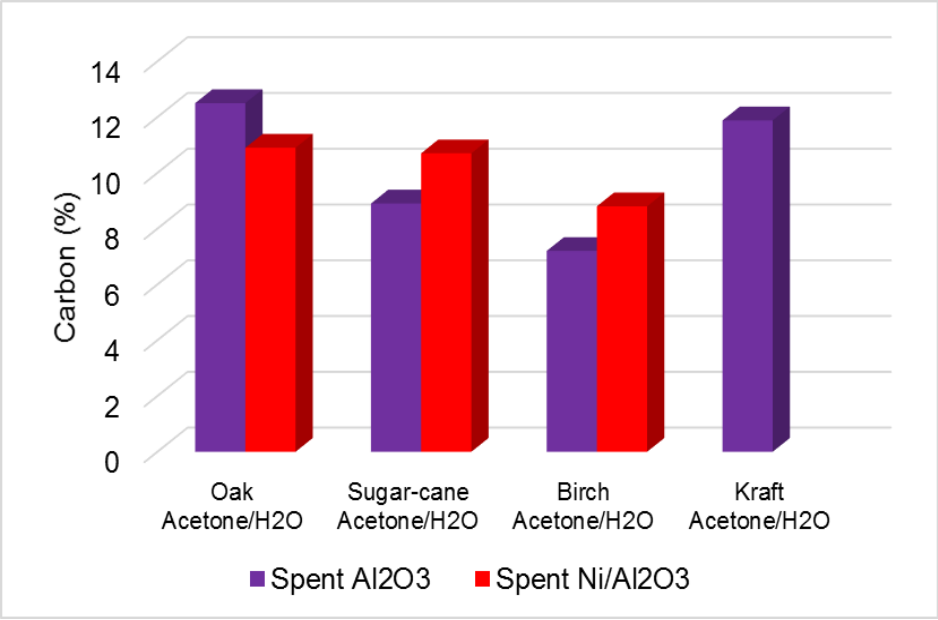

Figure 208 Carbon deposition over Al_2O_3 and Ni/Al_2O_3 catalyst according to CHN analysis

7.5.2 Coke deposition over spent catalysts

The complexity of lignin depolymerisation brings a gap in the understanding of coke formation and its attribution to a molecule fragment or active site in the catalyst. However, it is suggested that coke forms from lignin intermediates, including radical species that would adsorb onto the catalyst, forming highly condensed coke precursors through oligomerisation and polymerisation. These species along the reaction could undergo transformations resulting in the deposition of carbonaceous species.

7.5.3 Raman analysis

It was not possible to determine exactly what type of species was deposited onto the catalyst surface, but it was possible to detect by Raman spectroscopy graphitic and disordered bands in almost all analysed samples. They corresponded to the D and G bands at ~1380 cm^{-1} and ~1600 cm^{-1}[94], [95], respectively. In the TPO-MS analysis, it was found for Pt/Al_2O_3 (Section 4.2.1, Figure 55, Kraft, acetone/H_2O 50:50 v/v) a weight loss event at higher temperatures 800 K, indicating that there were more recalcitrant species produced from Kraft lignin. Graphite is reported to combust at higher temperatures than disordered carbon [94], the low intensities of the graphitic peaks, indicated that these species were present but not predominating. This was consistent with the TPO analysis, as there were not well defined peaks at high temperatures.

Figure 209 shows the variation of D:G ratio of the analysed catalysts. The reaction systems not shown had zero ratios. Pt/Al_2O_3 (4) was the lowest intensity detected. This catalyst was used in reaction with sugar-cane lignin and acetone. The highest value was for Pt/Al_2O_3 (1), which was regarded to Kraft lignin. These ratios depended on the type of reaction and in general, defective carbon had considerable low intensities. There was no obvious trend related to the type of lignin, solvent and catalyst analysed, but D:G ratios suggested that for most catalysts there were carbon species ordered in their nature.

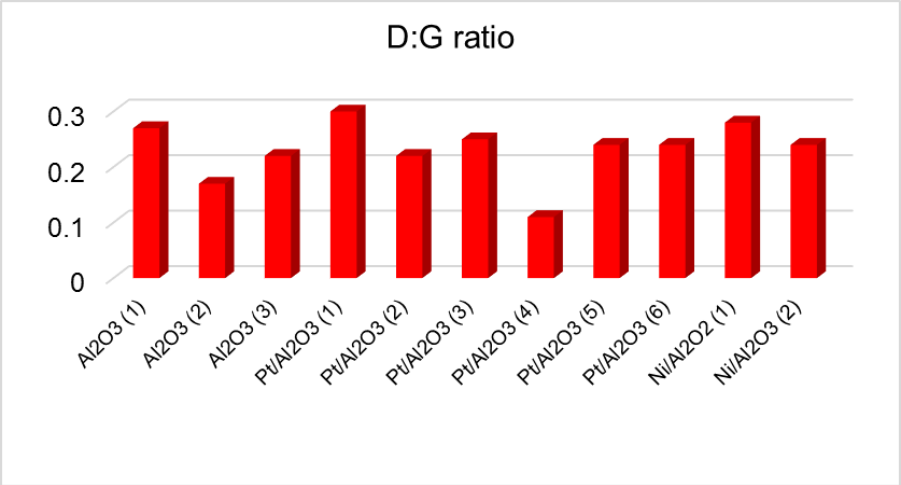

Figure 209 D:G ratio for Raman analysis. Reactions Key: Al_2O_3 (1) - Kraft Acetone/H_2O; Al_2O_3 (2) - Birch Acetone/H_2O; Al_2O_3 (3) - Oak Acetone/H_2O; Pt/Al_2O_3 (1) - Kraft EtOH/H_2O; Pt/Al_2O_3 (2) - Kraft IPA/H_2O; Pt/Al_2O_3 (3) - Kraft Acetone/H_2O; Pt/Al_2O_3 (4) - SC Acetone/H_2O; Pt/Al_2O_3 (5) - Birch Acetone/H_2O; Pt/Al_2O_3 (5) - Oak Acetone/H_2O; Ni/Al_2O_3 (1) - Birch acetone/H_2O; Ni/Al_2O_3 (2) - Oak Acetone/H_2O

8 Project conclusions

The interest in biomass has been growing over the years as an alternative renewable energy source. The polyaromatic nature of lignin holds a huge potential to obtain fine chemicals from its depolymerisation[50], [67], [112]. Within the biorefinery process, lignin can be included at three distinct stages: lignocellulose fractionation, lignin depolymerisation and upgrading [28]. Many methodologies have been applied over the years to optimise lignin utilisation [28], [31], [38]. This work contributed to this area of science by demonstrating how lignins with different types of bonds respond to the use of solvent mixtures and various metal based catalysts in depolymerisation reactions.

Lignin sources tend to originate as a by product or waste materials of existing industries and are often discarded or burnt. Kraft lignin used in this project was a technical lignin and is mostly burned as a low value fuel. Sugar-cane lignin was obtained by an Organosolv process from waste bagasse. The parr-lignin method developed in this project was a simple and efficient method to extracted lignin from sawdust biomass, possibly leaving hemicellulose and cellulose available for further use. In addition, the parr-lignins were less condensed than traditional technical lignins.

One of the main challenges in lignin depolymerisation is the variable or unknown chemical structure of the starting material and consequently how this molecule fragments during a reaction. Previous research has indicated a relationship between the amount of β-O-4 bonds in a lignin and the ease in which these linkages can be broken down. Thus, an increase in these labile bonds present in a lignin could allow more fine chemicals to be generated. This research used lignins with different amount of these bonds and it was confirmed that an increase in β-O-4 content produced a better response, with the addition of catalysts, to generate aromatic monomers. From these studies the following conclusions were made:

- The type of linkages and reactivity of a lignin were mainly governed by two aspects: the feedstock and the type of method used in the extraction process. Structural characteristics such as the type of units (H, S and G) or linkages (e.g. β-O-4 or β-β) changed between lignins. Consequently, the type of monomers obtained by depolymerisation of lignin was influenced mainly by the method used and the structural characteristic of the lignin. To promote direct comparisons with unambiguous assessments, the feedstock should be the same and the isolation method should reproduce most characteristics (linkages and units) that could be identified in

the lignin. Otherwise, these systems will behave in unique ways and should be analysed individually.

- Solvolysis of the lignins generated a range of products, with their yields influenced by the type of solvent mixture. The total yields were generally below 10 wt %, although slightly higher values were detected for Kraft lignin reactions. A trend was identified where less condensed lignins (more β-O-4 bonds) were not very susceptible for solvolysis but improved significantly when a catalyst was added to the reaction. Condensed lignin (Kraft) showed similar results in solvolysis and catalysed experiments. For Kraft lignin, these reference reactions yielded more unsubstituted and small chains of alky-substituted compounds, especially 2-methoxyphenol (guaiacol). Product selectivity was low and there was no clear pattern relating polarity of solvents and lignin conversion. It was difficult to establish if most of the linkages were cleaved by thermolysis, hydrolysis or solvent action. This highlighted the benefit of using catalysts.

- The use of heterogenous catalysts allowed the possibility of selective cleavage of C-O-C bonds in the lignin polymer. The monomers obtained from these reactions could undergo further transformations into fuels and chemical for use in industry. Zirconia catalysts did not show a good performance in the reactions even with changing of the type of solvent mixture or lignin. This could be due to the small surface area of these catalysts which was not able to contribute to the surface reactions responsible for the monomers formation. Reactions of Kraft lignin over alumina support showed overall better results compared to equivalent experiments with the noble metals. These results could be attributed to poisoning of the catalysts by the sulfur present in the lignin. Overall, the experiments involving alumina catalysts, sugar-cane and parr-lignins showed good results and successfully increased the monomer yields by more than double compared to the equivalent solvolysis. In addition, Ni/Al_2O_3 showed as good a performance in these reactions as the noble metals, revealing a promising catalyst for the cleavage of not only model compounds but the linkages of lignin itself.

- Carbon catalysts attained a considerable production of fine chemicals. Although the presence of metal over the support did not necessarily allow higher conversion. The highest overall yield (13.3 %) was obtained for oak parr-lignin (acetone/water 50:50 v/v) using only the support. Nevertheless and more importantly, the selectivity

towards aromatic compounds varied by changing the metal. Good results regarding individual and/or total yield were observed with nickel. Apart from the reaction with sugar-cane lignin, iron had the poorest performance. In addition, the solutions used in the reactions had an influence. Varying the solvent resulted in different selectivity and product distribution. Thus revealing a synergistic effect between catalyst and solvent.

- Kinetic isotope studies of Kraft lignin showed that the solvent was directly involved in the product formation. The change in values for the kinetic isotopic effects, when adding the catalyst, revealed that reference and catalysed experiments formed products from different reaction pathways. In addition, most compounds had different values, signifying that they were produced from different mechanisms, highlighting the complexity of lignin depolymerisation.

- Post reaction analysis showed that carbonaceous material was deposited over catalyst surface, including graphite and that there was not only one type of carbon. In addition, the amount of carbon deposited depended on the type of lignin. The change of metal also changed the carbonaceous complexity and no obvious trend was found relating these results to the solvents.

The results from sugar-cane and parr-lignins were different compared to Kraft. It was not possible to determine reaction mechanisms but as the increase in yields of individual compounds were considerably higher in most catalysed reactions, it was suggested hydrogenolysis was the prevailing route. The presence of monomers such as 2-methoxyphenol, 2,6-dimethoxyphenol and 1,2-dihydrozybenzene indicated dealkylation of lignin intermediates were favoured by the catalysts. In addition, hydrodeoxygenation was suggested to occur, due to the formation of 4-ethyphenol by methoxy cleavage of ethyl-guaiacol. The enhanced yield of a compound was also dependent on the type of catalyst used. The overall yields varied and the higher values were found for sugar-cane and oak parr-lignin with 13 % and 13.3 % of monomeric compounds with Pt/Al_2O_3 (acetone/water 50:50 v/v) and carbon support (acetone/water 50:50 v/v), respectively. Each catalyst showed a particular performance in the presence of solvent mixture and lignin. No obvious trend was found to simply classify an ideal system or the most successful reaction. The purpose is relevant and depends on whether it is desired to achieve high overall yield, a targeted compound or a mixture of certain products. For example, for higher overall yield (13.3 %) oak Par-lignin with carbon support and acetone/water 50:50 v/v would be the best system,

while for a specific compound, Kraft lignin with acetone/water 50:50 v/v and Rh/Al_2O_3 can yield up to 6.5 g/100 g of 2-methoxyphenol. In addition, the supports showed efficient catalytic activity, sometimes better than when the metal was present. It is interesting to keep the supports of catalysts as a candidate for further evaluation in reactions with other types of molecules.

The monomer product distribution was dependent on the raw material used, solvent mixture and catalyst. The reaction conditions used in this work did not overcome condensation issues related to Kraft lignin. However, the project successfully promoted cleavage of linkages by catalysts in sugar-cane and parr-lignins. For these lignins, the individual yields of products were significantly enhanced in most cases. Efficient use of catalysts and further understanding of these systems can increase the potential of reusing lignin in various industries across the world and converting it to valuable fine chemicals.

9 Recommendations for future work

To make lignin commercially valuable, the business case for converting it to useful products needs to be scalable, viable and for there to be a large enough demand. For this to occur, further research is required to overcome the technical challenges, including those described in this project, to develop a possible business model.

The results showed some limitations in terms of experimental set up. Due to the limited amount of biomass feedstocks (oak and birch) and lignin samples, the number of experiments conducted was limited. With larger volumes of samples, duplicates and triplicates would ensure that relative errors within experiments were appropriate.

Other peaks in the GC-MS were produced and their identification was not possible due to limitations of the GC-MS library and complexity of mass spectra information. Therefore, an improvement in the analysis methodology could contribute to clarification of non-identified peaks. The parr-autoclave reactor was a 300 mL vessel and for this reason 100 mL was the minimum of solvent mixture that could be used along with lignin and catalyst. An equipment with smaller vessel volume would allow better stoichiometry between catalyst, lignin and solvent, and the relevance of volume of solvent used in the reaction could be better investigated.

The proportion of lignin and catalyst was relatively high (0.5 g of lignin and 0.1 g of catalyst), however, this was an initial study of catalyst effects in these lignins depolymerisation. Changes in catalyst, solvent and lignin content could benefit these studies in terms of efficiency. In addition, an online GC-TCD coupled to the parr-autoclave would allow identification of gaseous compounds formed and reaction intermediates, providing kinetic information and mechanistical insights to avoid condensation issues. As described in Section 3.3.2, this research simplified the post reaction procedures compared to the previous methodology. However, optimisation of this methodology is still required. Due to losses during the manipulation of sample in the purification process (e.g. filtration, extraction) and slight release of gas when finishing the experiment, a mass balance was not achievable. The identification of gaseous components and products formed after reaction by an online GC-TCD would contribute to overcome this problem of mass balance closure.

The extraction method used in the parr-lignins successfully produced less condensed lignins than Kraft or soda pulping. Strategies such as distillation could be applied to recover the

solvent and re-use it in another cycle, making the process more sustainable. These lignins were produced in only one batch and did not pass for further purification steps. Investigation of carbohydrate content in these lignins would inform how efficient this method was in terms of cellulose and hemicellulose separation from lignin. This could be obtained by a two-step hydrolysis method [170] reported by Rémond (2010) with analysis carried out in a GC equipment [170]. In addition, purification methodologies, including lignin washed with organic solvents to remove impurities, could allow the parr-lignins to react more efficiently. These steps could produce higher quality lignins better suited for chemical valorisation.

One important point is that despite considerable higher yields of individual compounds in catalysed reactions compared to solvolysis, the overall yields were not considerable high compared to Kraft lignin. Maybe this was associated to condensation issues due to the reaction conditions. Perhaps these less condensed lignins would give even more promising results in catalysed experiments by optimising reaction conditions, such as change in reagents stoichiometry, time and temperature.

Kraft lignin (KL) is produced in large quantities annually [171]. This lignin is mostly burned and it is still a challenge to overcome the problems of its condensed character and impurities to make it suitable for value added chemicals production. Svensson and co-authors reported methodologies such as ion chromatography and inductively coupled plasma to identify sulfur species [172]. Hence, the type of sulfur present in the Kraft lignin could be detected, contributing to desulfurisation processes before depolymerisation, using hydrodesulfurization [173] for example. In addition, chemical modification of lignin has been showing as an efficient strategy[174], [175]. For example, esterification of KL resulted a decrease of OH groups and lower degradation temperature [175] and amination of KL successfully modified the chemical structure showing potential for value added applications [176]. The challenge faced in this project to study depolymerisation of Kraft lignin showed that other strategies should also be considered to ensure that a material that is produced in such large quantity is not wasted. This include research to produce activated carbon, biopolymers and adhesives from KL, for example.

The reactions carried out in this project focused on the catalytic chemistry behind it. However, it was difficult to establish trends and each system behaved in unique ways. This study allowed an overview about how lignins with different linkages levels reacted with noble metals, non-noble metals and supports. Studies to optimise catalyst systems could also be used, including changes in metal loading, influence of dispersion in the reactions and

more information about surface chemistry. The reaction product was composed of a complex mixture of chemicals. As some catalysts in sugar-cane and parr-lignins showed selective production of monomers such as 2,6-dimethoxyphenol, one strategy is to run reactions with target chemicals, enhancing the yields of specific compounds. Nevertheless, reactions from lignin generate mixtures of chemicals, one option is to use distillation to separate them by their boiling points (BP) or more selective mixtures with similar BP.

10 List of references

[1] A. McVeigh, F. P. Bouxin, M. C. Jarvis, and S. D. Jackson, "Catalytic depolymerisation of isolated lignin to fine chemicals: part 2 – process optimisation," *Catal. Sci. Technol.*, vol. 6, no. 12, pp. 4142–4150, 2016.

[2] F. P. Bouxin, A. McVeigh, F. Tran, N. J. Westwood, M. C. Jarvis, and S. D. Jackson, "Catalytic depolymerisation of isolated lignins to fine chemicals using a Pt/alumina catalyst: part 1—impact of the lignin structure," *Green Chem.*, vol. 17, no. 2, pp. 1235–1242, 2015.

[3] S. Borowitz, *Farewell Fossil Fuels*, 1st ed. Boston, MA: Springer US, 1999.

[4] World Energy Council, "World Energy Resources, Bioenergy," 2016. [Online]. Available: https://www.worldenergy.org/publications/2016/world-energy-resources-2016/. [Accessed: 02-Mar-2018].

[5] International Agency Energy, "Global energy demand grew by 2.1% in 2017, and carbon emissions rose for the first time since 2014," iea.org, Mar. 2018. [Online]. Available: https://www.iea.org/newsroom/news/2018/march/global-energy-demand-grew-by-21-in-2017-and-carbon-emissions-rose-for-the-firs.html. [Accessed: 14-Jun-2018].

[6] United Nations, "Sustainable development goals," [Online]. Available: https://www.un.org/sustainabledevelopment/sustainable-development-goals/. [Accessed: 12-Jun-2018].

[7] United Nations Climate Change, "The Paris Agreement," Framework Convention on Climate Change, 2018. [Online]. Available: http://unfccc.int/paris_agreement/items/9485.php. [Accessed: 12-Jun-2018].

[8] Z. Zhang, J. Song, and B. Han, "Catalytic Transformation of Lignocellulose into Chemicals and Fuel Products in Ionic Liquids," *Chem. Rev.*, vol. 117, no. 10, pp. 6834–6880, 2017.

[9] M. J. Climent, A. Corma, and S. Iborra, "Converting carbohydrates to bulk chemicals and fine chemicals over heterogeneous catalysts," *Green Chem.*, vol. 13, no. 3, pp. 520–540, 2011.

[10] W. Wang, M. Niu, Y. Hou, W. Wu, Z. Liu, Q. Liu, S. Ren, and K. N. Marsh, "Catalytic conversion of biomass-derived carbohydrates to formic acid using molecular oxygen," *Green Chem.*, vol. 16, no. 5, pp. 2614–2618, 2014.

[11] Z. Sun, L. Xue, S. Wang, X. Wang, and J. Shi, “Single step conversion of cellulose to levulinic acid using temperature-responsive dodeca-aluminotungstic acid catalysts,” *Green Chem.*, vol. 18, no. 3, pp. 742–752, 2016.

[12] H. Luo and M. M. A. Omar, “Lignin extraction and catalytic upgrading from genetically modified poplar,” *Green Chem.*, vol. 20, no. 3, pp. 745–753, 2018.

[13] H. Chen, *Biotechnology of Lignocellulose, Theory and Practice*, 1st ed. Dordrecht: Springer Netherlands, 2014.

[14] M. Möller and U. Schröder, “Hydrothermal production of furfural from xylose and xylan as model compounds for hemicelluloses,” *RSC Adv.*, vol. 3, no. 44, pp. 22253–22260, 2013.

[15] K. Wang, H. Yang, X. Yao, F. Xu, and R. C. Sun, “Structural transformation of hemicelluloses and lignin from triploid poplar during acid-pretreatment based biorefinery process,” *Bioresour. Technol.*, vol. 116, pp. 99–106, 2012.

[16] M. P. Ansell, "*Wood microstructure – A cellular composite*" in *Wood Composites*. Cambridge, Elsevier Ltd., 2015, pp. 3-26..

[17] S. Y. Lin and C. W. Dence, Eds., Methods in Lignin Chemistry, 1st ed. Berlin, Heidelberg: Springer Berlin Heidelberg, 1992.

[18] S. Laurichesse and L. Avérous, “Chemical modification of lignins: Towards biobased polymers,” *Prog. Polym. Sci.*, vol. 39, no. 7, pp. 1266–1290, 2014.

[19] Á. T. Martínez, J. Rencoret, G. Marques, A. Gutiérrez, D. Ibarra, J. Jiménez-Barbero, and J. C. del Río, “Monolignol acylation and lignin structure in some nonwoody plants: A 2D NMR study,” *Phytochemistry*, vol. 69, no. 16, pp. 2831–2843, 2008.

[20] R. Rinaldi, R. Jastrzebski, M. T. Clough, J. Ralph, M. Kennema, P. C. A. Bruijnincx, and B. M. Weckhuysen, “Paving the Way for Lignin Valorisation: Recent Advances in Bioengineering, Biorefining and Catalysis,” *Angew. Chemie - Int. Ed.*, vol. 55, no. 29, pp. 8164–8215, 2016.

[21] C. Wang, H. Li, M. Li, J. Bian, and R. Sun, “Revealing the structure and distribution changes of Eucalyptus lignin during the hydrothermal and alkaline pretreatments,” *Sci. Rep.*, vol. 7, no. 1, pp. 1–10, 2017.

[22] S. K. Ritter, “Lignocellulose: A Complex Biomaterial,” *Chemical & engineering news*, 2008. [Online]. Available: https://cen.acs.org/articles/86/i49/Lignocellulose-

Complex-Biomaterial.html. [Accessed: 15-Jun-2018].

[23] M. Zaheer and R. Kempe, "Catalytic hydrogenolysis of aryl ethers: A key step in lignin valorization to valuable chemicals," *ACS Catal.*, vol. 5, no. 3, pp. 1675–1684, 2015.

[24] Z. Strassberger, S. Tanase, and G. Rothenberg, "The pros and cons of lignin valorisation in an integrated biorefinery," *RSC Adv.*, vol. 4, no. 48, pp. 25310–25318, 2014.

[25] M. Yáñez-S, B. Matsuhiro, C. Nuñez, S. Pan, C. A. Hubbell, P. Sannigrahi, and A. J. Ragauskas, "Physicochemical characterization of ethanol organosolv lignin (EOL) from Eucalyptus globulus: Effect of extraction conditions on the molecular structure," *Polym. Degrad. Stab.*, vol. 110, pp. 184–194, 2014.

[26] A. McVeigh, "The Conversion of Lignin to Alkylphenolic Monomers using Heterogeneous Catalysis". Ph.D. thesis. Dep. Chem. The University of Glasgow, Glasgow, 2016.

[27] S. Gillet, M. Aguedo, L. Petitjean, A. R. C. Morais, A. M. Da Costa Lopes, R. M. Łukasik, and P. T. Anastas, "Lignin transformations for high value applications: Towards targeted modifications using green chemistry," *Green Chem.*, vol. 19, no. 18, pp. 4200–4233, 2017.

[28] H. Chen, "*1-Lignocellulose biorefinery engineering: an overview*," in *Lignocellulose Biorefinery Engineering*, Cambridge: Elsevier, 2015, pp. 1–17.

[29] A. Berlin and M. Balakshin, "*Industrial Lignins: Analysis, Properties, and Applications,*" in *Bioenergy Research: Advances and Applications*, Oxford, Elsevier, 2014, pp. 315–336.

[30] Sarah Delooze, "Bulk Chemicals VS Fine Chemicals," *Syntor Fine chemicals*, 2017. [Online]. Available: http://www.syntor.co.uk/bulk-chemicals/. [Accessed: 20-Jun-2018].

[31] C. Xu, R. A. D. Arancon, J. Labidi, and R. Luque, "Lignin depolymerisation strategies: Towards valuable chemicals and fuels," *Chem. Soc. Rev.*, vol. 43, no. 22, pp. 7485–7500, 2014.

[32] D. Ekeberg, K. S. Gretland, J. Gustafsson, S. M. Bråten, and G. E. Fredheim, "Characterisation of lignosulphonates and kraft lignin by hydrophobic interaction chromatography," *Anal. Chim. Acta*, vol. 565, no. 1, pp. 121–128, 2006.

[33] S. Laurichesse and L. Avérous, "Chemical modification of lignins: Towards biobased polymers," *Prog. Polym. Sci.*, vol. 39, no. 7, pp. 1266–1290, 2014.

[34] W. F. Cowan, V. B. Diebold and J. K. Walsh, "Solvent pulping process," U.S. Patent 4,100,016, 11 July., 1978.

[35] M. J. de la Torre, A. Moral, M. D. Hernández, E. Cabeza, and A. Tijero, "Organosolv lignin for biofuel," *Ind. Crops Prod.*, vol. 45, pp. 58–63, 2013.

[36] P. Sannigrahi and A. J. Ragauskas, "Fundamentals of Biomass Pretreatment by Fractionation," *Aqueous Pretreat. Plant Biomass Biol. Chem. Convers. to Fuels Chem.*, pp. 201–222, 2013.

[37] W. J. J. Huijgen, J. H. Reith, and H. Den Uil, "Pretreatment and fractionation of wheat straw by an acetone-based organosolv process," *Ind. Eng. Chem. Res.*, vol. 49, no. 20, pp. 10132–10140, 2010.

[38] F. P. Bouxin, S. David Jackson, and M. C. Jarvis, "Isolation of high quality lignin as a by-product from ammonia percolation pretreatment of poplar wood," *Bioresour. Technol.*, vol. 162, pp. 236–242, 2014.

[39] T. Renders, S. Van den Bosch, T. Vangeel, T. Ennaert, S.-F. Koelewijn, G. Van den Bossche, C. M. Courtin, W. Schutyser, and B. F. Sels, "Synergetic effects of alcohol/water mixing on the catalytic reductive fractionation of poplar wood," *ACS Sustain. Chem. Eng.*, pp. 6894–6904, 2016.

[40] C. S. Lancefield, I. Panovic, P. J. Deuss, K. Barta, and N. J. Westwood, "Pre-treatment of lignocellulosic feedstocks using biorenewable alcohols: Towards complete biomass valorisation," *Green Chem.*, vol. 19, no. 1, pp. 202–214, 2017.

[41] R. J. A. Gosselink, "Lignin as a renewable aromatic resource for the chemical industry," Ph.D. thesis. Dep. Wageningen Food & Biobased Research, Wageningen University, Wageningen, 2011..

[42] S. Bauer, H. Sorek, V. D. Mitchell, A. B. Ibáñez, and D. E. Wemmer, "Characterization of Miscanthus giganteus lignin isolated by ethanol organosolv process under reflux condition," *J. Agric. Food Chem.*, vol. 60, no. 33, pp. 8203–8212, 2012.

[43] T. Renders, S. V. D. Bosch, S. F. Koelewijn, W. Schutyser, and B. F. Sels, "Lignin-first biomass fractionation: The advent of active stabilisation strategies," *Energy Environ. Sci.*, vol. 10, no. 7, pp. 1551–1557, 2017.

[44] A. Jensen, J. B. Nielsen, A. D. Jensen, and C. Felby, "Chapter 4 Thermal and Solvolytic Depolymerization Approaches for Lignin Depolymerization and Upgrading," in *Lignin Valorization: Emerging Approaches*, The Royal Society of Chemistry, 2018, pp. 74–107.

[45] C. S. Lancefield, B. M. Weckhuysen, and P. C. A. Bruijnincx, "Chapter 7 Catalytic Conversion of Lignin-derived Aromatic Compounds into Chemicals," in *Lignin Valorization: Emerging Approaches*, The Royal Society of Chemistry, 2018, pp. 159–198.

[46] A. Rodriguez, D. Salvachúa, R. Katahira, B. A. Black, N. S. Cleveland, M. Reed, H. Smith, E. E. K. Baidoo, J. D. Keasling, B. A. Simmons, G. T. Beckham, and J. M. Gladden, "Base-Catalyzed Depolymerization of Solid Lignin-Rich Streams Enables Microbial Conversion," *ACS Sustain. Chem. Eng.*, vol. 5, no. 9, pp. 8171–8180, 2017.

[47] J. E. Miller, L. Evans, A. Littlewolf, and D. E. Trudell, "Batch microreactor studies of lignin and lignin model compound depolymerization by bases in alcohol solvents," *Fuel*, vol. 78, no. 11, pp. 1363–1366, 1999.

[48] T. F. Hubbard, T. P. Schultz, and T. F. Fisher, "Alkaline Hydrolysis of Nonphenolic β–O-4 Lignin Model Dimers: Substituent Effeċts on the Leaving Phenoxide in Neighboring Group vs Direct Nucleophilic Attack," *Holzforschung*, vol. 46, no. 4, pp. 315–320, 1992.

[49] A. K. Deepa and P. L. Dhepe, "Lignin Depolymerization into Aromatic Monomers over Solid Acid Catalysts," *ACS Catal.*, vol. 5, no. 1, pp. 365–379, 2015.

[50] H. Wang, M. Tucker, and Y. Ji, "Recent Development in Chemical Depolymerization of Lignin: A Review," *J. Appl. Chem.*, vol. 2013, pp. 1–9, 2013.

[51] J. R. Gasson, D. Forchheim, T. Sutter, U. Hornung, A. Kruse, and T. Barth, "Modeling the lignin degradation kinetics in an ethanol/formic acid solvolysis approach. Part 1. Kinetic model development," *Ind. Eng. Chem. Res.*, vol. 51, no. 32, pp. 10595–10606, 2012.

[52] A. Toledano, L. Serrano, A. Pineda, A. A. Romero, R. Luque, and J. Labidi, "Microwave-assisted depolymerisation of organosolv lignin via mild hydrogen-free hydrogenolysis: Catalyst screening," *Appl. Catal. B Environ.*, vol. 145, pp. 43–55, 2014.

[53] Z. Fang and M. S. Meier, "Toward the oxidative deconstruction of lignin: Oxidation

of β-1 and β-5 linkages," *Org. Biomol. Chem.*, vol. 16, no. 13, pp. 2330–2341, 2018.

[54] IUPAC. Compendium of Chemical Terminology, 2nd ed. (the "Gold Book"). Compiled by A. D. McNaught and A. Wilkinson. Blackwell Scientific Publications, Oxford (1997). [Online]. Available: http://goldbook.iupac.org/html/P/P04961.html. [Accessed: 02-Mar-2018].

[55] J. A. Caballero, R. Font, and A. Marcilla, "Pyrolysis of Kraft lignin: Yields and correlations," *J. Anal. Appl. Pyrolysis*, vol. 39, no. 2, pp. 161–183, 1997.

[56] A. Roth, "Pyrolysis." *studentenergy.org*. [Online]. Available: https://www.studentenergy.org/topics/pyrolysis. [Accessed: 21-Jun-2018]..

[57] A. Dieguez-Alonso, A. Anca-Couce, N. Zobel, and F. Behrendt, "Understanding the primary and secondary slow pyrolysis mechanisms of holocellulose, lignin and wood with laser-induced fluorescence," *Fuel*, vol. 153, pp. 102–109, 2015.

[58] H. Kawamoto, "Lignin pyrolysis reactions," *J. Wood Sci.*, vol. 63, no. 2, pp. 117–132, 2017.

[59] M. Asmadi, H. Kawamoto, and S. Saka, "Gas- and solid/liquid-phase reactions during pyrolysis of softwood and hardwood lignins," *J. Anal. Appl. Pyrolysis*, vol. 92, no. 2, pp. 417–425, 2011.

[60] I. Brodin, E. Sjöholm, and G. Gellerstedt, "The behavior of kraft lignin during thermal treatment," *J. Anal. Appl. Pyrolysis*, vol. 87, no. 1, pp. 70–77, 2010.

[61] J. Li, H. Sun, J. xing Liu, J. jie Zhang, Z. xing Li, and Y. Fu, "Selective reductive cleavage of C–O bond in lignin model compounds over nitrogen-doped carbon-supported iron catalysts," *Mol. Catal.*, vol. 452, no. April, pp. 36–45, 2018.

[62] X. Wang and R. Rinaldi, "Solvent effects on the hydrogenolysis of diphenyl ether with raney nickel and their implications for the conversion of lignin," *Chem. Sus. Chem.*, vol. 5, no. 8, pp. 1455–1466, 2012.

[63] A. Yamaguchi, N. Mimura, M. Shirai, and O. Sato, "Bond cleavage of lignin model compounds into aromatic monomers using supported metal catalysts in supercritical water," *Sci. Rep.*, vol. 7, no. November 2016, pp. 1–7, 2017.

[64] J. Goldemberg, S. T. Coelho, and P. Guardabassi, "The sustainability of ethanol production from sugarcane," *Energy Policy*, vol. 36, no. 6, pp. 2086–2097, 2008.

[65] N. R. Baral, L. Slutzky, A. Shah, T. C. Ezeji, K. Cornish, and A. Christy, "Acetone-butanol-ethanol fermentation of corn stover: Current production methods, economic

viability and commercial use," *FEMS Microbiol. Lett.*, vol. 363, no. 6, pp. 1–11, 2016.

[66] D. Wang, C. Deraedt, J. Ruiz, and D. Astruc, "Sodium hydroxide-catalyzed transfer hydrogenation of carbonyl compounds and nitroarenes using ethanol or isopropanol as both solvent and hydrogen donor," *J. Mol. Catal. A Chem.*, vol. 400, pp. 14–21, 2015.

[67] B. Joffres, D. Laurenti, N. Charon, A. Daudin, A. Quignard, and C. Geantet, "Thermochemical Conversion of Lignin for Fuels and Chemicals: A Review," *Oil Gas Sci. Technol. – Rev. d'IFP Energies Nouv.*, vol. 68, no. 4, pp. 753–763, 2013.

[68] R. Connor and H. Adkins, "Hydrogenolysis of oxygenated organic compounds," *J. Am. Chem. Soc.*, vol. 54, no. 12, pp. 4678–4690, 1932.

[69] C. Hodge, "Neste Oil Corporation's NEXBTL® Renewable Diesel" in Climate Action Team Technology Symposium, California, 2006.

[70] A. Gutierrez, R. K. Kaila, M. L. Honkela, R. Slioor, and A. O. I. Krause, "Hydrodeoxygenation of guaiacol on noble metal catalysts," *Catal. Today*, vol. 147, no. 3–4, pp. 239–246, 2009.

[71] F. P. Bouxin, X. Zhang, I. N. Kings, A. F. Lee, M. J. H. Simmons, K. Wilson, and S. D. Jackson, "Deactivation study of the hydrodeoxygenation of p-methylguaiacol over silica supported rhodium and platinum catalysts," *Appl. Catal. A Gen.*, vol. 539, pp. 29–37, 2017.

[72] V. N. Bui, D. Laurenti, P. Afanasiev, and C. Geantet, "Hydrodeoxygenation of guaiacol with CoMo catalysts. Part I: Promoting effect of cobalt on HDO selectivity and activity," *Appl. Catal. B Environ.*, vol. 101, no. 3–4, pp. 239–245, 2011.

[73] J. He, C. Zhao, D. Mei, and J. A. Lercher, "Mechanisms of selective cleavage of C-O bonds in di-aryl ethers in aqueous phase," *J. Catal.*, vol. 309, pp. 280–290, 2014.

[74] J. He, L. Lu, C. Zhao, D. Mei, and J. A. Lercher, "Mechanisms of catalytic cleavage of benzyl phenyl ether in aqueous and apolar phases," *J. Catal.*, vol. 311, pp. 41–51, 2014.

[75] J. Dunleavy, "Sulfur as a Catalyst Poison," *Platin. Met. Rev.*, vol. 50, no. 2, pp. 110–110, 2006.

[76] H. Holik, Ed., "Handbook of Paper and Board," Weinheim: Wiley-VCH, 2013..

[77] M. C. Lok, G. J Kelly, G. Grey., "Catalysts with high cobalt surface area," U.S.

Patent 6,927,190 B2, 2005..

[78] E. A. Gelder, "The Hydrogenation of Nitrobenzene of Metal Catalysts," The University of Glasgow, 2005.

[79] E. A. Gelder, "The Hydrogenation of Nitrobenzene of Metal Catalysts," Ph.D. thesis. Dep. Chem. The University of Glasgow, Glasgow, 2005..

[80] P. L. Toth, B. R. Harnishfeger, and A. Shea, "Kinetic Isotope Effects," *Compr. Enzym. Kinet.*, vol. 16, no. 3–4, pp. 353–390, 2002.

[81] S. Brunauer, P. H. Emmett, and E. Teller, "Adsorption of Gases in Multimolecular Layers," *J. Am. Chem. Soc.*, vol. 60, no. 1, pp. 309–319, 1938.

[82] Particle Analytical, "Introduction to BET (Brunauer, Emmett and Teller)." [Online]. Available: http://particle.dk/methods-analytical-laboratory/surface-area-bet-2/. [Accessed: 03-Apr-2018]..

[83] H. S. Kaufman and I. Fankuchen, "X-ray diffraction," *Anal. Chem.*, vol. 21, no. 1, pp. 24–29, 1949.

[84] T. B. Barrett, C. S. Massalski, *Structure of metals: crystallographic methods, principles, and data*, 3rd ed. New York: McGraw-Hill Book Company, 1966.

[85] Sigma-Aldrich, "Silylation Derivatization Reagent; BSTFA." [Online]. Available: https://www.sigmaaldrich.com/analytical-chromatography/analytical-reagents/derivatization-reagents/silylation.html. [Accessed: 03-Apr-2018]..

[86] M. Rynkowski, JM. Paryjczak, T. Lenik, "On the nature of oxidic nickel phases in NiO/y-Al203 catalysts," *Appl. Catal. A Gen.*, vol. 106, no. 1, pp. 73–82, 1993.

[87] X. Zhu, P. Huo, Y. Zhang, D. Cheng, and C. Liu, "Structure and reactivity of plasma treated Ni/Al2O3 catalyst for CO2 reforming of methane," *Appl. Catal. B Environ.*, vol. 81, no. 1–2, pp. 132–140, May 2008.

[88] A. Aljishi, G. Veilleux, J. A. H. Lalinde, and J. Kopyscinski, "The effect of synthesis parameters on ordered mesoporous nickel alumina catalyst for CO_2 methanation," *Appl. Catal. A Gen.*, vol. 549, no. July 2017, pp. 263–272, 2018.

[89] X. Zhang, Q. Zhang, N. Tsubaki, Y. Tan, and Y. Han, "*Influence of Zirconia Phase on the Performance of Ni/ZrO_2 for Carbon Dioxide Reforming of Methane*," in *Advances in CO_2 Capture, Sequestration, and Conversion*. Washington: American Chemical Society, 2015, pp. 135–153.

[90] K. Chen, Y. Fan, Z. Hu, and Q. Yan, "Study on the structure and reduction

behaviour of the iron-zirconium oxide system," *J. Mater. Chem.*, vol. 6, no. 6, pp. 1041–1045, 1996.

[91] C. Li and P. C. Stair, "Ultraviolet Raman spectroscopy characterization of coke formation in zeolites," *Catal. Today*, vol. 33, no. 1–3, pp. 353–360, 1997.

[92] C. Li and P. C. Stair, "Ultraviolet Raman spectroscopy characterization of sulfated zirconia catalysts: fresh, deactivated and regenerated," *Catal. Letters*, vol. 36, no. 3–4, pp. 119–123, 1996.

[93] M. D. Garba, "Valorisation of alkanes and alkynes by transhydrogenation in petrochemical processes," Ph.D. thesis. Dep. Chem. The University of Glasgow, Glasgow, 2017.

[94] J. J. H. B. Sattler, A. M. Beale, and B. M. Weckhuysen, "Operando Raman spectroscopy study on the deactivation of Pt/Al2O3 and Pt–Sn/Al2O3 propane dehydrogenation catalysts," *Phys. Chem. Chem. Phys.*, vol. 15, no. 29, p. 12095, 2013.

[95] A. Sadezky, H. Muckenhuber, H. Grothe, R. Niessner, and U. Pöschl, "Raman microspectroscopy of soot and related carbonaceous materials: Spectral analysis and structural information," *Carbon N. Y.*, vol. 43, no. 8, pp. 1731–1742, 2005.

[96] C. Crestini, H. Lange, M. Sette, and D. S. Argyropoulos, "On the structure of softwood kraft lignin," *Green Chem.*, vol. 19, no. 17, pp. 4104–4121, 2017.

[97] S. Constant, H. L. J. Wienk, A. E. Frissen, P. de Peinder, R. Boelens, D. S. van Es, R. J. H. Grisel, B. M. Weckhuysen, W. J. J. Huijgen, R. J. A. Gosselink, and P. C. A. Bruijnincx, "New insights into the structure and composition of technical lignins: a comparative characterisation study," *Green Chem.*, vol. 18, no. 9, pp. 2651–2665, 2016.

[98] Q. Song, F. Wang, J. Cai, Y. Wang, J. Zhang, W. Yu, and J. Xu, "Lignin depolymerization (LDP) in alcohol over nickel-based catalysts via a fragmentation-hydrogenolysis process," *Energy Environ. Sci.*, vol. 6, no. 3, pp. 994–1007, 2013.

[99] E. Buncel and C. C. Lee, Eds., Isotopes in organic chemistry: Secondary and solvent isotope effects., Amsterdam: Elsevier, 1987.

[100] Biology online Dictionary, "Amphipathic." biology-online.org. [Online]. Available: https://www.biology-online.org/dictionary/Amphipathic. [Accessed: 01-Jul-2018].

[101] B. Bagchi, "*The amphiphilic effect: the diverse but intimate world of aqueous binary*

mixtures," in *Water in Biological and Chemical Processes*, Cambridge: Cambridge University Press, 2018, pp. 243–260.

[102] S. M. Sami and M. A. Comeau, "Experimental study of non-azeotropic thermodynamic behaviour of binary mixtures in heat pumps," *Heat Recover. Syst. ClIP*, vol. 1, no. 6, pp. 505–515, 1991.

[103] Encyclopaedia Britannica, "Azeotrope." *britannica.com*. [Online]. Available: https://www.britannica.com/science/azeotrope. [Accessed: 01-Jul-2018].

[104] L. H. Horsley, "Table of Azeotropes and Nonazeotropes," *Anal. Chem.*, vol. 19, no. 8, pp. 508–600, Aug. 1947.

[105] R. B. Lebo, "Properties of mixtures of isopropyl alcohol and water," *J. Am. Chem. Soc.*, vol. 43, no. 5, pp. 1005–1011, 1921.

[106] B. L.. Theodore, H. E. LeMay and B. E. Bursten,, Chemistry the central science, 11th ed. Pearson Prentice Hall, 2009.

[107] D. Russo and V. Birolini, "Towards the right formulation of a technical problem," *Procedia Eng.*, vol. 9, pp. 77–91, 2011.

[108] Encyclopaedia Britannica, "Critical Point." britannica.com. [Online]. Available: https://www.britannica.com/science/critical-point-phase-change. [Accessed: 10-Jul-2018]..

[109] G. Price, Thermodynamics of chemical processes. Oxford: Oxford University Press, 1998.

[110] L. H. Bowen, and M. L. Benevides, "Critical point phase separation in binary liquid mixtures," J. Chem. Educ., vol. 70, no. 9, p. 1993.

[111] X. Huang, T. I. Korányi, M. D. Boot, and E. J. M. Hensen, "Catalytic depolymerization of lignin in supercritical ethanol," *Chem. Su. sChem.*, vol. 7, no. 8, pp. 2276–2288, 2014.

[112] X. Erdocia, R. Prado, J. Fernández-Rodríguez, and J. Labidi, "Depolymerization of Different Organosolv Lignins in Supercritical Methanol, Ethanol, and Acetone to Produce Phenolic Monomers," *ACS Sustain. Chem. Eng.*, vol. 4, no. 3, pp. 1373–1380, 2016.

[113] Z. Yuan, M. Tymchyshyn, and C. (Charles) Xu, "Reductive Depolymerization of Kraft and Organosolv Lignin in Supercritical Acetone for Chemicals and Materials," *Chem. Cat. Chem.*, vol. 8, no. 11, pp. 1968–1976, 2016.

[114] M. Saisu, T. Sato, M. Watanabe, T. Adschiri, and K. Arai, "Conversion of Lignin with Supercritical Water - Phenol Mixtures," *Energy & Fuels*, no. 17, pp. 922–928, 2003.

[115] National Institute of Standards and Technology, "Ethanol." NIST Web chemistry book, SRD 69, 2017 [Online]. Available: https://webbook.nist.gov/cgi/cbook.cgi?ID=C64175&Mask=4. [Accessed: 14-Jul-2018].

[116] National Institute of Standards and Technology, "Isopropanol." NIST Web chemistry book, SRD 69, 2017. [Online]. Available: https://webbook.nist.gov/cgi/cbook.cgi?ID=C67630&Mask=4. [Accessed: 14-Jul-2018].

[117] National Institute of Standards and Technology, "Acetone," NIST Web chemistry book, SRD 69, 2017. [Online]. Available: https://webbook.nist.gov/cgi/cbook.cgi?ID=C67641&Mask=4. [Accessed: 14-Jul-2018]..

[118] T. D. H. Nguyen, M. Maschietti, T. Belkheiri, L.-E. Åmand, H. Theliander, L. Vamling, L. Olausson, S.-I. Andersson, "Catalytic depolymerisation and conversion of Kraft lignin into liquid products using near-critical water," *J. Supercrit. Fluids*, Vol.86, pp. 67-75, 2014.

[119] N. Mahmood, Z. Yuan, J. Schmidt, and C. C. Xu, "Hydrolytic depolymerization of hydrolysis lignin: Effects of catalysts and solvents," *Bioresour. Technol.*, vol. 190, pp. 416–419, 2015.

[120] S. S. Toor, L. Rosendahl, and A. Rudolf, "Hydrothermal liquefaction of biomass: A review of subcritical water technologies," *Energy*, vol. 36, no. 5, pp. 2328–2342, 2011.

[121] Z. Fang, T. Sato, R. L. Smith, H. Inomata, K. Arai, and J. A. Kozinski, "Reaction chemistry and phase behavior of lignin in high-temperature and supercritical water," *Bioresour. Technol.*, vol. 99, no. 9, pp. 3424–3430, 2008.

[122] J. B. Nielsen, A. Jensen, C. B. Schandel, C. Felby, and A. D. Jensen, "Solvent consumption in non-catalytic alcohol solvolysis of biorefinery lignin," *Sustain. Energy Fuels*, vol. 1, no. 9, pp. 2006–2015, 2017.

[123] F. O. Rice and R. E. Vollrath, "The thermal decomposition of acetone in the gaseous state," *Pnas*, vol. 15, no. 1, p. 702, 1929.

[124] D. Royon, S. Locatelli, and E. E. Gonzo, "Ketalization of glycerol to solketal in supercritical acetone," *J. Supercrit. Fluids*, vol. 58, no. 1, pp. 88–92, 2011.

[125] S. C. Oh, D. I. Han, H. Kwak, S. Y. Bae, and K. H. Lee, "Kinetics of the degradation of polystyrene in supercritical acetone," *Polym. Degrad. Stab.*, vol. 92, no. 8, pp. 1622–1625, 2007.

[126] M. Bicker, D. Kaiser, L. Ott, and H. Vogel, "Dehydration of D-fructose to hydroxymethylfurfural in sub- and supercritical fluids," *J. Supercrit. Fluids*, vol. 36, no. 2, pp. 118–126, 2005.

[127] T. J. McDonough, "The chemistry of organosolv delignification," *Inst. Pap. Sci. Technol.*, no. 455, p. 17, 1992.

[128] M. Kumar, J. Singh, M. K. Singh, A. Singhal, and I. S. Thakur, "Investigating the degradation process of kraft lignin by β-proteobacterium, Pandoraea sp. ISTKB," *Environ. Sci. Pollut. Res.*, vol. 22, no. 20, pp. 15690–15702, 2015.

[129] K. Sarkanen and C. Schuerch, "A Quantitative Study of the Alcoholysis of Lignin," *J. Am. Chem. Soc.*, vol. 79, no. 15, pp. 4203–4209, 1957.

[130] B. Gómez-Monedero, M. P. Ruiz, F. Bimbela, and J. Faria, "Selective hydrogenolysis of α–O–4, β–O–4, 4–O–5 and C–O bonds of lignin-model compounds and lignin-containing stillage derived from cellulosic bioethanol processing," *Appl. Catal. A Gen.*, vol. 541, pp. 60–76, 2017.

[131] X. Cui, H. Yuan, K. Junge, C. Topf, M. Beller, and F. Shi, "A stable and practical nickel catalyst for the hydrogenolysis of C–O bonds," *Green Chem.*, vol. 19, no. 1, pp. 305–310, 2017.

[132] T. K. Sherwood, "Diffusion phenomena in heterogeneous catalysis," *Pure Appl. Chem.*, vol. 10, no. 4, pp. 595–610, 1965.

[133] C. Chmelik and J. Kärger, "In situ study on molecular diffusion phenomena in nanoporous catalytic solids," *Chem. Soc. Rev.*, vol. 39, no. 12, pp. 4864–4884, 2010.

[134] University of Cambridge, "Mass Transport,". Department. of chemical engineering and Biotechnology. [Online]. Available: https://www.ceb.cam.ac.uk/research/groups/rg-eme/teaching-notes/mass-transport. [Accessed: 10-Jul-2018].

[135] J. H. Wang, "On the role of diffusion in catalysis," *J. Phys. Chem.*, vol 59, no.10, pp. 1115-1116, 1955.

[136] Mineralogy Database, "Boehmite Mineral Data." webmineral.com. [Online]. Available: http://webmineral.com/data/Boehmite.shtml#.W0R-hRKn_IU. [Accessed: 10-Jul-2018].

[137] S. H. Cai, S. Rashkeev, S. Pantelides, and K. Sohlberg, "Phase transformation mechanism between γ- and θ-alumina," *Phys. Rev. B*, vol. 67, pp. 1–10, 2003.

[138] K. Wefers and C. Misra, "Oxides and Hydroxides of Aluminum," *Alcoa Tech. Pap.*, vol. 19, pp. 1–100, 1987.

[139] E. M. Anderson, R. Katahira, M. Reed, M. G. Resch, E. M. Karp, G. T. Beckham, and Y. Román-Leshkov, "Reductive Catalytic Fractionation of Corn Stover Lignin," *ACS Sustain. Chem. Eng.*, vol. 4, no. 12, pp. 6940–6950, Dec. 2016.

[140] M. R. Mostafa, A. M. Youssef, and S. M. Hassan, "Conversion of ethanol and isopropanol on alumina, titania and alumina-titania catalysts," *Mater. Lett.*, vol. 12, no. 3, pp. 207–213, 1991.

[141] E. Furimsky, "Catalytic hydrodeoxygenation," *Appl. Catal. A Gen.*, vol. 199, no. 2, pp. 147–190, 2000.

[142] K. A. Rogers and Y. Zheng, "Selective Deoxygenation of Biomass-Derived Bio-oils within Hydrogen-Modest Environments: A Review and New Insights," *Chem. Sus. Chem.*, vol. 9, no. 14, pp. 1750–1772, 2016.

[143] S. De, B. Saha, and R. Luque, "Hydrodeoxygenation processes: Advances on catalytic transformations of biomass-derived platform chemicals into hydrocarbon fuels," *Bioresour. Technol.*, vol. 178, pp. 108–118, 2015.

[144] N. P. Vasilakos and D. M. Austgen, "Hydrogen-donor solvents in biomass liquefaction," *Ind. Eng. Chem. Process Des. Dev.*, vol. 24, no. 2, pp. 304–311, Apr. 1985.

[145] C. Zhu, J. P. Cao, X. Y. Zhao, T. Xie, J. Ren, and X. Y. Wei, "Mechanism of Ni-catalyzed selective C–O cleavage of lignin model compound benzyl phenyl ether under mild conditions," *J. Energy Inst.*, pp. 1–8, 2018.

[146] J. Chen, Y. Ge, Y. Guo, and J. Chen, "Selective hydrogenation of biomass-derived 5-hydroxymethylfurfural using palladium catalyst supported on mesoporous graphitic carbon nitride," *J. Energy Chem.*, vol. 27, no. 1, pp. 283–289, 2018.

[147] J. L. Santos, M. Alda-Onggar, V. Fedorov, M. Peurla, K. Eränen, P. Mäki-Arvela, M. Á. Centeno, and D. Y. Murzin, "Hydrodeoxygenation of vanillin over carbon

supported metal catalysts," *Appl. Catal. A Gen.*, vol. 561, pp. 137–149, 2018.

[148] M. Goswami, S. Meena, S. Navatha, K. N. P. Rani, A. Pandey, R. K. Sukumaran, R. B. N. Prasad, and B. L. A. P. Devi, "Hydrolysis of biomass using a reusable solid carbon acid catalyst and fermentation of the catalytic hydrolysate to ethanol," *Bioresour. Technol.*, vol. 188, pp. 99–102, 2015.

[149] X. Cao, S. Sun, and R. Sun, "Application of biochar-based catalysts in biomass upgrading: a review," *RSC Adv.*, vol. 7, no. 77, pp. 48793–48805, 2017.

[150] E. Lam and J. H. T. Luong, "Carbon materials as catalyst supports and catalysts in the transformation of biomass to fuels and chemicals," *ACS Catal.*, vol. 4, no. 10, pp. 3393–3410, 2014.

[151] H. L. Riley, "Amorphous carbon and graphite," *Q. Rev. Chem. Soc.*, vol. 1, no. 1, p. 59, 1947.

[152] F. Rodriguez-Reinoso, "The role of carbon materials in heterogeneous catalysis," *Carbon N. Y.*, vol. 36, no. 3, pp. 159–175, 1998.

[153] T. Torres, "Graphene chemistry," *Chem. Soc. Rev.*, vol. 46, no. 15, pp. 4385–4386, 2017.

[154] H. C. Lee, W.-W. Liu, S.-P. Chai, A. R. Mohamed, A. Aziz, C.-S. Khe, N. M. S. Hidayah, and U. Hashim, "Review of the synthesis, transfer, characterization and growth mechanisms of single and multilayer graphene," *RSC Adv.*, vol. 7, no. 26, pp. 15644–15693, 2017.

[155] M. I. Zaki, M. A. Hasan, F. A. Al-Sagheer, and L. Pasupulety, "Surface chemistry of acetone on metal oxides: IR observation of acetone adsorption and consequent surface reactions on silica-alumina versus silica and alumina," *Langmuir*, vol. 16, no. 2, pp. 430–436, 2000.

[156] S. Kouva, K. Honkala, L. Lefferts, and J. Kanervo, "Review: monoclinic zirconia, its surface sites and their interaction with carbon monoxide," *Catal. Sci. Technol.*, vol. 5, no. 7, pp. 3473–3490, 2015.

[157] C. S. Lancefield, G. M. M. Rashid, F. Bouxin, A. Wasak, W. C. Tu, J. Hallett, S. Zein, J. Rodríguez, S. D. Jackson, N. J. Westwood, and T. D. H. Bugg, "Investigation of the Chemocatalytic and Biocatalytic Valorization of a Range of Different Lignin Preparations: The Importance of β-O-4 Content," *ACS Sustain. Chem. Eng.*, vol. 4, no. 12, pp. 6921–6930, 2016.

[158] C. Peng, Q. Chen, H. Guo, G. Hu, C. Li, J.-L. Wen, H. Wang, T. Zhang, Z. K. Zhao, R. Sun, and H. Xie, "Effects of Extraction Methods on Structure and Valorization of Corn Stover Lignin by a Pd/C Catalyst," *Chem. Cat. Chem*, vol. 9, no. 6, pp. 1135–1143, 2017.

[159] M. Rogošić, H. J. Mencer, and Z. Gomzi, "Polydispersity index and molecular weight distributions of polymers," *Eur. Polym. J.*, vol. 32, no. 11, pp. 1337–1344, 1996.

[160] R. Pagni, "Modern Physical Organic Chemistry," *J. Chem. Educ.*, vol. 83, no. 3, p. 387, Mar. 2006.

[161] J. Kestin, S. T. Ro, and W. A. Wakeham, "Viscosity of the isotopes of hydrogen and their intermolecular force potentials," *J. Chem. Soc.*, vol. 68, pp. 2316–2323, 1972.

[162] M. Gómez-Gallego and M. A. Sierra, "Kinetic Isotope Effects in the Study of Organometallic Reaction Mechanisms," *Chem. Rev.*, vol. 111, no. 8, pp. 4857–4963, 2011.

[163] K. B. J. Schowen, "*Solvent Hydrogen Isotope Effects*" in *Transition States of Biochemical Processes*, Boston: Springer, 1978, pp. 225–283.

[164] G. Hou and Q. Cui, "Stabilization of Different Types of Transition States in a Single Enzyme Active Site: QM/MM Analysis of Enzymes in the Alkaline Phosphatase Superfamily," *J. Am. Chem. Soc.*, vol. 135, no. 28, pp. 10457–10469, Jul. 2013.

[165] H. Esaki, F. Aoki, M. Umemura, M. Kato, T. Maegawa, Y. Monguchi, and H. Sajiki, "Efficient H/D exchange reactions of alkyl-substituted benzene derivatives by means of the Pd/C-H2-D2O system," *Chem. - A Eur. J.*, vol. 13, no. 14, pp. 4052–4063, 2007.

[166] H. J. Richard, "Nickel-catalyzed hydrogen isotope exchange," *J. Label. Compd. Radiopharm.*, vol. 53, pp. 716–721, 2010.

[167] E. E. Wolf and F. Alfani, "Catalysts Deactivation by Coking," *Catal. Rev.*, vol. 24, no. 3, pp. 329–371, 1982.

[168] M. Argyle and C. Bartholomew, "Heterogeneous Catalyst Deactivation and Regeneration: A Review," *Catalysts*, vol. 5, no. 1, pp. 145–269, 2015.

[169] J. C. Afonso, D. A. G. Aranda, M. Schmal, and R. Frety, "Regeneration of a Pt-SnAl2O3 catalyst: influence of heating rate, temperature and time of regeneration," *Fuel Process. Technol.*, vol. 50, no. 1, pp. 35–48, 1997.

[170] C. Rémond, N. Aubry, D. Crônier, S. Noël, F. Martel, B. Roge, H. Rakotoarivonina, P. Debeire, and B. Chabbert, "Combination of ammonia and xylanase pretreatments: Impact on enzymatic xylan and cellulose recovery from wheat straw," *Bioresour. Technol.*, vol. 101, no. 17, pp. 6712–6717, 2010.

[171] S. Huang, N. Mahmood, M. Tymchyshyn, Z. Yuan, and C. C. Xu, "Reductive de-polymerization of kraft lignin for chemicals and fuels using formic acid as an in-situ hydrogen source," *Bioresour. Technol.*, vol. 171, pp. 95–102, 2014.

[172] S. Svensson, "Minimizing the sulfur content in Kraft lignin," Master thesis. Sch. of. Dev. of Soc. and Tech. STFI-Packforsk, Stockholm, 2008.

[173] M. Al-Sabawi and J. Chen, "Hydroprocessing of Biomass-Derived Oils and Their Blends with Petroleum Feedstocks: A Review," *Energy & Fuels*, vol. 26, no. 9, pp. 5373–5399, Sep. 2012.

[174] M. Wang, Y. Zhao, and J. Li, "Demethylation and other modifications of industrial softwood kraft lignin by laccase-mediators," *Holzforschung*, vol. 72, no. 5, pp. 357–365, 2018.

[175] Y. Chen, N. M. Stark, Z. Cai, C. R. Frihart, L. F. Lorenz, and R. E. Ibach, "Chemical Modification of Kraft Lignin: Effect on Chemical and Thermal Properties," *Bioresources*, vol. 9, no. 3, pp. 5488–5500, 2014.

[176] X. Du, J. Li, and M. E. Lindström, "Modification of industrial softwood kraft lignin using Mannich reaction with and without phenolation pretreatment," *Ind. Crops Prod.*, vol. 52, pp. 729–735, 2014.

[177] S. Harrisson, "The downside of dispersity: Why the standard deviation is a better measure of dispersion in precision polymerization," *Polym. Chem.*, vol. 9, no. 12, pp. 1366–1370, 2018.

Appendix

i Calculation of the molecular weight, molecular number and polydispersity of lignin

The GPC analyses were performed according to the method developed by Dr Bouxin and Dr McVeigh (2016) [26] at The University of Glasgow as described in Section 3.4.9. Figure 210 shows a plot of intensity (UV response) and molecular weight distribution over time (minutes). Where Mi is the retention time and Ai is the value in the curve related to Mi. The Mi and Ai values could be used for all data points and the molecular weight, molecular number and polydispersity calculated [26] according to Equation 13, Equation 14 and Equation 15.

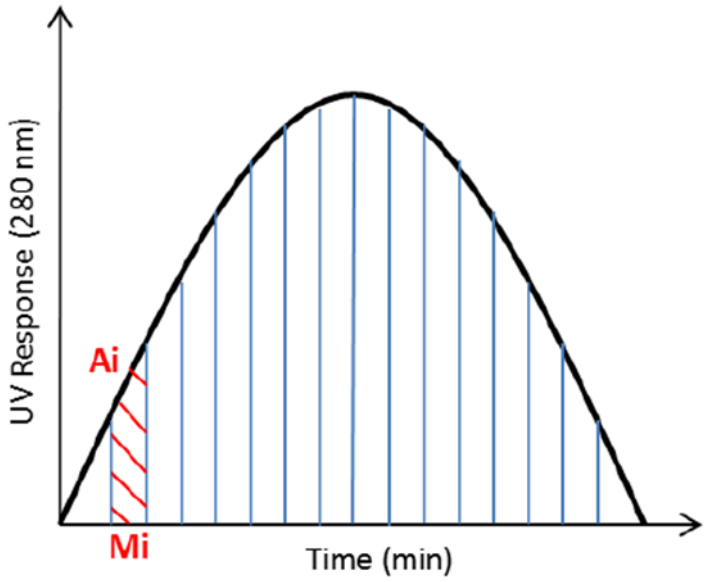

.

Figure 210 Example for GPC integration [26]

Equation 13 Equation for molecular weight calculation[26]

$$Mw = \frac{\sum(Ai * Mi)}{\sum Ai}$$

Equation 14 Equation for molecular number calculation[26]

$$Mn = \frac{\sum Ai}{\sum(\frac{Ai}{Mi})}$$

Equation 15 Equation for polydispersity calculation[26]

$$\mathrm{Ip} = \frac{\mathrm{Mw}}{\mathrm{Mn}}$$

ii Standard deviation calculation

The standard deviation (σ) was calculated according to Equation 16. Where ∑ is the summation, x is a value in the data set, μ is the mean of the data set, and N is the number of data points [177].

Equation 16 Formula for standard deviation calculation [177]

$$\sigma = \sqrt{\sum \frac{(xi - \mu)^2}{N}}$$

Glossary

Lignins

Kraft	KL
Sugar-cane	SC
Parr-lignin	PL
Birch parr-lignin	Birch Parr-lignin
Oak parr-lignin	Oak Parr-lignin

Catalyst Metal

Platinum	Pt
Rhodium	Rh
Nickel	Ni
Iron	Fe

Catalysts support

Aluminium oxide	Al_2O_3
Zirconium (IV) oxide	ZrO_2
Carbon	Carbon

Gases, compounds, solvents and reagents

Hydrogen	H_2

Nitrogen	N_2
Oxygen	O_2
Argon	Ar
Helium	He
Carbon monoxide	CO
Carbon dioxide	CO_2
Nitric oxide	NO
Nitrogen dioxide	NO_2
Deuterium	D_2
Water	H_2O
Acetone	C_3H_6O
Ethanol	C_2H_6O
Isopropanol	C_3H_7OH
Dichloromethane	DCM
Tetrahydrofuran	THF
Benzene, toluene and xylene	BTX
Hexadecane	Hexadecane
Polystyrene	PS
N,O-Bis(trimethylsilyl)trifluoroacetamide	BSTFA
Nickel (II) nitrate hexahydrate	$Ni(NO_3)_2x(H_2O)_6$
Iron nitrate nonahydrate	$Fe(NO_3)_3x(H_2O)_9$
Nickel (II) carbonate hydroxide tetrahydrate	$Ni_4CO_3(OH)_6x(H_2O)_4$
Nickel oxide	NiO
Iron(III) oxide	Fe_2O_3

Analyses Methods

Brunauer, Emmett and Teller	BET
X-ray Diffraction	XRD
Thermogravimetric Analysis	TGA
Temperature-Programmed Reduction	TPR
Temperature-Programmed Oxidation	TPO
Elemental analysis (CHN)	CHN
Gel Permeation Chromatography	GPC
Gas Chromatography	GC
Mass Spectroscopy	MS
HSQC NMR	HSQC NMR

Other terms

Total Ion Chromatogram	TIC
Intensity of Reference	IReference
Intensity of Internal Standard	IInternal Standard
Mass of Reference	mReference
Mass of Internal Standard	MInternal Standard
Molecular Weight	Mw
Molecular Number	Mw
Polydispersity	Ip
Hydrodeoxygenation	HDO
Hydrodesulfurisation	HDS

Products detected in the reactions

2-methoxyphenol	(1)
4-methyl-2-methoxyphenol	(2)

4-ethylphenol	(2A)
4-ethyl-2-methoxyphenol	(3)
4-propyl-2-methoxyphenol	(4)
1,2-dihydroxybenzene	(5)
4-ethylbenzene-1,2-diol	(6)
2,6-dimethoxyphenol	(6A)
4-(3-hydroxypropyl)-2-methoxyphenol	(7)
4-(3-methoxypropyl)-2-methoxyphenol	(8)
4-methyl-2,6-dimethoxyphenol	(9)
4-(2-hydroxyethyl)-2,6-dimethoxyphenol	(10)
4-ethyl-2,6-dimethoxyphenol	(11)
4-propenyl-2,6-dimethoxyphenol	(12)
4-(2-hydroxyethyl)-2-methoxyphenol	(13)
4-propyl-2,6-dimethoxyphenol	(14)
4-(1-hydroxy-2-methyl-pent-3-enyl)-2,6-dimethoxyphenol	(15)
4-(3-hydroxypropyl)-2,6-dimethoxyphenol	(15A)